CHARACTERIZING THE FUNCTION OF HUNTINGTIN IN THE CELL STRESS RESPONSE AS A TARGET FOR DRUG DISCOVERY IN HUNTINGTON'S DISEASE

By LISE MUNSIE B.Sc.

A Thesis Submitted to the School of Graduate Studies in Partial Fulfilment of the Requirements for the Degree Doctor of Philosophy

McMaster University © Copyright by Lise Munsie, June 2012

DOCTOR OF PHILOSOPHY (2012) **McMaster University**

(Biochemistry and Biomedical Science) **Hamilton, Ontario**

Title: Characterizing the function of huntingtin in the cell stress response as a target for drug discovery in Huntington's disease

Author: Lise Munsie, B.Sc

Supervisor: Dr. Ray Truant

Number of Pages: XVIII, 191

Abstract:

Huntington's disease (HD) is a devastating autosomal dominant neurodegenerative disorder for which there are no disease modifying treatments. Owing to this are the multiple biological functions of the huntingtin protein and the lack of understanding of the exact pathways being affected in HD. It is clear that the huntingtin protein normally provides anti-apoptotic support and that there are underlying energetic problems and cell stress defects associated with disease. Work from our group has shown that huntingtin acts as a stress sensor and translocates from the endoplasmic reticulum to the nucleus upon cell stress. We therefore hypothesized that huntingtin has a nuclear function in the cell stress response; which would tie together what is currently known about huntingtin, its pro-apoptotic function and the energetic defects of neurodegeneration. In this thesis we describe huntingtin as having a role in the nuclear cofilin-actin rod stress response. Cofilin is an actin binding protein normally involved in actin treadmilling. During stress, cofilin saturates F-actin leading to rod formation which functions to alleviate ATP. We show that this response is impaired in the presence of mutant huntingtin and that the aberrations in this response can be mediated through the enzyme tissue transglutaminase. Little is known about the physiological role and requirement of the cofilin-actin rod response. Therefore we created a system to test if rod formation was required in cells during stress, which indicates if and how targeting this pathway will be possible. We additionally looked at targeting the nuclear import and export properties of the cofilin protein, which directly affect rod formation and may be targetable in cofilin modifying drug discovery efforts. Overall, this work has described a specific and relevant pathway affected by mutant huntingtin and started the process of assessing this pathway as a therapeutic avenue for Huntington's disease.

Acknowledgements:

I would first and foremost like to thank my supervisor Dr. Ray Truant for making this project a reality, generating ideas, giving me support, encouragement and scientific freedom over the course of my PhD. I would like to thank CIHR for providing me with a doctoral scholarship, and the additional funding agencies, including CHDI inc. and the Krembil foundation who funded this work. I would like to thank my committee members Dr. David Andrews and Dr. Eric Brown for their guidance and constructive criticism that kept this project focused and moving forward. A sincere thank you to all past and present Truant lab members, we have always had a fantastic, encouraging and supportive group. Special thanks goes to Dr. Randy Singh Atwal and Carly Desmond, who initially trained me and provided endless insight and thoughtful discussion in my early years. Additional thanks to Jianrun Xia, Nick Caron, Leanne Stalker and Dr. Tamara Maiuri for all the help in and out of the lab.

Thank you to my friends who have always supported me throughout my scholarly endeavours.

And finally, thank you to my family.

My parents John and Maureen, I am who I am today because of you both, you have never stopped helping me through this journey; and my brothers, Tim and Reed, who are there for me unwaveringly.

Abbreviations:

17-AAG - 17-*N*-Allylamino-17-demethoxygeldanamycin

3NP – 3-nitroproprionic acid

A – Acceptor

AAV – Adeno-associated virus

Aβ - Amyloid beta

AD – Alzheimer's disease

ADF – Actin depolymerizing factor

ADP – Adenosine diphosphate

AFP – Aequorea fluorescent protein

ALS – Amyotrophic lateral sclerosis

AMP – Adenosine monophosphate

AMPAR – 2-amino-3-(5-methyl-3-oxo-1,2- oxazol-4-yl)propanoic acid Receptor

APP – Amyloid precursor protein

ASO – Antisense oligonucleotide

ATP – Adenosine triphosphate

BAC – Bacterial Artificial Chromosome

Bax – Bcl-2-Associated X protein

BDNF – Brain derived neurotrophic factor

β-Gal – β-Galactocidase

c. elegans – Caenorhabditis elegans

C9ORF72 – C9 open reading frame 72

CAFE miCELLS – Classification analysis and feature extraction from micrograph of cells

CaM - Calmodulin

cAMP – Cyclic adenosine monophosphate

CaN - Calcineurin

CBP – CREB binding protein

cDNA – Complementary DNA

ChIP – Chromatin immunoprecipitation

CIN – Chronophin phosphatase

CMV – Cytomegalovirus

CNS – Central nervous system

CoQ10 – Coenzyme Q10

CREB – cAMP response element-binding

CRM1 – Exportin 1

CSF – Cerebrospinal fluid

D – Donor

DAPI – 4'6'-Diamindino-2-Phenylindole, Dihydrochloride

DM1/2 – Myotonic dystrophy 1/2

DMSO – Dimethyl sulfoxide

DNA – Deoxyribonucleic acid

DRPLA – Dentatorubral-pallidoluysian atrophy

EF3 – Elongation Factor 3

ELISA – Enzyme-linked immunosorbent assay

ER – Endoplasmic Reticulum

EYFP – Enhanced yellow fluorescent protein

F-actin – Filamentous actin

FBS – Fetal bovine serum

FDA – Food and drug administration

FLIM – Fluorescent lifetime imaging microscopy

FRET – Förster Resonant energy transfer

FTD – Frontotemporal dementia

G-actin – Globular actin

GAPDH – Glyceraldehyde-3-phosphate dehydrogenase

GFP – Green fluorescent protein

GM1 – Monosialotetrahexosylganglioside

GST – Glutathione-S-transferase

GTP – Guanosine triphosphate

HAP1 – Huntingtin associated protein 1

HCL – Hydrochloric acid

HCS – High content screening

HD – Huntington's disease

HDAC – Histone deacetylase

Hdh – Murine HTT homolog

HDL2 – Huntington's disease like 2

HEAT – Huntington, elongation Factor 3, the regulatory subunit A of protein phosphatase 2A, TOR1

HEPES – 4-(2-hydroxyethyl)-1-piperazineethanesulfonic acid

HSE – Heat shock element

HSF – Heat shock factor

HSP – Heat shock protein

HSP90 – Heat shock protein 90

HSR – Heat shock response

HTS – High throughput screening

HTT – Huntingtin

IL – Interleukin

IPTG – Isopropyl-β-D-1-thiogalactopyranoside

IT15 – Interesting transcript 15

JMY – Junction mediating and regulatory protein

KA – Kainic acid

kDa- Kilodaltons

KMO – Kynurenin 3-monoxygenase

LIMK – Lin11, Isl-1 & Mec-3 domain kinase

MAL – Myelin and lymphocyte protein

MP – Multi-photon

MPTP – 1-Methyl-4-phenyl-1,2,3,6-tetrahydropyridine

MRI – Magnetic resonance imaging

mRNA – Messenger RNA

MSN - Medium Spiny Neuron

N.A – Numerical Aperture

NES – Nuclear export signal

NIH 3T3 – Mouse embryonic fibroblast cell line

NLS – Nuclear localization signal

NMDA – N-methyl-D-Aspartate

NMDAR – N-methyl-D- Aspartate Receptor

NP-40 – Nonidet P-40

NPC – Nuclear pore complex

OH_8dG – 8-hydroxydeoxyguanosine

PBS – Phosphate buffered saline

PCM1 – Pericentriolar material-1

PCR – Polymerase chain reaction

PD – Parkinson's Disease

PINK1 – PTEN induced kinase-1

Pol – RNA polymerase

PP2A – Protein phosphatase 2A

PRC2 – Polycomb recessive complex 2

PVDF – Polyvinylidene fluoride

QA – Quinolinic Acid

REST – Repressor element 1 silencing transcription factor

RFP – Red fluorescent protein

RNA – Ribonucleic acid

RNAi - RNA interference

ROCK –Rho-associated protein kinase

ROS – Reactive oxygen species

SBMA – Spinal and bulbar muscular atrophy

SCA – Spinocerebellar ataxia

SDS-PAGE – Sodium dodecyl sulfate polyacrylamide gel electrophoresis

shRNA – Short hairpin RNA

siRNA – Small interfering RNA

SN – Substantia nigra

SNP – Single nucleotide polymorphism

SP1 – Specificity protein 1

SSH1 – Slingshot 1 phosphatase

ST14 – Conditionally immortalized striatal derived cell line (from E14 striatal primordial)

ST*Hdh* – ST14 cells from a mouse striatum, Hdh refers to huntingtin

SV40 – Simian virus 40

TAFII130 – Tata-binding protein associated factor II130

TBST – Tris buffered saline with tween

TCSPC – Time correlated single photon counting

TESK – Testicular protein kinase

TG2/tTG – Tissue transglutaminase

TNF-α – Tumour necrosis Factor alpha

UPR – Unfolded protein response

UTR – Untranslated region

YAC – Yeast artificial chromosome

TABLE OF CONTENTS

List of Figures:

List of Tables:

List of Videos:

Video 2.1: Nuclear Rod Forming Dynamics in Wildtype STHdh Cells. Stable mCerulean-cofilin STHdh$^{Q7/Q7}$ were heated to 42°C using the delta T heated stage and objective system. Rod formation, rod breakdown and cell death is visualized by live cell fluorescence microscopy at 100X while heat shock was sustained. Images were acquired every 60 seconds from the time the dish reached 42°C.

Video 2.2: Nuclear Rod Forming Dynamics in Mutant STHdh Cells Stable mCerulean-cofilin STHdh$^{Q111/Q111}$ cells were heated to 42°C using the delta T heated stage and objective system. Rod formation, rod breakdown and cell death is visualized by live cell fluorescence microscopy at 100X while heat shock was sustained. Images were acquired every 60 seconds from the time the dish reached 42°C.

Video 2.3: Nuclear Rod Forming Dynamics in Wildtype STHdh Cells in the Presence of Scrambled siRNA. Stable mCerulean-cofilin expressing STHdh$^{Q7/Q7}$ cells were treated with control siRNA for 72 hours. Transfected cells were visualized by co-transfection with Block-iT™Alexa Fluor® red (Figure 4). Cells were heated to 42°C using the delta T heated stage and objective system. Rod formation, rod breakdown and cell death is visualized by live cell fluorescence microscopy at 100X while heat shock was sustained. Images were acquired every 60 seconds from the time the dish reached 42°C.

Video 2.4: Nuclear Rod Forming Dynamics in Wildtype STHdh Cells in the Presence of *hdh* siRNA hours. Transfected cells were visualized by co-transfection with Block-iT™Alexa Fluor® red (Figure 4). Cells were heated to 42°C using the delta T heated stage and objective system. Rod formation, rod breakdown and cell death is visualized by live cell fluorescence microscopy at 100X while heat shock was sustained. Images were acquired every 60 seconds from the time the dish reached 42°C.

Video 3.1: Visualization of the cofilin-actin rod stress response. Stable mCerulean-cofilin expressing STHdh cells were heated to 42°C using the Delta T heated stage and objective system. Rod formation, rod breakdown and cell death is visualized by live cell fluorescence microscopy at 100X while heat shock was sustained. Images were acquired every 60 seconds from the time the dish reached 42°C.

Video 3.2: Real-time, live cell observation of leptomycin B effect on cofilin NES activity. EYFP-cofilin NES was transfected into STHdh cells. Cell was imaged prior to addition of leptomycin B and then every 10 seconds after the addition of leptomycin B for 6 minutes to visualize nuclear entry.

Video 3.3: Cofilin knockdown by shRNA causes cell shrinkage during heat shock stress. STHdh cells were transfected with cofilin-shRNA-EYFP and construct was expressed for 48 hours. Cells were heated to 42°C using the delta T heated stage and objective system. Cell response to heat shock is visualized at 20X while heat shock was sustained. Images were acquired every 60 seconds from the time the dish reached 42°C. Video shows that cells cannot respond to stress and rapidly shrink in response to stress.

Video 3.4: EYFP-Cofilin in trans can complement the knockdown of endogenous cofilin during stress rescuing the cell shrinkage phenotype. STHdh cells were transfected with cofilin-shRNA-EYFP-cofilin and construct was expressed for 48 hours. Cells were heated to 42°C using the delta T heated stage and objective system. Cell response to heat shock is visualized at 20X while heat shock was sustained. Images were acquired every 60 seconds from the time the dish reached 42°C. Video shows that over-expression of EYFP-cofilin can rescue the change in cell size during stress phenotype shown when cofilin is knocked down. Cells maintain their size and rods form in both the nucleus and cytoplasm in response to stress.

Chapter 1: General Introduction

1.1 Huntington's Disease History

Huntington's disease (HD) has a rich history in the field of genetics and neurodegenerative disease. Prior to the eighteenth century, individuals with HD were said to be afflicted with St. Vitus dance, which specifically referred to any patients suffering from choreic movement. Chorea literally translates to "dancelike" movements and comes from the greek "khoreia", a word meaning dance. Chorea manifests as increasing involuntary movements over the course of disease, and is the distinguishing physical symptom of HD (Cardoso et al., 2006). Although chorea is the main symptom associated with HD and other neurological movement disorders, it was as early as 1621 that these disorders were characterized as not just physical, but also having cognitive and psychiatric components, as Robert Burton described those suffering from Chorus Sancti Viti (or St. Vitus dance) as having "a disease of the minde"(Wexler, 2008).

The groundwork for the full, and what remains accurate, description of HD came from a family medical practice in East Hampton in the eighteenth century. There was a population of East Hampton families afflicted with St. Vitus dance. A doctor named Abel Huntington arrived in East Hampton in 1797 and became the local family physician, treating families whose pedigrees can be traced back to this era. His practice would be taken over by his son, George Lee Huntington, who would continue to observe and treat the families in the community. This family history lay the groundwork for George Huntington, son of George Lee and grandson of Abel, to publish his seminal paper "On Chorea" in 1872 (Huntington, 2003; Wexler, 2008). It was the collective insight of George Huntington, his father and grandfather that led to the breakthrough publication describing hereditary chorea. Although some features of HD had been previously queried, this manuscript specifically describes a certain form of hereditary chorea that George Huntington noted in the East Hampton population. His description included three marked characteristics of HD, including:

1. its hereditary nature;

"When either or both the parents have shown manifestations of the disease, and more especially when these manifestations have been of a *serious* nature, one or more of the offspring almost invariably suffer from the disease, if they live to adult age. But if by any chance these children go through life *without* it, the thread is broken and the grandchildren and great-grandchildren of the original shakers may rest assured that they are free from the disease."(Huntington, 2003)

What he was describing, we now know, was that the disease is inherited in an autosomal dominant fashion (Conneally, 1984).

2. A tendency to insanity and suicide;

"As the disease progresses the mind becomes more or less impaired, in many amounting to insanity, while in others mind and body both gradually fail until death relieves them of their sufferings."(Huntington, 2003)

These are the cognitive and emotional symptoms in HD we know today to be characteristic and equally debilitating to the patient as the physical symptoms (Sturrock and Leavitt, 2010).

And finally,

3. It's manifesting as a grave disease in adult life;

"I do not know of a single case that has shown any marked signs of chorea before the age of thirty or forty years, while those who pass the fortieth year *without* symptoms of the disease, are seldom attacked."(Huntington, 2003)

HD typically has an adult onset manifesting in midlife and progressing for 10-20 years before invariably leading to death, although it is notable that there is also juvenile onset HD that occurs in individuals as early as age 10 (Sturrock and Leavitt, 2010).

"On Chorea" not only eloquently and succinctly described what would soon after come to be called Huntington's Chorea, and now more accurately to reflect the range of symptoms, Huntington's Disease, but also posed new questions about modes of inheritance in people; something at the time that was not appreciated, even though Gregor Mendel had published his work on dominant inheritance in 1866. George Huntington's paper brought this genetic inheritance of traits to the forefront until Mendel's work "Experiments on Plant Hybridization" was re-introduced in the 1900's (Mendel, 1865; Wexler, 2008).

In George Huntington's manuscript, the pathology of chorea was assumed to be nervous system and brain associated and circumstantial evidence led him to believe the affected region was the cerebellum (Huntington, 2003). However in 1880, clinical papers describing reports from post-mortem autopsies of patients who suffered from chorea, detailed a loss of brain cells in the region of the brain we know as the corpus striatum (Macleod, 1881). Although not his most notable achievement, the Noble laureate Camillo Golgi had a hand in this work when he used his famous technique of staining nerve cells (called the "black reaction") on post mortem chorea patient brains. He discovered a distinct atrophy of nerve cells located in the striatum and was possibly the first to link some cases of neurodegeneration with this brain structure, as opposed to the cerebellum (Macchi, 1999; Macleod, 1881). This obvious deterioration of a subset of the brain was initially thought to be caused by bacterial or viral infection, or possibly a susceptibility caused by other diseases. However the prevailing theory became that there was a wasting of neurons with unknown cause (Huntington, 2003; Wexler, 2008). One of the first reports to note this was by Charles Loomis Dana, from Cornell Medical school, where he described his hypothesis that HD was, in fact, not caused by inflammation, microbe, poison or anything environmental, but caused by "simply a death at the age of thirty of cells which should do in ordinary people live to

the age of seventy"(Dana, 1895). We still do not know the biochemical basis of cell death that leads to neurodegeneration, but we do know the genetics behind it.

1.1.1 The Discovery of the Gene

The next major chapter in the HD story came at a time when the field of genetics was just in its infancy. In the 1950's a clinician native to Venezuela, Dr. Américo Negrette, noted a dense population of individuals in Venezuela with choreic movements and characterized them as HD patients. The Venezuelan population remains the largest, most dense, and best characterized HD population in the world (Moscovich et al., 2011). Negrette published his findings and presented them, setting in motion a series of events that would ultimately lead to the discovery of the gene associated with the disease. Dr. Nancy Wexler, daughter of Milton Wexler - founder of the Hereditary Disease Foundation, was in the audience at one of Dr. Negrettes talks. Realizing the potential that such a closely genetically related population can provide, Dr. Wexler set off on an international expedition and initiated a large collaboration in search of the genetic cause of HD, basing her studies out of Lake Maracaibo, Venezuela. She initially set up the Venezuela Collaborative Huntington's Disease project, where a large amount of quality DNA from the Venezuelan kindred was obtained (Venezula-Project-Collaborators, 2008). In 1983, using DNA from the Venezuelan kindred and an American kindred, the group utilized restriction fragment length polymorphisms, specifically a *HindIII* digest of human genomic DNA, coupled with southern blot analysis of DNA from human-mouse somatic cell hybrids, and mapped the HD mutation to an unknown fragment of chromosome 4 (Gusella et al., 1983). This, the first example of a disease associated gene being mapped to a human chromosome, prompted the formation of a collaboration of gene hunters called the Huntington's Disease Collaborative Research Group. This group subsequently spent the next ten years working to determine the exact mutation that causes HD. The group hypothesized that the HD mutation was in a coding region of DNA and thus probed the region of interest on chromosome 4 for areas of DNA that were actively

transcribed. This led them to the *IT15* gene. After determining the DNA sequence of the *IT15* gene from a healthy individual, they found that the first exon contained 21 CAG repeats, encoding the amino acid glutamine in tandem repeats (The-Huntington's-Disease-Research-Collaborative-Group, 1993). Upon examining this region of DNA in HD affected individuals, this group was able to show that the DNA repeat element was expanded in HD, and that all affected individuals in their study had greater than 35 CAG repeats in the first exon of the *IT15* gene (The-Huntington's-Disease-Research-Collaborative-Group, 1993). When this seminal work was published, they named the protein encoded by *IT15* "huntingtin". The gene is now alternatively named *HTT*.

1.2 Genetics of Huntington's disease

HD is an autosomal dominant disorder, meaning to be affected you only need one copy of the mutant gene and the affected have a fifty percent chance of passing the disease on to their offspring. HD is a monogenetic disorder, caused by a single mutation in the DNA sequence located at chromosome 4p16.3 (The-Huntington's-Disease-Research-Collaborative-Group, 1993). The causative mutation occurs in the coding region of the actively transcribed *IT15 (HTT)* gene. The *HTT* gene encodes the huntingtin protein, which consists of 3144 amino acids, 67 exons and has a molecular weight of 350 kDa (The-Huntington's-Disease-Research-Collaborative-Group, 1993) (Figure 1.1 A). The mutation manifests as a CAG trinucleotide expansion in the *HTT* gene. CAG encodes for the amino acid glutamine and mutant huntingtin has an expansion in the polyglutamine tract contained in the first exon of the *HTT* gene (The-Huntington's-Disease-Research-Collaborative-Group, 1993). A normal unaffected individual will have 36 or less CAG repeats in their DNA sequence. Anyone with greater than 40 CAG repeats has completely penetrant HD (Figure 1.1 B). Typical age of onset is middle age (mean age of onset being 40) followed by unrelenting progression for 10-20 years before leading to death (Sturrock and Leavitt, 2010) . Individuals with greater than 60 repeats are said to have juvenile onset HD, which means they will typically

display symptoms before age 20 and experience a faster rate of progression compared to adult cases (Sturrock and Leavitt, 2010). CAG repeat lengths between 36-40 exhibit incomplete penetrance and an individual with this length of CAG may or may not exhibit HD symptoms in their lifetime (McNeil et al., 1997; Quarrell et al., 2007). CAG repeat lengths of 29-36 are said to be unstable, and although the individual with this length of CAG in their *HTT* gene will not clinically show HD symptoms, the CAG tract may expand during meiosis allowing the disease allele to emerge de novo in their children; this is the cause of sporadic HD and is more likely to occur through the paternal line during spermatogenesis (Kremer et al., 1995; McNeil et al., 1997). CAG length in the expanded allele is a dominant modifier for age of onset of HD symptoms and is inversely correlated; however there are other genetic and environmental factors that contribute to age of onset in HD (Lee et al., 2012). There is further somatic instability of the CAG tract causing different tissue specific CAG tract lengths within an affected organism, along with the instability in the germline. This somatic instability is tissue-specific and seems to affect the brain to a greater extent than other tissues in HD; and may therefore be a further genetic modifier of disease age of onset (Kennedy et al., 2003; Swami et al., 2009). HD is the most commonly inherited neurodegenerative disorder, and the prevalence of HD in the population is currently statistically thought to be at least 12.4/100,000 (Rawlins, 2010). This is most certainly an underestimate since these statistics come from the Huntington's Disease Association in England and Wales and cannot possibly account for areas that the association does not serve and the large number of undiagnosed or misdiagnosed cases of HD (Rawlins, 2010). Efforts into finding the true prevalence of HD are going on worldwide.

1.2.1 Polyglutamine Expansion Disorders

The nature of the mutation in huntingtin groups HD in with a broader range of disorders known as polyglutamine expansion neurodegenerative disorders. All of these disorders are hereditary neurodegenerative disorders that are caused by a CAG

expansion above a certain threshold, in the disease causing gene. There are currently nine known polyglutamine expansion disorders, including: HD, Spinal and bulbar muscular atrophy (SBMA), dentatorubral-pallidoluysian atrophy (DRPLA) and the spinocerebellar ataxia types (SCA) 1,2,3,6,7 and 17 (Zoghbi and Orr, 2000). Each disorder is caused by a CAG expansion occurring in a different gene, and the affected proteins share nothing in common: functionally, structurally or homologically, aside from the expanded polyglutamine tract (Gatchel and Zoghbi, 2005; Zoghbi and Orr, 2000). Each disease does lead to neurodegeneration, but with different affected regions in the brain and different neuronal sub-populations that undergo degeneration. Symptoms vary with different motor and psychological impairments; however disease similarities include the fact that almost all polyglutamine disorders are inherited in an autosomal dominant fashion, are characterized by genetic anticipation and instability, and typically have middle age onset with a 10-20 year disease progression. This implies that it is not just the toxic CAG expansion that dictates disease, but the context of the protein in which the polyglutamine expansion occurs that directs disease course and severity.

1.2.2 Repeat Expansion Disorders

Polyglutamine disorders in general are part of a growing family of diseases caused by repeat expansions in the DNA sequences, which can occur both in coding and non-coding DNA regions. Currently, the most common repeat expansion is trinucleotide, and there are at least 17 of these disorders, including HD and the other polyglutamine expansion disorders previously mentioned (Orr and Zoghbi, 2007). Other well-known trinucleotide repeat expansion disorders include: Fragile X syndrome, which is the most common form of mental retardation, caused by an unstable CGG expansion in the 5' untranslated region (UTR) of the *FMR1* gene, leading to loss of protein product (Fu et al., 1991; Orr and Zoghbi, 2007); and Myotonic Dystrophy (DM1), a multi-systemic disorder, caused by a CTG expansion in the 3' UTR of a gene encoding a protein kinase.

DM1 is not caused by an alteration in the coded protein, but by toxic RNA with an expanded CUG (Brook et al., 1992; Orr and Zoghbi, 2007). It is of note that Huntington disease-like2 (HDL2), a disease that presents clinically and neuropathologically with almost identical symptoms to HD, is caused a CAG/CTG repeat expansion in an alternatively spliced exon of the *Junctophilin-3* locus (Margolis et al., 2005). HDL2 pathogenesis is thought to be caused by toxicity elicited by both toxic RNA containing the CUG expansion and an antisense transcript encoding a polyglutamine expanded protein (Orr, 2011; Wilburn et al., 2011). There are also tetra, penta and hexa-nucleotide repeat expansions that cause disease. DM2, a disease with very similar symptomology to DM1, is caused by a tetra (CCUG) nucleotide expansion in an intron of the *zinc finger 9* gene, and pathogenesis results from toxic RNA via RNA binding proteins in a similar manner to DM1 (Liquori et al., 2001). Recently, a hexanucleotide repeat (GGGGCC) in the *C9ORF72* gene, leading to the loss of one alternatively spliced transcript, was found to be responsible for a large percentage of both familial frontotemporal dementia (FTD) and amyotrophic lateral sclerosis (ALS) (DeJesus-Hernandez et al., 2011; Renton et al., 2011). As sequencing and genetic technology advances we will continue to discover diseases caused by repeat expansions in DNA. However due to marked variability in the context of where in the DNA these expansions occur and what the resulting disease phenotype is, each disorder will need to be examined on a case by case basis in hopes of finding ways to treat each expansion disease individually.

1.3 Pathology

1.3.1 Development

HD is caused by neurodegeneration in a sub-population of neurons in specific regions of the brain. The *HTT* gene and the huntingtin protein are both ubiquitously expressed in the brain and peripheral tissues of the body, however expression levels

may be enriched in the brain and testes (Li et al., 1993; Sharp et al., 1995). Huntingtin is also an essential protein required for development. Targeted disruption of the *Hdh* gene (murine *HTT* homolog) in mice is embryonic lethal at embryonic day 8.5 indicating that huntingtin is expressed very early during development and that there are no other proteins in the cell with functional redundancy that can rescue huntingtin knockout (Nasir et al., 1995). Based on the timing of in utero death caused by huntingtin knockout, it is suggested that huntingtin is required for proper gastrulation, neurulation and neurogenesis (Nasir et al., 1995; White et al., 1997). A single copy of the huntingtin allele, with either a wildtype or mutant polyglutamine tract length, is sufficient to reverse the embryonic lethal huntingtin knockout phenotype (White et al., 1997). This is the first evidence to support the fact that mutant huntingtin does not interfere with normal huntingtin functions during development but rather elicits an obvious gain or loss of function only in adult cells. HD patients with a homozygous genotype develop normally, further indicating that mutant huntingtin can compensate for wildtype huntingtin with respect to functions during development (Wexler et al., 1987). There does seem to be a certain dosage of huntingtin required for normal development. A serendipitous mutation made during the homologous recombination process while producing a transgenic mouse resulted in a mutation causing about a two thirds decrease in normal huntingtin expression. It was found that when less than fifty percent of huntingtin was available during development there are resulting defects in CNS development in the mouse (White et al., 1997).

1.3.2 Neuropathology

In HD, progressive neurodegeneration is classically noted in the striatum, the main input of the basal ganglia (Vonsattel et al., 1985). The basal ganglia is made up of subcortical brain structures which are involved in motor control and cognition (Han et al., 2010). Within the striatum there are two main sub-populations of neurons: Medium Spiny Neurons (MSN), which are the projection neurons responsible for signalling to

other parts of the brain, and interneurons, which are much smaller neurons responsible for signalling within the striatum. The projection neurons are exquisitely susceptible to the insult of mutant huntingtin while the interneurons are largely spared (Reiner et al., 1988). Other parts of the brain including the cerebral cortex undergo some level of progressive degeneration over the course of HD. Pyramidal projection neurons, similar in morphology and size to MSNs, are more vulnerable to degeneration in the cerebral cortex than cell types with other morphologies (Cudkowicz and Kowall, 1990). Although there is massive cell loss in these brain structures at end point HD, it seems that neuron dysfunction precludes cell death and is responsible for early symptoms. This was initially observed in mouse models of HD. Although there is no validated mouse model that accurately recapitulates all of HD pathology, many models recapitulate some of the major pathological events in HD and the autosomal dominant inheritance pattern (Cepeda et al., 2010; Heng et al., 2008). In these mouse models, and specifically in knock-in mouse models which have an appropriate genetic context, symptomology, both behavioural and motor, were found to be present prior to any apparent cell loss or neurodegeneration (Levine et al., 2004; Menalled, 2005). Current worldwide effort is going into characterizing prodromal HD patients using advanced imagining techniques, specifically magnetic resonance imaging (MRI) to detect early changes in the brain either prior to symptoms or in early stages of HD (Tabrizi et al., 2012). These studies highlighted previously uncharacterized degeneration and atrophy in parts of the brain that occur prior to observation of clinical symptoms. Atrophy and cell loss in the white matter and striatum appear to be the earliest detectable changes present in the patient using sensitive imaging methods, supporting the hypothesis of early brain atrophy prior to degeneration and the idea that symptoms likely become present when the plasticity in the brain can no longer compensate for neuronal atrophy and loss (Dumas et al., 2012). These studies also highlight the fact that brain changes extend beyond the obvious areas of cell loss in the striatum and cortex and show that other areas including the white matter are affected, which is not surprising based on the ubiquitous

expression of huntingtin. However how these changes fit into the neuropathological profile of HD remain unclear.

1.3.3 Symptomology

HD patients are generally afflicted with a triad of symptoms (physical, cognitive and behavioural), that vary in severity from patient to patient. As previously described, the physical symptoms, largely the choreic movement, is the most characteristic symptom and is generally used to diagnose HD. There are both voluntary and involuntary movement afflictions. The involuntary movements initially present as "twitches" and progress to full chorea, which is a rapid, irregular and jerky movement of the limbs, trunk and face (Sturrock and Leavitt, 2010). The voluntary movement afflictions include gait ataxia, which leads to the inability to remain standing and eventually causes patients to become completely non-ambulatory. Deficits in fine motor control as well as dysphagia accompany this part of the disease (Sturrock and Leavitt, 2010). The cognitive deficits in HD can arise prior to the actual movement disorder; these include changes in personality, bradyphrenia (slow thought), inability to concentrate, inability to coordinate and initiate actions, and defective memory recall; all are reported over the course of HD (Butters et al., 1985; Caine et al., 1977; Pillon et al., 1991; Sturrock and Leavitt, 2010). The psychiatric component of the disease causes the patient to experience depression, irritability, obsessive compulsive symptoms and aggressive behaviours (Craufurd et al., 2001; Sturrock and Leavitt, 2010). Depression is the most common symptom and major depression occurs in up to forty percent of HD patients (Shiwach, 1994). The incidence of suicide in HD patients as a result of the cognitive and psychiatric symptoms is 4-6 times higher than average in the unaffected population (Schoenfeld et al., 1984).

1.3.4 Peripheral Pathology

It is important to further note peripheral changes that occur in cell types and tissues outside of the brain. HD patients suffer metabolic defects including severe weight loss, in spite of increased appetite and caloric intake (Sturrock and Leavitt, 2010), deficiencies in the endocrine system and problems related to the immune system. The peripheral immune system seems to be especially affected, as indicated by the presence of mitochondrial defects in lymphocytes and over-activity of monocytes in response to stimulation (Kwan et al., 2012; Sassone et al., 2009). There are many increased markers of inflammation, including pro-inflammatory cytokines and chemokines, found in HD blood samples (Bjorkqvist et al., 2008; Wild et al., 2008). Interestingly, when bone marrow transplant is performed from a wildtype mouse into a lethally irradiated HD transgenic mouse, effectively replacing the peripheral immune system, a partial rescue of pathology is observed in the brain as well as a normalization of peripheral cytokine levels (Kwan et al., 2012). This confirms that mutant huntingtin has cell autonomous effects in immune cells, and likely many other populations in the body. Many transcriptional and energetic defects that are characteristic of HD neurons are also found in most other cell types throughout the body. This implies that HD is not just a disease of the brain. However since the brain is most severely affected and causes the most devastating symptoms it has classically been the most studied organ in HD. Peripheral tissues will be important in discovering biomarkers for HD that can be used in drug discovery efforts as small molecules and other therapies reach clinical trials. Since brain sample availability is generally limited to post-mortem, it is not adequate for the monitoring of drug activity and effectiveness in clinical trials. As we discover more about the peripheral changes in HD, it is becoming clear that easily accessible tissues such as blood and fibroblasts offer significant potential in terms of biomarker development. More investigation into the dysfunction of huntingtin in these cell types will be needed, alongside the use of actual HD patient samples.

1.4 Huntington's Disease in the Context of Neurodegeneration at Large

There are commonalities between multiple neurodegenerative disorders. The greatest commonality between the three most studied neurodegenerative disorders, Huntington's disease (HD), Parkinson's disease (PD) and Alzheimer's disease (AD) is a common theme of bioenergetics failure. Although the etiologies and pathologies differ greatly between these disorders, mitochondrial dysfunction, problems with ATP and cell stress response, as well as excitotoxic stress as a mechanism for neuron death, are common to all. The brain has a disproportionately high energy requirement. Although only accounting for two percent of total body weight, it consumes up to twenty percent of the bodies energy. Neurons have a high energy consumption rate and are responsible for most of the energy consumption in the brain (Belanger et al., 2011). Because of this, the nervous system is exquisitely sensitive to energetic stress and it is foreseeable why cell autonomous defects in energetics would differentially affect neurons to a greater extent than other cell populations.

1.4.1 External Evidence of Energetics Failure

Both HD and PD can be mimicked in animal models by mitochondrial toxins. In both mice and primates, injecting the brain with 3-nitropropionic acid (3NP), an irreversible inhibitor of the tricarboxylic acid cycle through the respiratory chain enzyme succinate dehydrogenase, induces preferential degeneration of the striatum as well as abnormal movements mimicking some of the physical symptoms associated with HD in humans (Brouillet et al., 2005). 1-Methy-4-phenyl-1,2,3,6-tetrahydropyridine (MPTP), a heroin analog, inhibits both oxidative phosphorylation and the respiratory chain, and when administered systemically, induces PD symptoms and regional degeneration in primates. Some PD symptomology is also recapitulated in mice by this method (Porras et al., 2012; Przedborski et al., 2004).

1.4.2 Intrinsic Evidence of Energetics Failure

Genetically, a role for bioenergetics deficiencies is supported in both PD and AD. Some of the genes responsible for forms of familial PD are tightly linked to cellular energetics. For instance, mutations to the PTEN-induced-kinase 1 (PINK1) gene, which is responsible for mitochondrial maintenance, causes an autosomal recessive form of PD (Valente et al., 2004). DJ-1, a gene responsible for another form of familial PD, is also thought to have a role in the oxidative stress response and localizes to mitochondria (Junn et al., 2009). Although AD is largely sporadic, familial AD, caused by mutations in either amyloid precursor protein (APP) or presenilin, are also associated with mitochondrial dysfunction. Mutations to either of these proteins causes both increased cellular calcium leading to internal cell stress, and increased amyloid β peptide (Aβ) production. Increased Aβ leads to depressed mitochondrial function, impaired metabolism and increased oxidative stress (Eckert et al., 2010). A problem with a specific stress response pathway that occurs due to energetic failure has also been linked to AD. The cofilin-actin rod stress response is a cytoskeletal stress response that occurs when there is a decrease of ATP in the cells; under these low ATP conditions, cofilin, an actin binding protein, saturates actin and causes it to bundle into rods. Actin treadmilling is an energetically costly process. By formation of rods and inhibition of actin treadmilling during stress, the cell is able to free up ATP so it can be used elsewhere (Bernstein et al., 2006). Rod formation is triggered by oxidative stress conditions and can be induced using several methods: mimicking oxidative stress using hydrogen peroxide; depleting the cell of ATP by uncoupling oxidative phosphorylation and subsequently inhibiting glycolysis using sodium azide and 2-deoxyglucose; excitotoxic stress induced by glutamate; direct rod formation can occur in the presence of Aβ; or general cell stress including heat shock (Iida et al., 1992; Minamide et al., 2000). Neurons are typically more sensitive to these stressors compared to other cell types (Minamide et al., 2000). A defect in the cofilin-actin rod stress response is

thought to cause rods to persist in neurites in AD models, blocking vesicular transport and causing neurite dystrophy prior to cell death (Gallo, 2007; Maloney and Bamburg, 2007). There is further evidence that these rods may be associated with the plaques that build up in AD brains (Minamide et al., 2000).

1.4.3 Excitotoxicity as a Factor in Neurodegeneration

When nerve cells are exposed to an excessive amount of neurotransmitter they can be damaged and undergo cell death, this is known as excitotoxic stress or excitotoxicity, and is a pathology that occurs in the brain. Neurotransmitters bind their receptors allowing an influx of calcium into the cell and it is this excess of calcium ions that causes cell death (Dong et al., 2009). This was first demonstrated in HD, when injections of Kainic acid (KA) or Quinolinic acid (QA), which over-activate the N-methyl-D-aspartate (NMDA) receptors (NMDAR), resulted in an HD-like phenotype and cellular degeneration pattern in rats (Beal et al., 1986; McGeer and McGeer, 1976). Subsequently it was shown that toxicity elicited by the mitochondrial toxin, 3NP, in mice was abrogated when the mice were pre-treated with an NMDAR antagonist, thus tying together the observations of energetic deficiency and excitotoxicity and implying that mitochondrial dysfunction may lead to the abnormal activation of NMDAR (Dong et al., 2009). Excitotoxicity is also a common theme in AD and PD. In AD, an NMDAR antagonist, memantine, has been shown to reduce neuronal degeneration caused by increased levels of Aβ (Miguel-Hidalgo et al., 2002). Subsequently, in HD models, NMDAR were found to be mislocalized on synapses causing excitotoxicity and apoptosis, and memantine has been shown to have positive outcomes in the excitatory pathology and overall phenotype in HD mouse models (Milnerwood et al., 2010). Treating neurons with excess glutamate causing excitotoxic stress is one of the stressors that leads to the formation of persistent cofilin-actin rods in neurites, which results in blocked trafficking and the accumulation of Aβ and tau, the proteins involved in the formation of AD lesions (Minamide et al., 2000). Genetic PD is also linked to excitotoxicity due to the

function of the parkin protein, which regulates the stability of excitatory glutamatergic synapses. Parkin mutations, associated with some cases of familial PD, lead to enhanced synaptic efficacy and increased vulnerability to excitotoxic stress (Helton et al., 2008). As was demonstrated by the 3NP model of HD, a link between mitochondrial dysfunction and excitotoxicity also exists in PD, as the MPTP induced degeneration model of PD is also blocked by pre-treatment with NMDAR antagonists (Zuddas et al., 1992).

1.4.4 Aging, Energetics and Cell Stress Response

In neurodegenerative disease the common risk factor is aging. Aging is essentially the merciless accumulation of damaged biomolecules in the cell. These biomolecules are required for normal cellular function and their accumulation leads to senescence. The excess in damaged macromolecules is thought to be caused by hindered cellular stress response (Kirkwood and Austad, 2000). Aging interventions are hypothesized to be useful in combating neurodegeneration for this reason. The exposure of a cellular system to unfavourable conditions generally induces the heat shock response (HSR) (Morimoto, 2008). These unfavourable conditions can be physical, chemical or biological, and trigger a series of cellular events in order to re-establish cellular homeostasis. The production of Heat Shock Proteins (HSP) is induced by the Heat Shock Factor (HSF) family of transcription factors. Under stress conditions HSF1 trimerizes and translocates to the nucleus, binding Heat Shock Elements (HSE) that are present in the promoters of HSP genes (Morimoto, 2008). During aging there is an increase in the amount of HSP present in the cell in the absence of external stress, suggesting a certain level of intrinsic stress in the cell as they age (Macario and Conway de Macario, 2005). The HSR is also not as effective in aged animals (Heydari et al., 2000). It is likely that the populations of neurons affected in each disorder are exceptionally sensitive to this additional stress. There is already a reduced threshold for cell death in aged animals and cells, so an additional level of dysfunction in a cell stress

pathway caused by the neurodegenerative insult may render certain sub-populations of neurons more sensitive to stress while aging, leading to apoptosis and degeneration. Additionally, some cell stress response pathways, if over-activated, lead to apoptosis. The Endoplasmic Reticulum (ER) unfolded protein response (UPR) fails in response to persistent stress, and apoptosis is induced (Szegezdi et al., 2006). Severely damaged DNA, which cannot be repaired by traditional DNA repair pathways needs to be eliminated to prevent passing genetic errors through to subsequent cell divisions, and thus can also lead to apoptosis (Roos and Kaina, 2006).

1.4.5 Biomolecular Evidence for Impaired Energetics and Cell Stress Response in Neurodegeneration

Hallmarks of oxidative damage caused by reactive oxygen species (ROS), and increased accumulation of damaged biomolecules that normally result from aging, are present in models and tissue samples in all three neurodegenerative disorders. The footprints of increased oxidative stress in brains that have undergone neurodegeneration are present as modified macromolecules in the cell. Oxidative damage to DNA can be measured by looking at levels 8-hydroxydeoxyguanosine (OH^8dG) in nuclear DNA. In HD there is an increase of OH^8dG in DNA from the basal ganglia, but not other parts of the brain (Browne et al., 1997). An increase of OH^8dG is found in AD cerebrospinal fluid (CSF) and in PD is preferentially found in the substantia nigra (SN), the affected region of the brain in PD (Lovell et al., 1999; Zhang et al., 1999). Under oxidative conditions proteins can undergo carbonyl formation which is a modification that can lead to loss of protein function (Levine et al., 1994). Increased carbonylation has been found in multiple models of HD. Using 2D gel electrophoresis one group actually probed which proteins were subject to carbonylation in HD brains and found that most of the damaged proteins were involved in energy metabolism, protein folding and oxidative stress defense (Sorolla et al., 2008). An increased number of carbonyl modified proteins are found in AD and PD as well (Levine, 2002). The

increased carbonylation of some chaperone proteins, specifically those associated with the UPR, is noted in all aging populations (Nuss et al., 2008). It seems that these indicators of cell stress are increased in HD, AD and PD populations, supporting increased cell stress and ROS compared with a normal aging population.

1.4.6 Decreased ATP Levels in Neurodegenerative Disease

The increase in ROS leading to these modified macromolecules is indicative of mitochondrial dysfunction. Any problems associated with mitochondrial function would presumably lead to, or is indicative of, alterations of available ATP levels in the cell. As previously described, neurons are energy hungry and require high levels of ATP for normal functions. In cell extracts, from cells derived from a full length HD knock-in mouse model, there are decreased levels of ATP and a decrease in the ATP/ADP ratio which occurs early in the disease process (Gines et al., 2003). There are reports of low ATP levels in an AD neuron model in response to the presence of the AD associated protein tau (Thies and Mandelkow, 2007) and in PD patient fibroblast cell lines from patients afflicted with familial PD (Mortiboys et al., 2010). Decreased levels of ATP could presumably be responsible for many of the defects noted in neurodegeneration. For instance, a decrease in the ATP pool would lead to a decrease in production of glutathione causing an increase in oxidative stress and mitochondrial dysfunction, which would lead to apoptosis in the affected cell population. It is not difficult to see why neurons, which require so much energy, would be the first to be affected by a toxic insult causing decreases in ATP.

1.4.7 Cause and Effect of Energetic Problems in Neurodegeneration: A Case for Disease Specific Therapies

A paradigm is clearly emerging with respect to oxidative damage and neurodegenerative disease. It is clear that there is a contribution of oxidative stress, ROS and mitochondrial dysfunction to neurodegeneration, and thus correcting these

energetic failures could have implications in multiple devastating disorders. As such, anti-oxidants have been an attractive candidate for therapy, however there have been no successful clinical trials using anti-oxidants in these diseases (Delanty and Dichter, 2000). Generally increasing the expression of HSPs has also been proposed, but doing this has not been successful, likely because the presence of too many HSPs in the cell leads to inactivation of HSF which causes more damage than good long term (Labbadia et al., 2011). This leads to a cause and effect argument of energetic stress with relation to neurodegeneration and it would seem that many of these symptoms depend on the nature of the initial insult. It is becoming clear that targeting the symptoms is not proving to be effective. Perhaps parts of the pathway, such as breakdown in neuronal energy production, are being overlooked, and new ways to probe the crux of the issues in a disease specific manner needs to be investigated to discover new disease modifying therapies. The initial insult in HD is the mutated huntingtin protein, and learning more about the protein and what it does may lead to an understanding of how it could specifically cause the energetic failures characteristic of HD.

1.5 Huntingtin Structure and Cellular Localization

1.5.1 Huntingtin Structure

In studying the function of the huntingtin protein it is important to consider what we know about its structure. Full length huntingtin is thought to have a large flexible α-helical solenoid overall structure based on huntingtin being comprised of HEAT repeats almost exclusively (Andrade and Bork, 1995; Kobe and Kajava, 2000; Li et al., 2006) (Figure 1.1 A). The name HEAT comes from the original four proteins in which the repeat was detected: huntingtin, elongation factor 3 (EF3), the regulatory subunit A of protein phosphatase 2A (PP2A) and TOR1(Andrade and Bork, 1995). A single HEAT is made up of 2 hydrophobic helices forming an anti-parallel helical hairpin. These hairpins occur in tandem repeated sequences and stage to form a single solenoid or

HEAT repeat (Andrade and Bork, 1995). These tandem repeats share hydrophobicity but little sequence similarity (Kobe and Kajava, 2000). According to the amino acid sequence that makes up a HEAT repeat, huntingtin is thought to have anywhere from 40-70 HEAT repeats based on bioinformatics analysis. Solenoid proteins are generally involved in protein-protein interactions and this is likely true for huntingtin (Kobe and Kajava, 2000). This type of α-solenoid, helical structure has also been shown to have a high level of flexibility and can handle mechanical forces that occur in the cell (Grinthal et al., 2010). Because of these unique properties, proteins with this structure often act as scaffold proteins (Grinthal et al., 2010).

1.5.2 Huntingtin Structural Domains

There are some structural domains of huntingtin that have been additionally characterized. The first 17 amino acids (N17) of huntingtin arrange into an α-helix and act as a stress dependent membrane targeting sequence (Atwal et al., 2007). N17 is subject to multiple post-translational modifications, including phosphorylation (Atwal et al., 2011), acetylation (Thompson et al., 2009) and SUMOylation (Steffan et al., 2004), that affect huntingtin localization and function. We have further recently found that the N17 domain has nuclear export activity (Tamara Mauiri, Truant lab, Unpublished results). Immediately adjacent to the N17 domain is the polyglutamine tract. Following the polyglutamine tract is a polyproline rich region. This region is responsible for many of the protein-protein interactions that occur at the amino terminus of huntingtin, since proline is critical for many of these interactions (Burnett et al., 2008; Kay et al., 2000; Modregger et al., 2002). Shortly after the polyproline rich region is the nuclear localization signal (NLS) of huntingtin (Carly Desmond, Truant lab, unpublished results). The only other described domain on huntingtin is a nuclear export signal (NES) located near the carboxyl terminus of the protein (Xia et al., 2003) (Figure 1.1 A). The fact that some of the only described domains of huntingtin are import and export signals highlight the fact that huntingtin is a shuttling protein with functions in the nucleus and

cytoplasm. The remainder of the protein is made up of two large α-helical domains (comprised of HEAT repeats) that are separated by an unstructured, accessible and evolutionarily conserved hinge, confirmed by tryptic digestion and mass spectrometry (Seong et al., 2010). This structure means that purified recombinant huntingtin has, literally, hundreds of different conformations when analyzed by electron microscopy (Seong et al., 2010) (Figure 1.1 C). This supports huntingtin as being a multi-functional protein.

1.5.3 Huntingtin Cellular Localization and Protein Evolution

Huntingtin is classically a difficult protein to study due to its large size and promiscuous nature. At 350kDa it has been hard to work with using classic biochemical assays. In the cell, full length huntingtin can be found localized to the cytoplasm, nucleus (Kegel et al., 2002; Seong et al., 2010) and multiple organelles including mitochondria (Choo et al., 2004), ER, endocytic and autophagic vesicles (Atwal et al., 2007), the golgi and the plasma membrane (Strehlow et al., 2007) and most recently has been found localized at the base of primary cilia (Keryer et al., 2011) (Figure 1.1 D). Huntingtin has further been found to associate with both the actin (Angeli et al., 2010) and microtubule cytoskeleton, including being found at the mitotic spindle, cytokinetic cleavage furrow and centrosomes (Atwal et al., 2011; Godin et al., 2010). Huntingtin further has a seemingly unending list of proteins it interacts with, but also interacts with mRNA and DNA (Benn et al., 2008; Savas et al., 2010). As discussed previously, huntingtin appears to have not just one, but multiple functions in the cell, however, it lacks any catalytic activity. Huntingtin has no sequence homology to any other protein in the cell. It is evolutionarily conserved, with orthologs in most vertebrates, but is poorly conserved in drosophila and some invertebrates and completely absent in yeast and other invertebrates (Gissi et al., 2006; Li et al., 1999). This evolutionary conservation supports the important role of the huntingtin protein.

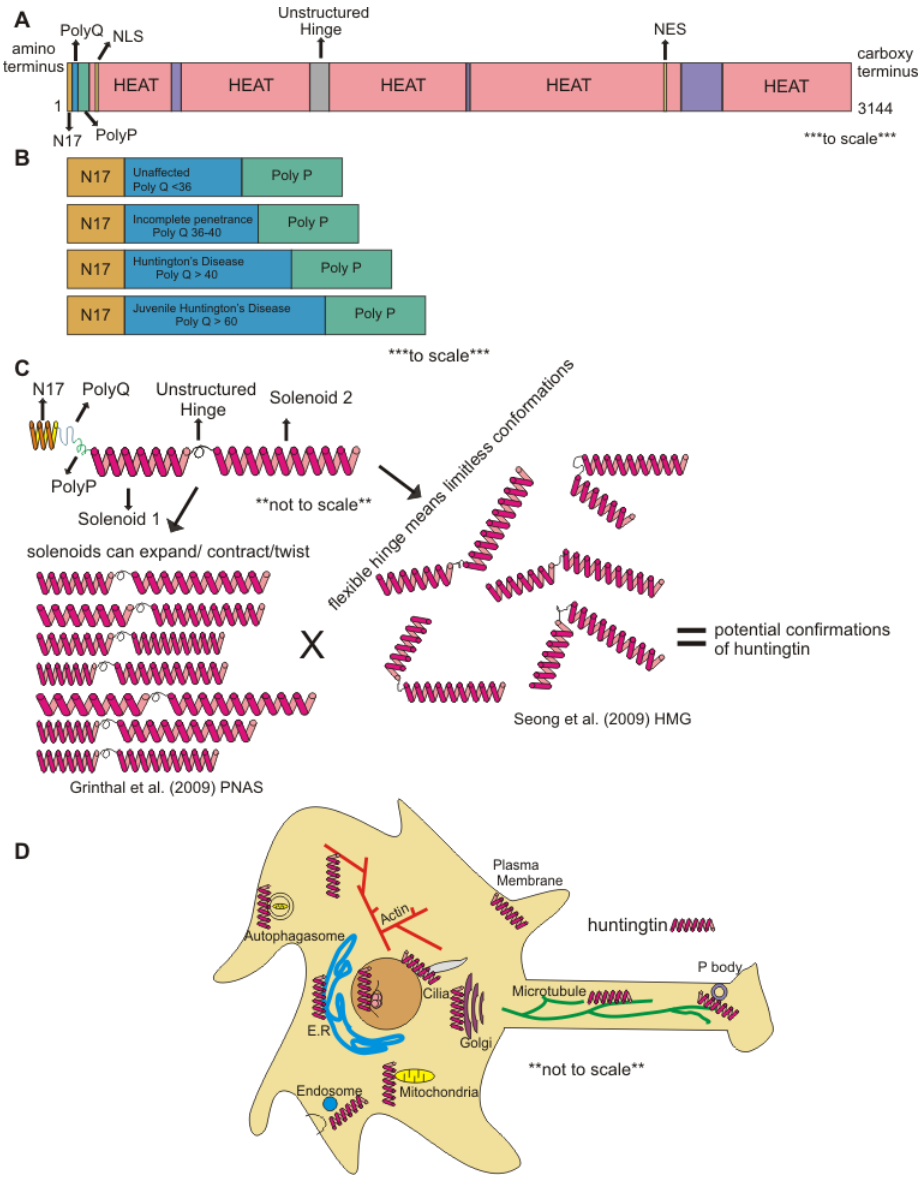

Figure 1.1

Figure 1.1: Schematic figure of the huntingtin protein, known domains, structures and cellular localization. A. Described known domains of the huntingtin protein shown to scale. **B.** Exon one of the huntingtin protein showing different polyglutamine tract lengths leading to different penetrance and disease state **C.** Huntingtin protein assumes a flexible solenoid confirmation with an unstructured hinge in the first half of the protein. **D.** Localization of huntingtin within the cell.

1.5.4 Hypothesis: Huntingtin is a scaffold protein

Huntingtin structure, protein interactions and multiple cellular and organelle localizations strongly support the hypothesis that huntingtin is acting as a scaffold protein within the cell and is a multifunctional protein involved in multiple facets of cell biology.

1.6. Huntingtin, a Protein of Many Functions

As previously described, huntingtin likely has many functions, and different functions during development versus later in adult tissue. Knowing the function of huntingtin is important and could lead towards a treatment in HD. An important question that is continually asked but still remains unanswered is if HD is caused by a gain or loss of function. It seems that there is no good answer to this question, likely because huntingtin is multi-functional, and some, many or all of huntingtin functions may be affected in a gain or loss of function manner. At first glance HD seems to be caused by a toxic gain of function of the mutant protein, as are most dominantly inherited diseases where some wildtype protein is still being expressed. Most studies to delineate huntingtin function are performed in controlled systems using overexpression or knock down of huntingtin, and these studies largely support a loss of function of wildtype huntingtin. Huntingtin has been shown to have multiple roles and contributes to different processes in the cell. Roles that have been shown to be mediated by full length huntingtin, that are supported by large bodies of literature, and that may be pathogenic will be discussed here.

1.6.1 The Role of huntingtin in Vesicular Trafficking

Membrane and macromolecular transport occurs in all eukaryotic cells, however in nerve cells with axons that are literally thousands of times longer than the cell body,

this becomes increasingly challenging due to the distance these molecules have to travel, and because components of the axon are made in the cell body and required during the entire life of the neuron. Huntingtin has an established role in vesicular transport, possibly transporting trophic factors in neuronal axons and acting as a scaffold protein in concert with Huntingtin associated protein1 (HAP1) and dynactin (Colin et al., 2008; Engelender et al., 1997). HAP1 is a protein that was found to associate with huntingtin in a polyglutamine length dependent manner, using a yeast two hybrid system, and then subsequently HAP1 was found to be associated with microtubule associated proteins dynactin and pericentriolar material-1 (PCM1), linking huntingtin to the microtubule cytoskeleton (Engelender et al., 1997). This is not surprising based on huntingtin having strong association with vesicles and multiple links to microtubules, trafficking proteins and molecular motors (Atwal et al., 2007; DiFiglia et al., 1995; Engelender et al., 1997; Godin et al., 2010; Hoffner et al., 2002; Tukamoto et al., 1997), and these associations may be the link between huntingtin and specific microtubule centers like the centrosome and mitotic spindle (Atwal et al., 2011; Godin et al., 2010). Specific post translational modifications also seem to affect huntingtin association with microtubule associated proteins and in turn affect the directionality of axonal transport. When phosphorylated at serine 421, huntingtin recruits kinesin to dynactin and anterograde transport increases, whereas lack of phosphorylation at this reside enhances retrograde transport (Colin et al., 2008). In the axon, huntingtin has been shown to be required for the trafficking of secretory vesicles moving brain derived neurotrophic factor (BDNF), which may be involved in striatal cell survival, and the disruption of this transport could lead to neurodegeneration (Colin et al., 2008; Gauthier et al., 2004). The role of huntingtin in trafficking has further extended to ciliogenesis. Huntingtin seems to be responsible for the trafficking of proteins, specifically PCM1, to the centrosome so that ciliogenesis can occur (Keryer et al., 2011). Interestingly huntingtin knockout causes a decrease in ciliogenesis, whereas mutant huntingtin causes an accumulation of PCM1 at the centrosome and thus abnormal ciliogenesis,

making it unclear if this is a gain or loss of function. One consequence of this aberrant ciliogenesis due to the presence of mutant huntingtin is irregular flow of CSF, which could contribute to or exacerbate disease processes (Keryer et al., 2011). Huntingtin has an additional transport role with respect to fast axonal trafficking in both drosophila and mammals (Gunawardena et al., 2003; Trushina et al., 2004). Live cell imaging reveals a decrease in motility of both endocytic vesicles and mitochondria, which travel by fast axonal transport within a nerve cell. *In vivo* there is a decreased uptake of a neurotracer upon administration into mouse brain, indicating a trafficking defect in the presence of mutant huntingtin. This effect is recapitulated with a decrease in wildtype huntingtin levels (Trushina et al., 2004), supporting a loss of function. Huntingtin has further shown to be involved specifically in the transport of RNA granules in the neuron to sites of local translation, this shows direct evidence of huntingtin trafficking and associates it with a neuron specific process (Savas et al., 2010). In these granules, huntingtin co-localizes with mRNA and may have the ability to down-regulate gene expression when associated with mRNA at post-transcriptional local sites of translation and gene control (Savas et al., 2010). The exact mechanism and role of huntingtin with respect to trafficking and the cytoskeleton is currently unclear, and although some evidence supports a neuronal specific role, it is likely that any effect on vesicular trafficking would be cell autonomous, but perhaps have greater effects if misregulated in neurons.

1.6.2 The Role of huntingtin in Transcription

Another established role of full length huntingtin is in transcriptional regulation. Single gene studies as well as microarray technology have shown that there are a large number of genes dysregulated in multiple HD systems from *in vitro* to actual patient samples (Cha, 2007). Although different gene expression profiles are likely expected in a diseased or sick cell versus a normal and healthy cell, there is some evidence to support an actual mechanism of transcriptional dysregulation that is attributed to direct function of the huntingtin protein and not just a consequence of a different disease process.

Huntingtin interacts with and affects the activity of transcription factors such as specificity protein 1 (Sp1), protein 53 (p53) and TBP associated Factor II130 (TAFII130). Although these interactions were originally found through yeast two hybrid, they were confirmed endogenously from human brain samples. Interaction with Sp1 was found to be enhanced in the presence of mutant huntingtin causing a decreased Sp1/TAFII130 association leading to impairment of Sp1 dependent transcription (Dunah et al., 2002). Huntingtin further binds to and affects transcriptional regulators such as repressor element 1 silencing transcription factor (REST) and CREB binding protein (CBP). The inappropriate binding of mutant huntingtin to REST inhibits the transcription of striatal neuron trophic factors, specifically BDNF. Presumably, huntingtin functions by binding and retaining REST in the cytoplasm. In the presence of the polyglutamine expansion there is decreased binding of REST, leading to an accumulation of REST in the nucleus and increased binding of REST to the promoter of BDNF inhibiting its expression (Zuccato et al., 2003). This was presumed to be a specific function of huntingtin in cortical neurons, which produce BDNF that is then trafficked to striatal neurons to act as a trophic factor, and thus decreased BDNF production in the cortex would lead to degeneration in the striatum (Zuccato et al., 2005). Recently, a conditional BDNF knockout mouse showed no change in number of striatal neurons, questioning the long standing assumption that BDNF is required for striatal neuron survival (Rauskolb et al., 2010). These studies did show a change in dendritic growth of striatal neurons (Rauskolb et al., 2010) which is a hallmark of HD in mice and humans (Ferrante et al., 1991; Milnerwood and Raymond, 2010), and thus the actual role and mechanism of BDNF depletion in HD will have to be the subject of further study. CBP has neuroprotective functions, and has dual action, acting as a transcriptional co-activator and as a histone acetyltransferase (Giralt et al., 2012). Mutant huntingtin has stronger binding to CBP than wildtype huntingtin and is thought to interfere with its acetyltransferase activity. This interaction may be responsible for some of the cognitive impairments in HD (Cong et al., 2005; Giralt et al., 2012). There is a large body of work

emerging suggesting that histone deactyltransferase (HDAC) inhibitors could provide potential therapy for HD, since it seems that mutant huntingtin binding histone modifiers such as HATs would change the histone modification landscape and this may lead to disease (Chuang et al., 2009; Giralt et al., 2012). It is of note that none of these inhibitors or other therapeutics affecting transcription have been successful in making it to clinical trials in HD to date. Although a lot of work is currently going into unveiling any potential mechanism huntingtin may have with respect to transcriptional regulation, it is hard to parse out which transcriptional changes are caused directly by the presence of mutant huntingtin and which are a secondary effect of what is going wrong in HD. New huntingtin functions with respect to transcriptional regulation are continuously being discovered. For instance, huntingtin itself has been found at promoters of genes *in vivo*. By performing Chromatin Immunoprecipitation (ChIP), and ChIP on chip, it has been shown that huntingtin directly interacts with DNA and is present at different promoters based on whether it has a wildtype or mutant polyglutamine tract (Benn et al., 2008). Huntingtin has also recently been found to be associated with the polycomb repressive complex 2 (PRC2) an epigenetic silencer (Seong et al., 2010). Huntingtin binds members of this complex and there is impaired PRC2 mediated gene silencing in response to loss of huntingtin in embryos (Seong et al., 2010). Therefore huntingtin may be affecting transcription both indirectly, by inappropriately binding and affecting the activity of transcription factors, transcription regulators and histone modifiers, or may have a direct role in the nucleus at DNA and chromatin.

1.6.3 The Role of Huntingtin in Cell Survival

Wildtype huntingtin has a role in promoting cell survival. Over-expressing wildtype huntingtin is protective to cells when challenged with stress. When either mutant full length or wildtype full length huntingtin is stably expressed in cultured ST14 cells, there is no obvious effect on cell health under normal growth conditions, however when challenged with temperature stress, serum starvation or mitochondrial toxins that

induce apoptosis, cells over-expressing wildtype full length huntingtin are more viable (Rigamonti et al., 2000). Interestingly, short amino terminal fragments of mutant huntingtin (ie. Amino acids 1-548) confer additional toxic properties leading to increased apoptosis when challenged with stress compared to control cells and mutant huntingtin is therefore thought to have a pro-apoptotic function. However, this increase in apoptosis is not noted when the polyglutamine expansion occurs in the context of full length huntingtin in this model (Rigamonti et al., 2000). Further evidence to support the induced toxic properties of over-expressing mutant huntingtin has been shown in primary neurons taken from a full length HD mouse model. Primary neurons from mice expressing a yeast artificial chromosome (YAC) carrying mutant huntingtin (Q72) are more sensitive to sub-lethal glutamate exposure (Leavitt et al., 2006). Over-expressing huntingtin in the same system (YAC with wildtype huntingtin – Q18) will then rescue these cultured neurons from lethal doses of NMDA which normally induces apoptosis through excitotoxic mechanisms (Leavitt et al., 2006). The anti-apoptotic properties of full length wildtype huntingtin are recapitulated *in vivo.* YAC mice expressing full length wildtype huntingtin (Q18), essentially overexpressing huntingtin, suffer less ischemic tissue injury following traumatic brain insults, indicating that wildtype huntingtin is protective *in vivo* (Zhang et al., 2003). This result was additionally reproduced in a model of excitotoxic stress. Excitotoxic stress is thought to be a contributing factor to HD pathogenesis, and intrastriatal injections of QA into normal mice causes excitotoxicy leading to neuronal degeneration that mimics HD (Beal et al., 1986). When QA is injected into mice over-expressing wildtype huntingtin (YAC Q18) the detrimental effects of QA are diminished (Leavitt et al., 2006). Additional confirmation of this protective effect of huntingtin comes from a corollary experiment using a conditional *in vivo* huntingtin knockout. Cre/*loxp* site-specific recombination was used to remove huntingtin from postnatal neurons in mice. This led to progressive neuronal degeneration and motor phenotypes, indicating that huntingtin is required for neuronal survival and that a loss of function may indeed contribute to pathogenesis by a loss of

the anti-apoptotic function of huntingtin (Dragatsis et al., 2000). This data indicates that over-expression of full length mutant huntingtin may render cells more sensitive to cell death through certain mechanisms, while confirming that full length huntingtin is protective. Indeed, this protective effect seems to be recapitulated in all models. This data indicates that huntingtin dosage is of key importance to cell survival and supports the premise of an anti-apoptotic property of wild type huntingtin, specifically under conditions of cell stress.

1.6.4 Hypothesis: Huntingtin is a Multi-Functional Protein that can Rescue Cells from Stress

The hypothesis that huntingtin is a multifunctional protein, acting as a scaffold for protein-protein interactions and different cellular functions, is supported by huntingtin known functions to date. Huntingtin has shown to function via the cytoskeleton in vesicle trafficking and gene regulation in the cytoplasm, binding multiple proteins including transcription factors, as well as binding many cellular organelles and structures such as RNA granules. Huntingtin is also found in the nucleus at DNA, binding nuclear proteins and affecting epigenetic complexes that regulate the nature of chromatin. The anti-apoptotic functions of huntingtin suggests that huntingtin is essential during stress and that its function during stress may be the central node that leads to cell specific degeneration and bioenergetics failure in HD.

1.7 Current Therapeutic Efforts in Huntington's Disease Research

1.7.1 Huntington's Disease: Treating the Symptoms

To date there has been little success in HD clinical trials. The aim of most clinical trials is just to treat the symptomology, yet still, there are few drugs with proven benefit available to help patients manage their symptoms. Tetrabenazine is the only FDA approved drug for the treatment of HD symptoms, and has some benefit in reducing

chorea, however it has several side effects, including increased depression, which is a major risk factor for HD patients (Paleacu, 2007). Currently undergoing clinical trials is pridopidine (huntexil), a dopaminergic stabiliser that is hypothesized to improve voluntary motor function (Feigin, 2011). Although the drug was well tolerated and highly touted, it has had little significant beneficial effects when brought to clinical trial (de Yebenes et al., 2011). Many standard antidepressants and mood stabilizers are prescribed for the psychiatric symptoms in HD, and there are some neuroleptic drugs, such as haloperidol, risperidone and olanzapine that have some benefits for both the movement and psychiatric symptoms, however, again with many unpleasant side effects (Bonelli et al., 2002; Dallocchio et al., 1999; Gimenez-Roldan and Mateo, 1989; Killoran and Biglan, 2012). The need for drugs that treat the symptoms of HD is great, but even more so is the need for disease modifying therapies.

1.7.2 Failed Clinical Trials

Based on the energetic deficiencies present in HD, a few clinical trials using anti-oxidants or drugs with anti-oxidant properties have been performed, but all have failed. Minocycline, a tetracycline antibiotic with anti-oxidant and neuroprotective effects was recently proven to be ineffective in HD after a large phase 3 clinical trial (Huntington-Study-Group, 2010; Kraus et al., 2005). Creatine, which is normally involved in maintaining cellular ATP levels and preventing ROS productions, has modest beneficial effects in HD models (Matthews et al., 1998). When taken to clinical trial for HD, creatine was largely found to be ineffective (Tabrizi et al., 2005). Coenzyme Q10 (CoQ10), another powerful antioxidant that acts as a cofactor of the electron transport chain in the mitochondrial membrane - accepting electrons and promoting ATP generation, has also been trialed in HD models and clinic (Turunen et al., 2004). In HD models CoQ10 had mixed results; initially showing benefit in some outcomes including motor impairment and survival in an HD mouse model (Smith et al., 2006). However, more recent data indicates that these results could not be reproduced, and although

CoQ10 went to clinical trial for HD, it failed there as well and likely will not be further pursued as a therapeutic agent (Huntington-Study-Group, 2001; Menalled et al., 2010).

1.7.3 A Need for Biomarkers

A large reason for the lack of clinical trials and potentially for the failed clinical trials is the lack of effective biomarkers available to track HD progression. The readout for most studies is an archaic method of assessing changes in patient movement disorder, moods and cognitive abilities over a six month to one year period. In a slowly progressing disease that presents with great variability it is almost impossible to get a meaningful outcome using these measures. As previously mentioned, HD can be genetically tested for long before clinical diagnosis based on an individual's gene status, and therefore HD is a great candidate for pre-symptomatic treatment. Treatment in this time period will likely yield the best results for disease outcome, however there needs to be ways to monitor the therapeutic effect of drugs on a patient prior to symptom onset. Ideal biomarkers are consistent between human and animal models, and can be easily traced using a renewable and easily obtainable biological sample. There are two main biomarker study attempts currently being used in HD research. Brain imaging is coming to the forefront as a potential biomarker for HD. Large cohorts are showing early changes in the brain that can be mapped with MRI, and these changes are clearly occurring in prodromal HD patients (Delmaire et al., 2012; Dumas et al., 2012; Tabrizi et al., 2012). These outcome measures include morphological changes in whole-brain, grey-matter, white-matter, and striatal atrophy that can be used to track disease progression and potentially be used as biomarkers for disease modifying treatment in the prodromal population (Tabrizi et al., 2012). Current work is going into performing MRI studies in rodent models of HD to see if these brain changes are recapitulated and to determine if disease modifying therapies can first be tested in these mouse models using similar outcome measurements (Cheng et al., 2011). Although the feasibility of using MRI to track disease progression is not overly restrictive, using readouts from

blood samples is the ideal biomarker. Blood is renewable and easily obtained in any laboratory. Also, the infrastructure for its analysis is available everywhere, and blood is easy to analyze in most model organisms. In human blood, a study was performed looking in an unbiased manner at the proteomic blood plasma profile, and many of the up-regulated proteins were directly linked to the innate immune response. Inflammatory cytokines, including interleukin (IL) 6, IL8 and tumor necrosis factor-α (TNF-α) are all elevated in plasma, track with disease progression, and are initially up-regulated in prodromal patients (Bjorkqvist et al., 2008). Inflammation seems to be linked to neurodegeneration, although it is not clear if this is cause or effect, but regardless, there are hallmarks of inflammation in both the brain and periphery in HD patients (Bjorkqvist et al., 2008; Dalrymple et al., 2007; Silvestroni et al., 2009; Wild et al., 2008). Some of these changes are further recapitulated in HD mouse modes, including increased IL6 levels in serum, as measured by ELISA (Dalrymple et al., 2007). Although these markers are of interest, an inflammatory response can go along with general illness and vary on a day to day basis. Therefore, validation and further work is needed before these cytokine and chemokine levels can be used as biomarkers. It is likely that there is no single biomarker that will suffice and a panel of imaging and wet biomarkers will increase the number of clinical trials possible in pro-dromal HD. As more functions of huntingtin are discovered there will be more pathways and markers available to probe in blood samples, in hopes of making this panel a reality.

1.7.4 Treating Huntington's Disease: The Future

Although it has been almost 20 years since the discovery of the *HTT* gene there has been no success in finding drugs that reverse or alter disease progression. This is not to say that great strides are not being made in understanding the disease. In understanding the normal functions of the huntingtin protein we are able to find better targets that may lead to treatment. There are currently two major efforts going into the treatment of HD. The only validated target for HD is the huntingtin protein itself, which

is known to be disease causing. Based on this, there is a lot of research and promise in *in vivo* huntingtin lowering strategies. However, there are major risks and hurdles associated with protein knockdown in humans, and as such, a second large effort and body of work is going into defining targetable pathways that will be amenable to small molecule drug discovery for the treatment of HD.

1.7.4.1 Huntingtin Lowering Strategies

There is a large school of thought that supports the huntingtin protein as the best target for HD. A lot of work is currently looking into the tolerability, safety and effectiveness of decreasing huntingtin protein levels *in vivo*. The two main methods being investigated are RNA interference (RNAi) and antisense oligonucleotides (ASO). RNAi using short hairpin RNA (shRNA) was the initial method of choice and was used in the pilot studies in this area. In transgenic HD mice, Adeno-associated Virus (AAV) was used to deliver the hairpin constructs directly into the brain, with some successful outcomes (Harper et al., 2005). However these pilot studies used shRNA targeted against a mutant human transgene and did not give indication to outcomes on silencing endogenous huntingtin. shRNAs have subsequently been shown to have off target effects and overwhelm the endogenous RNAi machinery causing toxicity in a whole organism, and using artificial miRNA and small interfering RNA (siRNA) has proven to be the safer approach (Boudreau et al., 2008). The follow-up experiments have also tested sequences targeted against the mutant human transgene alongside endogenous huntingtin using miRNA. These studies suggest that some level of endogenous wildtype huntingtin knockdown may be tolerated (Boudreau et al., 2009). This non-allele specific silencing of huntingtin is curious since wildtype huntingtin knockdown generally has toxic effects in cell models (Dragatsis et al., 2000). Some studies do suggest that reduced levels of huntingtin may be tolerated in a whole organism, and as such non-allele specific silencing of huntingtin is being pursued (White et al., 1997). To this end, the therapy has been brought into non-human primates, and forty-five percent

huntingtin reduction has been achieved by direct injection of miRNA into the brain. Observation for 6 weeks after surgery indicates that this is a safe approach up to this time point in primates and the reduced level of huntingtin shows no overt negative effects (McBride et al., 2011). Determining the long term effects, in humans, of knocking down an evolutionarily conserved protein with as many functions as huntingtin is going to be hard to justify from a safety perspective in clinical trials. As such the inimitable approach for huntingtin knockdown would be an allele specific method that would selectively knockdown the mutant huntingtin allele while leaving the expression of the wildtype allele unaltered. To accomplish this goal, different methods to identify single nucleotide polymorphisms (SNP) that are associated with the disease allele have been employed. Reports indicate that a panel of just five siRNAs targeted against different SNP sites could potentially treat up to seventy-five percent of HD patients if the siRNAs are potent, selective and safe, making clinical trials a possibility (Pfister et al., 2009). ASOs can be used to silence gene expression post-transcriptionally and are additionally beneficial because they are easy to modify. ASOs have been used to target both the expanded CAG tract and SNPs associated with the huntingtin allele to achieve some allele specific silencing (Carroll et al., 2011; Gagnon et al., 2010). Although there is a fair amount of promise with these techniques it is going to be a long road to finding successful, safe and feasible methods to deliver these compounds directly to the brain, assess the toxicity long term in humans, and determine if silencing huntingtin alone in the brain will be sufficient for treating HD, as huntingtin has many peripheral effects outside of the brain. Additionally, since much data indicates a loss of function component to the disease, knocking out the disease allele alone may not fully ameliorate disease processes.

1.7.4.2 Drug Discovery for Huntington's Disease

An ideal method for slowing or stopping the course of disease would be through the use of small molecules that could be administered and are effective systemically.

Towards this goal, pathways that mutant huntingtin specifically effects, and that lead to HD pathology need to be discovered so small molecule screens can be performed in search of compounds that reverse toxic effects of the mutant protein. Compounds of interest will likely require manipulation to be made blood-brain permeable. Although we know some general functions of the huntingtin protein: vesicular trafficking (Colin et al., 2008; DiFiglia et al., 1995; Engelender et al., 1997; Trushina et al., 2004), transcriptional regulation (Benn et al., 2008; Cha, 2007; Seong et al., 2010; Zuccato et al., 2003), and bioenergetics and cell survival (Dragatsis et al., 2000; Rigamonti et al., 2000; Zhang et al., 2003), we need to find what parts of these pathways are specifically affected to assess if they are realistically druggable targets.

1.7.4.2.1 Screening

A powerful method for the discovery of bioactives that modify disease is the utilization of high throughput and high content screening (HTS and HCS). HD research is quickly employing these powerful techniques and there are numerous reports of screens to discover molecules that will affect HD pathology. One problem with performing screening in HD currently is the lack of good read-out assays. Historically, *in vitro* protein aggregation assays were the readout of choice. Protein aggregates are found in the brains of HD patients and in the brains of individuals with many other neurodegenerative disorders (Scherzinger et al., 1997). Therefore it is hypothesized that inhibiting this aggregation could be therapeutic, however there are numerous studies that suggest these aggregates are in fact protective and therefore breaking them up would be toxic. Aggregates occur in most regions of the brain, not just the affected areas that undergo degeneration (Gutekunst et al., 1999), and in cell based assays, cells that form aggregates actually survive better in the presence of the toxic protein insult (Arrasate et al., 2004; Saudou et al., 1998). This debate has been reviewed at length (Ross and Poirier, 2005); never-the-less there are numerous reports of screens performed both *in vitro* and *in vivo* attempting to define molecules that inhibit

aggregation. In addition, since the purification of full length huntingtin is difficult and in cell based models the expression of full length huntingtin does not generally cause aggregate formation, aggregation screens tend to only look at systems with the over-expression of amino terminal fragments of the huntingtin protein; thus an incredibly artificial system (Heiser et al., 2002; Pollitt et al., 2003). Notably some of the compounds identified from these *in vitro* screens caused a decrease of aggregation *in vivo* in a full length mutant huntingtin transgenic mouse model, giving some validity to the approach (Wang et al., 2005a), although none of the targets obtained from these screens were successful at changing other phenotypes *in vivo* and are not being used in humans. Since a hallmark of neurodegeneration is inappropriate cell death in neurons, cell death is an attractive assay for compound screening. Cell death assays generally suffer the same problems as *in vitro* and aggregation assays. Since expressing full length huntingtin is difficult, these assays largely rely on massive over-expression of mutant huntingtin fragments, which induces cell death in different cell types. Multiple screens have been performed in the well characterized PC12 cell line, which undergoes cell death within 48-72 hours of overexpression of mutant huntingtin fragments. Multiple screens in these cell lines, performed in a similar manner with the same readout of Lactate Dehydrogenase as an indicator of cell death, had disparaging results and unfortunately did not find overlapping compounds as mediators of cell death (Aiken et al., 2004; Wang et al., 2005b). An additional screen has been performed in immortalized ST14A striatal neurons, overexpressing a longer, yet still amino terminal fragment of mutant huntingtin. This screen identified compounds that could rescue cell death based on a tryptan blue exclusion assay, and some of the hits were confirmed in brain slice models and *c. elegans* models, but all the follow up assays, again, were examining toxicity based on fragments of the huntingtin protein (Varma et al., 2007). Additionally, the compounds identified did not have known mechanism. More *in vivo* assays seem to be the future of HTS screening in HD. Brain slice cultures are being exploited as a nice cell based model that maintains the interplay of multiple cell types,

which is thought to be pertinent in HD. One group performed screening on brain slice cultures from rats, again over-expressing amino terminal mutant huntingtin fragments, and used number of healthy primary neurons as a read out (Reinhart et al., 2011). This screen had a narrower range of targets, and only used a small 74 compound library with drugs that act on cell death and inflammatory pathways, and thus picked out potential compounds that specifically affect these pathway in a somewhat biased manner (Reinhart et al., 2011).

It is difficult to perform screens in higher order *in vivo* models, like mice, however other model organisms like drosophila are more amenable to screening procedures. Although it is debatable if drosophila carry their own huntingtin gene (Li et al., 1999), drosophila do have some obvious phenotypes in the presence of recombinant human mutant huntingtin fragments, including aggregation of the protein, increased neuronal cell death and defective axonal trafficking (Schulte et al., 2011). This system is amenable to HTS and was used for RNAi and small molecule screening on primary neuron cultures obtained from this model, assaying aggregation and cell morphology (Schulte et al., 2011). This screen revealed interesting pathways and some new compounds that affect HD outcome. *lkb1*, an upstream kinase regulator of the mTOR/insulin pathways which have some implications in HD, was shown by RNAi knockdown to be a genetic modifier of toxicity in this system. However knocking out this protein has been found to induce hyperplasia and silencing this protein is not a viable target. Additional compounds with unknown mechanism were detected, however some did have roles in pathways known to affect HD, for instance DNA damage pathways, and thus may be worth pursuing (Schulte et al., 2011).

1.7.4.2.2 Hypothesis Driven Small Molecule Drug Discovery

It is clear from the screening data to date in the HD field that there are a lot of options available for performing these screens but it seems clear that we require more

meaningful readouts in order to find compounds that may be clinically relevant. Cell death as a readout is probably too broad, and aggregation is likely inappropriate. Therefore there is a need for more elegant and disease specific read outs and assays, likely pertaining directly to known huntingtin function. An ideal screen would look at a proposed function of full length huntingtin being driven off an endogenous promoter, with a novel assay that looks at a particular function that is negatively affected by the presence of mutant huntingtin, in a system that is amenable to performing screening on thousands of compounds. Therefore we currently need a more direct approach for drug discovery in HD. One way to go about this is by finding specific pathways that are affected by mutant huntingtin, through screening or hypothesis driven work, and finding small molecule agonists and antagonists against these pathways.

1.7.4.2.2.1 KMO Inhibition

An effective way to tackle this is by looking at genetic modifiers in model organisms, similar to the screen performed in Drosophila (Schulte et al., 2011). One group used yeast overexpressing fragments of mutant huntingtin in hopes of finding genetic modifiers of disease that indicate pathways that can be used for targeted drug discovery (Giorgini et al., 2005). Most of the genes that suppressed huntingtin toxicity in this screen were validated as genes involved in known mechanisms of disease, including transcriptional regulation, autophagy and vesicular transport (Giorgini et al., 2005). But the most potent suppressor of mutant huntingtin induced toxicity, was a gene encoding Bna4 (kynurenine 3-monooxygenase, KMO). KMO is a mitochondrial enzyme known to be activated in individuals with HD and the kynurenine pathway metabolite, QA, is elevated in early stage HD brains, likely due to the inflammatory response (Guidetti et al., 2000; Schwarcz, 2004), thus making KMO inhibition an interesting target. KMO inhibitors have had some efficacy in yeast and drosophila models of HD (Giorgini et al., 2005; Zhang et al., 2005). These KMO inhibitors were somewhat metabolically unstable so some groups have created more bioavailable

versions of the inhibitors which have increased their efficacy. These modified inhibitors do not cross the blood brain barrier, yet they are still showing effects in murine models of neurodegeneration indicating a non-cell autonomous mechanism and warranting further study (Zwilling et al., 2011).

1.7.4.2.2.2 Tissue Transglutaminase Inhibitors

Transglutaminases are a family of enzymes involved in many facets of cell biology by modifying proteins, either through the crosslinking of glutamine and lysine or attaching polyamine to, or deamidating, glutamine (Folk, 1983). Tissue Transglutaminase (tTG or TG2) is abundantly expressed in the human brain and unregulated TG2 activity has been linked to most neurodegenerative disorders (Jeitner et al., 2009; Muma, 2007), cancer (Herman et al., 2006) and celiac disease (Caputo et al., 2009). Although increased TG2 activity was initially hypothesized to be involved in the crosslinking of disease specific proteins in neurodegenerative disease leading to inclusions that were thought to be pathological, the role of TG2 in neurodegeneration seems to be more complicated. TG2 knockout mice indicate that TG2 has a role in mitochondrial energy production, which could be a link between all the related disorders that suffer energetic deficiencies (Mastroberardino et al., 2006). In HD models and patient samples there is an increase of TG2 levels and activity with unknown downstream pathological mechanisms (Bailey and Johnson, 2005; Caputo et al., 2009; Cariello et al., 1996). TG2 is unique from other transglutaminases in that it has activity outside of its crosslinking abilities in that is has GTPase activity (Monsonego et al., 1998). TG2 undergoes large conformational changes depending on whether it has GTPase activity or crosslinking activity in the presence of excessive levels of calcium. It is hypothesized that TG2 activity is causing some pathology in HD and therefore to test this we need specific TG2 inhibitors, which leave the other transglutaminases unaffected. There is a lot of research going into finding specific TG2 inhibitors. It is an interesting target because specific TG2 inhibitors will give insight into disease

mechanism as well as be useful for many disorders. Many groups have put substantial effort into finding and producing specific inhibitors using HTS and medicinal chemistry to improve compounds of interest, although some have limited specificity, no appropriate and specific inhibitors have been found to date (Prime et al., 2012).

1.7.4.2.2.3 Huntingtin N17 Kinase Inhibitors

Huntingtin is known to be subjected to many post translational modifications that affect its localization and function, specifically modifications to the first 17 amino acids (Atwal et al., 2011; Atwal et al., 2007; Steffan et al., 2004; Thompson et al., 2009). Our group initially found that the amino terminal 17 amino acids of huntingtin (N17) function as a membrane targeting sequence, and huntingtin, while normally localized to the ER and other membranous structures, comes off the ER and enters the nucleus during stress (Atwal et al., 2007). We subsequently hypothesized that some of the post translational modification at N17 may be responsible for this change in localization and that this may be mis-regulated in HD (Atwal et al., 2011). Mouse model experiments show that phosphomimicry of serines 13 and 16 in full length mutant huntingtin at N17 in a bacterial artificial choromosome (BAC) mouse model of HD results in a normal phenotype free of HD symptoms, indicating that modulating the phosphorylation state of N17 is a real therapeutic target (Gu et al., 2009). We found that the reversible phosphorylation at the two conserved serine residues in N17 affected the localization of huntingtin, both in the nuclear and at sub-nuclear compartments, in a polyglutamine dependent manner (Atwal et al., 2011). We then performed HCS on kinase inhibitors in live cells, using N17 localization as a readout and found specific kinase inhibitors that affected the localization of huntingtin, both drugs that increase and decrease N17 phosphorylation, and subsequently the toxicity of the mutant protein (Atwal et al., 2011). Following this work, GM1, a ganglioside involved in cell signaling with pivotal roles in neurotransmission (Posse de Chaves and Sipione, 2010), was found to be decreased in HD models and patients (Maglione et al., 2010). Based on this, the direct

injection of GM1, in order to restore GM1 levels, was hypothesized to be a potential therapeutic for HD. The administration of GM1 into the full length mutant huntingtin YAC model of HD restored normal behaviour and reduced pathology (Di Pardo et al., 2012). Of interest, GM1 triggered the phosphorylation of the N17 domain of huntingtin which may be part of the mechanism of the rescue when GM1 is administered, and confirms that the phosphorylation state and localization of N17 can be used as a new readout and assay for screening drugs for HD; the GM1 therapy is now en route to clinical trial (Atwal et al., 2011; Di Pardo et al., 2012).

1.8 Thesis Outline and Study Rationale

It is clear that there is a strong need for disease modifying therapies for neurodegenerative disorders as currently none exist. Although there are a lot of commonalities between neurodegenerative disorders, evidence suggests that we need to tackle therapeutics on a case-by-case basis, so to speak, as general therapies that help modify the common symptoms have been largely ineffective (Huntington-Study-Group, 2001). We need to understand the molecular mechanisms underlying the initial disease process and find the earliest points in the dysfunctional pathways that we can target. For HD, we are at an advantage since we know the disease is caused by a single mutation in the huntingtin protein. If we can ascertain the normal function of the huntingtin protein we will have a much better idea of what pathways to probe, to find what is going wrong to cause disease, and then try to find ways to modify these pathways. Unfortunately it has become clear that huntingtin likely has many functions in the cell, and affects many different pathways. It has now become important to parse out which of these pathways are most critical to disease.

Based on huntingtin having known functions with respect to cell survival during stress (Dragatsis et al., 2000; Leavitt et al., 2006), its localization changes from ER to nucleus during stress (Atwal et al., 2007), and the overwhelming evidence for

bioenergetics failure, excitotoxicity and stress response failure linked to neurodegeneration (Browne et al., 1999; Grunewald and Beal, 1999), we hypothesized that huntingtin has a functional role during cell stress. We hypothesize that this role likely occurs in the nucleus, and a dysfunction in cell stress response would contribute to the pathogenic process. We aimed to test our hypothesis by looking at the function of full length endogenous protein expressed at normal levels, under different stress conditions. We aimed to find pathways huntingtin is involved with during stress and determine if and how these pathways are altered in the presence of the polyglutamine expanded mutant huntingtin. Chapter 2 of this thesis describes a new stress pathway – the nuclear cofilin-actin rod stress response, which the huntingtin protein is involved in. We show that this pathway is disrupted in the presence of mutant huntingtin, and probe potential mechanisms causing this dysfunction, including aberrant crosslinking activity of TG2 at these cofilin-actin rods. From this work we further hypothesize that the cofilin-actin rod stress response may be a pathway that is amenable to small molecule drug discovery in HD. Chapter 3 describes domains in the cofilin protein which may lead to therapeutic targets for altering the cofilin-actin rod stress response, mainly a stress dependent nuclear import and export signal, and aims to delineate the requirement of the cofilin-actin rod stress response in hopes of determining if this pathway will be susceptible to manipulation in drug discovery efforts.

Chapter 2: Defining the role of huntingtin in the cell stress response

Preamble

The material presented in this chapter is a representation of the following publication with permission to reprint.

Munsie, L., Caron, N., Atwal, R. S., Marsden, I., Wild, E. J., Bamburg, J. R., Tabrizi, S. J. and Truant, R. (2011). Mutant huntingtin causes defective actin remodeling during stress: defining a new role for transglutaminase 2 in neurodegenerative disease. *Hum Mol Genet* **20**, 1937-51.

The only changes made were for thesis formatting and continuity purposes and copy editing.

LM wrote the manuscript and performed all experiments and data analysis except the experiments listed below.

NC performed the TG2 FLIM-FRET and analysis and contributed to writing the results section and materials and methods for this section

RSA assisted in heat shock live cell imaging experiments

IM cultured and performed immunofluorescence on the primary neurons

EJW performed the gradient density centrifugation-separated pellets from human blood and provided these samples

Mutant Huntingtin Causes Defective Actin Remodeling During Stress: Defining a New Role for Transglutaminase 2 in Neurodegenerative Disease

Lise Munsie[1], Nicholas Caron[1], Randy Singh Atwal[1], Ian Marsden[2], Edward J. Wild[3], James R. Bamburg[2], Sarah J. Tabrizi[3] and Ray Truant[1*]

[1]Department of Biochemistry and Biomedical Sciences, McMaster University, 1200 Main Street West, Hamilton, Ontario, Canada, L8N3Z5

[2]Department of Biochemistry and Molecular Biology, Colorado State University, Fort Collins, CO 80523-1870

[3]Department of Neurodegenerative Disease, UCL Institute of Neurology, National Hospital for Neurology and Neurosurgery, Queen Square, London WC1N 1NG, UK

*corresponding author, truantr@mcmaster.ca

2.1 Abstract

Huntington's disease is caused by an expanded CAG tract in the *IT15* gene encoding the 350 kDa huntingtin protein. Cellular stresses can trigger the release of huntingtin from the endoplasmic reticulum, allowing huntingtin nuclear entry. Here, we show that endogenous, full-length huntingtin localizes to nuclear cofilin-actin rods during stress and is required for the proper stress response involving actin remodeling. Mutant huntingtin induces a dominant, persistent nuclear rod phenotype similar to that described in Alzheimer's disease for cytoplasmic cofilin-actin rods. Using live cell temporal studies, we show that this stress response is similarly impaired when mutant huntingtin is present, or when normal huntingtin levels are reduced. In clinical lymphocyte samples from HD patients, we have quantitatively detected cross-linked complexes of actin and cofilin with complex formation varying in correlation with disease progression. By live cell FLIM-FRET studies and western blot assays, we quantitatively observed that stress-activated tissue transglutaminase 2 (TG2) is responsible for the actin-cofilin covalent cross-linking observed in HD. These data support a direct role for huntingtin in nuclear actin re-organization, and describes a new pathogenic mechanism for aberrant TG2 enzymatic activity in neurodegenerative diseases.

2.2 Introduction

In 1993, an expanded CAG tract in the *IT15* gene encoding the polyglutamine-expanded huntingtin protein was found to be the cause of Huntington's disease (HD): a progressive, neurodegenerative disorder with typical late-age onset affecting as many as 1 in 4000 individuals (Rawlins, 2010; The-Huntington's-Disease-Research-Collaborative-Group, 1993). This 350 kDa protein contains little homology to other known proteins, but does share a repetitive peptide structure termed HEAT-repeats, found in many large scaffolding proteins (Andrade et al., 2001). HEATs are seen to allosterically regulate the shape of proteins and allow multiple conformations and protein-protein interactions controlled by elastic and tensor forces, mediated by tethers to cell structural components or organelles (Grinthal et al., 2010). Normal huntingtin functions have been described in transcriptional regulation (Zuccato et al., 2001), epigenetic control (Benn et al., 2008; Seong et al., 2010), vesicle trafficking (Gauthier et al., 2004), endoplasmic reticulum (ER)-stress response (Atwal et al., 2007) and neurogenesis during development (Godin et al., 2010). Previously, we defined the amino-terminal 17 amino acids of huntingtin as a critical ER tether that mediates its release from the ER upon stress (Atwal et al., 2007). This 17-amino-acid signal in huntingtin, or N17, is a modulator of mutant huntingtin toxicity in many systems (Atwal et al., 2007; Rockabrand et al., 2007) and the target of post-translational modifications (Aiken et al., 2009; Gu et al., 2009; Steffan et al., 2004). This signal is also found in all mouse models of HD, and is protective to the effects of polyglutamine expansion if phospho-mimicked at serines 13 and 16 in the bacterial artificial chromosome (BAC) HD mouse model (Gu et al., 2009). From this work, we focused our cell biological studies on the effects of stress on the localization of normal, full-length, huntingtin protein that is endogenous to mouse striatal-derived cells (Trettel et al., 2000), without any over-expression of huntingtin fragments. Our goal was to observe normal huntingtin cell biology under

transient stresses, similar to those types of stresses associated with normal human aging.

Heat shock stress recapitulates a strong transient stress event that causes a global unfolding of proteins, or proteotoxic stress, a temporary drop in adenosine triphosphate (ATP) levels and spike in calcium signaling via the ER without having to use small molecules (Drummond et al., 1986; Morimoto, 2008). The heat shock stress response is well characterized, leading to the transient activation of several chaperones, transcription factors and components of the unfolded protein response (UPR) at the ER (Schroder and Kaufman, 2005). Some of these responses involve classic transcriptional activation, but other responses are at the post-translational level only, to rapidly respond to a potentially toxic cell stress event. The cell stress response has been of intense interest to the neurodegeneration community. Neuronal cells have a decreased ability to deal with oxidative and cellular stress during the aging process which has been tightly linked to neurodegeneration in HD, Alzheimer's disease (AD), and Parkinson's disease (PD) (Gibson et al., 2010; Hosoi and Ozawa, 2010; Keller, 2006). Upon induction of heat shock stress, we observed the nuclear localization of endogenous huntingtin, similar to previous studies using cold shock or UPR stresses with huntingtin fragments containing N17 (Atwal et al., 2007). However, we also observed the localization of huntingtin within the nucleus to numerous straight rod-like structures of 3-5 μm, which disappeared upon the relief of stress. Similar structures were reported as rods of cofilin and super-twisted F-actin in neurites, observed in models of AD (Maloney and Bamburg, 2007; Minamide et al., 2000). In the nucleus, during the heat shock response, cofilin, an actin binding protein normally required for actin treadmilling, saturates actin causing bundles of actin filaments. These bundles are referred to as 'cofilin rods' (Bamburg and Wiggan, 2002). Cofilin rods can form in the cytoplasm during certain cell stresses and stop a proportion of actin from treadmilling. This liberates ATP normally involved in this process so it can be used elsewhere in the cell during stress (Bernstein et al., 2006).

We observed a dominant loss of function of the ability of full length mutant huntingtin to respond to and recover from stress through the cofilin-actin pathway.

In order to determine the relevance of these observations to HD, we performed western blot analysis of cofilin on the lymphocytes of HD patient blood samples. Patients ranged from premanifest through the four clinically defined Shoulson-Fahn stages of disease. From this cohort, we detected the presence of a cross-linked cofilin-actin band by western blot in which higher degrees of cross-linking quantifiably correlated to disease stage. These correlations were apparent both across the population of each disease stage and also longitudinally within individuals.

Tissue transglutaminase 2 (TG2) is a calcium sensitive multifunctional enzyme. TG2 has guanosine triphosphate (GTP) signaling activity as well as transamidating activity. TG2 can catalyze the formation of a covalent bond between polyamine, or the ε-amino group of polypeptide-bound lysine, and the γ-carboxamide group of polypeptide bound glutamine to form polyamine or isopeptide bonds, respectively (Lesort et al., 2002). TG2 activity is known to be elevated in HD brains, and in HD lymphocytes (Cariello et al., 1996; Lesort et al., 1999). Others have shown that transglutaminase can cross-link cofilin and actin *in vitro* (Benchaar et al., 2007). We therefore hypothesized that the higher-order cross-link of cofilin and actin observed in the lymphocyte samples may be due to elevated TG2 activity. Using western blot assays, we show that cofilin-actin cross-linking, similar to what is observed in HD lymphocytes, was dependent not only on TG2 protein levels, but also stress, consistent with the requirement for activated TG2.

At the single cell level, we used biophotonic fluorescence lifetime imaging microscopy (FLIM) technology (Wallrabe and Periasamy, 2005)to measure Förster resonant energy transfer (FRET) between enhanced yellow fluorescent protein EYFP-TG2 and mCerulean-cofilin, at rods in live cells undergoing stress, to determine if the proteins directly (<8nm) interact *in vivo.* We show that TG2 interacts in a stress-

dependent manner with both nuclear and cytoplasmic cofilin rods, potentially mediating the cofilin-actin cross-link and the rod persistent phenotype observed in AD and HD. Thus, our data leads us to hypothesize a new model for TG2 hyperactivity in HD. This model describes defective actin turnover during stress due to the polyglutamine expansion in huntingtin causing ER disruption, increased calcium levels and activation of TG2, resulting in aberrant cofilin-actin covalent cross-links. This model predicts that actin turnover may be universally affected in all cell types in HD, but would be most critical to highly dendritic neurons (Hotulainen and Hoogenraad, 2010), such as the medium-sized spiny neurons (MSNs) which are predominantly affected in HD. Our data also shows that there may be subtle, but quantifiable HD phenotypes in peripheral cells that may be developed into biomarkers for HD.

2.3 Methods and Materials

Tissue Culture and Generation of Stable Cell Lines

Mouse striatal STHdh $^{Q7/Q7}$ cells, STHdh $^{Q111/Q111}$ and STHdh $^{Q7/Q111}$ (a kind gift of M. E. MacDonald, MGH), cell lines derived from the mouse striatum of wild-type mice and knock-in HD mice, were grown in Dulbecco's modified Eagle's medium (Invitrogen) with 10% fetal bovine serum (Invitrogen) at 33°C with 5% CO_2. Striatal cells were clonally selected and grown under G418 drug selection at 33°C to ensure temperature sensitive selection. Mouse Fibroblast NIH 3T3 Cells were grown in Dulbecco's modified Eagle's medium (Invitrogen) with 10% fetal bovine serum (Invitrogen) at 37°C with 5% CO_2. Stable STHdh$^{Q7/Q7}$ and STHdh$^{Q111/Q111}$ cell lines were generated by co-transfecting pmCerulean-Cofilin and pPuro using turbofect (Fermentas). Cells were grown under puromycin drug selection (Sigma) and positive colonies selected manually using colony selection rings. Stable cell lines were then maintained normally under only G418 selection.

Primary Cell Growth and Immunofluorescence

Sterile 0.1mg/mL Poly-D-Lysine (Sigma-Aldrich) was diluted in Borate Buffer (50mM Boric Acid, Sigma-Aldrich; 12mM Sodium Tetraborate, Fischer Scientific) and applied to a LAB-TEK™ 8 well chamber slide (Nalge Nunc International) and incubated at room temperature for 30 minutes. Each well was washed 5 times with NANOpure water and washed once with Neurobasal medium (Invitrogen). Cultures were prepared as described previously (Mila et al., 2009). 15,000 cells per well were plated in 400 µl of Neurobasal medium supplemented with B27 (Gibco) and GlutaMAX (Gibco) in a humidified 95% air/5%CO_2 incubator at 37°C. Medium was changed on days 2 and 4. On day 6 the medium was replaced with 10% DMSO (Sigma) in Neurobasal with B27 and GlutaMAX and incubated for 90 minutes in a humidified 95% air/5%CO_2 incubator at 37°C. Cells were fixed with 4% paraformaldehyde in PBS pH7.2 for 50 minutes at room

temperature. Cells were permeabilized in 0.05% Triton (Sigma), 2% FBS in PBS and this was applied to cells for 3 minutes at room temperature and then washed 3 times with 2% fetal bovine serum (FBS) (Atlas, Fort Collins, CO) in PBS over the course of one hour. Primary antibodies include: affinity purified rabbit IgG to chick ADF (2 ng/l rabbit 1439), which cross-reacts with mammalian ADF and cofilin, and MAB2166 ant huntingtin (Millipore; 1:50 dilution), which were both diluted in 2%FBS in PBS plus 0.05% Tween-20 (PBST) and incubated with the cells overnight at 4˚C. Cells were washed 2 times with 2% FBS in PBS. Secondary antibodies were diluted in 2% FBS in PBST at 1:1,000 and include Alexa 594 goat anti mouse (Invitrogen) and Alexa 488 goat anti rabbit (Invitrogen). DAPI (Invitrogen) was also added to the secondary antibody solution at 1:1,000. Secondary antibodies were incubated for 30 minutes and then washed 4 times with PBS. Antifade Gold (Invitrogen) was applied after final wash.

Plasmid Construct and expression

Primers to express human cofilin1 were made (McMaster Mobix facility) with 5' BspEI and 3' Acc651 overhangs and cloning was performed, using PCR product from human cofilin1 cDNA (OriGene), between BspEI/Acc651 sites of pemCerCI (BD Biosciences/Clontech) to create mCer-cofilin plasmid.

Forward 5’ GATCTCCGGAATGGCCTCCGGTGTGGC 3’

Reverse 5’ GATCGGTACCCAAAGGCTTGCCCTCCAG 3’

TG2 YFP was a kind gift from Dr. Gail Johnson. We used PCR primers to express TG2 with 5’BglI and 3’ ACC651 overhangs. Cloning was performed using PCR product from TG2 PCR between BglI/ACC651 sites of YFPCI (BD Biosciences/Clontech) to create YFP-TG2.

Forward 5’GATCAGATCTGGTGGCGGAGGGATGGCCGAGGAGCTGGTCTTAG3’

Reverse 5’CTATGGTACCCCCTCCGCCACCGGCGGGGCCAATGATGACATTC 3’

Huntingtin expression constructs were previously described (Atwal et al., 2007).

Plasmids were transfected using the transfection reagent Turbofect™ (Fermentas) according to manufacturer's instructions. For the full-length huntingtin FLIM-FRET experiments Lipofectamine 2000 was used as a transfection reagent according to manufacturer's protocol (Invitrogen). All co-transfections were performed using a 1:1 molar ratio of plasmids.

Heat Shock, Immunofluorescence and Recovery

Cells were cultured in 25 mM live-cell culture dishes at ~ 75-85% confluence. Once settled, media was exchanged for HEPES buffered (20 mM pH 7.4) media. Plates were wrapped with parafilm and placed in a pre-warmed water bath at 42.5˚C for 60 minutes. Cells were fixed in 4% paraformaldehyde for 45 minutes at room temperature. Cells were permeabilized using ice cold methanol at -20°C for 5 minutes and blocked in 1% FBS in PBS for 45 minutes. Primary antibody α-cofilin (mAB22 a kind gift from J. Bamburg 1/250), anti-actin (20-33 sigma 1/100) or anti huntingtin C20 (Santa Cruz 1/100) were applied in antibody solution (Blocker + 0.02% TWEEN-20) for 2 hours. Secondary antibodies conjugated to Alexa probes (Invitrogen) or Cy5 and FITC (Jackson laboratories) were used for 30 minutes at room temperature in antibody solution. For recovery experiments 3 dishes of each cell type were heat shocked as described. One dish from each cell type was fixed immediately. Recovery dishes had media exchanged for non- buffered media and were placed back in the incubator and allowed to recover for either 3 or 24 hours before fixation. After fixation of all dishes, immunofluorescence was performed as described. When immunostaining using the primary antibody mAB2166 anti huntingtin (1/250 Chemicon) and anti-actin(20-33 sigma 1/100) cells were permeabilized using 0.5% triton-X in PBS and 2% FBS for 12 minutes at 4°C with the rest of the immunofluorescence procedure being performed as described. All

double immunofluorescence was done in series with non-cross reactive secondary antibodies.

Stealth RNAi duplexes and transfection

Huntingtin Stealth™ Select RNAi was purchased from Invitrogen as a set of 3 (MSS205082, MSS205083, MSS205084). Stealth™ RNAi Negative Control Medium GC (Invitrogen) was purchased as a negative control. 120 pmol of RNAi was transfected into 25mm dishes plated at 50% confluency using the lipid based transfection reagent, Lipofectamine™2000 (Invitrogen) according to manufacturer protocol. Cells were treated for biochemical analysis or processed for fluorescence microscopy 72 hours after transfection. For delta T dish live cell experiments, Block-iT™ Alexa Fluor® red (Invitrogen) was co-transfected with huntingtin Stealth™ Select RNAi or Stealth™ RNAi Negative Control Medium GC, at a 1:3 ratio, as a control for transfected cells during live cell imaging experiments.

Protein extraction and Immunoblot assay

For STHdh cell lines, cells were grown in 10 cm dishes to confluence, washed with PBS and collected using a rubber scraper. Cells were pelleted, incubated and resuspended in NP-40 lysis buffer with protease inhibitor cocktail. Cells were spun at 14000X*g* for 10 minutes and the supernatant (protein fraction) was collected.

When protein from insoluble fraction was collected, protein was extracted as described above and pellet was re-suspended in NP-40 lysis buffer with protease inhibitors. Slurry was sonicated for 3 cycles of 15 pulses. The settings were set with a duty cycle of 10% and output control power of 3.

Lymphocyte samples were obtained by extracting the buffy coat from 3 mL total human blood using Accuspin Histopaque 1077 tubes from Sigma (Product code A6929, 3-6ml). Protein was extracted from lymphocyte samples as described for the cell lines.

Equal amounts of protein were loaded on 12% SDS–polyacrylamide gel and electroblotted to a polyvinylidene fluoride (PVDF) membrane. Membranes were blocked with 5% non-fat dry milk in TBST for 1 h followed by 1 h incubation at room temperature with anti cofilin mAB22 (1:5000, a kind gift from Dr. J. Bamburg), anti cofilin H12 (1:1000 Santa Cruz), anti htt-N18 (1:10000) or anti actin 20-33 (1:2500,sigma). After incubation with appropriate HRP-conjugated secondary antibody (Sigma) bands were visualized by enhanced chemiluminescence. Quantification of western blot bands was performed using the Image J software and pixel intensity analysis, normalized to actin. For Lymphocyte samples, pixel intensity analysis was performed individually on each lane and values are expressed as percent of total area in the higher order band.

Microscopy

All widefield fluorescence microscope images were captured on a Nikon TE200 epifluorescence inverted microscope equipped with a 60 X oil immersion plan apochromat NA1.4 objective and a Hamamatsu Orca ER digital camera (Hamamatsu Photonics, Japan). Qualitative images of nuclear rods were produced by obtaining a multichannel Z-stack and performing blind 3D non-iterative deconvolution (Autodeblur, Media Cybernetics). Images shown are mass-projections from deconvolved Z-stacks with gamma alterations (Figure 2.1 and Figure 2.2).

Live Cell Imaging

Live cell visualization was done using the Delta T4 heated stage, lid, and objective system (Bioptechs). Cells were seeded and treated in 0.17mm delta T dishes (Bioptechs). Cells were heated to 42.5°C using the heated stage and objective and visualized at 100 X plan apochromat oil N.A1.3 objective. As soon as dish reached temperature fluorescence images were recorded once every 60 seconds for the duration of the session.

Statistical Analysis

Statistical Analysis was performed using the SigmaPlot Software 11.0 (Systat Software Inc.) For single comparisons student T-tests were performed if data passed normality assumptions. If data did not pass normality assumptions it was analyzed by the Mann-Whitney method. For multiple comparisons ANOVA by the ranks was performed and multiple comparisons were performed using the Dunn Method.

Fluorescence Lifetime Imaging Measurement (FLIM)

FLIM was conducted using an inverted confocal laser-scanning microscope (Leica TCS SP5) with a 63x glycerol immersion NA 1.3 Plan apochromat objective. The SP5 is run using the LAS Advanced Fluorescence software from Leica. Two-photon excitation of samples was done using a tunable Chameleon laser, mode-locked to deliver femto-second pulses at a rate of 80MHz with an output power of 1.8W for a peak wavelength of 820nm.

mCerulean and EYFP fluorophores were used as FRET pairs. Excitation of the mCerulean donor using the MP laser was found to be optimal at 820nm. Collection of mCerulean fluorescence emission was limited to 480nm +/- 20nm. All live cell imaging and FLIM was done in Hank's saline HEPES buffer pH7.4

Photons from the donor fluorophores were collected, and counted using a Becker-Hickl photon counter and TCSPC software (SPC-830). The laser power was adjusted in order to give a photon collection count of ~10e5 photons/sec, where all FLIM measurements were conducted over a 60 second collection time. The lifetimes of all the pixels in the field of view (256x256) were calculated by the SPCImage analysis software (Becker & Hickl GmbH, Germany) to generate mono-exponential decay curves. Binning and thresholding values (bin=3, threshold=10) were kept constant to ensure consistency of lifetime measurements over multiple trials.

Förster Resonant Energy Transfer (FRET) Analysis

FRET analysis was performed using the Becker & Hickl FLIM plug-in for ImageJ software (McMaster Biophotonics Facility, www.macbiophotonics.ca). The lifetime of every pixel in the image was calculated to give a mean lifetime value for each cell when fit to a mono exponential decay curve. Pixels with lifetimes outside the range of 1750-3250 were excluded from further analysis, and visually identified via the intensity-weighted lifetime image to exclude areas of artifactual lifetimes due to very low or very high intensities. FRET efficiency for each image was determined using the equation EFRET = 1- (Average lifetime D.A/ Average lifetime D), where average lifetime D.A indicates the average lifetime of mCerulean-actin in the presence of the indicated acceptor and average lifetime D indicates the overall average lifetime of mCerulean-donor alone with no acceptor present.

2.4 Results

We have previously shown that huntingtin localizes to the ER under steady state growth conditions, and that it can be released from the ER and enter the nucleus under conditions of temperature or UPR stress (Atwal et al., 2007). In order to determine whether the huntingtin protein had any direct role in cellular stress response, we observed a mouse striatal neuron-derived cell line (STHdh) (Cattaneo and Conti, 1998) expressing full length endogenous levels of either wild-type (STHdh $^{Q7/Q7}$), or mutant (STHdh $^{Q111/Q111}$) huntingtin, under typical heat shock conditions of 42°C for 60 min. Huntingtin was then visualized by a fully validated huntingtin monoclonal antibody, MAb2166 , by immunofluorescence (Figure 2.1). Within the nucleus, we could visualize huntingtin localized to numerous 3-5 µm rod structures in STHdh $^{Q7/Q7}$ (Figure 2.1A, panels a-c, m-o), and to phenotypically different, fewer and longer rod structures in STHdh $^{Q111/Q111}$ (Figure 1A, panels d-l). These nuclear rods could be visualized with the amino-terminal epitope antibody MAb2166, as well as the carboxy-terminal epitope antibody C20 (Figure 2.1A, panels d-f), suggesting that full-length huntingtin localizes to these structures. Nuclear cofilin-actin rods have been observed by others in the past in response to various cell stress agents, including heat shock (Iida et al., 1992; Nishida et al., 1987; Ohta et al., 1989). To test if these huntingtin-positive nuclear structures may be cofilin–actin rods, we performed co-immunofluorescence with antibodies against huntingtin and cofilin (Figure 2.1A, panels d-f), huntingtin and actin (Figure 2.1A, panels g-i), and cofilin and actin (Figure 2.1A, panels j-l). From these data, we concluded that the huntingtin-positive nuclear rods induced by heat shock are cofilin-actin rods. This was confirmed directly by co-imaging and co-localization of mCerulean-cofilin fusion protein over-expressed in STHdh cells and immunofluorescence to visualize endogenous huntingtin using MAb2166 (Figure 2.1A, panels m-o). To verify that these observations were not artifactual to immortalized tissue culture cells, or to heat shock, we imaged endogenous cofilin and huntingtin in primary mouse hippocampal neurons, with and

without 10% dimethyl sulfoxide(DMSO) treatment (Ohta et al., 1989) to induce cofilin rods (Figure 2.1B, panels e-h), with similar localization of endogenous wild-type mouse huntingtin to cofilin rods. In summary, upon heat shock or DMSO induced cell stress, huntingtin protein entered the nucleus and localizes to cofilin-actin rods. We did not observe huntingtin at cytoplasmic cofilin-actin rods under any cell stress conditions tested in any cell type, indicating that this is likely a nuclear function of huntingtin during stress.

In order to quantify the effect of the polyglutamine expansion on nuclear cofilin-actin rods, we quantitatively compared rod formation in STHdh$^{Q7/Q7}$ and STHdh$^{Q111/Q111}$ cell lines during stress. STHdh $^{Q7/Q7}$ cells formed numerous (8 +/- 5) (Figure 2.2A, panels a-c, Figure 2.2B), short 3-5 µm rods upon heat shock (Nishida et al., 1987), whereas STHdh $^{Q111/Q111}$ cells formed fewer (2+/- 1) and longer rods that often spanned the nucleus to 10 µm (Figure 2.2A, panels d-f, Figure 2.2B), phenotypically similar to persistent rods previously defined by others in AD models (Minamide et al., 2000). The percentage of cells that formed rods during stress was not statistically different at the 60 min. time point (Figure 2.2C). We also observed endogenous huntingtin protein in a heat shocked mouse fibroblast cell line, NIH 3T3 (Figure 2.2A, panels g-i), and found that huntingtin localized to cofilin rods phenotypically similar to STHdh $^{Q7/Q7}$ cells. Thus, huntingtin localization to nuclear cofilin rods upon stress is not limited to neuron-derived cells. This is consistent with endogenous huntingtin protein expression in all cell types outside of the brain (The-Huntington's-Disease-Research-Collaborative-Group, 1993).

In AD, cytoplasmic cofilin-actin rods are shown to persist beyond the stress when cells are returned to normal conditions (Minamide et al., 2000). In order to assay whether mutant huntingtin rods were persistent or not, we heat shocked cells, and fixed them immediately following heat shock (t=0), or place them back at 33°C and allowed them to recover for 3 or 24 h (t=3, or t=24). This was followed by fixation and

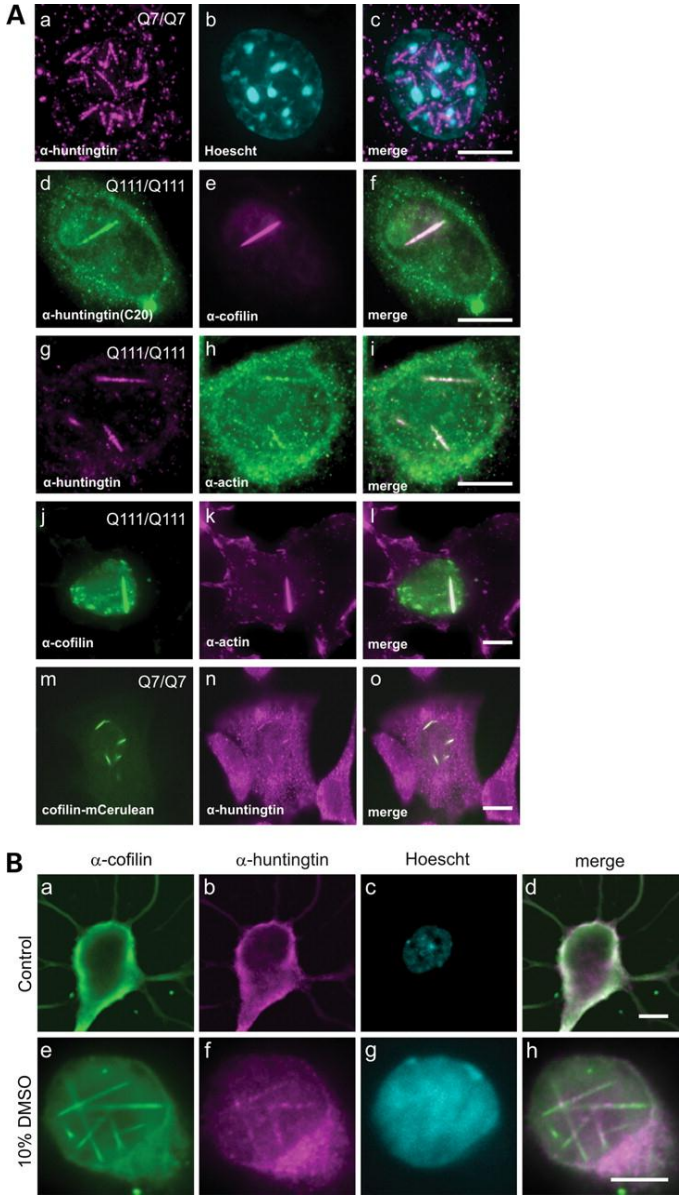

Figure 2.1: Full-length, endogenous huntingtin protein is a component of nuclear cofilin–actin stress rods. (A) Immunofluorescence in mouse STHdh$^{Q7/Q7}$ or STHdh$^{Q111/Q111}$ striatal-derived cell lines, in cells heat shocked at 42°C for 60 min. Secondary antibodies were either Alexa 488 (green) or Alexa 595 (magenta) labeled. (a–c) Huntingtin monoclonal antibody MAb2166, co-stained with Hoechst DNA dye (cyan). (d–f) Huntingtin monoclonal antibody C20, co-stained with cofilin monoclonal MAb22. (g–i) Huntingtin monoclonal MAb2166 co-stained with an antibody against actin. (j–l) Co-staining with antibodies against cofilin and actin. (m–o) Huntingtin monoclonal antibody MAb2166, in cells expressing an mCerulean–cofilin fusion protein. (B) Immunofluorescence on 6-day-old primary hippocampal neurons treated with 10% DMSO for 90 min to induce rod formation. Untreated cell (a–d) stained with affinity purified rabbit IgG to chick ADF (a), huntingtin monoclonal antibody MAb2166 (b) and co-stained with Hoechst DNA dye. Secondary antibodies were either Alexa 488 (green) or Alexa 595 (magenta) labeled. DMSO treated cell (e–h). Merged overlapping signal is pseudo-colored white. Scale bar is 10 μm.

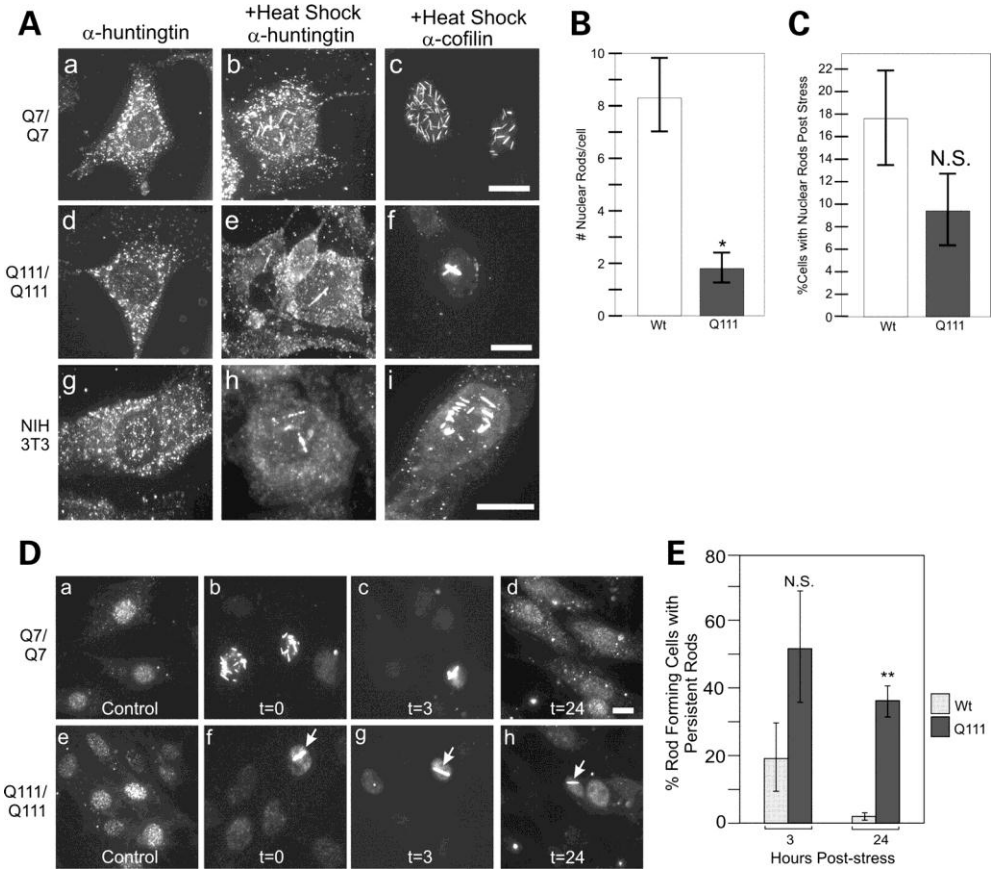

Figure 2.2 Mutant huntingtin protein affects nuclear cofilin rod formation and induces persistence of cofilin rods. Immunofluorescence with either huntingtin or cofilin antibodies in either STHdh$^{Q7/Q7}$ or STHdh$^{Q111/Q111}$ cell lines. (A) Mutant huntingtin protein affects the number and size of nuclear cofilin stress rods upon 60 min heat shock. (a–c) Huntingtin or cofilin immunofluorescence before (a), or after heat shock (b–c) in STHdh$^{Q7/Q7}$ cells. (d–f) Huntingtin or cofilin immunofluorescence before (d), or after heat shock (e–f) in STHdh$^{Q111/Q111}$ cells. (g–i) Huntingtin or cofilin immunofluorescence before (g), or after heat shock (h–i) in NIH 3T3 mouse fibroblast cell line. (B). Comparison of number of nuclear rods per cell immediately after 60 min heat shock in STHdh$^{Q111/Q111}$ or STHdh$^{Q7/Q7}$ lines. Rod forming cells were imaged as a z-stack and the mass projection was used to count number of rods per nucleus in each cell type. N = 3, n= 10 per replicate, total n= 30. *P-value of n< 0.001. (C) Comparison of number of cells with nuclear rods immediately after 60 min heat shock. Cells were fixed immediately after 60 min heat shock and 20 sequential images at a random area in the dish were taken at 63×. Number of cells with nuclear rods were counted and expressed as a percentage. N = 3, P-value of 0.210. N.S., not statistically significant. (D) Immunofluorescence staining against cofilin in either STHdh$^{Q7/Q7}$ (a–d) or STHdh$^{Q111/Q111}$ (e–h) cell lines. Images shown directly after heat shock stress (b, f) or after 3 h (c, g) or 24 h (d, h) recovery at optimal conditions. Control, no stress, images shown (a, e). (E) Quantification of percent rod forming cells with persistent nuclear rods after 3 and 24 h at 33°C was performed as described for (C). Percent cells with persistent rods expressed as a percentage of initial rod forming cells immediately after heat shock stress (t = 0) for each trial. N = 3; *P-value of 0.163; N.S., not statistically significant. **P-value of 0.003. Persistent rod phenotype highlighted with white arrows. All scale bars are 10 µm.

immunofluorescence with anti-cofilin MAb22 (Figure 2.2D). A minimum of 20 sequential frames at 63X magnification were imaged and the number of rod forming cells were counted. Recovery values were normalized to the number of rod forming cells observed at t=0. After 24 h recovery, the wild-type cell line recovered almost completely with only 2% of rods persisting, whereas mutant cells still had a 36% persistence rate (Figure 2.2E). Strikingly, 100% of nuclear rods that persist beyond 3 hours (in any cell type) have a persistent rod phenotype (Figure 2.2D, panels c,g,h , see arrows).

For subsequent experiments, based on our quantitative phenotyping of the different cell lines, we generated a phenotypic threshold defining a cell with the wild-type rod phenotype as having >4 rods/nucleus (rod length spanning 1-6 µm) and a cell that has a persistent rod phenotype to have between 1 and 4 rods/nucleus with at least 1 rod being >4 µm. Using these parameters, we quantified the percentage of rod forming cells with persistent rod phenotypes immediately following heat shock. We found that only 27.6±6.1% of rod forming STHdh$^{Q7/Q7}$ cells form nuclear rods with a persistent phenotype compared to 83±5.6% of rod forming STHdh$^{Q111/Q111}$ cells. Collectively, these results indicate that huntingtin has a normal universal role in the nucleus with respect to nuclear rod formation and that this role is disrupted by a polyglutamine expansion. In addition, the presence of mutant huntingtin causes an increase in the persistence of nuclear cofilin-actin rods once the cell has been allowed to recover from stress, thus directly implying huntingtin dysfunction in this stress response.

In order to consistently assay cofilin rod formation, we made a stable STHdh$^{Q7/Q7}$ cell line expressing the mCerulean-cofilin fusion protein. To assess any essential role of wild-type huntingtin in this cell stress response, we treated STHdh mCerulean-cofilin cell lines with specific small interfering ribonucleic acid (siRNA) to knockdown levels of huntingtin. After siRNA knockdown of huntingtin was confirmed by western blot (Figure 2.3A), we compared rod formation in STHdh mCerulean-cofilin cells treated with huntingtin siRNA or a control siRNA during and after heat shock stress by visualizing

mCerulean-cofilin (Figure 2.3B&C). We did not observe any difference in percentage of cells forming rods upon heat shock at 60 min whether huntingtin levels were reduced or not (Figure 2.3B). After 1h stress 35.5±2.3% of rod forming cells had a persistent rod phenotype when scramble siRNA was transfected versus 51.6±4.3% when huntingtin siRNA was transfected (Figure 2.3B). After 24 h recovery, we observed a significant increase in persistent rods after huntingtin knockdown; 3.5± 0.38% of rods persisted in cells transfected with scrambled siRNA vs. 21.4± 6.5% when huntingtin siRNA was transfected (Figure 2.3C). These results show that when wild-type huntingtin is knocked down, the cofilin-actin rod phenotype and defects are similar to cells expressing mutant huntingtin (Figure 2.3B), indicating a loss of function with polyglutamine expansion in huntingtin.

We then wanted to ascertain whether the effect of mutant huntingtin presence was dominant, an important factor when considering the genetics of HD. Immortalized striatal neurons from a heterozygous (STHdh $^{Q111/Q7}$) mouse were heat shocked and we performed similar immunofluorescence for cofilin. At the one hour time point, the heterozygous cells formed rods with a similar phenotype to mutant cells: 79±3.3% (SE) of rod forming cells had a persistent rod phenotype (Figure 2.3B). This indicates that the changes in rod formation can happen even when wild-type huntingtin is present, and thus the persistent rod phenotype is dominant.

In order to visualize the dynamics of cofilin rod formation during cell stress, we used STHdh$^{Q7/Q7}$ and STHdh$^{Q111/Q111}$ cell lines stably expressing mCerulean-cofilin fusion protein, and observed live cells over time during heat shock stress by fluorescence microscopy using a heated stage (Video 2.1 and Video 2.2). Cells were imaged every 60 s during heat shock. These temporal experiments were repeated multiple times and parameters of rod formation, rod persistence time, rod length, and time to cell death were quantified and compared (Table 2.1A). Typical results are presented in figure 2.4. These experiments revealed that the average time before nuclear cofilin rods

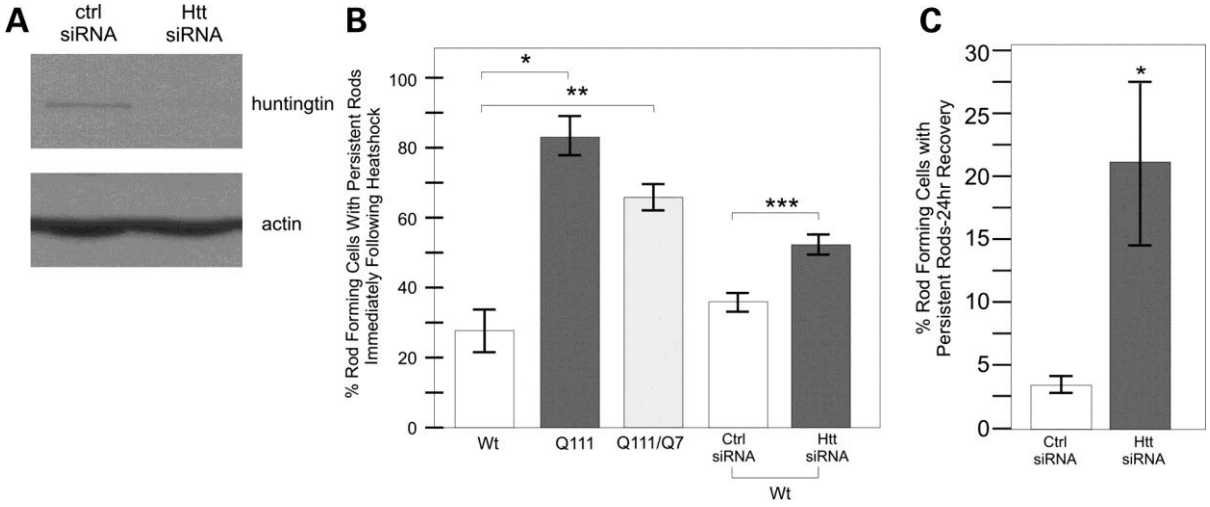

Figure 2.3 Huntingtin protein is required for proper cofilin nuclear rod formation and clearance following cell stress. (A) Western blot against huntingtin protein after control siRNA or huntingtin-specific siRNA was expressed in wild-type huntingtin STHdhQ7/Q7 cells for 72 h. Anti-actin shown as a loading control. (B) Comparison of percent nuclear rod forming cells with persistent rod phenotype in heat-shocked cells. Comparison between STHdhQ7/Q7, STHdhQ111/Q111 and STHdhQ7/Q111 cell lines as well as in STHdhQ7/Q7 cells following siRNA treatment. Experiment performed as described previously. N = 3, *P-value of <0.003, **P-value of 0.028. (C) Comparison of percent of rod forming cells with nuclear persistent rods after 72 h siRNA treatment, heat shock and 24 h recovery. Quantification performed as previously described. N = 3, *P-value of 0.046.

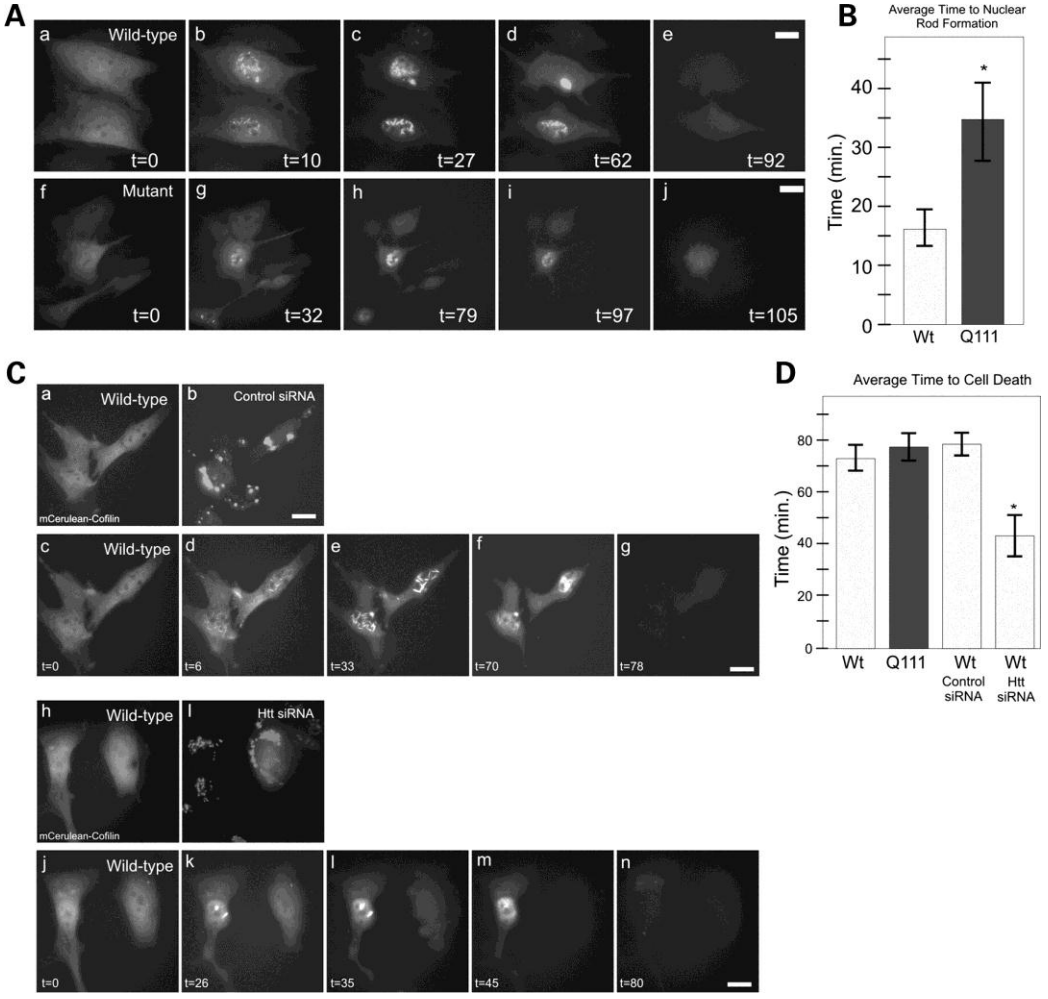

Figure 2.4 Huntingtin is required for normal cell heat shock stress response and mutant huntingtin affects the rate of the nuclear cofilin rod stress response. Temporal imaging in live STHdh$^{Q7/Q7}$ or STHdh$^{Q111/Q111}$ cells stably expressing mCerulean–cofilin fusion protein. (A) mCerulean–cofilin imaged over time showing nuclear cofilin rod formation in both wild-type and mutant cell lines at 10 and 32 min, respectively (b versus g), following panels show length of times rods exist and time of clearance during maintained heat shock at 42°C (c–e and h–j). (B) Comparison graph of average time to nuclear rod formation for stable mCerulean–cofilin wild-type (N = 15) and mutant (N = 9) STHdh cells during live cell imaging experiments. *P-value of 0.007. (C) Temporal imaging in live STHdh$^{Q7/Q7}$ cells stably expressing mCerulean–cofilin. Cells were co-transfected with control siRNA or huntingtin-specific siRNA and Block-iT™ Alexa Fluor® red for 72 h prior to experiments. Single-cell visualization of control (a–b) or huntingtin siRNA (h–i) transfection with labeled Block-iT™Alexa Fluor® red. Visualization of STHdh$^{Q7/Q7}$ cells with mCerulean–cofilin during heat shock, treated with control siRNA (c–g). STHdh$^{Q7/Q7}$ cells with cofilin–mCerulean during heat shock, treated with siRNA to huntingtin (j–n). (D) Comparison graph of average time to cell death in mCerulean–cofilin stable STHdh$^{Q7/Q7}$ (N = 13) or STHdh$^{Q111/Q111}$ (N = 24) cells imaged live and STHdh$^{Q7/Q7}$ mCerulean–cofilin cells treated with control siRNA (N = 5) or huntingtin siRNA (N = 6) imaged live during heat shock. *P-value of 0.003. Scale bars are 10 μm

were observed during cell stress was significantly longer in STHdh $^{Q111/Q111}$ (35 min) versus STHdh $^{Q7/Q7}$ (16 min) cell lines (Figure 2.4A&B) (Video 2.1 and video 2.2). A detailed quantitative comparison of the rod phenotypes between the two cell lines demonstrated that mutant huntingtin cell lines were significantly delayed in rod formation during stress, and that rods were typically fewer and longer, with a persistent phenotype (Table 2.1A). This is consistent with our earlier results in fixed cell lines expressing only endogenous cofilin. In contrast to fixed cells, live cell temporal observations demonstrate that fewer STHdh$^{Q111/Q111}$ cells form rods during stress in the presence of mutant huntingtin. These data highlight the importance of using live cell imaging for these observations.

We used the same assay to track huntingtin siRNA effects on a cell-by-cell basis using a siRNA transfection fluorescent marker indicator (Block-it™, Alexa Flour Red) in our mCerulean-cofilin stable STHdh$^{Q7/Q7}$ cell line (Figure 2.4C, panels a-b and h-i). When cells were transfected with huntingtin siRNA, the cells had a delayed rod formation response upon stress, and a persistent rod phenotype (Figure 2.4C, panels k-m) mimicking what occurred in our STHdh$^{Q111/Q111}$ cofilin stable cells. There was also a significantly faster cell death due to stress after siRNA treatment (44 min versus 79 min for the scrambled control) (Figure 2.4D, Table 2.1B, Video 2.3 and Video 2.4). Thus, huntingtin has a critical normal function in cell heat shock stress response, and the mutant huntingtin protein or knockdown of normal huntingtin protein appears to delay the onset of this stress response and affect the normal recovery from stress.

Under normal growth conditions, cofilin has an essential function in actin treadmilling, or turnover from the monomeric soluble state to the filamentous fibers. This function is controlled by the reversible phosphorylation of cofilin by LIM kinase (Endo et al., 2007). During stress, cofilin becomes hyper-dephosphorylated. Dephosphorylated cofilin has a strong affinity for adenosine diphosphate (ADP) actin and saturates F-actin, forming rods or bundles that sequester most of the cofilin and

thus slows turnover of the remaining F-actin sparing ATP for other cellular processes (Bamburg and Wiggan, 2002; Bernstein et al., 2006). LIM is targeted by Parkin in PD (Lim et al., 2007), and cofilin levels are highly variant in PD lymphocytes (Mila et al., 2009). Therefore, we western blotted cofilin in protein samples from HD patient lymphocyte samples obtained from gradient density centrifugation-separated pellets from blood. These samples were collected from patients at the four clinically defined (Shoulson-Fahn) stages of HD, including pre-manifest patients and age-matched controls, for a total of 39 individuals. We performed western blots using monoclonal antibodies raised against cofilin protein (Figure 2.5A). We observed a higher order cofilin complex that was enhanced with advancing stages of HD. The size of the higher order band was consistent with the additive molecular weights of actin and cofilin proteins, which have been shown by others to be capable of stably cross-linking *in vitro* (Mannherz et al., 2007). Blotting for actin revealed a band migrating at the same size in these samples (Figure 2.5A). Therefore this complex contained cofilin and actin, and was stable despite sodium dodecyl sulfate polyacrylamide gel electrophoresis (SDS-PAGE), boiling, and 1% dithiothreitol treatment, indicating a covalently linked complex. When quantitatively comparing the ratios of cofilin trapped in the cofilin-actin complex to the free cofilin (higher order band to lower order band) by pixel density analysis, we noted that more cofilin was present in the higher order complex as the stages of HD advanced. This effect was statistically significant between control or pre-manifest individuals and early or late stages of HD (Figure 2.5B). Thus, the degree of cross-linked cofilin-actin complex from patient lymphocytes could be tracked from pre-manifest patients to patients with advancing stages of HD.

We additionally obtained longitudinal primary lymphocyte samples from four HD patients, three of whom had progressed from pre-manifest to early HD, while one patient remained pre-manifest on both samplings. For all three individuals who had progressed to early HD, we observed an increase in trapped cofilin-actin complexes

(Figure 2.5C&D). No increase in cofilin-actin complex was observed in the pre-manifest individual (Figure 2.5D, patient #2) consistent with the population studies, and the greatest increase in ratio of cofilin-actin complex to free cofilin was observed in a patient who had progressed from pre-manifest to a later stage of HD (Figure 2.5D, patient #1). The two sets of data from different patient populations, and from individual patients over time similarly demonstrated that trapped cofilin-actin complexes increase with disease onset and increasing severity of HD. This raises the question as to what is actually mediating this cross-linkage and what connection there may be between cofilin and actin cross-links in lymphocytes and cofilin-actin rods in model systems.

In the past, others have observed the ability of cofilin and actin to be covalently cross-linked *in vitro* upon addition of transglutaminase (Benchaar et al., 2007) . Tissue transglutaminase (TG2) is an intracellular protein with many functions, but is known to catalyze the formation of a covalent bond between polypeptide-bound lysine and polypeptide-bound glutamine (Ruan and Johnson, 2007). Several lines of evidence prompted us to examine TG2 activity in our system. First, TG2 activity and expression are highly elevated in neurodegenerative diseases, including HD in the brain (Lesort et al., 1999), cerebrospinal fluid and plasma (Jeitner et al., 2008), as well as in AD (Johnson et al., 1997). For example, TG2 has been shown to co-localize with pathological lesions in AD brains (Wilhelmus et al., 2009) and isopeptide cross-links have been detected in paired helical Tau filaments (Norlund et al., 1999). Of relevance to this study, TG2 activity has been shown to be increased in HD patient lymphocytes, in a CAG-length dependent manner (Cariello et al., 1996). Furthermore, a TG2 knockout mouse crossed with an HD model mouse results in reduced neuronal death and increased lifespan (Mastroberardino et al., 2002). Regular polyglutamine (Kahlem et al., 1996) as well as expanded polyglutamine (Cooper et al., 1997) have been shown to be TG2 substrates and TG2 is mis-regulated in HD, however there is evidence showing that TG2, although

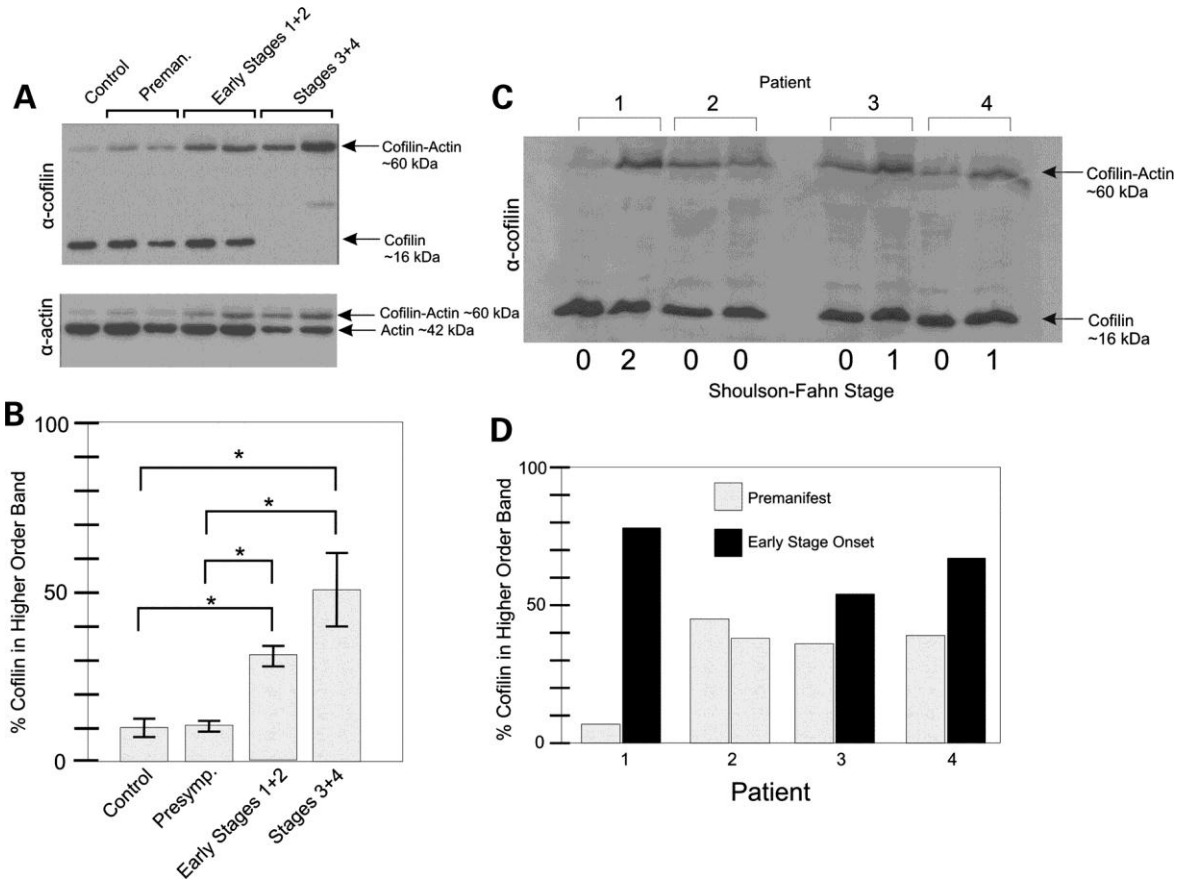

Figure 2.5 White blood cell populations from HD patients show a cross linked cofilin–actin complex on a western blot which increases with clinical onset and severity of disease. Western blots on the protein extracted from blood buffy coat histopaque-treated pellets from HD patients at different clinically defined stages of HD (the Shoulson–Fahn method). Western blot was done using MAb22 cofilin or anti-actin antibodies. (A) Typical comparison of samples between age-matched controls and either pre-symptomatic, early stage 1 and 2 patients and late stage 3 and 4 patients. Mobility of either cofilin or actin is indicated by black arrows. (B) Quantification of percent cofilin signal in higher order cofilin–actin band from western blots performed on control and HD patient blood samples. Analysis done using pixel intensity analysis using NIH Image J. Control (N = 7), pre-symptomatic (N = 11), early stages 1 + 2 (N = 9), late stages 3 + 4 (N = 12). *P-value < 0.05. (C) Western blot of cofilin in longitudinal blood samples (prepared as described previously) from four HD patients, three of whom had progressed in HD from pre-symptomatic to early HD between samplings. (D) Graph shows percent cofilin signal in higher order cofilin–actin band in western blot determined by pixel intensity analysis using NIH Image J.

involved in HD progression, does not cross-link or co-localize to inclusions of mutant huntingtin (Chun et al., 2001). Consistent with this, there is evidence showing that in an HD mouse model TG2 is involved in HD progression in an aggregate-independent manner (Bailey and Johnson, 2005). Recently TG2 has been shown to modulate transcriptional changes in HD indicating aberrant nuclear activity apart from aggregation (McConoughey et al., 2010). Given this data, we tested whether TG2 could be responsible for the cofilin-actin cross-links observed in clinical HD lymphocyte samples.

We wanted to ascertain whether TG2 could have activity at rods in our live cell STHdh system. FLIM, measures the change in fluorescence lifetime of the donor fluorophore, in this case mCerulean, which inversely correlates to FRET efficiency in the presence of an acceptor, in this case EYFP. This is not affected by spectral bleed-through or protein concentration, and thus is the best standard of FRET measurement between two individual proteins observed in live cells (Wallrabe and Periasamy, 2005). This method is used to determine whether two proteins are directly interacting within 8nm of 3D space *in vivo*, as FRET efficiency drops off to the sixth power with distance(Wallrabe and Periasamy, 2005). FRET efficiency, E, is calculated as 1 minus the lifetime of the donor in the presence of acceptor/lifetime of donor without acceptor. mCerulean-cofilin was used as our donor and EYFP (Venus yellow variant) or EYFP-TG2 as our acceptor. Under steady-state conditions, mCerulean-cofilin could be visualized in both the nucleus and cytoplasm, with mCerulean-cofilin having a fluorescent lifetime of 2600 ps, either with EYFP or EYFP-TG2 co-expressed (Figure 2.6A, panels a-c versus d-f shown on the color scale map as green and red dashed line). This indicated that there is no FRET under steady-state conditions, hence no interaction between the proteins. Under heat shock conditions in mCerulean-cofilin expressing cells, the lifetime of mCerulean-cofilin did not change from 2600 ps when only EYFP was co-expressed (Figure 2.6A, panels g-j and Figure 2.6B). Under heat shock conditions the lifetime of mCerulean-cofilin was significantly shorter due to FRET in the presence of EYFP-TG2

(Figure 2.6A, panels k-r and Figure 2.6B), with the strongest FRET efficiency at the cofilin-actin rods, from 2600 to under 2000 ps (indicated by yellow-orange in Figure 2.6B, panels l,m,p,q and arrows). The interaction between mCerulean-cofilin and YFP-TG2 gave an average of 15.6% FRET efficiency over the whole cell area (with the maximum possible being ~30% for this donor-acceptor FRET pair) versus the average of the EYFP control interacting with mCerulean-cofilin of 0.7% (Figure 2.6A, panel j vs. n, quantified in Figure 2.6B). These data show that EYFP-TG2 can directly interact with mCerulean-cofilin on both nuclear and cytoplasmic cofilin rods *in vivo* (see arrows in Figure 2.6B, panels l,p,q) which may lead to a cross-link of cofilin and actin, especially if elevated calcium levels are present, as seen in HD (Tang et al., 2005).

To ask whether TG2 could catalyze a cross-linked cofilin-actin band as observed in our HD lymphocyte sample western blots, we assayed for the presence of the cofilin-actin complexes in STHdh cells by western blotting for endogenous cofilin under conditions of steady state, heat shock, with TG2 over-expressed, and under heat shock with TG2 over-expressed (Figure 2.6C). When over-expressing EYFP-TG2 we had ~25% transfection rate by direct visualization of YFP. A cofilin-actin band co-migrating with a similar higher order cofilin-actin band in clinical HD patient lymphocytes was observed when TG2 was over-expressed coupled with stress conditions (Figure 2.6C). The effect seen in the HD patient sample was more robust that in our model system, which may indicate that the lymphocyte population in HD may be undergoing a chronic stress, as opposed to the transient stress of our assay. The data we provide indicates that a disrupted mechanism of TG2 in HD may be aberrant cross-linking of cytoskeletal proteins.

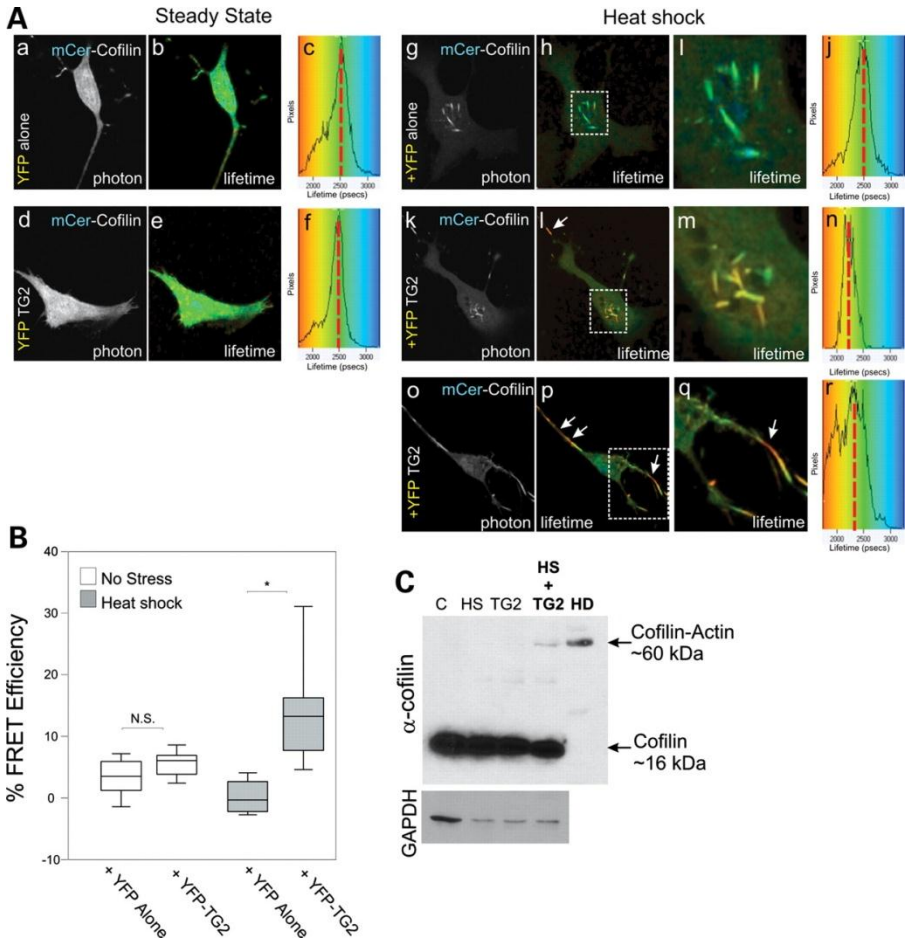

Figure 2.6 TG2 directly interacts with cofilin–actin rods during stress and TG2 over-expression induces a cofilin–actin complex in stressed cells. (A) STHdh cells were transiently transfected with mCerulean–cofilin and either EYFP alone (a–c, g–j) or EYFP-TG2 (d–f, k–r), and FLIM analysis was performed either before (a–c, d–f) or following a 45 min heat shock at 42.5°C (g–j, k–n, o–r). Fluorescence lifetimes for mCerulean blue are presented with a continuous pseudocolor rainbow scale representing time values ranging from 1750 to 3250 ps. The lifetime distribution curve of the mCerulean–cofilin is shown as a histogram on the right representing the number of pixels at each lifetime. The red vertical broken line marks the median lifetime distribution for the cell. Red arrows connect histogram value position with lifetime image value. (B) Box and whisker plot representing FRET efficiency, with FRET occurring at distances <8 nm for these FRET pairs. All imaging and FRET analysis were done in Hank's HEPES buffer pH 7.4. N = 3, n > 10 for each donor–acceptor pair. *P< 0.001. Line = mean; box = 1 standard deviation from the mean; whiskers = 2 standard deviations from the mean. (C) STHdh$^{Q7/Q7}$ cells were heat shocked (at 42.5°C for 45 min) and/or transfected with EYFP-TG2 (for ~36 h). Western blot using MAb22 anti-cofilin was performed on cell pellets to determine whether a higher order cofilin band would be observed. Higher order band observed only in stressed cells over-expressing TG2. Patient HD stage 4 lymphocyte sample was used as a size control for cofilin–actin band. Glyceraldehyde 3-phosphate dehydrogenase loading control was used. Cells were verified for YFP-TG2 expression by fluorescent microscopy

2.5 Discussion

Previous work has described the first 17 amino acids of huntingtin as being an amphipathic alpha helix with an affinity for the ER. Huntingtin has the ability to come off the ER and enter the nucleus during stress (Atwal et al., 2007), following the classic model of ER stress-sensor proteins (Zhao and Ackerman, 2006). Here, we demonstrate that huntingtin directly affects nuclear actin remodeling during the heat shock stress response. In the past, huntingtin has been shown to bind F-actin (Angeli et al., 2010) and localize to tubulin-rich structures at the mitotic spindle (Godin et al., 2010). Our data shows that huntingtin localizes to an additional form of the dynamic cytoskeleton, nuclear cofilin-actin rods, during stress. The cofilin rod stress response occurs to halt a small proportion of actin from treadmilling, so the ATP that would be used in this dynamic turnover can be used elsewhere for more crucial cell functions (Bernstein et al., 2006). Other than freeing up ATP, the exact role of nuclear actin rods is not known. Rods may influence chromatin structure and dynamics as well as transcription in response to stress, all of which are affected in HD (Benn et al., 2008; Luthi-Carter and Cha, 2003). All of our data studying nuclear cofilin rods was acquired by observing full-length endogenous huntingtin expressed at normal levels. While data suggests that the amino terminus of huntingtin is involved in cytoskeletal association (Angeli et al., 2010; Atwal et al., 2007), optimal huntingtin interactions with the cytoskeleton may require additional domains at the carboxyl-terminus of the protein (Pal et al., 2006). In live cells, FRET with cofilin was only observed with full-length huntingtin and not with smaller fragments (Figure 2.7), implying that this function is a loss of function of fragments of huntingtin. Our data shows that in the presence of mutant huntingtin this stress response is impaired: the stress response is slower, fewer cells respond and a persistent nuclear rod phenotype is induced. Defective actin turnover is quickly establishing itself as a common theme among other neurodegenerative diseases, including PD (Lim et al., 2007)

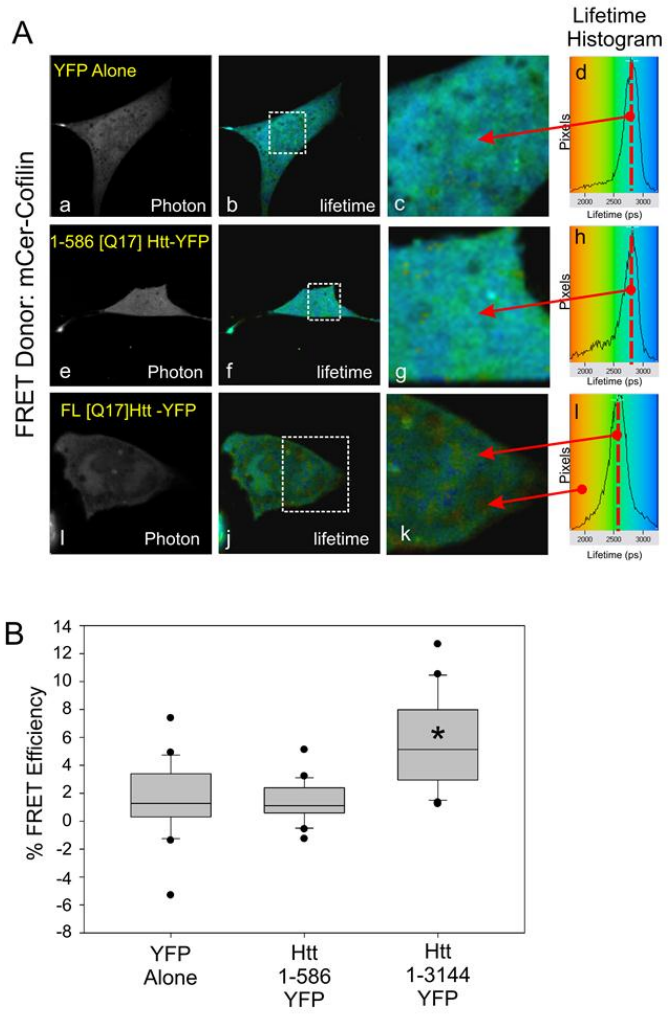

Figure 2.7: Full Length Huntingtin but not a Truncated Huntingtin Interacts with Cofilin. STHdh$^{Q7/Q7}$ cells were transiently transfected with mCerulean-cofilin (donor fluorophore) and either YFP alone (a-d) huntingtin 1-586 [Q17]-YFP (e-h) or full length huntingtin [Q17]-YFP (i-l) (acceptor fluorophores) and FLIM-FRET analysis was performed as described previously. Fluorescence lifetimes are presented with a continuous pseudocolor scale representing time values ranging from 1750 to 3250 psecs (1A, panels d,h,l). The lifetime distribution curve of the mCerulean-cofilin is shown as a histogram on the right representing the number of pixels at each lifetime. The red vertical broken line marks the mode lifetime distribution. Red arrows link histogram values with lifetime image. White dashed boxes indicate zoomed areas in c,g,k. 1B. Box and Whisker plot representing FRET efficiency. FRET efficiency was calculated using the formula EFRET = 1- (Average lifetime D.A/ Average lifetime D), where Average lifetime D.A indicates the average lifetime of mCerulean-Cofilin in the presence of the indicated acceptor and Average lifetime D indicates the overall average lifetime of mCerulean-Cofilin alone (no acceptor present). All imaging and FRET analysis was done in Hank's HEPES Buffer pH 7.4. N=3 n=10 for each Donor-Acceptor pair * $p<0.001$ compared to control of YFP alone or Huntingtin 1-586 [Q17]-YFP. Box = 1 standard deviation from mean D; Whiskers = 2 standard deviations from mean; Dots = statistical outliers.

and AD (AD) (Maloney and Bamburg, 2007; Minamide et al., 2000) indicating that defective actin remodeling through cofilin may be universally contributing to the age-onset progression of these neurodegenerative diseases. Specifically in AD, cofilin-actin rods have been shown to persist in neurites leading to axonal dystrophy (Minamide et al., 2000).

Cofilin rods can be induced by stresses that cause protein misfolding, increased calcium and decreased available ATP. These include temperature stress, 10% DMSO, ATP depletion with sodium azide and 2-deoxyglucose to inhibit metabolism, heavy metals, and hydrogen peroxide (Minamide et al., 2000; Nishida et al., 1987). Chronic low ATP levels have been described in HD patient brains and HD animal models (Gines et al., 2003; Koroshetz et al., 1997), presumably from defective mitochondrial metabolism (Seong et al., 2005). A defect in the actin stress response could further contribute to the aberrant ATP regulation in HD. Our findings suggest that defective actin remodeling during stress may lead to persistent rods causing a decline in the available cofilin in the cell, or that the altered actin dynamics during stress may be toxic. Either of these outcomes would predict that a population of neurons requiring higher levels of active actin turnover and having high ATP demands would be greatly affected in HD. Notably, the highly dendritic MSNs are predominantly affected in HD, whereas the smaller interneurons in the striatum, with fewer projections, are spared (Richfield et al., 1995). Dynamic actin turnover is critical to the health of neurons due to its role in maintaining the plasticity of dendritic spines, which is critical in projection neurons (Hotulainen and Hoogenraad, 2010). Furthermore, active actin remodeling to maintain synaptic and dendritic structures is a huge energy burden, using up to half of the total ATP in a steady-state cell (Bernstein and Bamburg, 2003). Therefore, the reduced ability of these cells to free up ATP during stress or defective actin turnover, even subtly, would conceivably lead to the changes in spine density, axonal atrophy and eventual neurodegeneration, all observed in MSNs in HD.

Although this is the first report of defective actin turnover via cofilin in HD, several previous studies have reported beneficial effects of the Rho associated kinase (ROCK) inhibitor, Y-27632, in HD model systems (Shao et al., 2008). ROCK is an upstream modulator of cofilin. ROCK inhibition effectively leads to reduced phosphorylation of cofilin and therefore increased actin binding cofilin activity (Maekawa et al., 1999). ROCK inhibitors have shown *in vivo* beneficial effects in both a mouse (Li et al., 2009) and Drosophila model (Agrawal et al., 2005) of HD. Thus, our findings provide a potential mechanistic link between the role of huntingtin in the cell stress response and the independent observations that ROCK inhibition has protective benefit in several HD models. This suggests that modulating the activity of cofilin and actin may have therapeutic potential in HD.

Given our findings that the polyglutamine expansion affects cofilin dynamics in neuronal populations we sought to test whether changes in cofilin properties could be observed in peripheral cells from HD patients. We performed western blotting against cofilin and actin from HD patient lymphocytes and observed a higher order protein band corresponding with the size of a putative cofilin-actin crosslink which increased with disease progression. In our attempt to determine what may cause the SDS insoluble, cofilin-actin crosslink, we noted that transglutaminase has the ability to cross-link cofilin and actin *in vitro* (Benchaar et al., 2007) and that tissue transglutaminase (TG2) is thought to be involved in multiple neurodegenerative disorders, including HD (Ruan and Johnson, 2007). TG2 is a transamidating enzyme that can crosslink the ε-amino group of polypeptide bound lysine and the γ-carboxamide group of polypeptide bound glutamine through an acyl transfer reaction forming a stable covalent cross-link. This reaction may be reversible and is highly dependent upon calcium levels for activation (Ruan and Johnson, 2007). TG2 binds calcium which activates its enzymatic activity in a concentration dependent manner (Kiraly et al., 2009). Disrupted calcium signaling is also noted in HD (Zhang et al., 2008) and an increase in calcium levels is a hallmark of

most cellular stress events. TG2 activity and expression is up-regulated in HD (Lesort et al., 1999), and notably has been shown to have aberrant activity in HD lymphocyte populations in a CAG length-dependent manner (Cariello et al., 1996). To test whether TG2 could cause a similar cofilin-actin cross-link *in vivo,* we over-expressed TG2 in STHdh cells and activated it using heat shock stress. In this manner, we can recapitulate the higher order cofilin protein band from patient lymphocytes in STHdh cells. Furthermore, using FLIM-FRET we show that TG2 can directly localize to cofilin rods during stress suggesting that TG2 may not only crosslink free cofilin and actin, but that its activity may be involved in the aberrant nuclear cofilin-actin rod stress response in HD. Consistent with our data highlighting the importance of full length huntingtin, disrupted calcium signaling in an HD mouse model requires the polyglutamine expansion in the context of the full huntingtin protein (Zhang et al., 2008). Calcium levels can also be elevated upon massive over-expression of a small fragment of polyglutamine-expanded huntingtin that requires the presence of N17 (Rockabrand et al., 2007). This indicates that aberrant TG2 activation may be present in many HD models, but for different reasons. It is especially notable that the cross between a TG2 knockout mouse and an HD model mouse can rescue HD toxicity supporting the dysfunctional role of TG2 as a strong contributor to the HD phenotype in this model (Mastroberardino et al., 2002).

Based on the findings presented here, we propose a model in which huntingtin protein acts as a cell stress response protein at the ER (Figure 2.8). Under cell stress conditions, which lead to ER stress and increased cellular calcium, full-length huntingtin translocates to the nucleus and plays a role in actin remodeling in response to stress. Once the cell has recovered from stress, actin remodeling should return to normal. However, when polyglutamine-expanded huntingtin is present this nuclear actin stress response is impaired; there is a prolonged aberrant regulation of calcium-causing activation of TG2 where it can act on cofilin-actin. This defective actin remodeling would have multiple undesirable effects in a neuron, such as synaptic and dendritic

dysfunction, leading to the initial synaptic dysfunction and changes in spine density observed in the early stages of HD. This would likely lead to additional cell stress, further decreases in cellular ATP and additional intracellular calcium increases, progressively augmenting the cycle.

The implications of our findings may lead to new therapeutic targets for HD, including: alteration of mutant huntingtin nuclear localization in response to stress; inhibition of TG2 enzymatic activity (Schaertl et al., 2010); or activation of alternative stress-response pathways that override or circumvent the function of the huntingtin protein in actin-mediated cell stress response. The ratio of free cofilin to cross-linked cofilin can be quantifiably measured in human blood pellets, suggesting that this assay may be developed into a potential biomarker for HD.

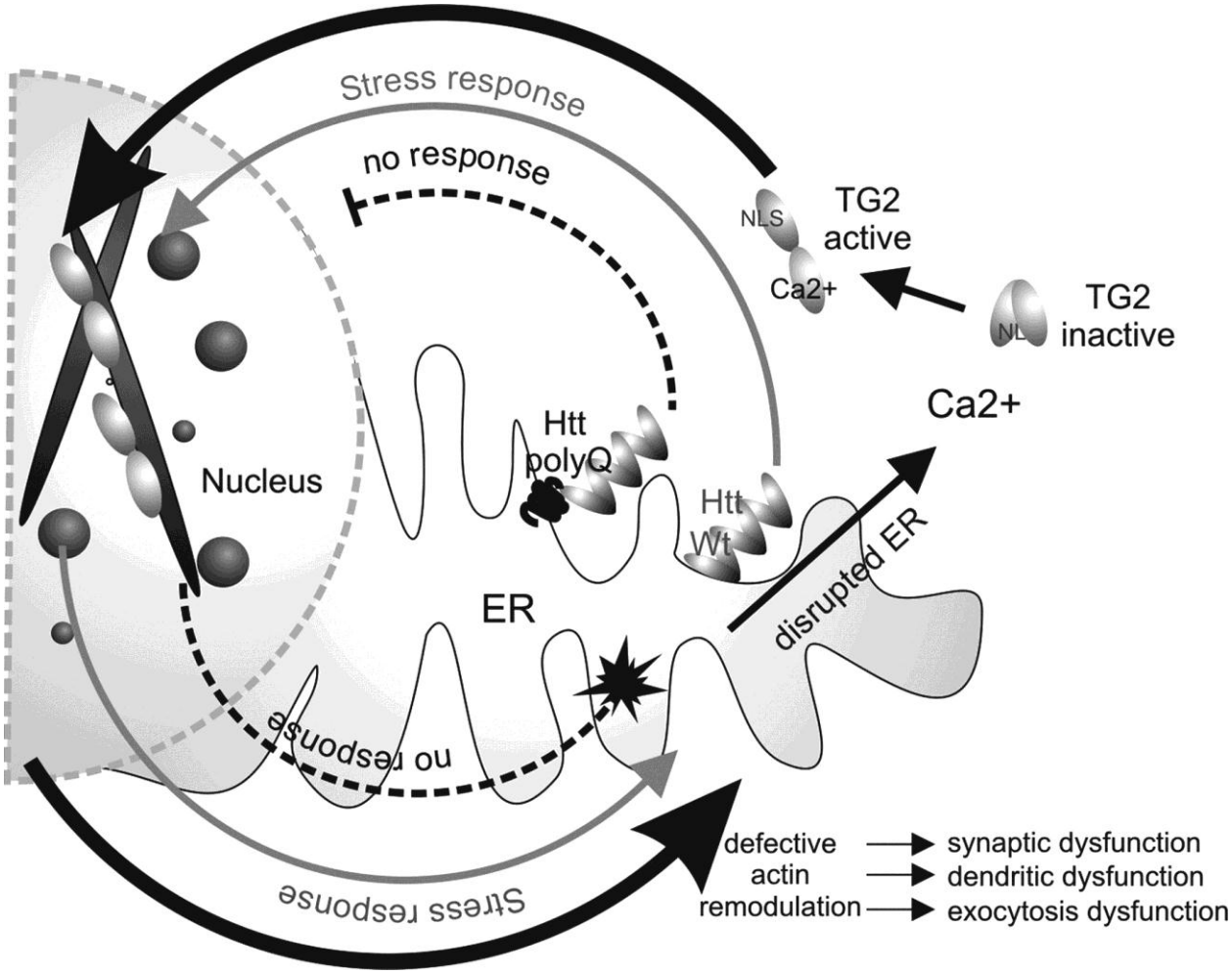

Figure 2.8 A model for defective huntingtin-mediated cofilin rod stress response leading to activation of TG2. The grey arrow pathway highlights normal huntingtin stress response by releasing from the ER, entering the nucleus and binding cofilin–actin rods, then exiting the nucleus upon stress relief. With mutant huntingtin present, the dashed arrow pathways show a defect in huntingtin stress response, resulting in less nuclear activity and persistent rods. Back in the cytoplasm, the black arrow pathways highlight elevated calcium due to a defective ER, which results in aberrant TG2 activation and cross-linking of cofilin–actin in both the nucleus and cytoplasm. Defective actin remodeling critically affects neurons at the level of dendritic and synaptic dysfunction, as well as exocytosis activity in peripheral cells.

1A. Comparison of Cofilin Response in ST*Hdh* Cells During Heat Shock Stress

Cell Line	Total Percent of Cells That Formed Nuclear Rods	Percent of Cells That Formed Nuclear Rods		Average Time to Nuclear Rod Formation (minutes)	Average Time to Nuclear Rod Formation (minutes)		Average time to Cell Death	Average time to Cell Death	
		Wildtype Phenotype	Persistent Phenotype		Wildtype Phenotype	Persistent Phenotype		Nuclear rod forming Cells	Non Rod-forming cells
ST*Hdh*$^{Q7/Q7}$	79%	74%	5%	16.2 ± 3.1**	13.2 ±1.2	57	73.5 ± 5	78.7 ± 4.8	68.3 ± 13
ST*Hdh*$^{Q111/Q111}$	40%	8%	32%	34.8 ± 6.6	12.5	41.1±6.2	78 ± 5.3	90.6 ± 9	77 ± 4.3

1B. Comparison of Cofilin Response in ST*Hdh* Cells With Huntingtin siRNA

siRNA Treatment	Total Percent of Cells That Formed Rods	Percent of Cells that formed rods		Average Time to Rod Formation (min)		Average time to Cell Death
		Wt Phenotype	Persistent Phenotype	Wt Phenotype	Persistent Phenotype	
Control siRNA	87.5%	75%	12%	8 ±1.2	51	79.1 ± 4.4**
Huntingtin siRNA	25%	0%	25%	NA	26	43.6 ± 8

Table 2.1: 1A.Comparison of cofilin response in STHdh$^{Q7/Q7}$and STHdh$^{Q111/Q111}$cells undergoing heat shock stress during live cell imaging. Several quantified parameters are compared. **= P Value equals 0.007. 1B. Comparison of cofilin response in STHdh$^{Q7/Q7}$ cells treated with either control or huntingtin siRNA undergoing heat shock stress during live cell imaging. Several quantified parameters are compared. **= P Values = 0.003.

2.6 Acknowledgements:

This work is supported by operating grants from the Canadian Institutes of Health Research (MOP-165174), the Krembil Foundation and CHDI Inc (to RT). LM has a CIHR Doctoral Research Award. SJT is funded by the MRC, Wellcome Trust, CHDI, and Brain Research Trust. The clinical evaluation, genetic testing and patient blood collections were undertaken at UCLH/UCL who received a proportion of funding from the UK Department of Health's NIHR Biomedical Research Centers funding scheme. NIH grant NS40371 to JRB. We gratefully acknowledge the technical assistance of Ms. L. S. Minamide , Dr. Nayana Lahiri and valuable discussions with Drs. O. Wiggan and B.W. Bernstein. We thank GVW Johnson for the gift of TG2 expression cDNAs and invaluable advice.

Conflict of Interests Statement

The authors declare no conflict of interests.

Chapter 3: Nuclear shuttling of cofilin as a therapeutic target

Preamble

The material presented in this chapter is a representation of the following publication with permission to reprint.

Munsie, L., Desmond, C.R., Truant, R. (2012) Cofilin Nuclear-Cytoplasmic Shuttling Affects Cofilin-Actin Rod Formation During Stress. *J. Cell Science*. **Epub ahead of print** doi: 10.1242/jcs.097667

The only changes made were for thesis formatting and continuity purposes and copy editing.

LM wrote the manuscript and performed all experiments and data analysis except the experiments listed below.

CRD assisted in cloning the GST plasmids and purifying the cofilin-GST tagged protein

Nuclear-Cytoplasmic Shuttling Affects Cofilin-Actin Rod Formation During Stress

Running title: Cofilin has nuclear export and import signals

Lise Nicole Munsie[1], Carly R. Desmond[1] and Ray Truant[1*]

*To whom correspondence should be addressed, truantr@mcmaster.ca

[1]Department of Biochemistry and Biomedical Sciences, McMaster University, 1200 Main Street West, Hamilton, Ontario, Canada, L8N3Z5

3.1 Abstract

Cofilin protein is involved in regulating the actin cytoskeleton during typical steady state conditions, as well as during cell stress conditions where cofilin saturates F-actin forming cofilin-actin rods. Cofilin can enter the nucleus through an active nuclear localization signal (NLS), accumulating in nuclear actin rods during stress. Here, we characterize the active nuclear export of cofilin through a leptomycin-B sensitive, CRM1-dependent, nuclear export signal (NES). We also redefine the NLS of cofilin as a bipartite NLS, with an additional basic epitope required for nuclear localization. Using fluorescence lifetime imaging microscopy (FLIM) and Förster resonant energy transfer (FRET) between cofilin moieties and actin, as well as automated image analysis in live cells, we have defined subtle mutations in the cofilin NLS that allow cofilin to bind actin *in vivo* and affect cofilin dynamics during stress. We further define the requirement of cofilin-actin rod formation in a system of cell stress by temporal live cell imaging. We propose that cofilin nuclear shuttling is critical for the cofilin-actin rod stress response with cofilin dynamically communicating between the nucleus and cytoplasm during cell stress.

3.2 Introduction

Cofilin and its family members are ubiquitously expressed proteins best characterized as actin binding and modulating proteins. These proteins have now been shown to be involved in multiple facets of cellular biology independent of their function with respect to actin tread-milling. These functions are as diverse as: involvement in membrane and lipid metabolism (Han et al., 2007); mitochondrial dependent apoptosis (Klamt et al., 2009); as well as the regulation of transcription and chromatin structure (Obrdlik and Percipalle, 2011). The improper regulation of the cofilin family members have been implicated in disease mechanisms (Bernstein and Bamburg, 2010). Cofilin1, the non-muscle specific isoform, is of particular interest to the field of neurodegeneration. We have previously reported the involvement of nuclear cofilin-actin rods in a Huntington's disease (HD) cell model and changes in the cofilin protein expression profile in HD patient lymphocytes (Munsie et al., 2011) and cytoplasmic cofilin-actin rods are involved in the progression of Alzheimer's disease (AD) (Maloney and Bamburg, 2007; Minamide et al., 2000). Cofilin-actin stress rods can form in either the nucleus or cytoplasm in response to stress (Minamide et al., 2000) as a potential means to stop actin tread-milling and in turn free up ATP for other more immediate cellular uses (Bernstein et al., 2006). Improper regulation of the actin cytoskeleton is becoming a focus in neurodegenerative diseases, as actin dynamics are critical for maintenance of healthy synapses and dendrites (Hotulainen and Hoogenraad, 2010). Thus, understanding actin dynamics under disease and aging related stresses will give important insights into disease mechanisms for neurodegeneration.

During our previous studies, we observed that cofilin could enter the nucleus upon cell stress. Cofilin is known to be actively imported into the nucleus through a classic importin or karyopherin alpha/beta(α/β)-dependent nuclear localization signal (NLS) (26-PEEVKKRKKAV-36) (Abe et al., 1993; Iida et al., 1992). Importinα/β dependent NLSs are defined by a stretch of basic amino acids that are recognized by the adapter

protein importinα and subsequently imported into the nucleus through the nuclear pore complex (NPC) with the assistance of the nuclear transport receptor importinβ (Lange et al., 2007). Directionality of nuclear transport is maintained through the small Ras family GTP-binding protein, Ran. Ran-GTP, which is maintained at high levels in the nucleus, binds the nuclear import factors facilitating cargo release in the nuclear compartment. This process is reversed for nuclear export proteins where Ran-GTP binding encourages cargo interaction in the nucleus. RanGAP-mediated nucleotide exchange to Ran-GDP in the cytoplasm disassociates the complex (Lange et al., 2007). Cofilin is an 18 kDa protein that should be able to freely diffuse across the NPC, which has a passive diffusion cut-off point of ~40 kDa in yeast (Fahrenkrog et al., 2001), but likely higher in mammalian cells (Seibel et al., 2007). Cofilin has been shown to be required for the nuclear transport of actin, although how it is mediating this nuclear entry is unknown (Dopie et al., 2012; Iida et al., 1992). Cofilin recently has been shown to have a role in the nucleus with respect to RNA polymerase II transcription elongation and is likely required for the function of F-actin in the nucleus (Obrdlik and Percipalle, 2011). During certain stress situations, such as DMSO treatment and heat shock, the majority of cofilin in the cell can be found in the nucleus, and at nuclear rods, indicating that the NLS may have a stress dependent function aside from transporting actin into the nucleus or steady state functions with respect to RNA polymerase activity (Nishida et al., 1987; Obrdlik and Percipalle, 2011; Ono et al., 1993). During our live cell imaging studies of heat shock in real time, we noted the rapid exit of cofilin from the nucleus after extended stress. We hypothesized that cofilin may have an active nuclear export signal (NES). The classic CRM-1/exportin-dependent NES has a conserved consensus of $LX_{2-3}LX_{2-3}LX_{1-2}L$, where L is typically a leucine but can be any hydrophobic amino acid and X is any amino acid (Bogerd et al., 1996). This consensus is recognized by the nuclear export protein, CRM1, which relies on the Ran gradient to transport its cargo across the NPC, releasing the cargo in the cytoplasm (Fornerod et al., 1997). This pathway can be disrupted by leptomycin B, which covalently links to, and inactivates mammalian CRM1

at a single cysteine residue (Kudo et al., 1998). During this study we examined the amino acid sequence of cofilin and defined a conserved CRM1 dependent NES sequence as well as redefined the cofilin NLS as a bipartite NLS.

Cofilin-actin rods are thought to be transiently neuroprotective in cellular models (Bernstein et al., 2006), but improper formation and clearance is thought to be neurotoxic in models of AD and HD (Minamide et al., 2000; Munsie et al., 2011). Since aberrant rod formation may be involved in the progression of AD and HD, it has been hypothesized that altering rod formation or breaking down persistent rods could be therapeutic (Bamburg et al., 2010). By mutating key residues in the cofilin NES and NLS, coupled with endogenous cofilin knockdown by short hairpin (sh)RNA, we investigated the actin binding activity of cofilin mutants in a cell based model. We made minimal mutations to the cofilin NLS that resulted in loss or decreased rod formation during stress and observed how cells responded to stress when they were unable to form cofilin-actin rods. Importantly, cells expressing cofilin mutants that had abolished rod formation had an impaired ability to respond to stress but a cofilin mutant that could still form rods was able to respond to stress. These data highlight the importance of cofilin activity in response to stress and also imply that altering, but not completely abolishing the rod forming capabilities of cofilin by targeting the NLS may be tolerated by the cell and may thus define cofilin as a new drug target for some neurodegenerative diseases.

3.3 Materials and Methods

Tissue culture

Mouse STHdh$^{Q7/Q7}$ cell line (a kind gift from M. E. MacDonald, MGH), derived from the mouse striatum, were grown in Dulbecco's modified Eagle's medium (Invitrogen) with 10% fetal bovine serum (Invitrogen) at 33˚C with 5% CO_2. Striatal cells were clonally selected and grown under G418 drug selection at 33˚C to ensure temperature sensitive selection and maintain SV40 Tag expression. Derivation and characterization of stable cell lines used were previously described (Munsie et al., 2011).

Mouse fibroblast NIH 3T3 Cells were grown in Dulbecco's modified Eagle's medium (Invitrogen) with 10% fetal bovine serum (Invitrogen) at 37˚C with 5% CO_2.

EYFP and 3xFLAG cofilin plasmid construction and expression

EYFP-human cofilin plasmid used was previously described (Munsie et al., 2011). All primers were synthesized and all sequencing was performed at McMaster MOBIX Facility. All primer sequences and detailed cloning protocols or constructs are available upon request. (Located in Appendix of this document)

Primers to mutate the NES (V20A) and the NLS (KR31-32AA) were made and mutations achieved according to manufacturer's protocol using the QuickChange kit (Stratagene). Primers to mutate the first part of the bipartite NLS: RK21-22AA, R21A or K22A, were made using inverse PCR on the EYFP-cofilin or e-EYFP-cofilin KR31-32AA plasmids. Cofilin shRNA plasmids were purchased (HuSH, Origene) in pRFP-C-RS vector. Cofilin shRNA F1575659 was used for all experiments. To make silent mutations in the EYFP-cofilin plasmid so that it would not be susceptible to the shRNA inverse PCR was used. Inverse PCR was used to remove the RFP cDNA from the cofilin shRNA vector. Primers to express EYFP-cofilin(with silent mutations) or EYFP were made with 5' MluI and 3' PmeI overhangs and cloning was performed, using PCR product from all EYFP-cofilin plasmids

or EYFP alone plasmid (previously described), between MluI/PmeI sites into the modified cofilin shRNA constructs. Primers to express human cofilin1 were made with 5' Acc651 and 3' XbaI overhangs and cloning was performed, using PCR product from our previously constructed cofilin and cofilin mutant plasmids, between Acc651/XbaI sites of 3xFLAG-CMV-14 (Sigma) to create the cofilin-3xFLAG plasmids.

mCerulean-human beta actin was a kind gift from Kotaro Oka, (Keio University, Japan).

Plasmids were transfected using the cationic polymer based in vitro transfection reagent Turbofect™ (Fermentas) according to manufacturer instructions for different sizes of culture dishes (i.e. 2.0 ug DNA for 25mm dishes). Expression time was 24 hours unless otherwise indicated in the methods.

Synthetic peptide cloning and nuclear import and export assays

The synthetic NES was made with 5' BspEI and 3' Acc651 overhangs and cloned using the annealed product into pEYFPC1 (BD Biosciences/Clontech) to create Synthetic NES-EYFP.

The assay for nuclear export was done as previously described (Xia et al., 2003).

The assay for NLS activity was based on the pHM830 GFP-β-galactosidase triple fusion plasmid construct and conducted as described (Sorg and Stamminger, 1999). Synthetic DNA oligonucleotides encoding the cofilin NLS, bipartite NLS and bipartite NLS mutations were made with 5' SacII and 3' XbaI overhangs (MOBIX, McMaster University) and cloned using the annealed products into GFP-MCS-βGalactosidase (pHM830 vector) to create GFP-"synthetic NLS"- β-Galactosidase.

To make the GFP-cofilin RK21-22AA KR31-32AA- β-Galactosidase construct, primers to express human cofilin1 were made with 5' SacII and 3' XbaI overhangs and cloning was performed as described previously.

Heat Shock, immunofluorescence and recovery

Cells were cultured in 25 mM live-cell culture dishes at ~ 75-85% confluence and transfected as described. If leptomycin B was required it was added for 4 hours prior to heat shock. Media was exchanged for HEPES buffered (20 mM pH 7.4) media for all live cell imaging and heat shock experiments. Plates were wrapped with Parafilm and placed in a pre-warmed water bath at 42.5ºC for 60 minutes. Cells were fixed in 4% paraformaldehyde for 45 minutes at room temperature. Cells were permeabilized by the addition of pre-cooled methanol and placed at -20 ˚C for 5 minutes. Cells were blocked in 1% FBS in PBS for 45 minutes. Primary antibody α-cofilin (mAB22 a kind gift from J. Bamburg, 1/250 dilution), α-3xFLAG (Sigma 1/500 dilution), and α-cytochrome C and α-Bax (6A7) (kind gifts from D. Andrews, 1/500 dilution) were applied in antibody solution (1% FBS blocker + 0.02% TWEEN-20) for 2 hours. Secondary antibodies conjugated to Alexa dyes 488 or 594 (Molecular Probes) were used for 30 minutes at room temperature in antibody solution.

Microscopy

All 60X widefield fluorescence microscope images were captured on a Nikon TE200 epi-fluorescence inverted microscope (Nikon, USA) equipped with a 60 X oil immersion plan apochromat NA1.4 objective and a Hamamatsu Orca ER digital camera (Hamamatsu Photonics, Japan). All 20X widefield fluorescence microscope images were captured on an Evos digital LED inverted microscope equipped with a 20 X air plan fluor NA1.2 objective (AMG, Seattle, USA).

Percent nuclear fluorescent signal image analysis

To determine the percent nuclear fluorescence, cells were imaged at 60X and then analyzed using Compix Simple PCI (Hamamatsu, Japan). To ensure unbiased data collection, the cells were co-transfected with pmCherry-C1 (Clontech/Invitrogen), and

cells were selected under the red channel before being imaged in the green channel, in a method of unbiased imaging data acquisition. Nuclear and total cell intensities were collected by manually defining the nuclear (nucleus was defined using either bright field or Hoechst staining) region and the outline of the entire cell. For each cell the total intensity was measured and compared to the total intensity of the nucleus. Areas of equal size to represent the image background were obtained. The intensities of the defined regions were then measured using the Simple PCI measurement tool. Percent Nuclear Fluorescence was calculated using the equation % nuclear fluorescence = [(nuclear fluorescence-background)/(total cell fluorescence-background)] / 100. For quantification of immunofluorescent images when looking at endogenous protein (Figure 3.2H), background subtraction was not performed since every cell in the image was fluorescent and there was not enough background area available.

Live cell imaging

Live cell visualization was done using the Delta T4 heated stage, lid, and objective system (Bioptechs Inc. Butler, PA, USA). Cells were seeded and treated in 0.17mm delta T dishes (Bioptechs Inc). Cells were heated to 42.0˚C using the heated stage and objective and visualized at 100 X oil immersion NA1.3 objective with an objective heater. As soon as dish temperatures reached 42.0˚C, fluorescence images were recorded once every 60 seconds for the duration of the session.

Protein extraction and immunoblot assay

Cells were transfected and plasmids expressed for 36 hours in 5cm dishes, washed with PBS and collected using a rubber scraper. Cells were pelleted, incubated and re-suspended in NP-40 lysis buffer with protease inhibitor cocktail. Cells were spun at 14000X*g* for 10 minutes and the supernatant (protein fraction) was collected.

Equal amounts of protein were loaded on 12% SDS–polyacrylamide gel and electroblotted to a poly-vinyl difluoride (PVDF) membrane. Membranes were blocked with 5% non-fat dry milk in TBST for 1 hour followed by 1 hour incubation at room temperature with anti cofilin mAB22, (a kind gift from Dr. J. Bamburg), anti-EYFP (Clontech/Invitrogen) or anti-Actin (Sigma). After incubation with appropriate HRP-conjugated secondary antibody (Sigma) bands were visualized by enhanced chemiluminescence using the MicroChemi system (DNR Bio-Imaging systems, Israel). Quantitation of western blot bands was performed using the NIH Image J software and pixel intensity quantification, normalized to actin or EYFP-cofilin.

Statistical analysis

Statistical Analysis was performed using the SigmaPlot Software 11.0 (Systat Software Inc.) For single comparisons student T-tests were performed if data passed normality assumptions. If data did not pass normality assumptions data was tested by the Mann-Whitney method.

Fluorescence Lifetime Imaging Microscopy (FLIM)

FLIM was conducted using an inverted confocal laser-scanning microscope (Leica TCS SP5) with a 63x glycerol immersion NA 1.4 Plan apochromat objective. The SP5 is run using the LAS Advanced Fluorescence software from Leica. Two-photon excitation of samples was done using a tunable multi-photon (MP) Chameleon laser (Coherent, USA), mode-locked to deliver sub-femtosecond pulses at a rate of 80MHz with an output power of 1.8W for a peak wavelength of 820nm. Laser output was restricted to 12.5%.

EYFP and mCerulean fluorophores were used as FRET pairs. Excitation of the mCerulean donor using the MP laser was found to be optimal at 820nm. Collection of mCerulean fluorescence emission was gated to 480nm +/- 20nm. All live cell imaging and FLIM was done in Hank's saline HEPES buffer pH7.4.

Photons from the donor fluorophores were collected, and counted using a Becker-Hickl photon counter and TCSPC software (SPC-830). The laser power was adjusted in order to give a photon collection count of ~10e5 photons/sec, where all FLIM measurements were conducted over a 60 second collection time. The lifetimes of all the pixels in the field of view (256x256) were calculated by the SPCImage analysis software (Becker & Hickl GmbH, Germany) to generate mono-exponential decay curves. Binning and thresholding values (bin=3, threshold=10) were kept constant to ensure consistency of lifetime measurements over multiple trials.

FRET analysis

FRET analysis was performed using the Becker & Hickl FLIM plug-in for ImageJ software (McMaster Biophotonics Facility, www.macbiophotonics.ca). The lifetime of every pixel in the image was calculated to give a mean lifetime value for each cell when fit to a mono exponential decay curve. Pixels with lifetimes outside the range of 1750-3250 nm were excluded from further analysis, and visually identified via the intensity-weighted lifetime image to exclude areas of artifactual lifetimes due to very low or very high intensities. FRET efficiency for each image was determined using the equation EFRET = 1- (Average lifetime D.A/ Average lifetime D), where average lifetime D.A indicates the average lifetime of mCerulean-actin in the presence of the indicated acceptor and average lifetime D indicates the overall average lifetime of mCerulean-actin alone with no acceptor present.

Automated image analysis

Automated image analysis for cell health was done using the CellProfiler cell image analysis software (http://www.cellprofiler.org). We created a pipeline to classify healthy versus unhealthy cells based on size. Cells were transfected with the shRNA constructs of interest and plasmids were allowed to express for 48 hours. Images at 20X were taken and cells were subjected to a one hour heat shock. Images were then taken

directly after heat shock. Images were loaded into cell profiler and analyzed for number of healthy versus unhealthy cells based on size and morphology.

Protein expression, purification and F-actin co-sedimentation assay

Primers to express human cofilin1 were made (McMaster Mobix facility) with 5' BamHI and 3' EcoRI overhangs and cloning was performed, using PCR product from all cofilin mutant plasmids previously made, between BamHI/EcoRI cut sites of pGEX 5X-1 (GE Healthcare) to create GST-Cofilin expression plasmid.

Wild-type and mutant cofilin constructs were then expressed as glutathione-S-transferase (GST) fusion proteins in E.coli BL21 cells. Cells were grown in 200 mL of LB medium to an optical density of 0.7 at 600 nm, and expression was induced with Isopropyl-beta-D-thiogalactosidase (IPTG, 0.2 mM). Cells were harvested 6 h after induction, washed with 200 mL of 150 mM NaCl, resuspended in 20 mL of PBS and lysed by sonication. GST fusion proteins were enriched using Glutathione Sepharose 4B (GE Healthcare), washed in 3X by PBS and then eluted using elution buffer (50mM Tris-HCL, 10mM reduced glutathione). The samples were dialyzed into 50mM Tris-HCL pH 6.8 overnight using Slide-a-Lyzer mini dialysis units (Thermo Scientific).

F-Actin co-sedimentation experiment was performed using the actin binding protein kit (non-muscle actin, catalog number BK013) from Cytoskeleton Inc. (Denver, USA). Changes to protocol include using the provided actin at 10 µM and cofilin mutants in excess at 10-15 µM. Actin buffer was made in 5mM tris-HCL pH 6.8, 0.2mM $CaCl_2$. Incubation of cofilin and actin was done for 40 minutes and fast spins for F-actin binding assay were done in a Beckman ultracentrifuge using the TLA100 rotor at 150,000X*g*. Slow spins for F-actin bundling assay were done on a table top microcentrifuge (VWR, Galaxy 16D) at 14,000X*g*. Equal amounts of supernatant or pellet fractions were loaded

onto an SDS-gel and western blotting was performed as described using antibodies to GST (Sigma) or actin (Sigma).

3.4 Results

Cofilin has a conserved CRM1-dependent NES

Under steady state conditions, cofilin is diffuse throughout the cell with varying levels in the nucleus (Figure 3.1A). During heat shock and other stresses cofilin has been shown to rapidly accumulate in the nucleus (Iida et al., 1992), which we could recapitulate in our cell model system (Figure 3.1B). During live cell imaging of cells stably expressing mCerulean-cofilin and undergoing heat shock stress, cofilin accumulates in the nucleus as predicted and nuclear rods form. If the stress stimulus is not removed following the cofilin rod stress response, cofilin is observed to rapidly exit the nucleus (Figure 3.1C and Supplemental Video 3.1). The rapid nature of this nuclear export led us to hypothesize the presence of an active nuclear export signal in cofilin. We identified a single sequence in cofilin that fits the putative CRM1 dependent NES consensus (11-VIKVFNDMKV-20) (Bogerd et al., 1996; Fornerod et al., 1997). This sequence is conserved between different species of cofilin and between cofilin1 (non-muscle) and cofilin2 (muscle enriched) (Figure 3.2A). To initially test this sequence for NES activity, the putative NES sequence, VIKVFNDMKV, was fused in frame to EYFP to see if it would mediate the localization of EYFP to the cytoplasm, compared with the 26 kDa EYFP which can freely diffuse into the nucleus (Figure 3.2B). Under normal conditions, EYFP appears diffuse throughout the cell (Figure 3.2B). Imaging revealed that the putative cofilin NES sequence can function as an NES since EYFP fused to this sequence appeared predominantly cytoplasmic (Figure 3.2B). When cells expressing VIKVFNDMKV-EYFP were treated with the CRM1 inhibitor, leptomycin B (Kudo et al., 1998; Wolff et al., 1997), the fusion protein was observed to be able to diffuse into the

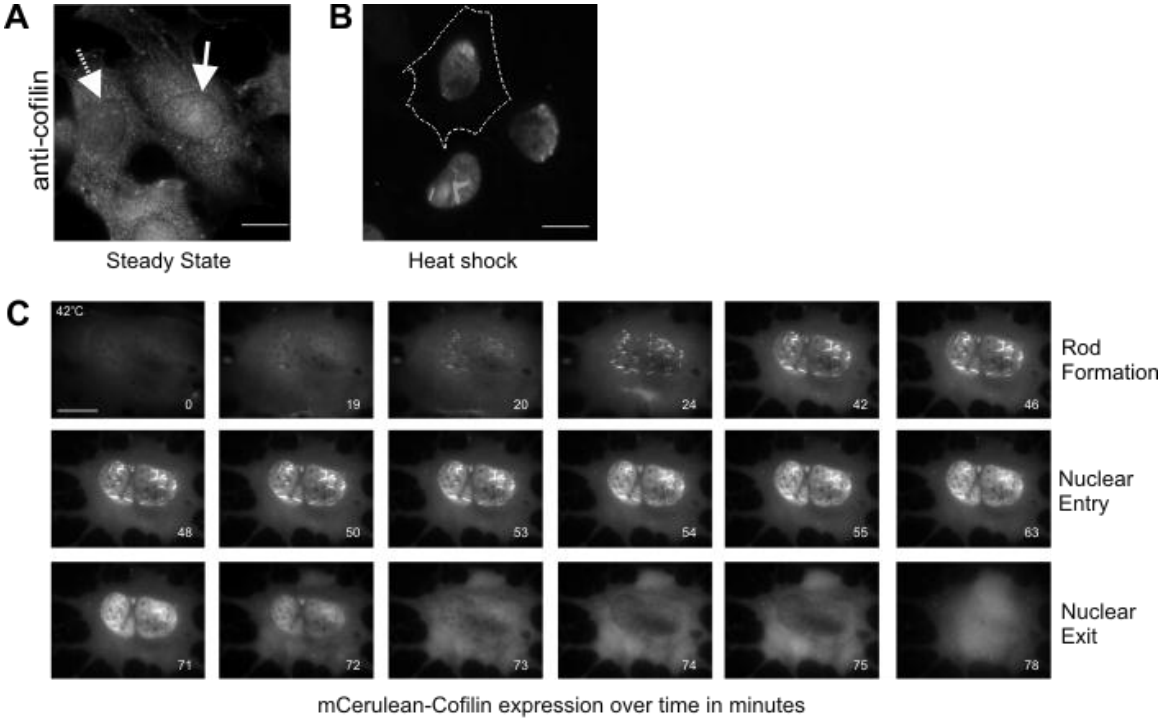

Figure 3.1: Cofilin has the ability to shuttle into and out of the nucleus. . Immunofluorescence of cofilin under steady state and heat shock conditions in STHdh cells. **(A)** Cofilin can have a nuclear (solid arrow) or cytoplasmic (dashed arrow) phenotype under steady state. **(B)** A large proportion of cofilin enters the nucleus during heat shock stress. Images taken at 60X on a widefield microscope. Scale bar = 10µm. **(C)** Temporal 100X wide field imaging in live cells stably expressing mCerulean-cofilin during the course of heat shock. Time represents the amount of time at 42°C in minutes. Cells imaged every 60 seconds. Scale bar = 10µm.

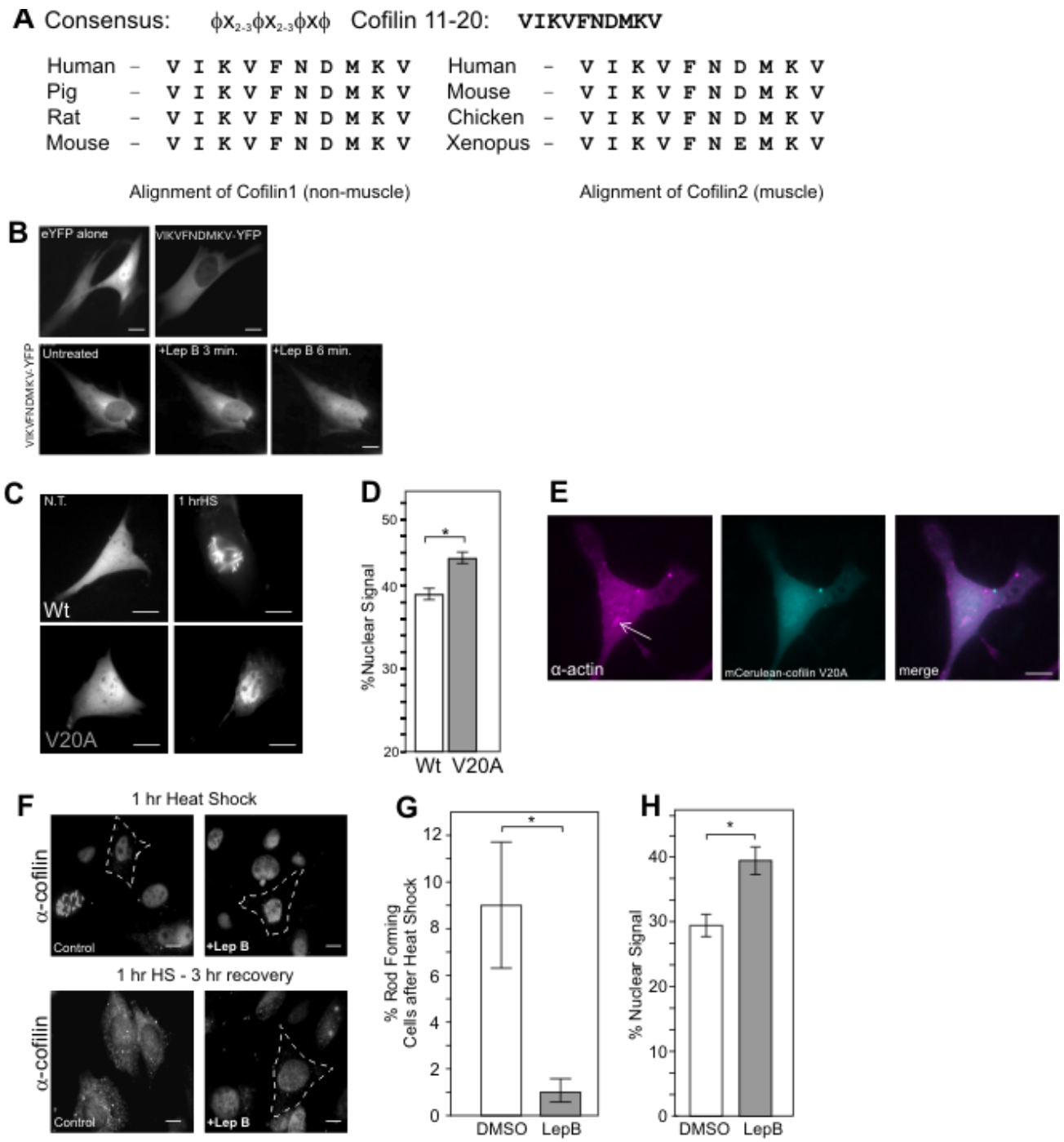

Figure 3.2 - Cofilin has a conserved putative NES sequence. LEGEND – see next page

Figure 3.2: Cofilin has a conserved putative NES sequence. (A) CRM1 dependent NES consensus and matching sequence in cofilin. Sequence comparison of the human cofilin1 and cofilin2 NES with that of other species of cofilin. **(B)** Cofilin NES functions out of context and is leptomycin B sensitive. EYFP alone or EYFP-cofilin NES were transfected into STHdh cells. EYFP-cofilin NES was transfected into STHdh cells and 5ng/mL leptomycin B was added to the media. Imaging was done in live cells. All images taken at 60X on a wide field microscope. All scale bars are 10µm **(C)** Cofilin NES works in context of the full length protein. EYFP-cofilin or EYFP-cofilinV20A was transfected into STHdh cells. Cells were imaged prior to, and after heat shock. V20A mutant accumulates more in the nucleus before stress and does not form nuclear rods during stress. **(D)** Graph represents percent nuclear fluorescent signal analysis for EYFP-cofilin vs. EYFP-cofilinV20A under steady state conditions in live cells. N= approximately 50 per construct/condition. *P value<0.005. **(E)** EYFP-cofilinV20A was transfected into STHdh cells and cells were heat shocked for 1 h. Cells were fixed and immunostained for actin. Endogenous rods still form in cells expressing the V20A mutant (white arrow). **(F)** STHdh cells were untreated or treated with 5 ng/mL leptomycin B for 4 h prior to heat shock stress then immunostained for cofilin or cells were allowed to recover for 3 h prior to immunostaining. Cofilin remains nuclear after heat shock in cells treated with leptomycin B and fewer cells form rods. **(G)** Effects of leptomycin B treatment on the percentage of cells with nuclear rods immediately after heat shock. Cells were fixed immediately after heat shock and were immunostained for cofilin. 25 sequential images at a random area in the dish were taken at 60X. Number of total cells and cells with nuclear rods were counted (percentage of cells with rods shown). N=3, n=500-900/dish *P value = 0.001. **(H)** Percent nuclear fluorescent signal analysis on endogenous cofilin after heat shock and 3 h recovery in the presence or absence of leptomycin B followed by cofilin immunostaining. 10 random and blinded images were taken at 60X, cells from these images were quantified for percent nuclear fluorescence. N= at least 30 cells/condition. *P<0.0035.

nucleus, but no longer exit the nucleus, indicating that this sequence can function as a CRM1-dependent NES (Fig. 3.2B and Video 3.2).

To test if this identified sequence works as an NES in the context of full length cofilin, we fused cofilin to EYFP and mutated one of the consensus hydrophobic amino acids in the NES, valine 20 to alanine (V20A). The V20A mutation caused a significant increase in detectable nuclear cofilin when percent nuclear fluorescent signal analysis was performed (Figure 3.2C&D and Table 3.1). This mutation also inhibited the ability of EYFP-cofilin to form rods in either the nucleus or cytoplasm during heat shock stress (Figure 3.2C and Table 3.1); however when immunofluorescence for actin was performed, we show that rods can still form endogenously, in cells expressing the V20A mutant during stress, indicating that over-expression of this protein does not

dominantly inhibit endogenous rod formation (Figure 3.2E). When cells were treated with leptomycin B and challenged with heat shock stress fewer rods formed endogenously (Figure 3.2F&G), and cofilin remained nuclear after stress was removed from the cells as compared to untreated control cells (Figure 3.2F&H). The endogenous data recapitulates some of what we observed with over-expressing the cofilin V20A mutant. Cofilin and actin have been shown to be the only required proteins for rod formation *in vitro* (Minamide et al., 2010) indicating that likely only cofilin-actin is affected in the *in vivo* leptomycin B rod forming assay. Although CRM1 has many target proteins for nuclear export, we believe that leptomycin B, through CRM1, is specifically affecting cofilin with respect to rod formation since actin nuclear export is mediated through profilin and exportin 6 and is not leptomycin B sensitive (Dopie et al., 2012; Park et al., 2010; Stuven et al., 2003). From these data, we conclude that cofilin has a CRM1-dependent NES and that the NES mutant V20A does not have the ability to form or be incorporated into cofilin-actin rods during stress.

Cofilin has a conserved bipartite NLS

Cofilin has a previously defined putative nuclear localization signal (NLS) at amino acids 26-PEEVKKRKKAV-36 (Iida et al., 1992), which is a monopartite, importin α/β-dependent NLS. To test whether inhibiting the ability of cofilin to enter the nucleus would also inhibit the formation of cofilin-actin nuclear rods in our system, we mutated critical amino acids lysine 31 and arginine 32 to alanines, KR31-32AA, in the context of the full length EYFP-cofilin construct, similar to what has been done previously (Iida et al., 1992). Contrary to previous studies by others, we observed no change in the ability of cofilin to enter the nucleus and cofilin KR31-32AA maintained its ability to form rods during stress (Figure 3.3A&B and Table 3.1), although fewer cells expressing this construct formed rods compared with the wild-type cofilin sequence (Table 3.1). During stress, a large proportion of cofilin is localized to the nucleus (Figure 3.1A&C) and nuclear import via cofilin has also been shown to be critical for actin nuclear entry

(Dopie et al., 2012; Iida et al., 1992). These data suggest that either cofilin may enter the nucleus alone by simple diffusion, or that additional amino acids are required for optimal active nuclear entry.

There is a second type of NLS that is recognized by importin α/β, known as a bipartite NLS. The bipartite NLS contains two basic rich regions, generally separated by 10-12 amino acids, with the consensus $(K/R)(R/K)X_{10\text{-}12}(K/R)_{3\text{-}5}$ where X can be any amino acid (Robbins et al., 1991). Seven amino acids upstream of the KKRKK sequence in cofilin there are two basic amino acids, RK. The sequence (21- RKSSTPEEVKKRKK-34) in cofilin loosely fits the bipartite NLS consensus. Both basic parts of the bipartite NLS in cofilin are evolutionarily conserved between different species of cofilin and between cofilin1 and cofilin2 (Figure 3.3C). In order to determine if either the monopartite NLS (cofilin amino acids 26-34) or the bipartite NLS (cofilin amino acids 21-34) were functional, these sequences from cofilin were taken out of context and fused between GFP and β-Galactosidase (β-Gal). β-Gal is 112 kDa, tetramerizes, and lacks an endogenous NLS. The triple fusion of GFP-putative NLS-β-gal allowed us to assess the activity of the cofilin NLS sequence by its ability to heterologously mediate GFP-β-Gal entry (>550KDa as tetramer) into the nucleus (Sorg and Stamminger, 1999). As a positive control, we expressed GFP-SV40NLS-β-Gal as the SV40 NLS is a well-defined monopartite NLS that is known to mediate β-Gal nuclear entry (Kalderon et al., 1984). While the positive control is active in our cell lines, the putative cofilin monopartite NLS sequence was not able to mediate β-Gal nuclear entry (Figure 3.3D&E), indicating that amino acids 26-36 in cofilin do not function as an NLS in this classic assay. The extended putative cofilin bipartite NLS was able to mediate the nuclear entry of GFP-β-Gal indicating that it can function as an active NLS (Figure 3.3D&E). When both critical basic regions were mutated to alanines in the triple fusion GFP-(AASSTPEEVKAAKK)-β-Gal, the sequence could no longer mediate nuclear entry of β-Gal (Figure 3.3D&E). Additional testing of these constructs in mouse NIH 3T3 fibroblasts confirmed that the NLS activity

was not cell type specific (Figure 3.4). To test whether the bipartite NLS sequence functions in the context of the full length cofilin protein, we mutated both basic regions to make the fusion EYFP-cofilin RK21-22AA KR31-32AA. Under steady state conditions, EYFP-cofilin RK21-22AA KR31-32AA had less percent nuclear fluorescent signal compared to wild type EYFP-cofilin (Figure 3.3F&G and Table 3.1). As with the cofilin NES mutant, the cofilin NLS mutant is no longer capable of forming nuclear or cytoplasmic rods (Table 3.1). The NLS mutant in the context of full length cofilin was also functional in NIH 3T3 fibroblasts indicating this is not a cell type specific effect (Figure 3.4 and Table 3.1).

To test if the decrease in nuclear signal of EYFP-cofilin KR21-22AA RK31-32AA, the NLS mutant (Figure 3.3F&G), is in part mediated by active nuclear export via the NES, and not simply an exclusion from the nucleus due to the cumulative size of EYFP fused to cofilin (44 kDa in total), we treated cells expressing EYFP-cofilin or EYFP-cofilin RK21-22AA KR31-32AA with leptomycin B. We also created a full-length, NLS mutant cofilin construct fused between GFP and β-Gal. Due to the high molecular weight of β-Gal in addition to cofilin and GFP (156kDa as monomer, 624kDa as tetramer), this construct far exceeds the predicted diffusion limit of the nuclear pore and is thus too large to diffuse into the nucleus upon leptomycin B treatment, even with an inactive NES. After leptomycin B treatment both EYFP-cofilin and EYFP-cofilin RK21-22AA KR31-32AA had an increase in nuclear fluorescence, however the GFP-cofilin RK21-22AA KR31-32AA β-Gal construct did not (Figure 3.3H&I and Table 3.2), indicating the NLS and NES are functional in the context of the EYFP-cofilin protein and that the EYFP-cofilin is not being excluded from the nucleus due to size when the NLS is mutated (Figure 3H&I).

In attempt to further verify these findings, we tested our cofilin NLS and NES mutants fused to the 22 amino acid tag, 3xFLAG (DYKDHD-G- DYKDHD-I-DHKDDDDK). We expressed these constructs and performed immunofluorescence using an α-FLAG monoclonal antibody. Under steady state conditions, we found no difference in percent

nuclear fluorescent signal regardless of mutation (Figure 3.5 and Table 3.3). However, during heat shock stress, we did observe a reduced ability of FLAG-tagged cofilin NLS mutant to enter the nucleus compared to those constructs where the NLS remained intact (Figure 3.5 and Table 3.3). We interpreted these results cautiously, since the cofilin-3xFLAG construct showed signs of functional impairment, forming almost no rods during heat shock, whereas EYFP-cofilin forms rods in a similar manner to endogenous cofilin (Munsie et al., 2011) (Table 3.1 and Table 3.3). This may have been due to the significant increase in acidic charge (11 of 22 residues) due to the 3xFLAG fusion to cofilin or due to differences and artifacts in immunofluorescent imaging versus direct live cell imaging (Schnell et al., 2012). The differences are not due to tag location since cofilin behaves the same when tagged with EYFP at either the amino or carboxyl terminus (data not shown).

Table 1: AFP-Cofilin constructs nuclear signal and ability to form rods during stress

					in Vitro actin binding assay	
Cell Line	**Construct**	**% Nuclear±SE**	**Rod Formation**	**Bind actin by FRET**	**Highspeed**	**Lowspeed**
ST*Hdh*$^{Q7/Q7}$	wildtype**	33.51±1.03	+++	Y	Y	Y
ST*Hdh*$^{Q7/Q7}$	V20A**	43.08±1.35**	-	N	Y	N
ST*Hdh*$^{Q7/Q7}$	KR31-32AA	32.01±1.39 NS	++	NA	NA	NA
ST*Hdh*$^{Q7/Q7}$	RK21-22AA** KR31-32AA	25.36±1.35**	-	Y	Y	N
ST*Hdh*$^{Q7/Q7}$	R21A**	29.29±0.89*	-	Y	Y	N
ST*Hdh*$^{Q7/Q7}$	K22A**	30.48±0.91*	+	Y	Y	Y
NIH 3T3	wildtype	27.54±1.15*	NA	NA	NA	NA
NIH 3T3	V20A	36.67±1.14**	NA	NA	NA	NA
NIH 3T3	RK21-22AA KR31-32AA	21.01±0.95**	NA	NA	NA	NA

Construct

** assay performed multiple times in cells with and without endogenous cofilin knocked down

% nuclear - student T-test compared to wildtype cofilin *p<0.05 **p<0.001 NS=not significant

Rod Formation - % of cells with rods after 60 min. heat shock +++ (average 20+) ++(average of 10-20%) +(average of 1-10%)

Table 3.1: Comparison of percent nuclear fluorescent signal, rod forming ability and actin binding ability of different cofilin NES and NLS mutants tagged to EYFP in different cell types.

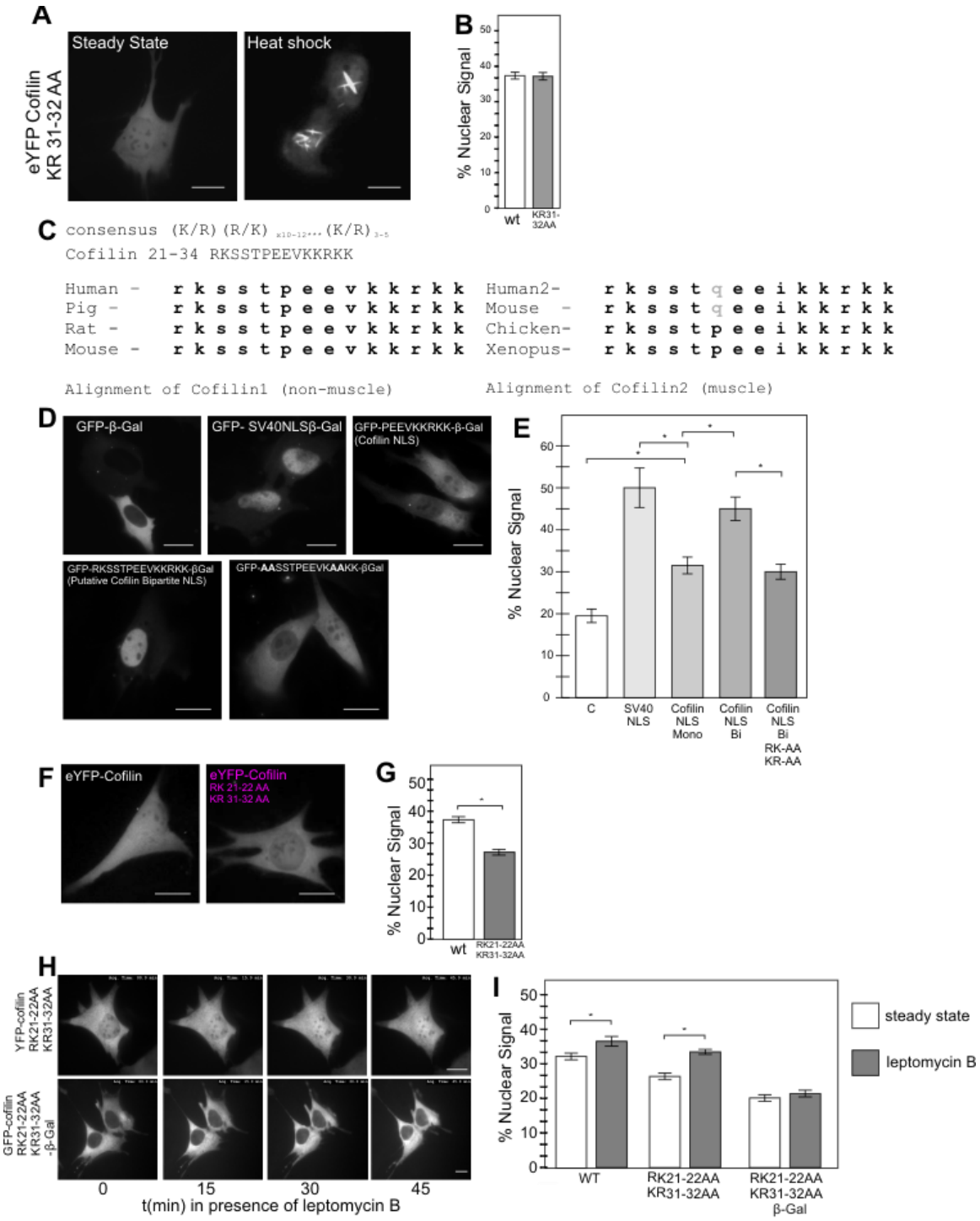

Figure 3.3 : Cofilin has a highly conserved putative bi-partite NLS. – LEGEND next page

Figure 3.3 : Cofilin has a highly conserved putative bi-partite NLS. (A) EYFP-cofilinKR31-32AA was transfected into STHdh cells and cells were heat shocked showing nuclear signal and rod formation. All images taken at 60X on a wide field microscope. All Scale bars = 10µm **(B)** Graph represents percent nuclear fluorescent signal analysis for EYFP-cofilin vs. EYFP-cofilin KR31-32AA under steady state conditions in live cells. N=at least 30 per construct/condition. **(C)** Bi-partite NLS consensus and matching sequence in cofilin. Sequence comparison of the human cofilin1 and cofilin2 bi-partite NLS with that of other species of cofilin. **(D)** The putative cofilin bipartite NLS mediates βGal nuclear entry. GFP-βGal, GFP-SV40NLS-βGal, GFP-cofilin NLS-βGal, GFP-cofilin-bipartite NLS-βGal and GFP-cofilin bipartite NLS-βGal RK21-22AA KR31-32AA were transfected into STHdh cells to look for active nuclear import. **(E)** Graph represents percent nuclear fluorescent signal analysis for each construct N= at least 30 cells/construct, *P<0.05. Images taken in fixed cells. **(F)** Mutating both parts of the bipartite NLS affects cofilin nuclear entry. EYFP-cofilin or EYFP-cofilin RK21-22AA KR31-32AA were transfected into STHdh cells. **(G)** Percent nuclear fluorescent signal analysis for each construct in live cells. N= at least 30 cells/construct *P<0.05. **(H)** EYFP-cofilin RK21-22AA KR31-32AA or GFP-cofilin RK21-22AA KR31-32AA- βGal were transfected into STHdh cells and treated with 5ng/mL leptomycin B. Live imaging was performed after leptomycin B addition at 5ng/mL. **(I)** Graph represents percent nuclear fluorescent signal analysis for EYFP-cofilin, EYFP-cofilin RK21-22AA KR31-32AA and GFP-cofilin RK21-22AA KR31-32AA- βGal in control and leptomycin B-treated cells. N= at least 30 cells/construct, *P<0.05.

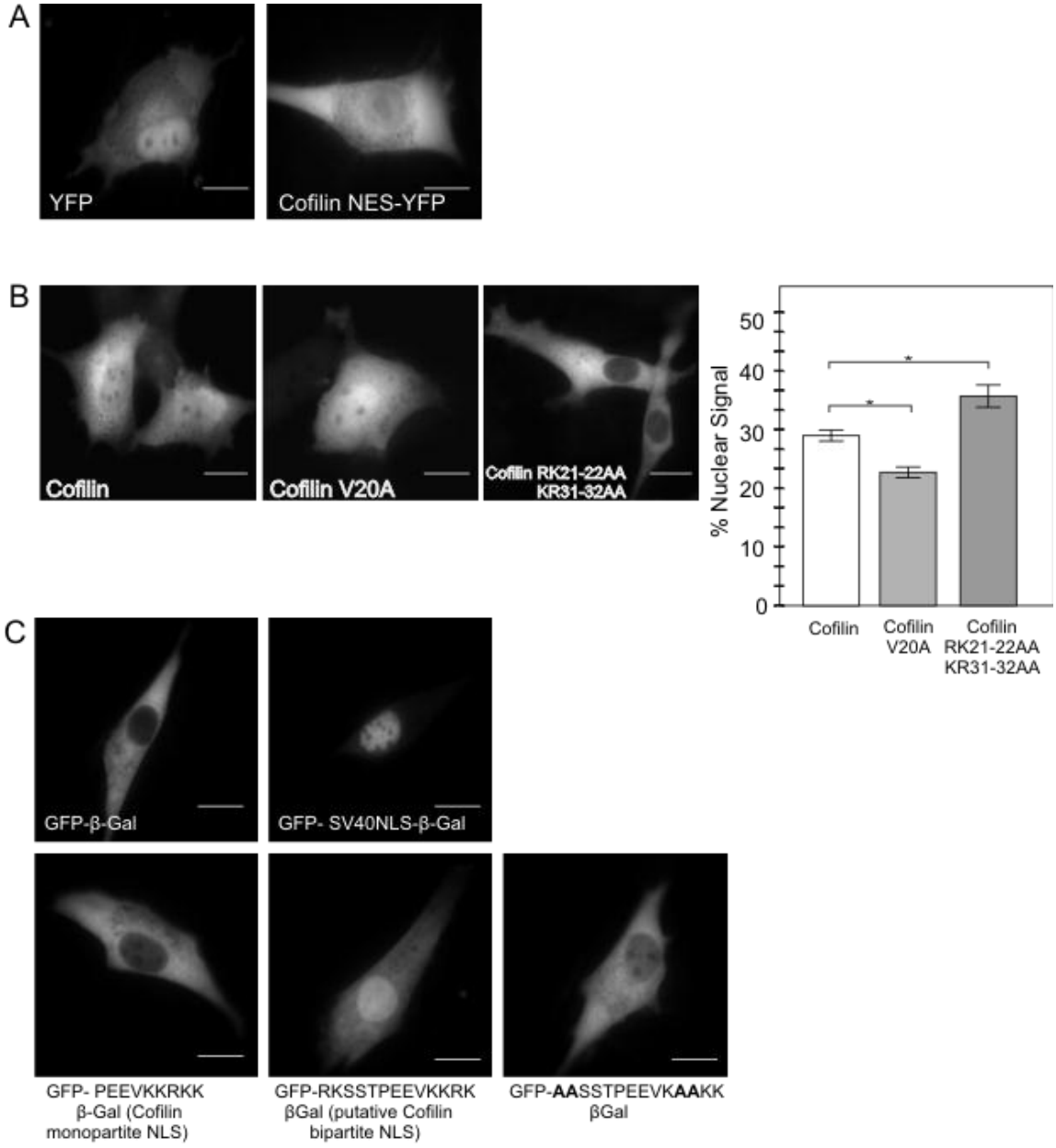

Figure 3.4: Cofilin NES and bipartite NLS function in multiple cell types. (A) EYFP and EYFP-cofilin NES were expressed in NIH3T3 cells showing that the cofilin NES sequence functions in multiple cell types. **(B)** EYFP-cofilin, EYFP-cofilin V20A and EYFP-cofilin RK21-22AA, RK31-32AA were transfected into NIH3T3 cells. Graph represents percent nuclear fluorescent signal analysis for all constructs in live NIH3T3 cells. N= at least 30 per construct/condition *P value<0.05. **(C)** All synthetic NLS reporter constructs were expressed in NIH3T3 cells. Cofilin localization was similar to STHdh cells. All imaging was done in live cells at 60X on a wide field microscope. All scale bars = 10µm.

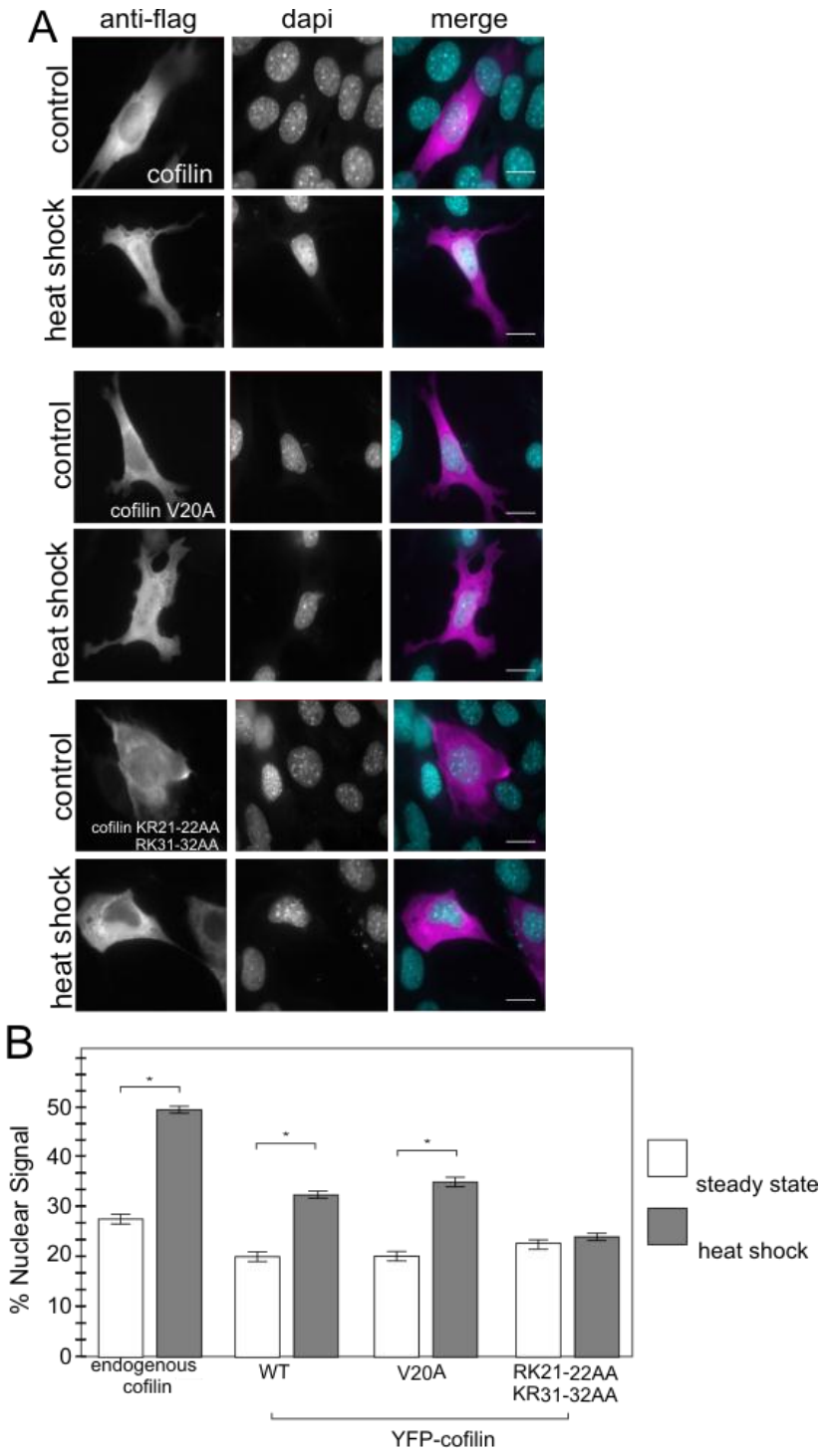

Figure 3.5: Endogenous cofilin and cofilin-3xFLAG constructs percent nuclear fluorescent signal analysis before and after heat shock by immunofluorescence. – Figure Legend on next page

Figure 3.5: Endogenous cofilin and cofilin-3xFLAG constructs percent nuclear fluorescent signal analysis before and after heat shock by immunofluorescence. (A) Cells were transfected with cofilin-3xFLAG, cofilin-3xFLAG V20A or cofilin-3XFLAG RK21-22AA RK31-32AA. Cells were then immediately fixed or subjected to heat shock for 1 h prior to fixing. Cells were immunostained using α-FLAG antibody. Images taken at 60X on a wide field microscope. Scale bar = 10μm. **(B)** Graph represents percent nuclear fluorescent signal analysis performed prior to and after heat shock stress on endogenous cofilin visualized by immunostaining with α-cofilin or cells expressing cofilin-3xFLAG constructs and visualized by immunostaining with α-FLAG antibody. N= at least 40 per dish/condition. *P value<0.05.

Table 1: Changes in percent nuclear signal for cofilin constructs in the presence of Leptomycin B

Cell Line	Construct	Leptomycin B	% Nuclear±SE
ST*Hdh*$^{Q7/Q7}$	YFP-cofiin	-	33.17±1.03
ST*Hdh*$^{Q7/Q7}$	YFP-cofilin	+	36.06±0.87*
ST*Hdh*$^{Q7/Q7}$	YFP-Cofilin RK21-22AA KR31-32AA	-	26.72±0.54
ST*Hdh*$^{Q7/Q7}$	YFP-Cofilin RK21-22AA KR31-32AA	+	33.98±0.94**
ST*Hdh*$^{Q7/Q7}$	GFP-Cofilin RK21-22AA KR31-32AA-β-Gal	-	20.39±1.45
ST*Hdh*$^{Q7/Q7}$	GFP-Cofilin RK21-22AA KR31-32AA-β-Gal	+	21.61±0.85 NS

% nuclear - student T-test compared to no leptomycin B *p<0.05 **p<0.001 NS=not significant

Table 3.2: Comparison of changes in percent nuclear fluorescent signal on cofilin and cofilin NLS mutations in the presence of leptomycin B.

Table 3: Changes in percent nuclear signal for cofiln during stress using immunofluorescence

Cell Line		Heat Shock	% Nuclear±SE	Rod Formation
ST*Hdh*$^{Q7/Q7}$	endogenous	-	27.05±0.77	NA
ST*Hdh*$^{Q7/Q7}$	endogenous	+	50.54±1.39**	+++
	FLAG Construct			
ST*Hdh*$^{Q7/Q7}$	wildtype	-	21.46±0.86	NA
ST*Hdh*$^{Q7/Q7}$	wildtype	+	32.74±0.98*	+
ST*Hdh*$^{Q7/Q7}$	V20A	-	20.36±1.14	NA
ST*Hdh*$^{Q7/Q7}$	V20A	+	34.74±1.06*	-
ST*Hdh*$^{Q7/Q7}$	RK21-22AA KR31-32AA	-	23.45±0.84	NA
ST*Hdh*$^{Q7/Q7}$	RK21-22AA KR31-32AA	+	25.33±0.91 NS	-

% nuclear - student T-test compared to no heat shock *p<0.05 **p<0.001 NS=not significant

Rod Formation - % of cells with rods after 60 min. heat shock +++ (average 20%+) ++(average of 10-20%) +(average of 1-10%) - (0%)

Table 3.3: Comparison of changes in percent nuclear fluorescent signal and rod forming ability of endogenous cofilin and FLAG tagged cofilin constructs before and after heat shock.

The cofilin NLS-inactive mutant can bind actin *in vivo*

It has been hypothesized that being able to inhibit rod formation or break down rods could be a novel therapeutic approach for HD or AD (Bamburg et al., 2010), however the absolute requirement of cofilin-actin rod formation during cell stress response is unknown. We hypothesized that regulating cofilin nuclear import and export may be an avenue to modulate rod formation and that we could use these mutants to test our hypothesis *in vivo*. Therefore, we had to ascertain if these mutants could still bind actin and therefore still be able to perform other critical cellular functions. Using an *in vitro* F-actin co-sedimentation assay, we show that both V20A and RK 21-22AA KR31-32AA have some ability to bind F-actin, however neither bound as strongly as wild-type cofilin (Figure 3.6). To measure the cofilin-actin interaction *in vivo*, we employed Fluorescent Lifetime Imaging Microscopy (FLIM) to accurately measure Förster Resonance Energy Transfer (FRET) between cofilin and actin in a live cell environment. FRET can be used to measure protein-protein interactions at the nanometer scale in live cells by calculating efficiency of the resonant transfer of energy from a donor to an acceptor fluorophore. For mCerulean and EYFP donor-acceptor pairs, optimal FRET efficiency occurs at 8 nm or less, for a maximal possible FRET efficiency of ~30%, as dictated by the degree of spectral overlap between mCerulean emission and EYFP excitation. FLIM measures this transfer of energy by measuring the change in the lifetime of the donor fluorophore in the absence and presence of the acceptor fluorophore (Lleres et al., 2009; Lleres et al., 2007). FRET determination by this method is independent of donor/acceptor fluorophore concentrations, as only the donor lifetime is being measured, thus is optimal for two molecule FRET, without concern of spectral overlap as with other methods. FRET efficiency is calculated using the formula E_{FRET} = 1- (Average lifetime D.A/ Average lifetime Donor), where average lifetime D.A

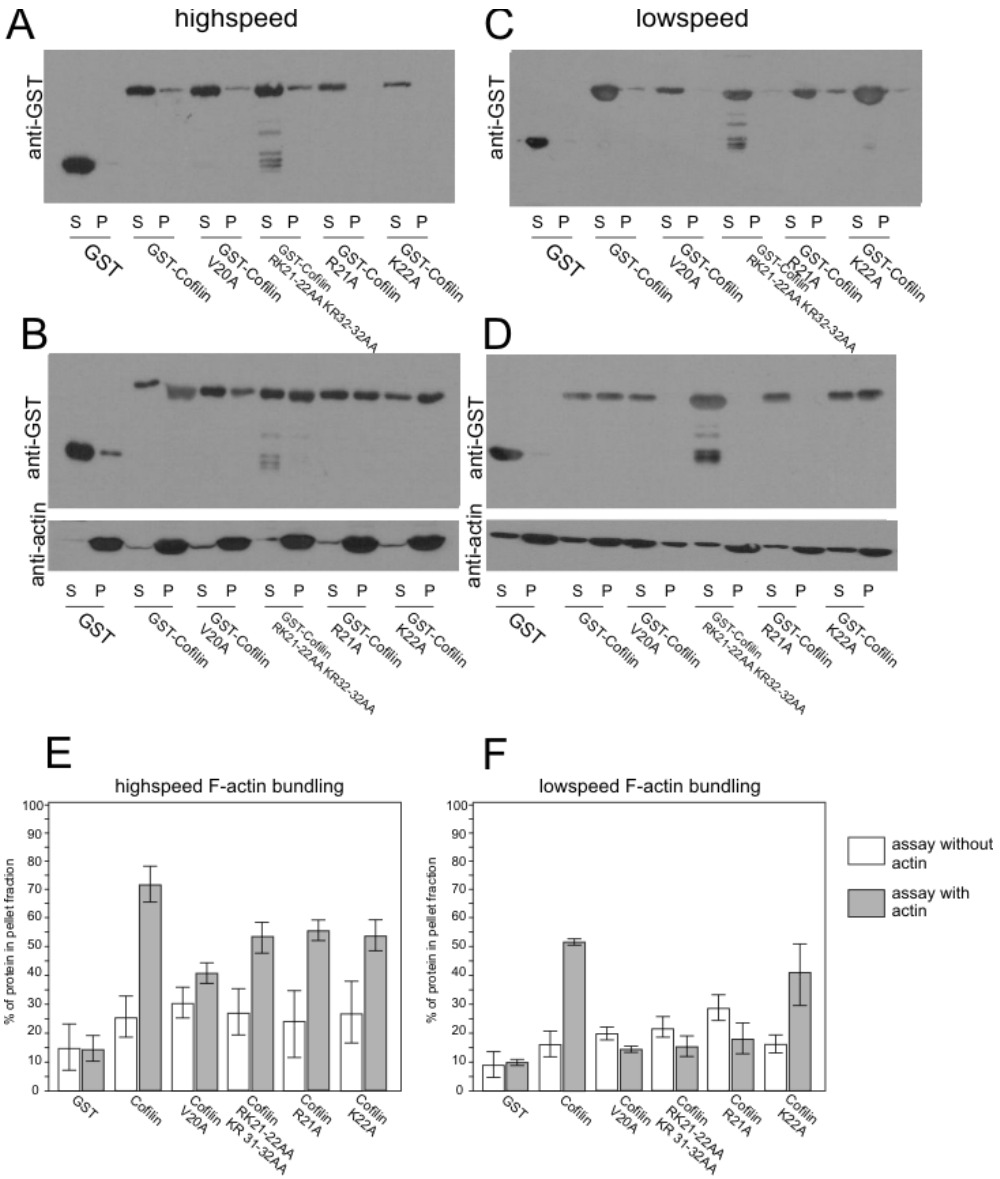

Figure 3.6: F-actin binding and bundling co-sedimentation assays. Cofilin mutants tagged to GST were incubated alone **(A) (C)** or cofilin mutants were incubated with F-actin for 40 minutes **(B) (D)**. The samples were then centrifuged at 150,000X*g* (high speed) **(A) (B)** for F-actin binding activity or 14,000X*g* (low speed) **(C) (D)** for F-actin bundling activity. Equal portions of the pellet (P) and supernatant (S) were subjected to SDS-PAGE and western blotting for GST and actin was performed. Graphs **(E) (F)** shows percent of GST construct in pellet fraction from western blot determined by pixel intensity analysis using NIH Image J. Graphs are representative of the average amount of protein in the pellet fraction from 3 separate trials. Error = standard error from the mean.

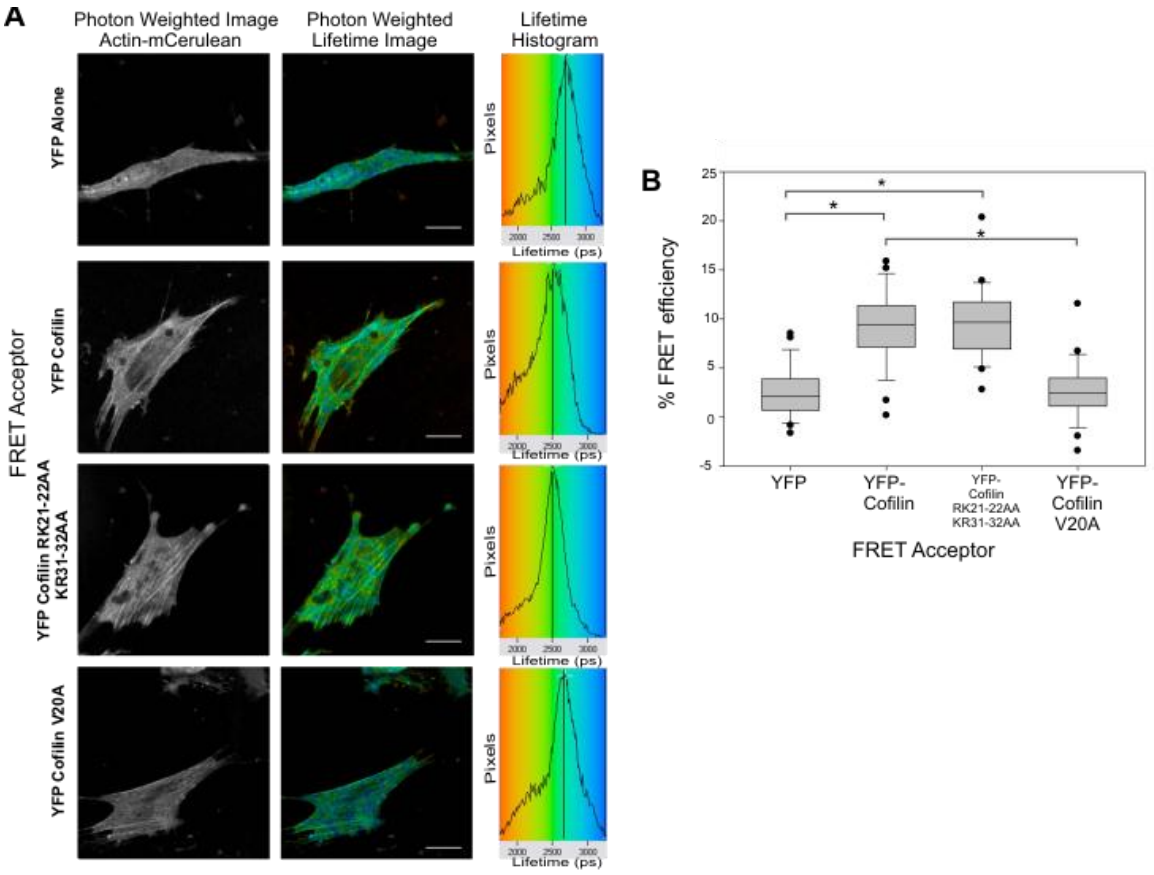

Figure 3.7: Mutant NLS cofilin can bind actin *in vivo*, while mutant NES cofilin cannot. **(A)** STHdh cells were transiently transfected with mCerulean-actin and either EYFP alone, EYFP-cofilin, EYFP-cofilinV20A or EYFP-cofilin RK21-22AA KR31-32AA for FRET analysis. Fluorescence lifetimes are presented in a continuous pseudo-color scale representing time values ranging from 1750 to 3250 ps. The lifetime distribution curve of the mCerulean-actin is shown as a histogram on the pseudo-color scale. The vertical line marks the mode lifetime distribution for the ROI. **(B)** Box and whisker plot of calculated percent FRET efficiency. Percent of FRET efficiency was calculated using the formula E_{FRET} = 1- (Average lifetime D.A/ Average lifetime D) * 100, where Average lifetime D.A = the average lifetime of mCerulean-actin in the presence of the indicated acceptor and Average lifetime D= the overall average lifetime of mCerulean-actin alone (no acceptor present). N=3, n=10 for each Donor-Acceptor pair. *P<0.001 Box = 1 S.D. from mean; Whiskers = 2 S.D. from mean; spots = outlier data points.

indicates the average lifetime of the donor in the presence of the indicated acceptor. We used mCerulean-actin as the donor and EYFP alone as a negative control acceptor, EYFP-cofilin as a positive control acceptor and EYFP- cofilin NES and NLS mutants as the experimental acceptors (Figure 3.7). The lifetime of mCerulean alone is approximately 2.9 nanoseconds (ns) (Rizzo et al., 2004) , and when mCerulean was tagged to actin this construct had an average lifetime of approximately 2.7 ns. In the presence of molar excess of EYFP alone (negative control) the lifetime of mCerulean-actin was slightly decreased giving a FRET efficiency of 2.6%. In the presence of EYFP-cofilin (positive control), which is known to interact with mCerulean-actin to allow FRET, the mCerulean-actin lifetime was decreased and FRET efficiency was 9.0%. In the presence of the cofilin NLS mutant there was a FRET efficiency of 9.6%, similar to EYFP-cofilin indicating that this mutant retains the ability to interact with actin *in vivo*. In the presence of the cofilin NES mutant the FRET efficiency was 2.6%, which was the same as EYFP alone, indicating that this cofilin mutant has lost its ability to interact with actin in our live cell based assay (Figure 3.7B). Based on this data, we decided to further assay the requirement of rod formation using the cofilin NLS mutant.

Cofilin NLS mutants affect rod forming ability during stress

Although the cofilin NLS mutant, RK21-22AA KR31-32AA, could still bind actin *in vivo*, we wanted to test if a minimal mutation to the cofilin NLS would have the same effect on nuclear localization, actin binding and rod formation as RK21-22AA KR31-32AA. We created two new mutations in the first basic region of the bipartite NLS, resulting in EYFP-cofilin R21A and EYFP-cofilin K22A. We did not focus on KR31-32AA as we already had found mutating these residues did not affect cofilin nuclear localization and this mutation did not abolish rod formation (Figure 3.3A and Table 3.1). We measured the ability of the R21A and K22A cofilin mutant's ability to bind F-actin *in vitro* and found that these mutants maintained some F-actin binding ability (Figure 3.6). As

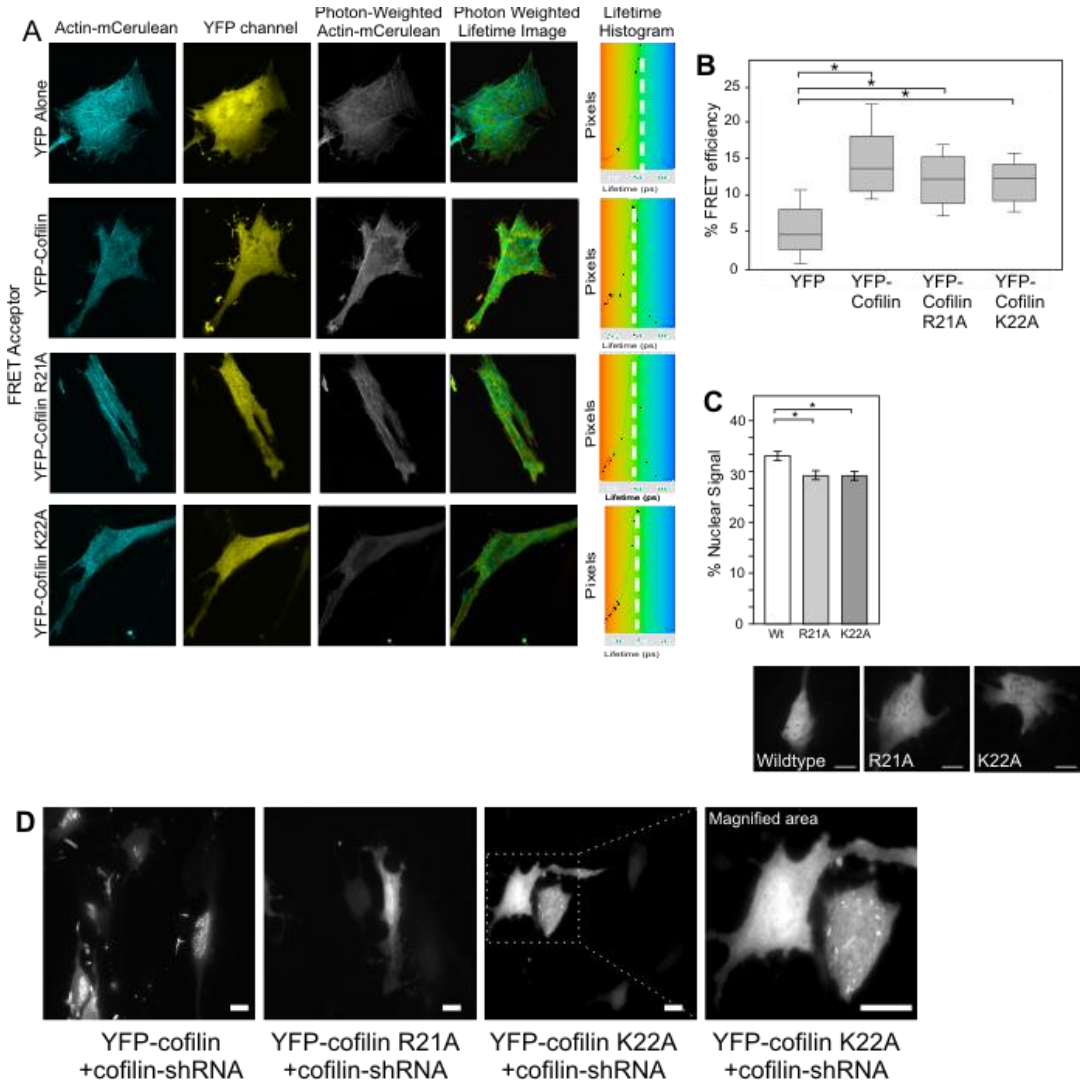

Figure 3.8: Analysis of R21A and K22A cofilin mutations on nuclear shuttling of cofilin, actin binding and rod formation during stress. (A) Cells were transfected with plasmids encoding EYFP-cofilin, EYFP-cofilin R21A or EYFP-cofilin K22A. Representative images show expression levels of EYFP and mCerulean, microscope settings kept consistent within each channel. Cells shown have similar mCerulean and EYFP intensities (intensity quantified using NIH Image J). Fluorescence lifetimes are presented in a continuous pseudo-color scale representing time values ranging from 1750 to 3250 ps. The lifetime distribution curve of the mCerulean-actin is shown as a histogram on the pseudo-color scale. The vertical line marks the mode lifetime distribution for the ROI. (**B**) Box and whisker plot of calculated FRET efficiency shown. For each Donor-Acceptor pair - N=3, n= at least 10. * P<0.05. Box = 1 S.D. from mean; Whiskers = 2 S.D. from mean **(C)** Graph represents percent nuclear fluorescent signal analysis for each construct. N = at least 30 cells. Images were taken in live cells. *P<0.05. Representative image shown for each construct. Imaging done at 60X on a wide field microscope. **(D)** Representative image of rod formation in each construct after 1 h heat shock at 20X magnification. Scale bars = 10µm

expected, both the R21A and K22A cofilin mutant fusion proteins retained the ability to bind actin *in vivo* by measuring FLIM-FRET (Figure 3.8A&B). Quantification of percent nuclear fluorescent signal showed that each of these mutations affected the ability of cofilin to enter the nucleus (Figure 3.8C) but not to the same extent as mutating both halves of the NLS (Table 3.1). We subjected cells expressing the R21A and K22A constructs to cofilin/actin rod-inducing stress. Under conditions of heat shock or ATP depletion, the R21A mutant did not form any cofilin rods (Figure 3.8D and Table 3.1), however the K22A mutant still formed rods in 2.8% of cells after a one hour heat shock, although fewer than wild type EYFP-cofilin which formed rods in 37% of cells (Figure 3.8D and Table 3.1). We additionally performed an *in vitro* F-actin co-sedimentation assay at low speed centrifugation, to determine actin bundling activity of our cofilin mutants and found that only wild-type cofilin and cofilin K22A had actin bundling activity, whereas all other mutants, NLS and NES had no F-actin bundling activity *in vitro* (Figure 3.6C,D&F) which may correspond to rod forming ability *in vivo*. This assay could just be detecting F-actin binding and further work would need to be done to show any bundling or rod forming activity, however during low speed spins wild-type cofilin and K22A cofilin were the only proteins to co-sediment with F-actin consistently, although varying amounts of F-actin were detected in pellet and supernatant during these low speed experiments.

To reduce effects of endogenous wild-type cofilin, we created a system where cofilin mutants could be expressed on the same plasmid as an shRNA to endogenous cofilin allowing simultaneous knockdown of the endogenous protein and over-expression of our cofilin mutants. The EYFP-cofilin contains a silent mutation in the cofilin DNA sequence which makes it immune to shRNA knockdown (Figure 3.9A). We tested these constructs for knockdown of endogenous cofilin and found that the shRNA worked effectively on endogenous cofilin but allowed our EYFP constructs to be expressed (Figure 3.9B-E). Knocking down endogenous cofilin had no effect on our

EYFP-cofilin and cofilin mutants ability to enter the nucleus or form rods (Table 3.1). When observing cells undergoing heat shock with cofilin knocked down we noted that cells would rapidly shrink, a sign of poor cell health or apoptosis (Figure 3.10A and Video 3.3) whereas cells where wild-type EYFP-cofilin was re-expressed tolerated cell stress by forming rods and generally maintained their cell shape and size (Figure 3.10A and Video 3.4). During heat shock stress rods formed by endogenous cofilin and actin almost exclusively form in the nucleus, however when over-expressing cofilin we often get rods forming in the nucleus and cytoplasm in response to heat shock likely due to a higher local cofilin-actin ratio in the cell, as shown in Video 3.4. The ability of cofilin to form rods in general appears to be protective, and it seems that the shuttling capabilities of cofilin is required for both nuclear and cytoplasmic rods, likely through a similar mechanism. Since cell shrinkage is a sign of apoptosis (Friis et al., 2005), we wanted to investigate if these cells with knocked-down levels of cofilin and undergoing heat shock stress were shrinking due to apoptosis or shrinking due to another reason, since cofilin knockdown can actually inhibit some forms of oxidant-induced apoptosis (Klamt et al., 2009). To analyze this we used immunofluorescence against two proteins that change localization during apoptosis: cytochrome C and activated Bax (Annis et al., 2001), in cells expressing our cofilin-shRNA plasmid before and after heat shock. For the Bax immunofluorescence, we used an antibody that recognizes an epitope to Bax that is only exposed when it undergoes a conformation shift during apoptosis (Eskes et al., 1998). After heat shock we found a shift in localization from mitochondria (Figure 3.11A) to diffuse cytochrome C staining (Figure 3.11B) indicating apoptosis, as well as an increase and change in localization of Bax in cells expressing cofilin-shRNA-EYFP (Figure 3.11). These cells are also visibly smaller than surrounding cells not expressing cofilin-shRNA-EYFP, indicating that these shrinking cells are likely undergoing apoptosis under stress conditions. We therefore used cell size after stress to measure cell health in our cofilin knockdown-EYFP-cofilin over-expression system.

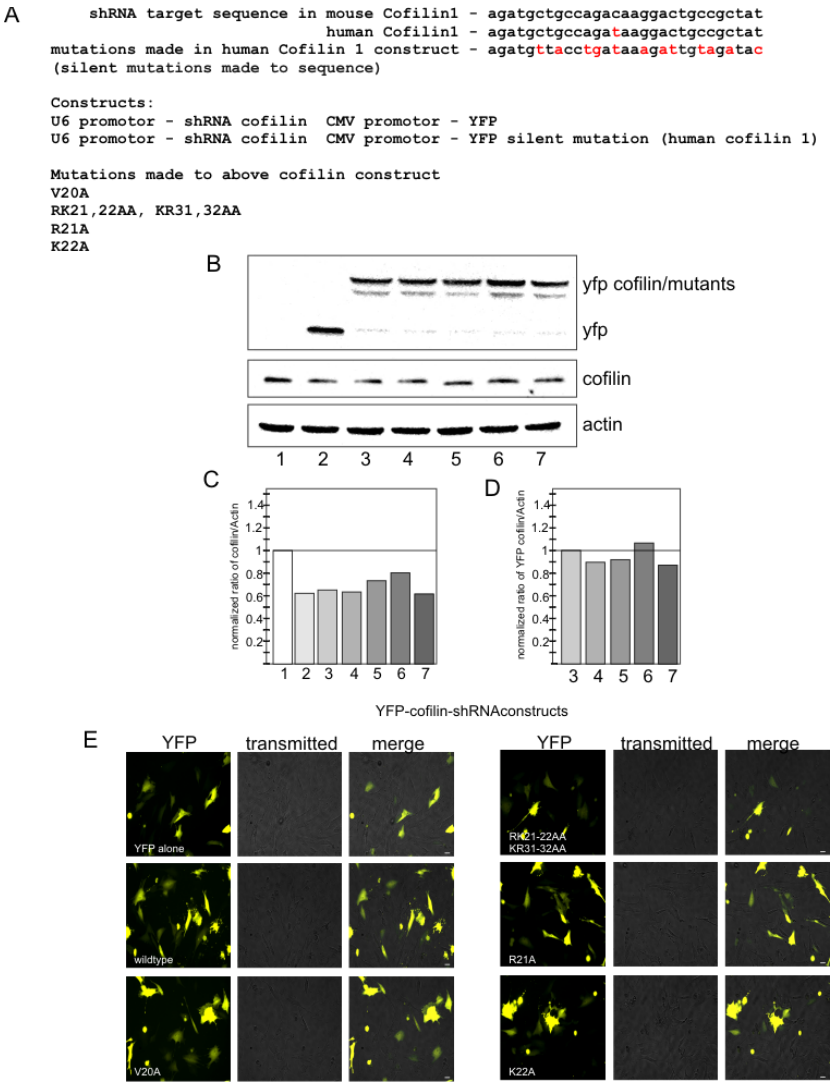

Figure 3.9: Cofilin shRNA knocks-down endogenous levels of cofilin and EYFP-cofilin over-expression is unaffected. (A) Cofilin shRNA target sequence and silent mutation made to human cofilin1 cDNA for over-expression. Vector components shown and cofilin mutations that were made in these constructs defined. **(B)** STHdh cells were either untransfected (1), or transfected with cofilin shRNA constructs tagged to EYFP (2), EYFP-cofilin (3), EYFP-cofilin V20A (4), EYFP-cofilin RK21-22AA KR31-32AA (5), EYFP-cofilin R21A(6) or EYFP-cofilin K22A (7). Constructs were expressed for 36 hours prior to cell imaging and cell lysis. Protein was extracted and western blot using α-EYFP, α-actin and α-cofilin was performed. **(C)** Normalized comparison of endogenous cofilin protein levels to actin by pixel intensity measure using NIH Image J for western blots. All constructs had similar levels of cofilin knockdown. **(D)** Normalized comparison of EYFP-cofilin and EYFP-cofilin mutant protein levels to actin by pixel intensity measure using NIH Image J. All constructs had similar levels of expression and similar break-down products. **(E)** Representative 20X images of cofilin-shRNA constructs showing similar transfection efficiency and expression levels of all constructs. Scale bar = 10µm.

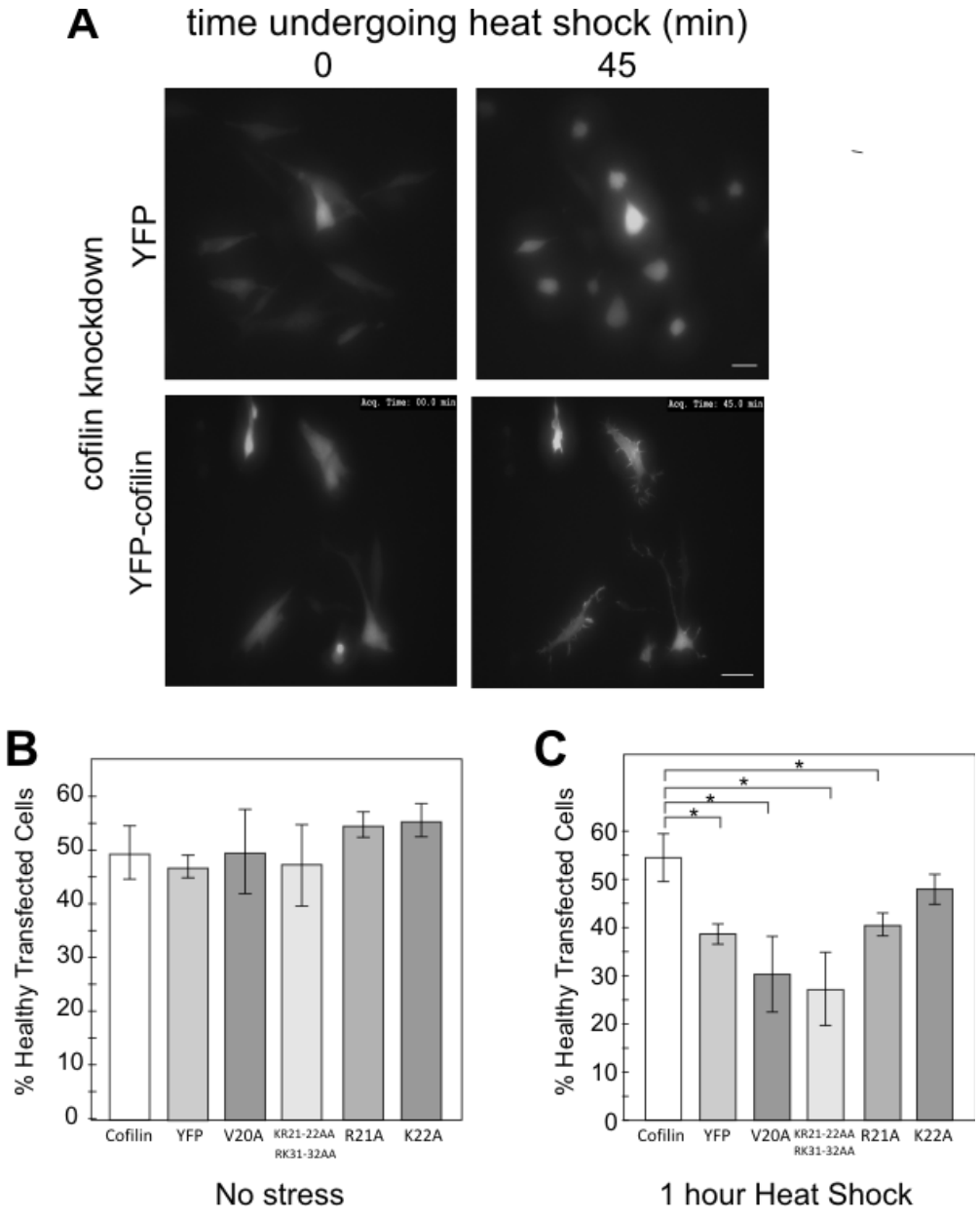

Figure 3.10: Ability of different cofilin mutations to rescue cell stress phenotype in cofilin knock-down cells. (A) Temporal 20X widefield imaging in cells expressing cofilin-shRNA-EYFP or cofilin-shRNA-EYFP-cofilin and imaged during the course of heat shock. Time represents the amount of time at 42°C in minutes. Cells imaged every 60 seconds. Scale bar = 10µm. **(B)** STHdh cells were transfected with cofilin-shRNA/EYFP-cofilin expression plasmids. Cells were imaged before and directly after 1 h heat shock in live cells at 20X. Images were run through a CellProfiler pipeline designed to detect healthy vs. unhealthy cells based on cell size along with other parameters. Prior to stress there are no significant differences in percent of cells with a healthy morphology. **(C)** After stress only the K22A mutation was not significantly different from wild-type cofilin in cell health. N=4, n=200-500 cells/construct/trial. *P<0.001.

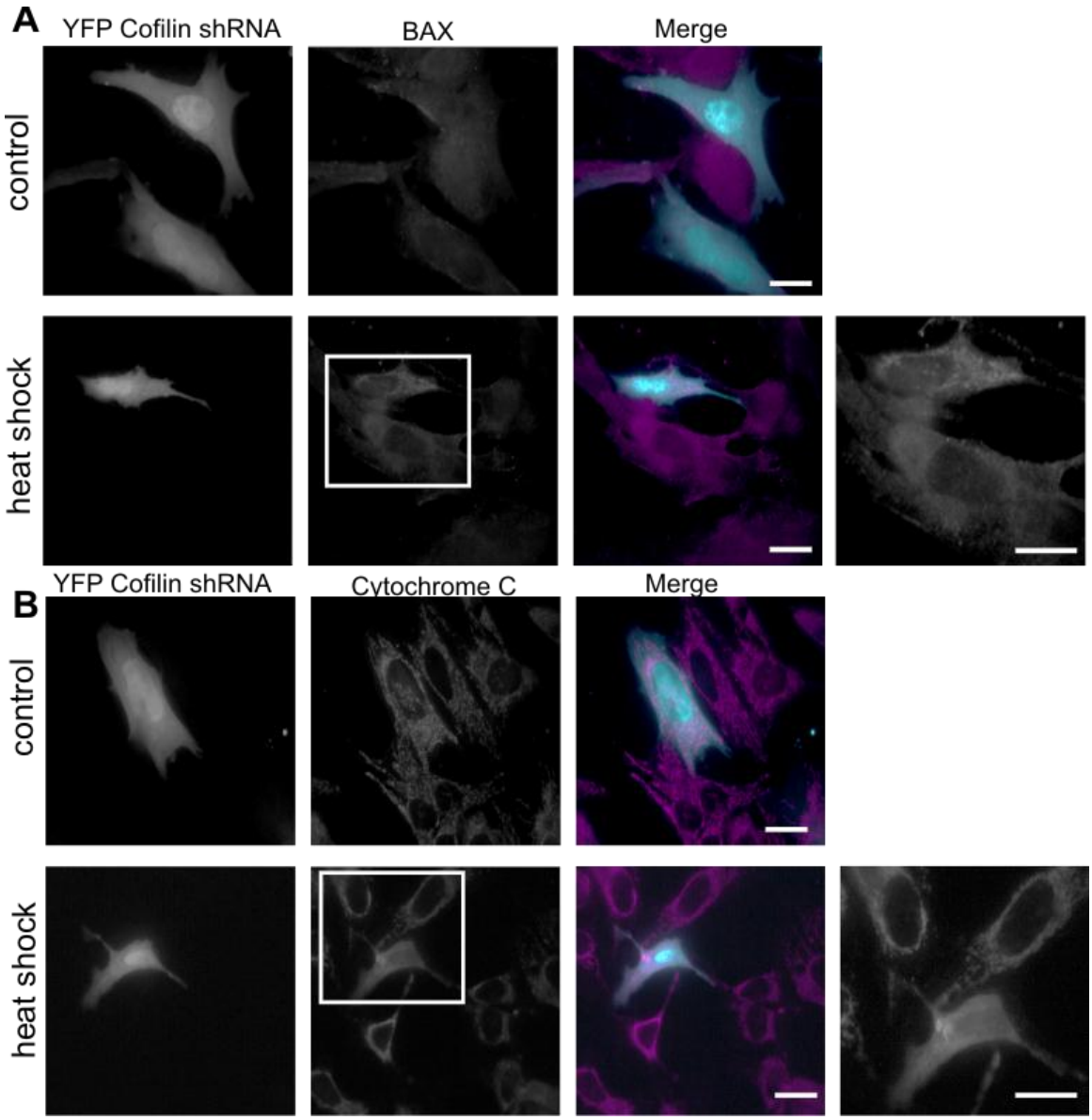

Figure 3.11: Cofilin knockdown causes cell shrinkage during cell stress that is linked to markers of apoptosis. STHdh cells were transfected with cofilin-shRNA-EYFP expression plasmid. Cells were fixed or heat shocked and fixed followed by immunostaining for markers of apoptosis: activated Bax **(A)** or cytochrome C **(B).** Wide field images at 60X, scale bar is 10µm.

To objectively quantify our assays with robust numbers and avoid investigator bias, we used an image based assay coupled with open-source software, CellProfiler™, to determine cell health based on cell morphology by automated image scoring (Lamprecht et al., 2007). The software can automatically identify objects from an image, measure and sort them based on pre-defined guidelines (pipelines). This method allows the unbiased quantification of large numbers of cells. An example of the pipeline we created is shown in Figure 3.12. We imaged cells expressing these constructs both prior to stress and directly after heat shock stress in live cells at 20X. Using cell size, approximately fifty percent of cells had a "healthy phenotype" based on cell size prior to cell stress (Figure 3.10B). All of our knockdown constructs had baseline toxicity, possibly due to the knockdown of cofilin and the over-expression of the EYFP-cofilin constructs from the CMV promoter. There were no differences in any of our constructs at steady state, likely due to the fact that some aspects of cofilin1 knockdown can be rescued by other family members including ADF (actin depolymerizing factor) (Hotulainen et al., 2005). Immediately after stress there was a significant increase in the unhealthy cell population when EYFP alone, V20A, RK 21-22AA KR31-32AA or R21A cofilin mutants were expressed, however there was less of a toxic effect when the K22A mutant was expressed compared to re-expression of wild-type cofilin (Figure 3.10C). This indicates that although cofilin mutants that cannot form rods can still bind actin, and under steady state do not have an obvious effect on cell health, they cannot rescue cells during stress. However, the K22A mutant maintained some ability to form rods, had some actin bundling activity *in vitro* and could mediate a better stress response than the other cofilin mutants (Figure 3.6D, Figure 3.8D and Figure 3.10C). This indicates that the cofilin protein is likely integral to cell health during stress and the rod forming function may be required for cell survival under stress conditions.

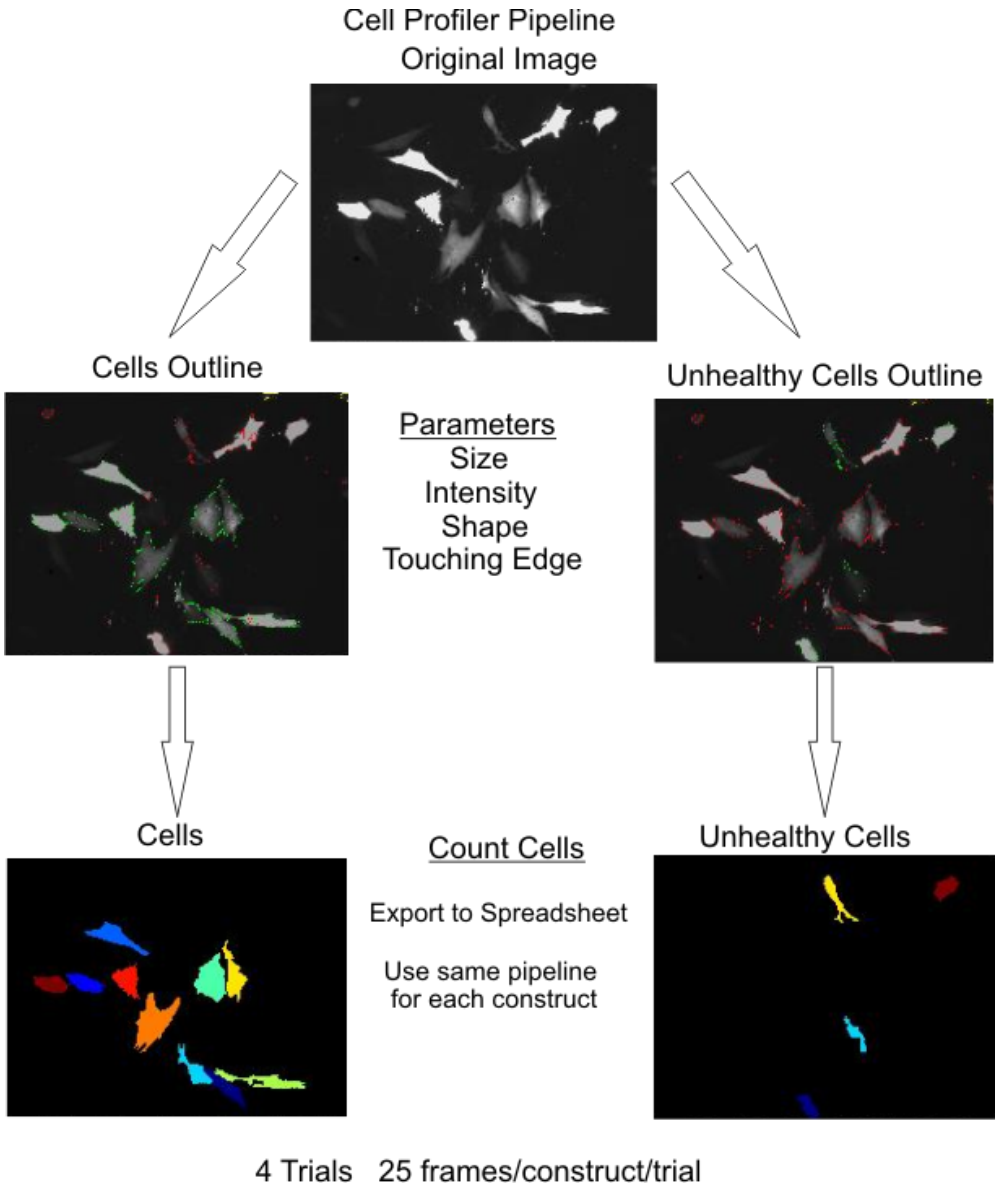

Figure 3.12: Derivation of cell profiler pipeline for quantification of cell health. Images were taken at 20X in live cells and cells divided into healthy and unhealthy populations based on size and morphology.

3.5 Discussion

At 18kDa, cofilin can passively diffuse in and out of the nucleus, however a large proportion of cofilin localizes to the nucleus during stress (Iida et al., 1992; Nishida et al., 1987) and recently cofilin has been shown to be required for actin nuclear import (Dopie et al., 2012). Actin is known to be transported out of the nucleus when bound to profilin through the exportin 6 pathway, and does not require cofilin for export (Dopie et al., 2012; Stuven et al., 2003). Although actin is now known to be active in the nucleus and therefore many actin binding proteins may be as well, cofilin seems to have its own nuclear functions aside from actin transport. Cofilin has been shown to be in complex with actin and phosphorylated RNA polymerase (pol) II and depleting cofilin from the cell affects active transcription (Obrdlik and Percipalle, 2011). It is hypothesized that cofilin is involved in regulating actin polymerization in the nucleus to accomplish this function; when cofilin is depleted from the cell actin no longer enters the nucleus and there is a decrease in pol II transcription, however simply forcing actin into the nucleus by tagging it with an NLS when cofilin is knocked down does not rescue these defects (Dopie et al., 2012). We further show that during certain stress events a large proportion of cellular cofilin can be found in the nucleus and is found at nuclear cofilin-actin rods. Small proteins, i.e. the 7 kDa HIV-1 Rev protein, can have active nuclear transport signals as the facilitated diffusion mediated by these signals through nuclear transport factors is far faster than passive diffusion (Mohr et al., 2009). We initially noted that cofilin rapidly exits the nucleus during prolonged cell stress and hypothesized the existence of an NES in cofilin. By visually searching the protein amino acid sequence we found a single sequence that fit the CRM1-dependent NES consensus. We found that this sequence was functional as an NES and was responsive to leptomycin B, indicating that export is through the classic CRM1 pathway. Using live cell imaging FLIM-FRET, we found that when this sequence was mutated at a single valine, V20A, cofilin lost its ability to bind actin *in vivo*. Subsequently, other amino acid

substitutions were assayed at position 20, but with similar loss of actin association (data not shown). While any actin-binding mutant of cofilin is likely to have pleiotropic effects on cofilin or cytoskeletal functions, the coincident phenotypes of NES inactivation and abrogated actin binding with V20A may suggest that actin association may competitively inhibit the NES by competing CRM1 and actin interactions.

Recently, actin was shown to compete with importins for binding to JMY, a regulator of transcription and actin filament assembly. In the presence of actin monomers, the nuclear import signal of JMY is inhibited (Bradley Zuchero et al., 2012). Other actin associated protein import and export is controlled by actin binding; including MAL, the serum-response factor co-activator. MAL has CRM1 dependent nuclear export activity that requires it to be bound to G-actin for nuclear export (Vartiainen et al., 2007). MAL has a bipartite NLS with a long intervening sequence that is activated when the G-actin pool is depleted (Pawlowski et al., 2010). The nuclear-cytoplasmic trafficking of these proteins is dependent on the polymerization state of actin. We propose that under cell stress events, the enhanced association of cofilin with F-actin in the nucleus at rods may prevent CRM1 interaction, thus allowing increased nuclear cofilin levels by active import of cofilin and the prevention of CRM1-mediated nuclear export of cofilin. The release of cofilin from actin rods would permit CRM1 interaction and thus reduce nuclear cofilin levels by active nuclear export (see model in Figure 3.13). This model would connect the higher order structural state of nuclear actin with cofilin sub-cellular localization, and hence compartmental activity.

When the putative cofilin NLS (26-PEEVKKRKKAV36) was mutated, we found no effect on nuclear localization under steady state conditions or stress conditions, and cofilin maintained its ability to form some rods in the nucleus, contrary to previously reported data (Iida et al., 1992). Discrepancies between data may reflect the different mutations: we chose to use alanine substitution with hopes of not disrupting the secondary structure of the protein, but still removing some critical basic charge, and

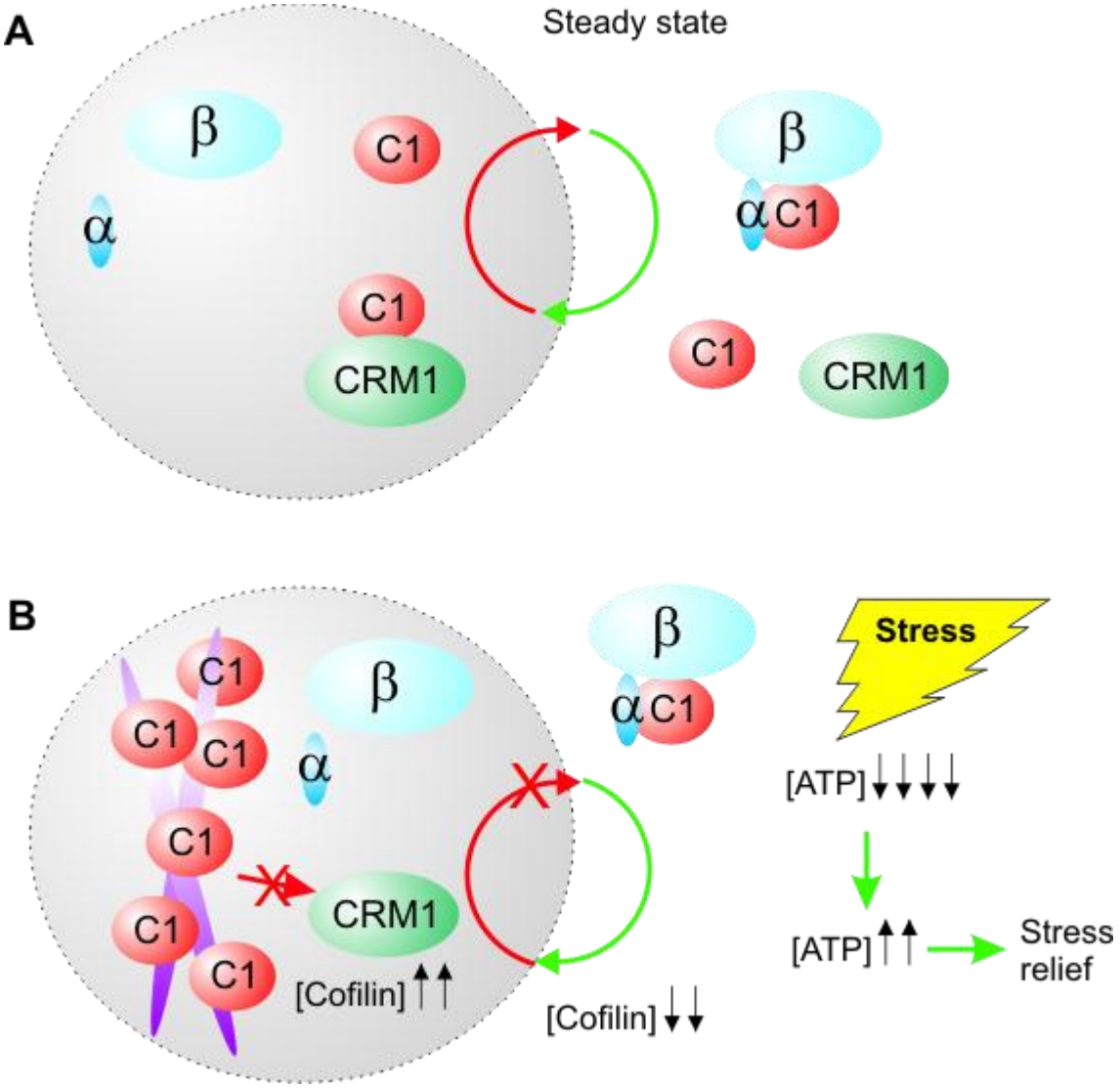

Figure 3.13: A model of cofilin interaction with F-actin rods regulating cofilin nuclear export during stress. **(A)** Under steady state conditions, cofilin shuttles between the nucleus and cytoplasm using the importin α/β and CRM1 pathways of import and export across the nuclear pore complex. **(B)** Under stress conditions, cofilin associates with F-actin in the nucleus, causing the formation of cofilin-actin rods, thus preventing interaction with CRM1, resulting in increased nuclear concentration of cofilin. Post stress, cofilin dissociates from rods and is allowed to interact with CRM1 to export from the nucleus as shown in live cell imaging in Fig. 1 and Supplemental Video 1.

that we performed direct imaging rather than indirect imaging methods. Upon closer examination of the amino acid sequence we found that seven amino acids upstream of the basic rich "KKRKK" sequence there was a conserved "RK" sequence. The sequence (21-RKSSTPEEVKKRKK-34) is consistent with a bipartite NLS sequence. The intervening sequence between the two basic rich sequences in a bipartite NLS is generally 10-12 amino acids long. In the cofilin NLS, this intervening sequence is shorter than predicted, however, it has been reported that the number of amino acids between the basic regions of a bipartite NLS can vary greatly, being either longer (Lange et al., 2010) or shorter (Taniguchi et al., 2002) than the earlier defined consensus. When we mutated both basic regions of the bipartite NLS (AASSTPEEVKAAKK) the nuclear localization signal was not functional, either out of context or in context of full length cofilin. We treated cells expressing the NLS mutant or wild-type cofilin with leptomycin B which induced increased nuclear accumulation of both constructs. If leptomycin B treatment were to cause a generalized cell stress, the increased nuclear accumulation of EYFP-cofilin could be attributed to its normal stress related function. However, since the NLS mutant also became more nuclear in response to leptomycin B, we can conclude that the compound is working more directly, by blocking the activity of the cofilin NES. This further supports our conclusion that cofilin has an active NES that is CRM1 dependent, and indicates that EYFP-cofilin RK21-22AA KR31-32AA exclusion from the nucleus under steady state conditions is due to active nuclear export and not simply protein size. However tagging EYFP to cofilin does bring the size of the protein closer to the diffusion limit of the nuclear pore. To try and determine if the NLS and NES are constitutively active and not just stress dependent signals, we tagged full length cofilin NLS or NES mutants to the 3xFLAG tag, which is much smaller than EYFP, and assessed nuclear localization of cofilin-3xFLAG using immunofluorescence. No changes were seen in the nuclear localization of cofilin under steady state conditions by immunofluorescence (Figure 3.5), however we did observe that when the NLS is mutated in this context, cofilin did not enter the nucleus during stress. The wild-type cofilin-3xFLAG vector did not form rods

as efficiently as endogenous or EYFP tagged cofilin (Tables 3.1 and 3.3). To date, the EYFP-cofilin construct has behaved the most appropriately in comparison to endogenous cofilin with respect to nuclear localization and rod formation during stress.

The ability of cofilin to enter the nucleus in the presence of leptomycin B was different when the cofilin NLS mutant was fused to EYFP as opposed to β-gal, indicating that EYFP-cofilin, although larger and possibly having different dynamics than endogenous cofilin, is still being shuttled out of the nucleus by some active transport and not simple diffusion. Although it is likely that active shuttling of cofilin is required during stress (Figure 3.1); the changes in localization of EYFP-cofilin NLS and NES mutants under no stress conditions suggests that there may be active shuttling of cofilin into and out of the nucleus under steady state conditions as well. With the newly defined role of cofilin in RNA polymerase activity (Obrdlik and Percipalle, 2011), it will be interesting to determine if the cofilin NLS is required for this function under steady state conditions; either bringing actin into the nucleus or if a specific pool of nuclear cofilin is required to regulate the polymerization of actin at actively transcribing genes. However, we focused our studies on the requirements of active transport of cofilin in response to stress.

The RK21-22AA KR31-32AA mutation did not impair the ability of cofilin to bind actin *in vivo*. This mutant did inhibit rod formation and its expression under stress conditions affected cell health. Single mutations to the first basic regions in the bipartite NLS, R21A and K22A affected nuclear localization of cofilin, however not to the same extent as mutating both halves of the NLS, but also maintained their ability to bind actin. There were differences in these mutants abilities to bind F-actin *in vitro* and therefore may have different affinities for F-actin versus G-actin or may differ in their abilities to sever F-actin. While the R21A mutant could not form rods under any stress condition tested, the K22A mutant could still form rods, although to a lesser extent than wild-type cofilin, and was the only mutant that had F-actin bundling/binding activity *in*

vitro when co-sedimentation was performed at low speeds. When analyzing cell health in cells expressing these constructs, the R21A mutant had fewer healthy cells after stress compared to the K22A mutant or wild-type cofilin, indicating that the ability of cofilin to properly bind actin and form cofilin-actin rods may be critical to cell health under stress conditions. Cofilin-actin rods form rapidly in response to many ATP depleting stresses (Minamide et al., 2000; Nishida et al., 1987), stresses that likely affect all cells in the body under different conditions. This may be particularly relevant in neurodegeneration since ATP levels are critical to neuronal health, as are actin dynamics (Hotulainen and Hoogenraad, 2010). This may be additionally relevant to neurons undergoing stresses associated with the aging process (Gibson et al., 2010).

Aberrant rod formation has been described in AD and HD, in the form of persistent rods, or improper rod formation and dynamics (Bamburg et al., 2010; Minamide et al., 2000; Munsie et al., 2011). Persistent rods could lead to trapped cofilin and altered cytoskeletal dynamics after stress leading to neurite and dendrite dystrophy or dysfunction. Alternatively, improper rod formation could mean that cells do not have the required ATP levels available to respond to stress, leading to cell dysfunction or death. Notably, cofilin-actin inclusions have been visualized in AD brains (Minamide et al., 2000). The involvement of both actin and actin binding proteins (Lim et al., 2007; Maloney and Bamburg, 2007; Mila et al., 2009) as well as microtubule related proteins (Atwal et al., 2011; Godin et al., 2010) in neurodegeneration is becoming more evident, and cell stress has been hypothesized to be involved in these disorders (Gibson et al., 2010; Keller, 2006). Thus, being able to modulate the stress response in relation to the cytoskeleton may be a novel therapeutic approach for neurodegeneration and was the driving force behind this work. To this end, we have defined the import and export signals of cofilin, and have further defined two cofilin mutants, discovered by altering cofilin shuttling activity that affect rod formation and cell health during stress. The cofilin R21A mutant binds actin *in vivo*, affects nuclear localization and does not form

rods, and thus would be a good model to discern the requirement of rod formation *in vivo*. As more is revealed about the necessity of cofilin-actin rod formation for cell health and survival, the K22A mutant will offer valuable insight into the level which modulating rod formation can be tolerated since this mutant has all the same features of the R21A mutant except it has increased *in vitro* F-actin bundling activity as well as some limited capacity to form rods. If rod formation is intimately tied into the proper ability of cofilin to bind actin, it may not be possible to target rod formation directly through cofilin. However, if the R21A or K22A mutations are tolerated in stress conditions or cell types tested, then compounds that specifically inhibit or alter cofilin nuclear shuttling may be therapeutic without affecting other essential actin dynamics. The cofilin NLS is bipartite with a unique intervening sequence, thus it may be possible to target this nuclear import activity without affecting other proteins NLSs. Notably, there is a conserved serine-serine-threonine, (SST) motif in the intervening sequence of the cofilin bipartite NLS (Fig. 3C). This SST motif in the cofilin NLS may be a target of post-translational modification and is the subject of further study.

3.6 Acknowledgements

This work is supported by operating grants from the Canadian Institutes of Health Research (MOP-119391) and the Krembil Foundation (to RT). LM has a CIHR Doctoral Research Award.

Conflict of Interests Statement

The authors declare no conflict of interests.

Chapter 4: Discussion

Chapter 4: Discussion

The body of work in this thesis describes a new function of the huntingtin protein in response to stress, which occurs in the nucleus and involves the actin cytoskeleton, namely the nuclear cofilin-actin rod stress response. Many aspects of this work tie in with previous reports of energetic failures in neurodegeneration. By providing mechanistic details of the dynamics of the cofilin-actin rod stress response as well as strategies to specifically tackle the defect imposed by mutant huntingtin with respect to the formation of cofilin-actin rods, this thesis introduces a novel and much needed avenue for drug discovery in HD.

Much can be inferred from this work with respect to the current state of literature in HD as well as neuronal energetics and nuclear actin. It cannot go unnoticed that cofilin-actin rods have also been linked to AD indicating that they may be a target for multiple neurodegenerative disorders. The connections of this work to current literature will be discussed in this chapter, arguing that the cofilin-actin rod stress response could be intimately tied to the pathology in HD and that targeting the defects in this response is a viable and worthwhile target for efforts in drug discovery with respect to neurodegeneration.

4.1 Cofilin-Actin Rods as a Target for Neurodegeneration

4.1.1 Cofilin-Actin Rods in Alzheimer's Disease

Our work shows the involvement of cofilin-actin rods in HD, however the connection of cofilin-actin rods to neurodegenerative disease was initially made by observations of aberrant cytoplasmic cofilin-actin rod formation in AD. Cytoplasmic cofilin-actin rods are formed under low ATP conditions (Minamide et al., 2000), and were found in models examining hippocampal neurons and ATP depleting stresses thought to mimic neurodegeneration (Minamide et al., 2000). The current prevailing

hypothesis with respect to cytoplasmic rods in AD is that they form in neurites under times of ATP depleting stress, however for some reason in the presence of AD related pathology including high levels of amyloid beta (Aβ), they persist in the neurite. These persistent rods block trafficking causing the accumulation of proteins leading to the hallmark plaques in AD and causing downstream synaptic loss and neurite dystrophy, preceding cell death (Bamburg et al., 2010; Cichon et al., 2012; Minamide et al., 2000). Increased amyloid beta peptide ($A\beta_{1-42}$) is unequivocally linked to AD progression and increasing levels of this peptide causes persistent cofilin-actin rod formation in neurons, therefore tightly linking this specific rod formation to AD (Davis et al., 2009; Maloney et al., 2005). Although cytoplasmic rods seem to be found in aging brains, the rods induced in AD models and found in AD brains seem to cause the accumulation of protein at rod sites and problems occur distal to where the rods form which may lead to AD pathology (Cichon et al., 2012). It has been proposed that in familial AD cytoplasmic rods are induced directly by an increase in $A\beta_{1-42}$ caused by the mutations in associated proteins. In sporadic AD it is other aging related stresses that result in a decreased level of ATP leading to rod formation and this may happen in the entire aging population; however in some cases due to predisposition or other environmental factors, these rods persist and lead to blocked transport and formation of Aβ plaques. Thus, two separate mechanisms would result in the same disease (Bamburg et al., 2010). Since these rods presumably form early in disease and are responsible for the initial dystrophy in neurons and not cell death, they are proposed to be a good therapeutic target for AD that would lead to changes early in disease course (Bamburg et al., 2010).

4.1.2 Evidence to Support Cofilin-Actin Rod Dysfunction in Huntington's Disease

In the literature with respect to HD, there are many small molecules that have been tested in many different models that have positive outcomes with unknown mechanism. Upon our discovery of cofilin-actin rods in disease we find that many of these compounds may be directly affecting pathways that affect cofilin-actin rod

formation and many of these positive outcomes can be re-examined from a fresh perspective.

4.1.2.1 Nuclear Rod Formation and its Link to Huntington's Disease

In this thesis we provide the first evidence of dysregulated cofilin-actin rods in HD and the first correlation of aberrant nuclear rod formation in a neurodegenerative disorder. Historically, intranuclear rods have been found in a large percentage of neurons in aged rats, but these early studies did not address whether the rods were comprised of actin or if they are similar structures to what we know today to be cofilin-actin stress rods (Feldman and Peters, 1972). It was in the 1970s that certain nuclear rods were first described as containing actin and as being induced by cell stress agents (Fukui and Katsumaru, 1979). Subsequently, nuclear actin rod structures have been induced by: general stress including DMSO and heat shock (Abe et al., 1993; Fukui and Katsumaru, 1979; Iida et al., 1992; Nishida et al., 1987), altering actin dynamics using Cytochalasin D (Yahara et al., 1982), affecting calcium levels in the cell through inhibiting calmodulin (CaM) using trifluoperazine (Osborn and Weber, 1980), as well as by raising levels of cyclic AMP using forskolin (Osborn and Weber, 1984). Many of these drugs and stress inducing agents have some link to the dysfunction noted in HD.

General stress induces the Heat Shock Response (HSR), which has involvement in HD that has already been described at length (see section 1.4). We hypothesize that an age-related increase in general cell stress inducing the HSR is mitigating the rod forming response in neurons, and it is this kind of stress that would cause the effects of any rod related HD pathology. However, exogenous rod-inducing compounds not only give insight into potential mechanisms of rod dysfunction with respect to mutant huntingtin, but also support altering rod formation as a therapeutic in HD. Two such compounds, as well as their links to HD, will be described in this section.

4.1.2.2 Compounds that Induce Normal Nuclear Rod Formation Lead to Positive Outcomes in Huntington's Disease Models

Calmodulin (CaM) is a eukaryotic calcium binding protein that regulates many intracellular processes. Inhibiting CaM using trifloperazine induces rod formation (Osborn and Weber, 1980). Inhibiting CaM also has positive outcomes in an HD model (Dudek et al., 2010). CaM has been shown to increase transglutaminase activity of TG2 and overactive TG2 is a hallmark of HD (Cariello et al., 1996; Cooper et al., 1997; Jeitner et al., 2009; Karpuj et al., 2002; Lesort et al., 1999; Puszkin and Raghuraman, 1985) (Described in section 1.7.8.2). Huntingtin has been shown to bind CaM in the presence of calcium and this binding is enhanced in a polyglutamine dependent manner (Bao et al., 1996). Mutant huntingtin may bind CaM and be involved in the activation, or potential over-activation, of TG2. In this model huntingtin acts as the scaffold and CaM provides the calcium required for activation of the transglutaminase enzyme (Bao et al., 1996; Zainelli et al., 2004) (Figure 4.1). As such, inhibiting the binding of CaM to mutant huntingtin and thus reducing TG2 activity may be protective in HD models (Dudek et al., 2010). Our work provides a potential mechanistic link between trifloperazine-mediated rod formation and the protective effects of CaM inhibition in an HD mouse model(Dudek et al., 2010), in that mutant huntingtin may inappropriately interact with CaM in the presence of high levels of cellular calcium, leading to persistent rods or inappropriate rod formation through the activity of TG2 (Figure 4.1).

A second, mechanistically unrelated method of inducing rods also has links to HD. Increasing cycling AMP (cAMP) levels using forskolin induces normal rod formation, implying that high levels of cAMP can induce rods or that normal cAMP levels may be required for normal rod formation (Osborn and Weber, 1984). It is of note that there is a decreased level of cAMP specifically in the striatum of full length mutant huntingtin transgenic mice starting at 10 weeks of age that coincides with a decreased ratio of ATP/ADP (Gines et al., 2003). This decreased level of cAMP was shown to lead to

impaired cAMP response element-binding (CREB) mediated transcription and is thought to contribute to some of the transcriptional defects in HD (Gines et al., 2003). CREB is responsible for the transcription of BDNF and, as described in section 1.6.3, decreased BDNF levels are a hallmark of HD and are hypothesized to be a contributing factor to the disease (Milnerwood et al., 2010; Milnerwood and Raymond, 2010; Zuccato et al., 2001; Zuccato et al., 2005). Additionally, decreased cAMP levels in both patient brains and peripheral lymphocytes have been observed, validating the finding in the mouse model (Gines et al., 2003). Compounds that cause an increase in cAMP levels, including forskolin, rescued cell death and dysfunctional neurite outgrowth phenotypes in an amino-terminal mutant huntingtin fragment cellular model (Wyttenbach et al., 2001). The mechanism of this rescue was assumed to be changes in transcription of CREB related genes, but it is additionally possible that this could have led to a change in actin dynamics since forskolin induces nuclear rod formation (Osborn and Weber, 1984) (Figure 4.1). Therefore, two unrelated compounds that induce rods through completely different mechanisms have both been found to affect huntingtin polyglutamine expansion induced toxicity, and further support cofilin-actin nuclear rod defects in pathology through different mechanisms (Figure 4.1).

In addition to these mechanisms that directly affect rod formation there are potential indirect mechanisms linking compounds tested in HD to rod formation, specifically compounds that would affect the phosphorylation and activity state of cofilin.

4.1.2.3 Phosphorylation State of Cofilin Controls Actin Dynamics

Cofilin binding to actin is essential for treadmilling, where cofilin has dual action either causing the breaking of an actin filament resulting in the nucleation of new filaments or actin monomer dissociation from the minus end of an actin filament allowing monomer recycling and turnover (Carlier et al., 1997; McGough et al., 1997).

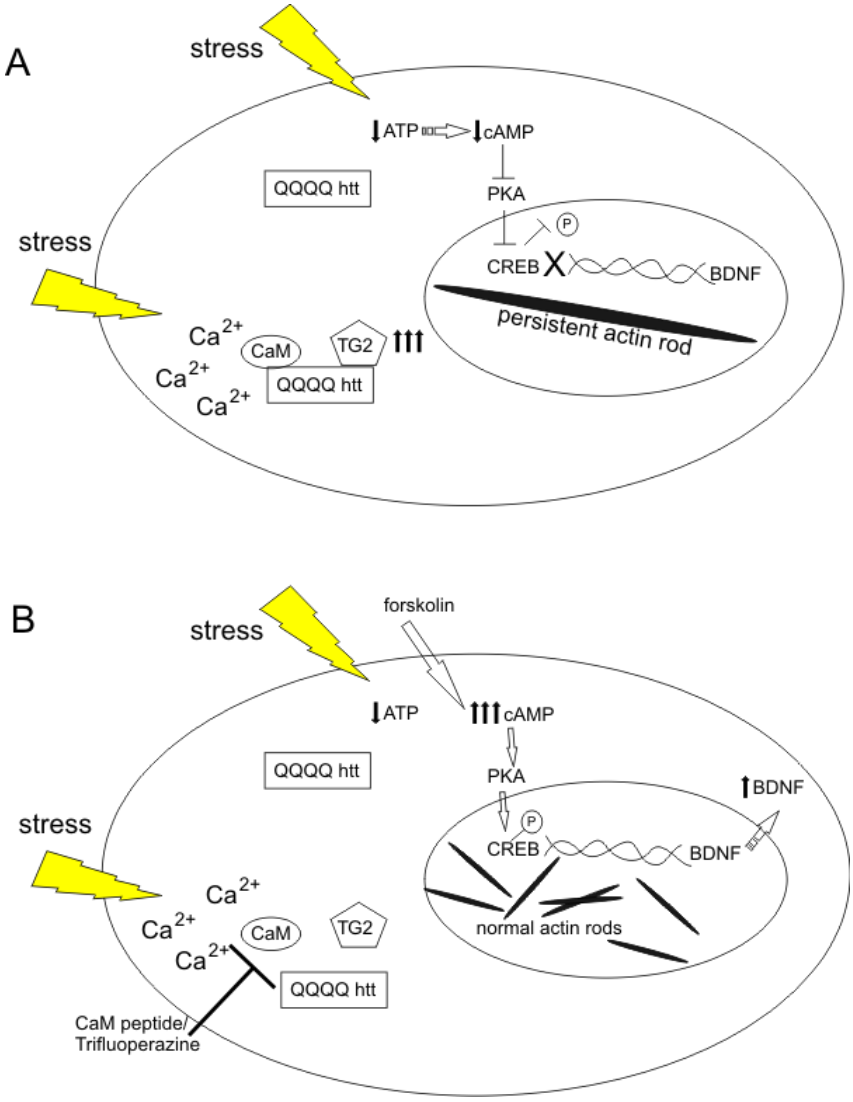

Figure 4.1: Compounds that induce nuclear cofilin rods have positive outcomes in Huntington's disease models. A. Cell stress conditions can cause a decrease in ATP levels and an increase in calcium levels. Decreased ATP levels occur in concert with cAMP decreases in the presence of mutant htt. Decreased cAMP leads to decreased activity of protein kinase A (PKA) which in turns down regulates CREB dependent gene transcription including BDNF. Increased calcium levels lead to increased activity of calmodulin (CaM). CaM inappropriately binds polyglutamine expanded huntingtin and causes the overactivation of TG2. Both of these outcomes could conceivably lead to inappropriate rod formation. **B.** Compounds that affect both cAMP levels and calmodulin binding to huntingtin are compounds that induce normal rod formation. Forskolin increases cAMP levels and leads to both proper gene transcription and positive outcomes in HD. The calmodulin inhibitor trifluoperazine induces cofilin rods. Calmodulin peptides that also act as inhibitors have positive outcomes in HD models.

Cofilin is therefore a key regulator of actin filament reorganization and its dynamics are almost exclusively regulated by reversible phosphorylation at serine 3 (Moon and Drubin, 1995). There is a negative effect on cofilin-actin dynamics when cofilin is phosphorylated at serine 3 and this activity is reinstated by cofilin dephosphorylation (Arber et al., 1998; Moriyama et al., 1996). This reversible phosphorylation of cofilin is required for all actin dynamics. Modifying levels of phospho-cofilin (from here forward phospho-cofilin will describe cofilin phosphorylated at serine 3) may have direct impact on rod formation and positive outcomes in HD models.

4.1.2.3.1 Control of Actin Dynamics and Rod Formation through Kinase and Phosphatase Activity on Cofilin

Our interest lies in the cofilin-actin stress response, which occurs when cofilin is hyper-dephosphorylated at serine 3, and an increased concentration of dephosphorylated cofilin in comparison to actin causes cofilin to saturate F-actin, leading to a decrease in filament turnover and the bundling of filaments into rods (Fukui and Katsumaru, 1979; Nishida et al., 1987). Cofilin can be phosphorylated at serine 3 by either LIM kinases or testicular protein kinases (LIMK1, LIMK2, TESK1, TESK2) (Arber et al., 1998; Okano et al., 1995; Toshima et al., 2001). LIMK activity is controlled by the Rho family of GTPases, while TESK activity on cofilin is controlled by integrin mediated signal transduction (Toshima et al., 2001; Yang et al., 1998). Thus, the phosphorylation of cofilin seems to be controlled by external stimuli.

The dephosphorylation of cofilin is controlled by at least two phosphatases, slingshot1 (SSH1) and chronophin (CIN) (Huang et al., 2008; Kurita et al., 2007). The activity of these phosphatases on cofilin is tied to the intracellular environment. Increased intracellular concentration of calcium leads to an increased pool of dephosphorylated cofilin through the activity of SSH1 (Wang et al., 2005c) and CIN activity is intimately tied to Heat Shock Protein 90 (HSP90) and ATP levels in the cell

(Huang et al., 2008). Upon stimuli that induce cell stress and ATP depletion, HSP90 is released from CIN, and CIN is free to dephosphorylate cofilin, favouring rod forming conditions (Huang et al., 2008). Modulating the activity of these kinases and phosphatases would result in altered levels of phospho-cofilin, with an increased pool of dephosphorylated cofilin resulting in conditions favourable to rod formation.

4.1.2.4 A Connection between Phospho-Cofilin Levels and Positive Outcomes in Huntington's Disease Models

Significantly, compounds that promote the dephosphorylated state of cofilin, either by inhibiting LIMK1 or increasing CIN activity, lead to positive outcomes in HD models (Bauer et al., 2009; Fujikake et al., 2008; Li et al., 2009; Pollitt et al., 2003). As described in section 2.5, Rho-associated protein kinase (ROCK) is an upstream activator of LIMK. The small molecule Y-27632 is a ROCK inhibitor that consequently inhibits the activation of LIMK causing a decrease in the pool of phosphorylated cofilin. Y-27632 has been found to be effective in aggregation models of HD, leading to decreased aggregation and cell toxicity, as well as improving motor symptoms in short fragment HD model transgenic mice (Bauer et al., 2009; Li et al., 2009). The mechanism behind these positive outcomes is not known. We propose that it may be due to an increased pool of dephosphorylated (therefore activated) cofilin, which may improve the stress response or overall actin activity in the presence of mutant huntingtin via phospho-cofilin levels (Figure 4.2A). Unfortunately, the activity of Y-27632 and ROCK inhibitors is an unlikely therapeutic due to the vast cellular effects it would have and much work needs to go into the safety of inhibiting ROCK in humans (Kubo et al., 2008).

Geldanamycin is a potent HSP90 inhibitor which acts by binding the ATP-binding pocket of HSP90, leading to the inhibition of the steady state activity of HSP90 effectively inducing the Heat Shock Response (HSR) through the activity of HSF-1 (Whitesell et al., 1994). Geldanamycin treatment has had positive outcomes in HD

fragment models and the positive outcomes were thought to be caused by an induction of the HSR leading to the degradation of mutant huntingtin and a decrease in protein aggregation (Sittler et al., 2001). However, geldanamycin and geldanamycin derivates (17-demthoxygeldanamycin – 17-AAG) also cause the activation of CIN, which leads to a large increase in the pool of dephosphorylated cofilin and actually induces cofilin rod formation (Huang et al., 2008). Therefore activating the HSR in this manner, in theory, has the dual benefit of activating chaperones in the cell as well as mediating phospho-cofilin levels (Figure 4.2B). Since geldanamycin and 17-AAG have some negative side effects, specifically liver toxicity, and they are unable to cross the blood-brain barrier, new HSP90 inhibitors have been created and tested in HD models (Labbadia et al., 2011). These inhibitors, while having initial beneficial effects in transgenic HD mouse models motor symptoms, do not appear to be effective in the long term (Labbadia et al., 2011). It is possible that either the HSR is further impaired as HD progresses, or that the cell responds in a negative feedback manner to having the HSR activated constitutively. For these reasons, HSP90 inhibitors may not be viable drug options.

There is another interesting connection between phospho-cofilin levels and HD. The calcium sensitive phosphatase, calcineurin (CaN), activates SSH1 leading to dephosphorylated cofilin, and CaN inhibitors lead to an increased pool of phospho-cofilin (inactive) via decreased SSH1 activity (Wang et al., 2005c) (Figure 4.2C). CaN over-activity has been hypothesized to be involved in HD through the over-activation of NMDAR leading to excitotoxic cell stress via increased calcium levels (Xifro et al., 2008). Therefore CaN inhibitors have also been tested for activity in HD models. It was therefore surprising that the CaN inhibitor FK506 resulted in faster progression of HD symptoms in a transgenic HD mouse model (Hernandez-Espinosa and Morton, 2006). This inhibitor was also tested in cell based HD models and had some beneficial effects under very mild stress conditions, however it had no effect on outcome under more aggressive stress conditions (Rosenstock et al., 2011). Taking the work from this thesis

into account, it must be considered that FK506 would cause an increased pool of inactive cofilin as a by-product of its inhibitory action on CaN which would inhibit proper rod formation. Additionally, in actively firing neurons, it has been shown that active cofilin is required for spine morphology and changes in spine morphology in the postsynaptic neuron. Specifically, it has been shown that cofilin is required to be dephosphorylated through CaN activity on SSH1 upon receptor activation and intracellular calcium increases (Pontrello et al., 2012). This highlights the importance of having active cofilin in the cell, both under steady state and cell stress conditions, and can explain why CaN inhibitors increased symptom progression in HD mice (Pontrello et al., 2012).

It is interesting that two separate studies defined compounds that have benefits in HD models through two very different mechanisms (ROCK inhibition and HSP90 inhibition), with a side effect of both of these compounds leading to increased levels of phosphorylated cofilin which would increase favourable rod forming conditions (Bauer et al., 2009; Li et al., 2009; Sittler et al., 2001); whereas a small molecule that would lead to inactive, or dephosphorylated-cofilin as a side effect had negative or neutral outcomes in HD models (Hernandez-Espinosa and Morton, 2006; Rosenstock et al., 2011) (Figure 4.2).

This data suggests the requirement of certain pools or a certain threshold of active-dephosphorylated cofilin during cell stress in HD models, or an inherent deficiency thereof in the presence of mutant huntingtin. If targeting cofilin is going to be therapeutic, it is pertinent to find other ways to alter its stress dependent activity, aside from controlling its phosphorylation state through off-target inhibitors. This data additionally supports looking at levels of phosphorylated cofilin in human patients. We have shown that the western blot profile of cofilin changes as HD progresses in lymphocyte samples, and propose this should be further looked at as an HD biomarker. However we did not investigate changes in the level of phospho-cofilin which may show

differences over the course of HD and based on the presented data may further function as a biomarker.

Cofilin-actin rods have now been linked to both AD and HD, and converging hypothesis indicate that targeting the rod forming ability of cofilin may be a therapeutic target for both diseases. It is possible that the mechanisms are quite different since the rods occur in different compartments. In AD it seems that the requirement to breakdown or not form rods could be therapeutic, whereas in HD breaking down persistent nuclear rods or alternatively encouraging proper rod formation may be therapeutic. It is additionally possible that there is something going wrong with normal rod forming dynamics in sporadic AD which is causing the persistent rods, and encouraging normal rod formation could be therapeutic in AD. Our work in chapter 3 shows that the nuclear shuttling capabilities of cofilin affects both cytoplasmic and nuclear rod formation and that the mechanism of rod formation might not be completely different. Thus any drugs or target compounds we find looking at nuclear rod formation are worthy of testing in AD models. Before going on to alter rod formation as a therapeutic it would be ideal to know the physiological requirement and role of the nuclear rods which will lead to hypothesis about how to alter them and if an organism may tolerate changes in this response.

4.2 Roles of Nuclear Actin and Potential Functions of Nuclear Cofilin-Actin Rods

4.2.1 Physiological Requirement of Nuclear Cofilin-Actin Rods

It is important to note that the physiological role and requirement of nuclear cofilin-actin rods is currently unknown. One function of cytoplasmic rod formation is the alleviation of ATP used in actin treadmilling (Bernstein et al., 2006). Presumably nuclear rods would function in a similar manner but it is unlikely that freeing up ATP in the nucleus is the only function of such a striking and localized response. Additionally

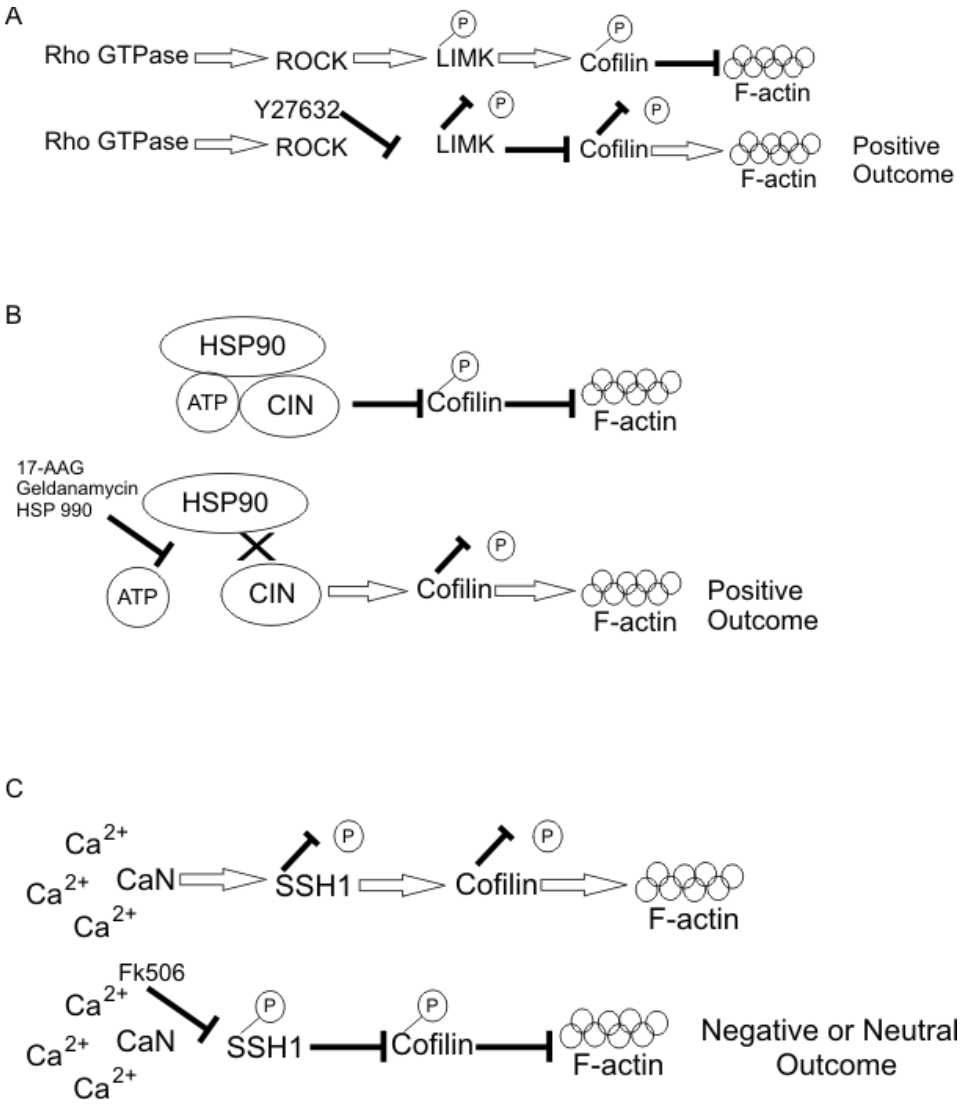

Figure 4.2 Compounds that decrease the pool of phospho-cofilin leading to conditions favourable for rod formation have positive outcomes in Huntington's disease models. A. Y27632, a ROCK inhibitor, leads to the inhibition of the cofilin kinase LIMK which inhibits its activities on cofilin leading to positive outcomes in an HD aggregation model and mouse model. **B.** Chronophin phosphatase (CIN) is found in a complex with HSP90 and ATP under steady state conditions rendering it ineffective. Under cell stress conditions or when ATP binging to HSP90 is inhibited, CIN is able to dephosphorylate cofilin and induce cofilin rods. HSP90 inhibitors have positive outcomes in HD cell and mouse models. **C.** Calcineurin (CaN) is a calcium dependent phosphatase that normally acts on the cofilin phosphatase Slingshot 1 (SSH1), activating it and leading to an increased pool of dephosphorylated cofilin. CaN inhibitors which would lead to SSH1 inactivation and an increased pool of phospho-cofilin cause increased progression of HD in a mouse model.

the question remains as to why certain stressors and compounds cause the formation of cytoplasmic rods and others the formation of nuclear rods, but suggests that rods forming in different cellular compartments may have different functions. Only two proteins are required for cytoplasmic rod formation: cofilin and actin (Minamide et al., 2010). As we show in chapter 2, huntingtin only localizes to nuclear cofilin rods, indicating that nuclear and cytoplasmic rods have different compositions or at least that different proteins localize to them. The third chapter of this thesis shows that rod forming capabilities of cofilin are required for cell survival upon stress and may be an anti-apoptotic function. Therefore the ability to form stress rods overall is a required function of both cofilin and actin in a cell based system.

The requirement for nuclear cofilin-actin rods may be related to nuclear actin specific functions. Nuclear actin has been shown to be imperative for most aspects of transcription (de Lanerolle and Serebryannyy, 2011; Zheng et al., 2009), it is therefore possible that nuclear rod formation has a function with respect to transcription during stress and that rod formation may be physiologically required for this function.

4.2.2 Nuclear Actin Function in Transcription and Implications for Rod Formation

It is now undisputable that actin resides in the nucleus, both in monomeric and polymeric forms (de Lanerolle and Serebryannyy, 2011), and new evidence supports an expansive array of previously unappreciated functions of nuclear actin. Actin has been shown to be involved in multiple steps of transcription through binding of all three RNA polymerases, recruiting chromatin remodelling complexes as well as in the export of mRNA (Hofmann et al., 2004; Hu et al., 2004; Obrdlik et al., 2008; Obrdlik and Percipalle, 2011; Percipalle et al., 2001). In addition to these functions, nuclear actin and its associated motor protein myosin have been implicated in the actual movement of gene loci in response to transcription activation (Dundr et al., 2007). Experiments in epithelial cells show that a decreased pool of nuclear actin is required for cells to obtain a

quiescent state (Spencer et al., 2011), while increased levels of nuclear actin are required for macrophage differentiation (Xu et al., 2010) indicating that nuclear actin dynamics are closely linked to cell state which may be specifically important to post-mitotic neurons. Because of this expansive array of activities regarding transcription and cell state, actin, a protein previously regarded as being excluded from the nucleus, is now being considered as a master regulator of transcription. It follows that fine regulation of nuclear actin and polymerization states are likely required to maintain cell state and most transcription related activities.

Recently, cofilin has been shown to be intimately involved in the nuclear transport of actin, which supports our work in chapter 3, characterizing the nuclear import signal of cofilin and implying that cofilin actively shuttles in and out of the nucleus under steady state and cell stress conditions (Dopie et al., 2012). Profilin, an actin binding protein with opposite actions of cofilin, being involved in the polymerization of F-actin, is required for the nuclear export of actin through exportin6 (Stuven et al., 2003). It is of note that profilin levels are additionally altered in HD (Burnett et al., 2008). Thus, actin binding proteins are required for the transport of actin and have been shown to be necessary for the transcriptional activities of actin in the nucleus (Dopie et al., 2012), likely through modulating the polymerization state of actin in the nucleus. The large influx of cofilin and actin into the nucleus during stress and the formation of cofilin-actin rods will likely impact the transcriptional functions of actin.

It is not beyond reason to predict that differential remodelling of actin in the nucleus occurs under stress conditions to change the transcriptional landscape in response to stress. It is well documented that cell stress induces a large shift in transcriptional activities, leading to decreased transcription of most steady state proteins and increased transcription and translation of chaperones and other stress related proteins (Morimoto, 2012). The role of actin as a master regulator of transcription, as well as its rod-forming function, are likely involved in these cell stress

associated transcriptional changes. During stress, actin may act directly via changes in which DNA promoters it binds during stress versus steady state conditions or indirectly through altered chromatin modification or movement of chromosomes within the nucleus. Inappropriate execution of this response could lead to many of the transcriptional defects noted in HD, could be tied to cell stress and energetics failure in HD, and may correlate to some of the nuclear functions of huntingtin, through its scaffold activity. Changes in actin related transcription changes should be looked at as a target or as a readout for neurodegeneration in general and looking at transcriptional alterations caused by nuclear cofilin rods is discussed in Chapter 5.

4.3 A Model for Differential Cell Susceptibility in Huntington's Disease Due to Aberrant Cofilin-Actin Rod Formation

We have demonstrated a dysfunctional cell stress response via the actin cytoskeleton in the presence of full length mutant huntingtin. We propose that this function is a good target for drug discovery since it seems to be directly affected by mutant huntingtin and ties into the energetic defects, transcriptional defects and problems with cell stress and aging hypothesized to cause neurodegeneration, and therefore is a good pathway to experimentally test for rescue. An altered cell stress response would likely be cell autonomous but we propose that a stress response involving both ATP alleviation and the actin cytoskeleton would conceivably differentially affect projection neurons, the population of neurons that are most sensitive to the insult of mutant huntingtin. We propose a mechanism that would lead to the increased susceptibility of these neurons based on an impairment of the cofilin-actin rod stress response.

Projection neurons are large cells with long axons and dendrites, and many spines. The cytoskeleton is required for structure and trafficking along these axons and active actin remodelling through cofilin activities is required at spines for plasticity

through changes in spine morphology (Hotulainen and Hoogenraad, 2010). Recently, cofilin activity has been found to be critical in response to activities of NMDAR as well as AMPA receptors (AMPAR) for motility of synapses, controlling spine morphology and post-synaptic potentiation and depression (Pontrello et al., 2012; Rust et al., 2010). Cofilin knockout is embryonic lethal, therefore selective knockout of cofilin from postnatal neurons in the forebrain has been performed to specifically probe cofilin function at synapses using a floxed system. This system reveals that cofilin is essential in controlling the turnover of F-actin at synapses. The consequence of an overload of F-actin at synapses results in problems with post synaptic physiology including spine morphoplogy, number of synapses and decreased receptor mobility leading to impaired associative learning (Rust et al., 2010). Interestingly, actin depolymerizing factor (ADF) gets up-regulated when cofilin is depleted in this model (Rust et al., 2010), ADF can sometimes compensate for cofilin knockdown in other actin related functions (Hotulainen et al., 2005), however, it cannot fully compensate for the loss of cofilin in neurons with respect to spine morphology (Rust et al., 2010). In chapter 3 of this thesis, we noted that cofilin knockdown did not seem to affect steady state functions in our cells, likely due to compensating mechanisms by ADF, however ADF cannot compensate for the stress dependent function of cofilin in our cofilin-knockdown cell stress model. Additionally it has been shown that upon NMDAR activation and calcium level increases associated with this, activated calcineurin (CaN) causes a dephosphorylation of cofilin through SSH1 activity and cofilin is translocated to dendritic spines for remodeling activities (Pontrello et al., 2012), agreeing with the specific need for active dephosphorylated cofilin in actin remodeling at spines. Therefore the normal regulation of cofilin and phospho-cofilin is intimately and specifically tied to proper neuron function.

Between the large cytoskeleton of neurons and the active remodeling of actin required at synapses it is clear that neurons have a high demand for actin turnover. This

high demand for active actin turnover is energetically costly. It has been found that inhibiting treadmilling of actin after stopping ATP production in neurons alleviated approximately fifty percent of the already produced ATP In the cell, indicating that actin turnover may have been overlooked as a major energy drain for neurons (Bernstein and Bamburg, 2003). An additional large pool of ATP is required in neurons for electrical activity and restoring transmembrane ionic gradients (Attwell and Laughlin, 2001). Overall, projection neurons in particular, including MSN and pyramidal neurons, have high energy demands associated with maintaining the ionic gradient and high levels of actin turnover in spines, and are unique from other cell types in this way. The cofilin-actin rod stress response is currently shown to be involved in alleviating a pool of ATP that is normally used for active actin processes, so it can be used elsewhere in the cell during times of stress (Bernstein et al., 2006). Since neurons are already using up so much ATP under normal condition, dysregulation of the cofilin-actin rod stress response may have additional negative effects in neurons compared with other cell types if ATP is not being relieved.

Medium spiny neurons (MSN), the population of neurons that are exquisitely sensitive to the mutant huntingtin insult may have amplified negative effects due to a deficiency in ATP alleviation compared with other projection neurons. MSNs are named such based on the fact that they have a medium sized cell body and notably spiny dendrites (DiFiglia et al., 1976). MSNs have both AMPA and NMDA neurotransmitter receptors, highlighting the importance of the active actin cytoskeleton and active cofilin in these neurons in particular (Han et al., 2010). MSNs are additionally thought to have distinct electrophysiology in that they are kept in a hyperpolarized state. There is a more relaxed environment in other neurons that spontaneously discharge, however this almost never happens in MSNs and the maintenance of this state would be a further energy burden (Calabresi et al., 1995; Han et al., 2010; Mitchell et al., 1999). Recent advances in technology have led to different experimental platforms suggesting this may

not be strictly true and MSN may not require as many concerted inputs as previously thought to fire (Plotkin et al., 2011). Regardless of their physiology, MSN spine morphology is tied to signalling in a way that is unlike other neurons. MSN are extremely plastic and have changing spine formation and morphology in the presence of the neurotransmitter glutamate (Kaufman et al., 2012), indicating constant changes in spine number and morphology which would require massive amounts of F-actin turnover. This would require them to have different and higher actin requirements compared with other neuron types where spine morphology is not tied into activity. In support of this, HD mouse models consistently have decreased spine density in the MSN population leading to altered plasticity (Cepeda et al., 2010; Milnerwood and Raymond, 2010; Singaraja et al., 2011), and loss of spines and dendritic morphology is characteristic of the disease in humans (Ferrante et al., 1991). Therefore, MSNs are especially spiny, have distinct actin requirements for spine morphology and plasticity in response to neurotransmission, and additionally may have a higher energy demand associated with their unique physiology that differs from other projection neurons (Figure 4.3A). Based on this, we propose two scenarios connected to our analysis of the cofilin rod stress response in the presence of mutant huntingtin that would lead to the differential neuronal vulnerability in HD. We propose that cells can compensate for the defective stress response imposed by mutant huntingtin under normal stress conditions; however the accumulation of damaged proteins and dysfunctional pathways that occur during aging and the increased and more severe levels of stress are not being compensated for in these vulnerable neuronal populations in HD. We found first of all that in the presence of mutant huntingtin cofilin rods formed slower and in some cells they did not form at all. Cells that did not form rods had a propensity to cell death prior to cells that did form rods. If indeed this response is required to free up ATP during stress, we would predict that cells that already have a high energy demand and in general likely do not have a large pool of ATP readily available during stress, would be the first to succumb to the adverse effects of not having ATP alleviated during stress

(Figure 4.3 B&C). Second-of-all, cofilin-actin rods form under stress conditions and should break apart once the stress is removed, however we find that in the presence of mutant huntingtin the phenotype of the nuclear rods differs and these rods persist once stress has been alleviated. Additionally in AD models, rods in neurites also have a tendency to persist and not break down (Maloney and Bamburg, 2007; Minamide et al., 2000). Specifically in the case of nuclear rods, a large pool of the cellular cofilin enters the nucleus and is localized to these rods; if cofilin is stuck at these rods it is not available to perform its other essential functions with respect to actin treadmilling in neurons along axons and at synapses. This defective cell stress response may indicate that there is not the correct level of active cofilin in the cell to perform essential functions on F-actin in neurons. This would lead to problems at synapses and in trafficking since cofilin has essential roles in both of these functions in neurons and may lead to the initial dystrophy and loss of connections and synapses in neurons prior to cell death (Figure 4.3 B&C).

The next question is how to test if altering cofilin and the cofilin-actin rod stress response is a therapeutic avenue for drug discovery in HD. The requirement of cells to form rods has never been looked at and we found a correlation between cell survival during stress and the ability of cofilin to form rods. Therefore we hypothesize that inhibiting rod formation may not be the way to target this, although this needs to be tested in higher order model organisms; the mutations we found in chapter 3 that affect cofilin rod forming ability but not its other functions, can be used in a transgenic model to test this. We also found that the active shuttling of cofilin through nuclear import and export signals seems to be intimately tied to the ability of cofilin to respond to stress and form rods, and as such finding compounds that alter this ability may answer some of these questions, or be therapeutic. We further propose that restoring the correct ability of cofilin to form normal cofilin-actin nuclear rods in the presence of mutant huntingtin may be a screening tool for drugs since we have an obvious defective

rod phenotype in cells expressing mutant huntingtin, which may easily be screened for compounds that alter this activity with positive outcomes. Preliminary data and the future direction with respect to this work will be presented in chapter 5.

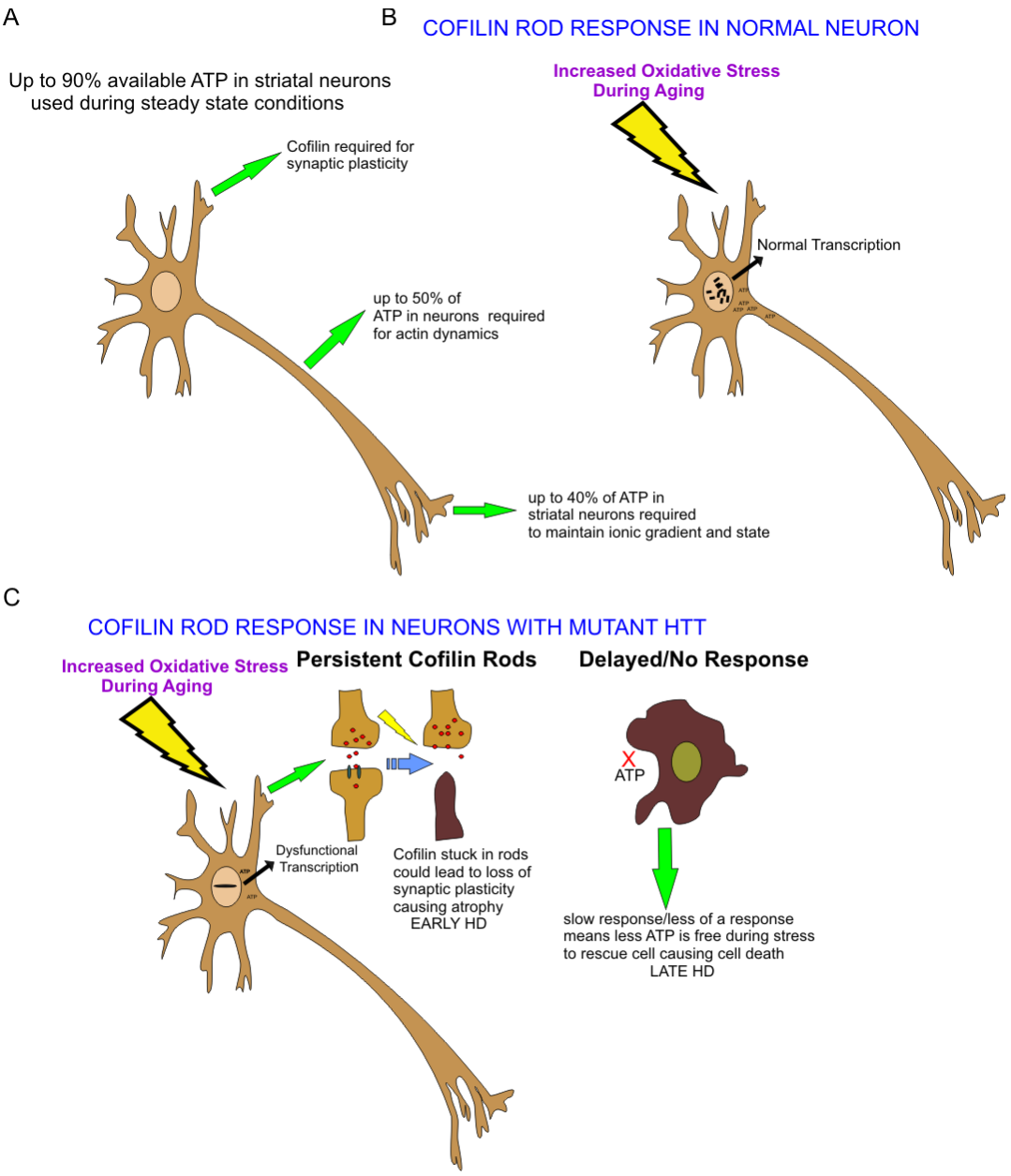

Figure 4.3 A model for differential susceptibility of neurons in Huntington's Disease. **A.** Under normal conditions neurons, specifically medium spiny neurons (MSNs) have high ATP demands due to unique cytoskeleton remodeling and electrophysiology. **B.** In normal cells cofilin-actin rods with a normal phenotype form, alleviating ATP, and normal transcription occurs. These rods break down once stress is removed. **C.** Model of aberrant rod formation in the presence of mutant huntingtin. The rod phenotype differs in the presence of mutant huntingtin, these rods persist once the stress is removed. This traps a large proportion of cofilin at the rods which may lead to dysfunction in cellular cytoskeleton dynamics, specifically causing dystrophy in neurites where active actin remodeling via cofilin is required for spine morphology. Alternatively, in cells where rods do not form, ATP is not alleviated and may lead to cell death specifically in cell populations where there is not a lot of ATP readily available under steady state conditions. Both of these outcomes predict transcriptional dysregulation based on the fact that actin dynamics are tightly linked to all levels of transcription.

Chapter 5: Future Direction and Conclusion

Preamble

This chapter presents some unpublished results from preliminary experiments done in hopes of probing drug discovery pathways with respect to cofilin-actin rod formation.

Experiments in section 5.1 were done in collaboration with the McMaster Biophotonics Facility (www.macbiophotonics.ca) and automated image acquisition and analysis was performed by Jarkko Ylanko.

Chapter 5: Future Direction and Conclusion

The body of work described in this thesis has led to discoveries in different facets of the drug discovery pipeline for HD. We have first and foremost defined a new and specific target, the nuclear cofilin-actin rod stress response, which ties in with many features of neurodegeneration. We then looked at different ways to probe this pathway directly for drug discovery. This work can now be taken forward and used to define new assays and readouts for HD screens, with additional biomarker development potential. Follow-up experiments need to be performed, looking at the biochemical features of this pathway and if these can be further exploited for drug discovery. Here we will describe some preliminary data obtained in these efforts as well as suggest follow up experiments that are directly relevant to this body of work.

5.1 Nuclear Cofilin-Actin Rod Phenotype as a Screening Tool for Huntington's Disease Modifying Compounds

In chapter 2 of this thesis we described visually different phenotypes of nuclear cofilin rods based on the presence of either wildtype or mutant huntingtin in the cell. In the presence of wildtype huntingtin rods form with a normal phenotype which is more than four rods per nucleus with rod length varying between 1-6 µm. In the presence of mutant huntingtin there are only 1-4 rods that form in the nucleus with at least one rod having a length of greater than 4 µm. These rods can be easily visualized either endogenously using cofilin or actin antibodies, or by the over-expression or stable expression of a fluorescent cofilin fusion. We hypothesized that these different phenotypes would be acceptable to use as a read out for high throughput screening (HTS) using automated microscopy and computer based image analysis. Our goal of setting up a HTS in this manner would be to find compounds that cause cells with a mutant huntingtin background, overexpressing EYFP-cofilin to have a normal rod phenotype after compound treatment and exposure to stress (Figure 5.1A). Towards

this goal we have created STHdh $^{Q7/Q7}$ (wildtype huntingtin) and STHdh $^{Q111/Q111}$ (mutant huntingtin) cell lines stably expressing EYFP-cofilin to be used in screening since YFP has bright fluorescence amenable to automated imaged acquisition. We tested plating these cells in a 384 well dish at cell densities of 2500 cells/50µl, 5000 cells/50 µl and 7500 cells/50 µl. The cells were allowed to settle overnight and the following day were subjected to a 1 h heat shock at 42˚C using a heated water bath. Immediately following heat shock, media was aspirated off and replaced with 4% paraformaldehyde which was allowed to incubate with the cells for 45 minutes. Wells were washed twice with PBS and once with DRAQ5 diluted in PBS at concentrations of 2.5 µm, 5 µm, 10 µm or 15 µm. These different cell density and DRAQ5 concentrations were used to test automated image acquisition and image analysis software for optimal cell segmentation. We took 15 images per well and performed 8 replicates of each condition for each cell type using the Perkin-Elmer automated Opera confocal microscope. We visualized the cells using a 40X water immersion objective and obtained 120 images of each condition for the Acapella high-content imaging and analysis software to analyze. The DRAQ5 stain is membrane permeable and has a high affinity for double stranded DNA and can be imaged using far red fluorescence and therefore has no bleed-through or spectral overlap with YFP. We found that this dye could be used to successfully segment our whole cells and the nucleus of the cell within the whole cell (Figure 5.1B). We found that using a cell density of 5000 cells/ 50 µl and between 5-10 µm DRAQ5 gave us optimal segmentation of both the wildtype and mutant cells. The optimized images from either the wildtype or mutant cell lines were analyzed using the CAFE miCELLS scripts (Classification Analysis and Feature Extraction from Micrographs of Cells – www.macbiophotonics.ca). This program is able to classify different cell types based on the features extraction performed by the acapella software and the training images you provide (ie. Images of wildtype cells vs. images of mutant cells) (Figure 5.2A). This was successfully done as a proof of principle to see if the software could assign differences in our cells morphologies (Figure 5.2B&C), and this may be used as a

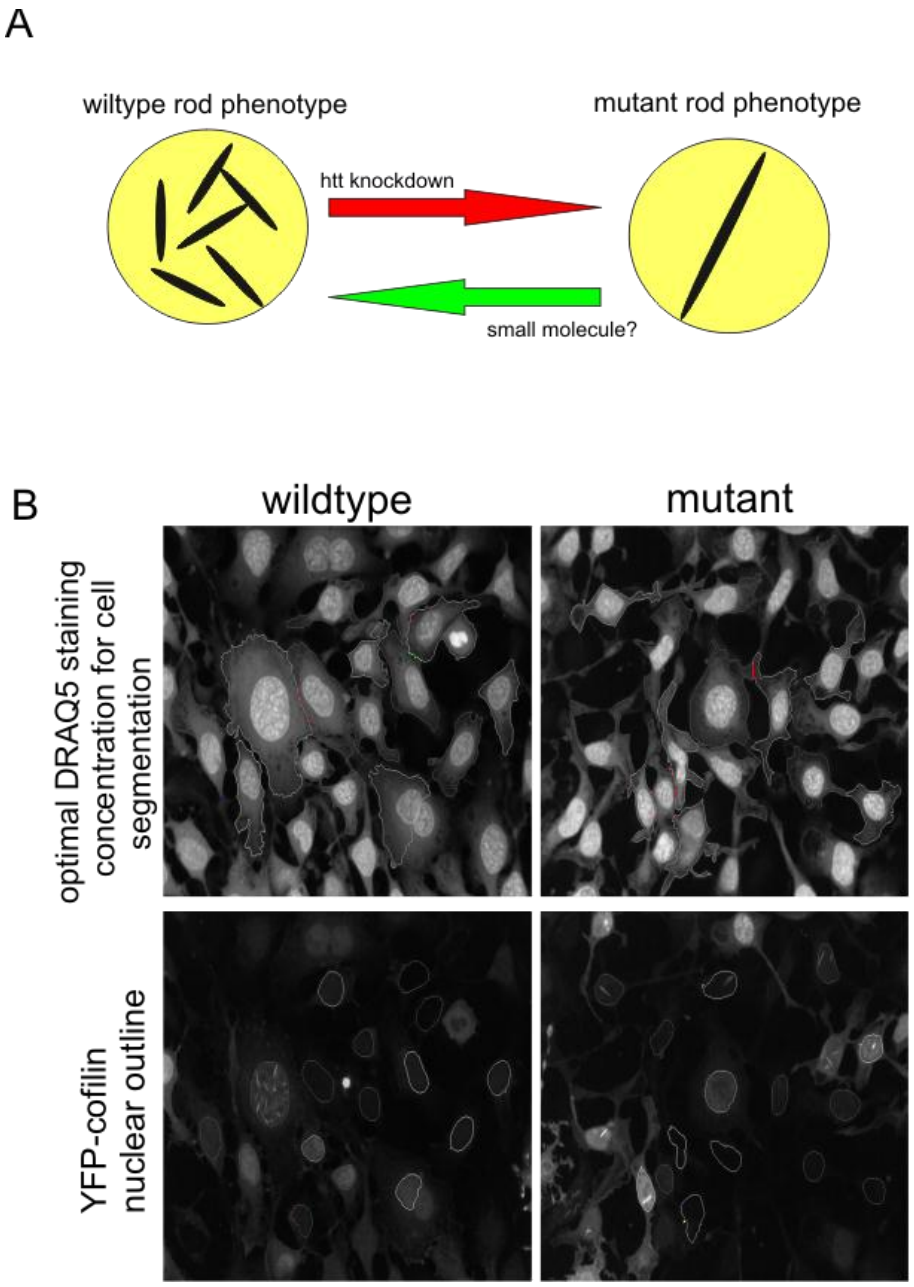

Figure 5.1 Proposed screening using nuclear rod phenotype assay. A. There are two distinct rod phenotypes depending on whether STHdh cells have a mutant or wildtype huntingtin protein background. Reducing levels of wildtype huntingtin induces a mutant rod phenotype. We aim to screen for compounds that cause cells expressing mutant huntingtin to behave like cells expressing wildtype huntingtin with respect to rod phenotype. **B.** Screening parameters obtained using YFP-cofilin stable cell lines after heat shock. Imaging done at 40X using the evotech Opera automated imaging system. Optimal plating conditions for segmentation found to be a cell density of 5000cells/50µl and a DRAQ5 concentration of 7.5µm. Segmentation performed using the Acapella software.

secondary read-out since we predict some of the morphological difference in our wildtype vs. mutant cells is a result of aberrant cytoskeletal remodelling. Our specific and primary interest lies in the rod phenotype. Therefore we used the cell segmentation based on DRAQ5 staining to assign the nucleus vs. cytoplasm of the cell, and then used a nuclear spot identifier to find the rods in the nucleus using the YFP channel. Acapella could successfully detect rods in the YFP channel and we are currently developing an assay where we can define a wildtype vs. mutant rod based on the percentage of the nucleus that is covered in identified "nuclear spots" (Figure 5.3). Since in general more rods form in wildtype cells the phenotype should be detectable and distinguishable based on this parameter. Alternatively it may be possible to train CAFE miCELLS to assign cells as having either mutant or wildtype rods based on the feature extraction of the nuclear spots. Our future goal is to prepare 384 well dishes as described with our STHdh$^{Q111/Q111}$ EYFP-cofilin cell line and treat the cells with different libraries of chemical compounds prior to exposing them to stress. Following fixation, DRAQ5 staining, automated image acquisition and analysis we will have identified compounds that alter the rod forming ability and phenotype of this cell line causing it to behave more like cells with a wildtype huntingtin background (Figure 5.1A). We will be looking for changes in the percentage of cells that form rods as well as changes in rod phenotype. We will manually examine the images from the wells with hit compounds to ensure that it is detecting a change in rod formation and not other artifacts or nuclear changes induced by chemical compounds. We will also see if any hit compounds alter the over-all morphology of the cell to determine if there are additional benefits making the mutant huntingtin cell line behave more like the wildtype huntingtin cell line.

Once we have identified compounds of interest we will use these compounds in secondary assays looking at changes of S13S16 phosphorylation levels of huntingtin by immunofluorescence and western blot, which have already successfully been used as a secondary screen in testing drugs in HD models (Di Pardo et al., 2012). An increased

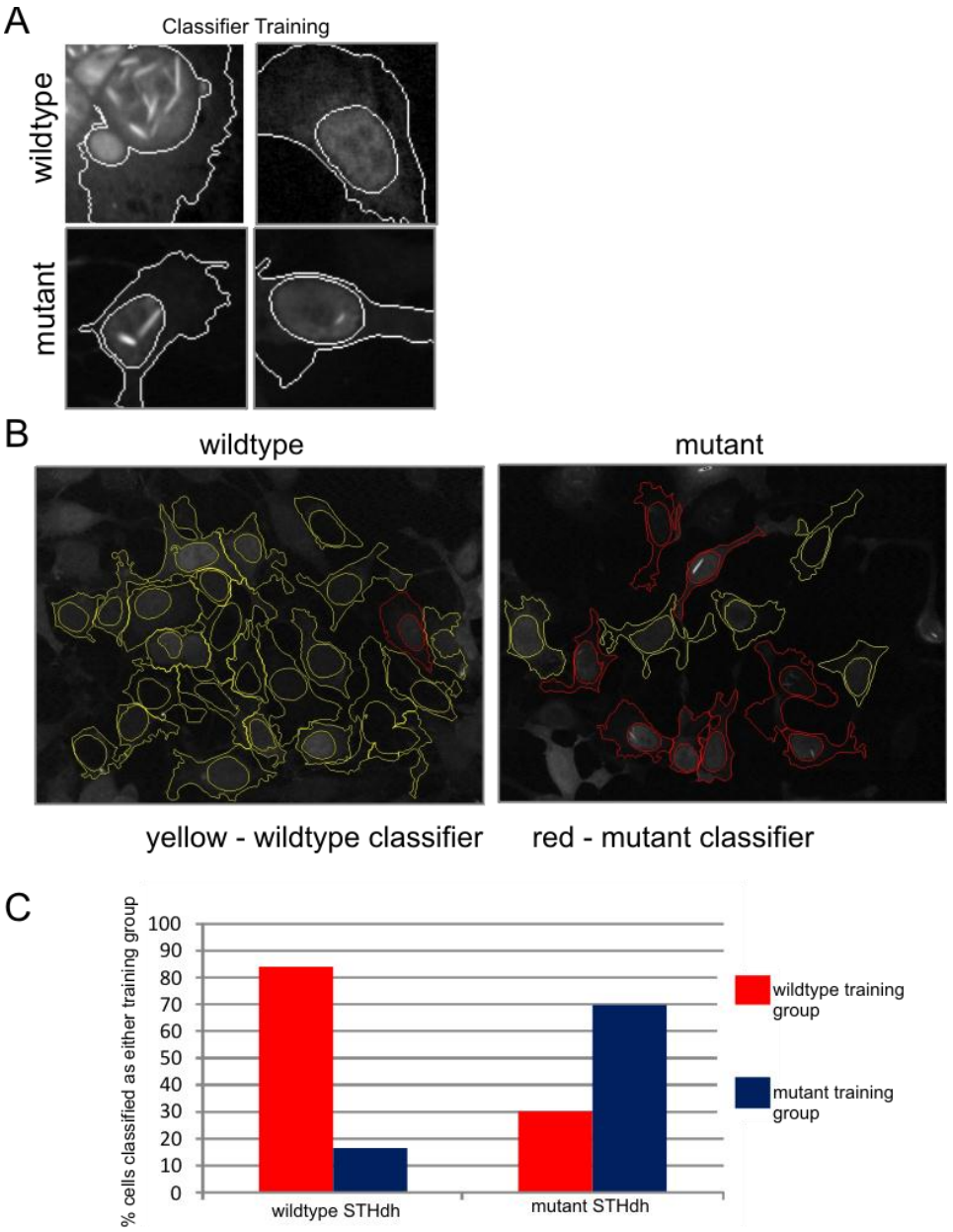

Figure 5.2 Wildtype and mutant cell morphologies can be distinguished by CAFE miCells using features extracted from the Acapella software. A. Examples of cells distinguished by Acapella software and used to train CAFE miCells to determine differences between mutant and wildtype cells based on morphological characteristics. **B.** Example image of each cell type showing cells distinguished as either wildtype or mutant based on morphology. **C.** Quantification of cells in each population distinguished as having a wildtype or mutant morphology.

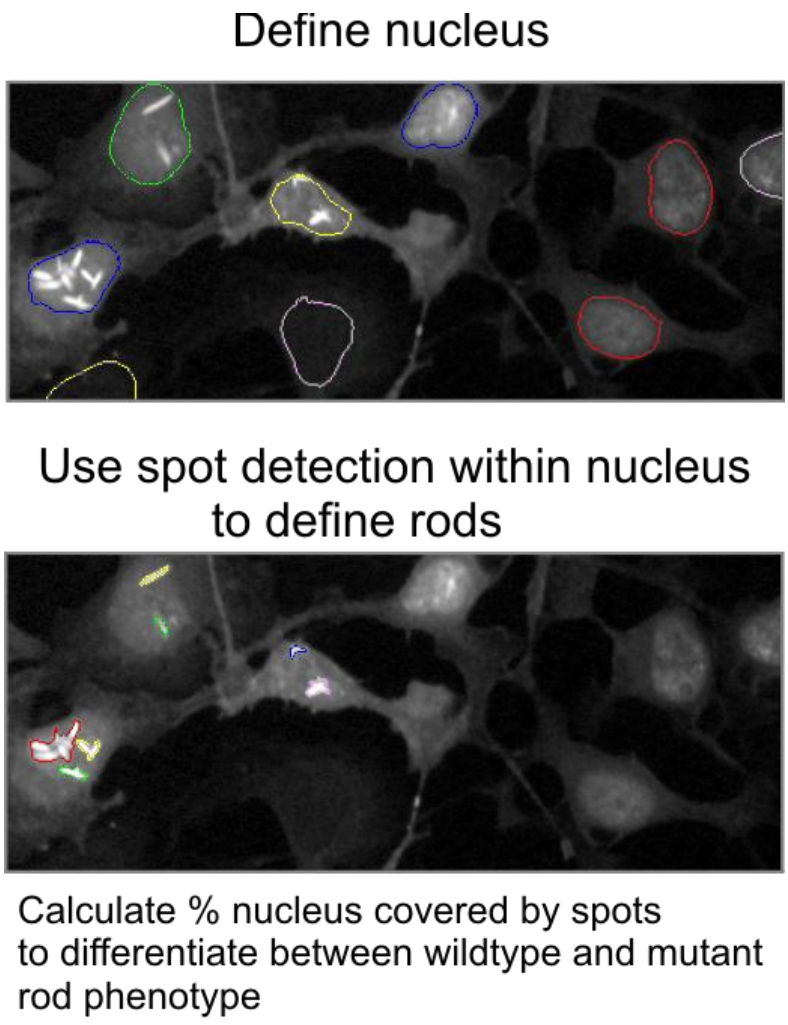

Figure 5.3 Rods can be found in nucleus using nuclear spot identifier. Example images showing that the Acapella software can distinguish the nucleus using the DRAQ5 stain and then subsequently pick out rods in the nucleus in the YFP channel using the large nuclear spot identifier.

level of phosphorylated huntingtin in the nucleus is linked to a successful outcome with respect to drug treatment. We will examine the effects these compounds have on cofilin levels and phospho-cofilin levels since we know these are altered in HD cells and predict that compounds that affect this will also affect rod formation. We will also use our β-galactosidase reporter system to assess any affects these compounds have on the ability of cofilin to enter the nucleus and assess if altering this ability may have successful outcomes for HD. Other secondary screens can be performed with respect to the role of huntingtin in cell survival, which is additionally important with respect to disease. Once these screens have been done, if there are any compounds that are having overwhelming beneficial effects they can be assessed for feasibility as drugs. They will have to be assessed based on if they are deliverable, non-toxic and cross the blood brain barrier and can then be tested for behavioural and neuronal degeneration rescue, or biomarker changes depending on the state of research at that point, in mouse models of HD.

5.2 Targeting the Intervening Sequence of the Cofilin NLS to Alter Rod Forming Ability

In chapter 2 we found that the nuclear cofilin-rod stress response is affected by the presence of mutant huntingtin in the cell, and in chapter 3 we describe how mediating the nuclear entry and exit of cofilin directly impacts this response. Therefore we are looking at ways to affect the nuclear import and export of cofilin to see if we can mitigate this stress response by manipulating these biochemical pathways. The nuclear export of cofilin is mediated by CRM1, the major export pathway in the cell (Fornerod et al., 1997). We predict based on the NLS sequence of cofilin, that its nuclear import is mediated by the major nuclear import pathway in the cell, the importin α/β pathway (Lange et al., 2007). Globally disrupting either of these pathways to mediate the nuclear shuttling of cofilin is not a viable option since these pathways are used for the nuclear transport of many target proteins. Thus, we need to find ways to specifically alter the shuttling capabilities of cofilin with as few off target effects as possible. The cofilin NLS

is a bipartite NLS, which means it has two basic regions required for nuclear import with an intervening sequence between the regions. This intervening sequence would presumably affect the confirmation of the NLS or its interactions with the import protein and may be amenable to biochemical manipulation. We specifically noted that the intervening sequence of this NLS has a conserved SST motif. All three of these residues are capable of being phosphorylated and the activity of many NLSs are controlled by reversible phosphorylation of residues near the consensus import sequence (Harreman et al., 2004). We would like to test the effects that phosphorylation at these residues has on the ability of the NLS to function. We have done an initial experiment, phosphomimicking each residue individually in the context of our GFP–RKSSTPEEVKKRKK- β-galactosidase reporter, to make either an S23D, S24D or T25D mutation (amino acid residues corresponding to full length cofilin sequence) (Figure 5.4A). We found that making the S23D mutation, thus mimicking constitutive phosphorylation at this residue, resulted in less nuclear accumulation of the reporter, indicating that phosphorylation of this residue may be involved in regulating the nuclear shuttling of cofilin (Figure 5.4A&B). We find this data encouraging and will pursue making alanine mutations in this model to inhibit phosphorylation at those residues to assess this effect on nuclear accumulation of the reporter, as well as making in context mutations to see if the full length cofilin is affected in the same manner. This will tell us if we might be able to use kinase inhibitors to modulate cofilin nuclear entry, a viable option in drug discovery (Zhang et al., 2009). We can initially screen our reporter for change in activity upon administration of kinase inhibitors, and then screen our EYFP-cofilin stable lines for change in localization both before and after stress, as well as for any associated changes in rod forming dynamics. If we find any compounds that modulate these outcomes they can be used to assay the cofilin dynamics changes in the presence of mutant huntingtin, and follow up screens can be performed as described previously.

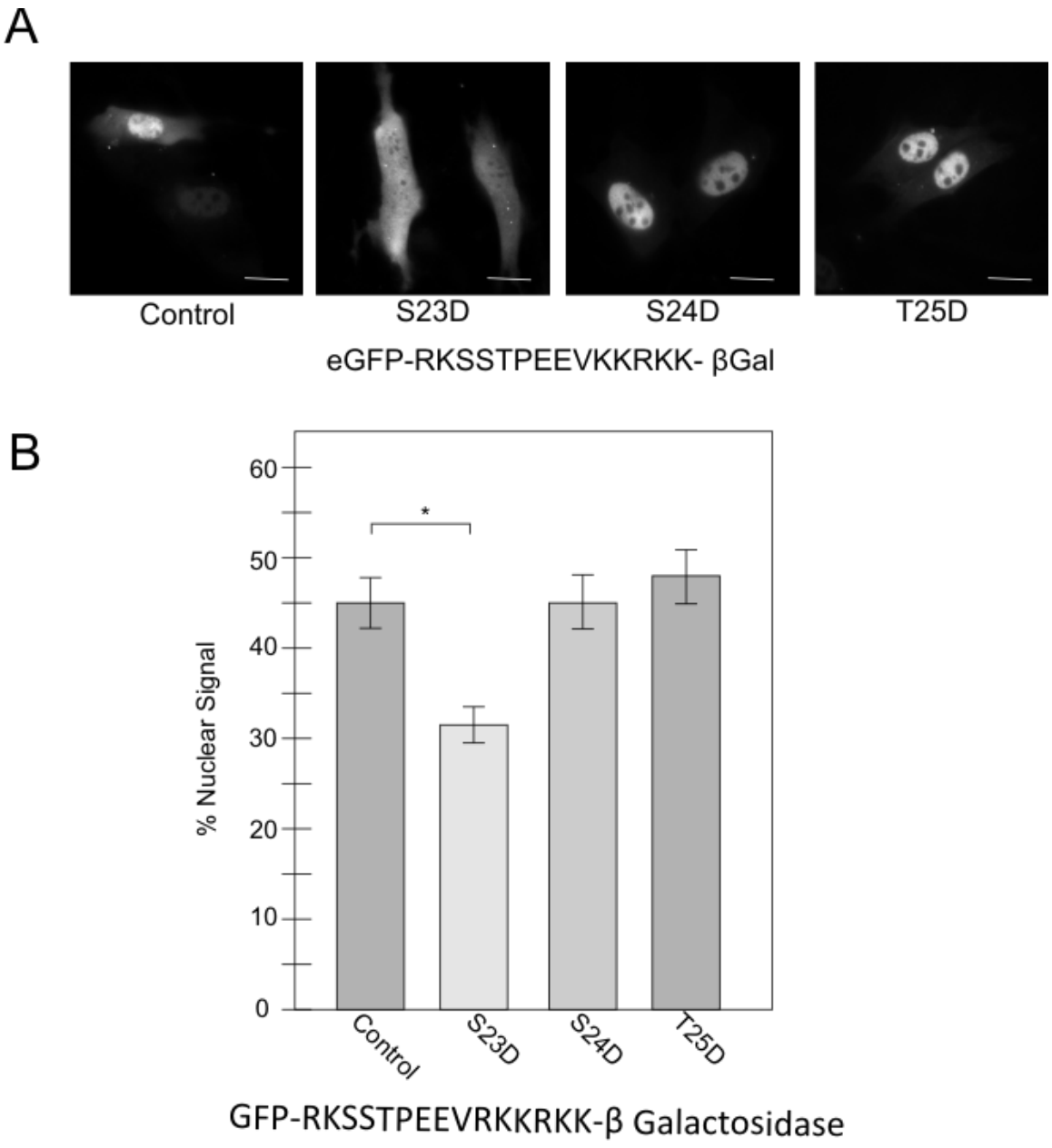

Figure 5.4 Phosphomimicking intervening sequence of cofilin NLS affects nuclear localization A. We know that the putative cofilin bipartite NLS mediates βGal nuclear entry. GFP-RKSSTPEEVRKKRKK-β Galactosidase or this construct with mutations S23D, S24D or T25D were made to assess the effects of phosphomimicking on nuclear entry of the constructs Imaging done at 60X. Scale bar = 10µm **B.** Graph represents percent nuclear fluorescent signal analysis for each construct N= at least 30 cells/construct, Images taken in fixed cells *P<0.05.

5.3 Answering New Questions about Cofilin-Actin Dynamics

This body of work has posed additional questions that need to be answered with respect to cofilin and actin dynamics in general, as well as with respect to disease. We have redefined the cofilin NLS as a bipartite NLS with an amino acid sequence that is similar to the importin α/β bipartite NLS consensus (Robbins et al., 1991), however we have not shown a direct interaction between cofilin and a specific nuclear import factor. At the time of these experiments cofilin was thought to be required for actin nuclear transport, but this was not unequivocally shown. With no evidence to the contrary we were able to assume that the cofilin NLS matched importin α/β bipartite NLS closely enough to be mediated through this pathway (Lange et al., 2010; Taniguchi et al., 2002). New evidence shows that cofilin is absolutely required for the nuclear import of actin, and that this import is linked not to importin α/β but to importin 9 (Dopie et al., 2012). It is possible that cofilin nuclear import is mediated through importin 9 as the consensus sequence for this import factor is unknown and the amino acid sequence in cofilin in slightly shorter than the normal bipartite NLS consensus for importin α/β. Targeting the nuclear import of cofilin may be more realistic if it is being imported through an obscure import pathway like importin 9, which has few known substrates at this point. Disrupting a major import pathway like importin α/β would be harder to do in a specific manner, and likely have more off target effects due to the large amount of import substrates that utilize this pathway.

We additionally hypothesize that knocking down cofilin, specifically in stress conditions, will have strong implications on transcriptional regulation. It has been shown that cofilin knockdown affects steady state transcription through activity in concert with actin in the nucleus under steady state conditions (Dopie et al., 2012; Obrdlik and Percipalle, 2011). Therefore global transcriptional changes should be examined in our cofilin knockdown system, both at steady state conditions and during heat shock stress and both in the background of wildtype and mutant huntingtin. This

will answer what genes cofilin is specifically involved in regulating and these genes can be cross referenced for being affected in HD or other HD models.

Based on the important regulation of transcription imposed by actin and cofilin, and based on the cellular requirement for transcriptional changes after the heat shock response has been induced, we hypothesize that one function of nuclear rods is in regulating transcription in some manner. To initially test this we can use our cofilin mutants that specifically affect rod formation, R21A and K22A, to probe how rod formation affects transcriptional changes during stress and if rod formation does indeed influence stress dependent transcription changes. This will additionally answer if these non-rod forming cofilin mutants can perform the transcriptional functions of cofilin both under steady state and stress conditions. This will give us information about the biological requirement of rods with respect to transcription during stress and will provide an additional potential read-out or assay for screening of compounds by analyzing gene transcription changes caused by aberrant actin reorganization in the nucleus during stress.

5.4 Conclusion

This body of work describes a new role of huntingtin with respect to the cell stress response. Specifically, huntingtin localizes to nuclear cofilin-actin rods during stress, and this cytoskeletal stress response is impaired by the presence of mutant huntingtin in the cell, in a dominant fashion. We find that part of the pathogenic mechanism may be mediated by the enzyme TG2, indicating that this could be part of the TG2 pathology in neurodegeneration. We find aberrant cofilin-actin crosslinks in patient blood samples that increases with disease progression. It is our hope, that with some optimization, this inappropriate cofilin-actin crosslink western blot profile from patient blood may become part of a panel of biomarkers that can be used for outcome testing in clinical trials for HD.

We went on to further characterize actual cofilin-actin rods, trying to find if and how this stress pathway may be used in drug discovery efforts. We find that cofilin has a highly conserved import and export signal that seems to be required for cofilin activity under steady state and cell stress conditions. The functionality of these signals is required for proper rod formation and therefore we propose that altering the shuttling abilities of cofilin may alter rod formation and be a way to manipulate this pathway. We went on to answer the question if rod formation is required in the cell, in hopes of finding if ablation of rod formation would be an acceptable therapeutic. We find that cells cannot appropriately respond to stress in the absence of a correct cofilin-actin rod stress response and thus ways to mediate, but not abolish this stress response will be probed as a therapeutic.

The literature strongly supports an energetic failure and problems with neurons responding to stress as a causative factor in neurodegeneration. This body of work not only supports that, but describes a pathway that would contribute to most known factors in neurodegeneration, including differential cellular susceptibility to neurodegenerative insults. It is our hope that this pathway will be used to look for small molecules that have disease modifying activity in future work.

APPENDIX 1 - Detailed cloning information for Chapter 3 plasmids

A1.1 NES and NLS mutations

EYFP-cofilin plasmid used was previously described (Munsie et al., 2011), and in detail with primers in Chapter 2 methods and materials.

Primers to mutate the NES (V20A) and the NLS (KR31-32AA) were made (McMaster Mobix facility) and mutations achieved according to manufacturer's protocol using the QuickChange kit (Stratagene). All plasmids constructs were verified by DNA sequencing (McMaster Mobix facility).

V20A

5'CATCAAGGTGGTCAACGACGCGAAGGCGCGTTAGTCTTCAACGCC3'

5' GGCGTTGAAGACTTACGCGCCTTCGCGTCGTTGTTGAACACCTTGATG3'

NOTE: Primers encode M18AV20A but sequencing showed one clone with a mutation only at V20A. Both EYFP-cofilin M18AV20A and EYFP-cofilin V20A have been used with the same results therefore we based our studies off the minimal mutation, V20A.

KR31-32AA

5' CAGAGGAGGTGAAGGCGGCCAAGAAGGCGG 3'

5' CCGCCTTCTTGGCCGCCTTCACCTCCTCTG 3'

To create the full NLS mutant EYFP-cofilin RK21-22AA, KR31-32AA primers to mutate the first part of the bipartite NLS (RK21-22AA) were made using inverse PCR on the eYFP-cofilin KR 31-32 AA vector:

5' CAACGACATGAAGGTGGCTGCGTCTTCAACGCCAGAGG 3'

5' CCTCTGGCGTTGAAGACGCAGCCACCTTCATGTCGTTG 3'

Primers to make single mutations R21A or K22A were made using inverse PCR

R21A:

5’GCAAAGTCTTCAACGCCAGAGG3’

5’CACCTTCATGTCGTTGAAC3’

K22A:

5’GCATCTTCAACGCCAGAGGAGGTG3’

5’ACGCACCTTCATGTCGTTGAAC3’

A1.2 Synthetic NES and NLS constructs

The synthetic NES was made with 5' BspEI and 3' Acc651 overhangs and cloned using the annealed product into peYFPC1 (BD Biosciences/Clontech) to create Synthetic NES-YFPN1:

5’ CCGGAGTGATCAAGGTGTTCAACGACATGAAGCTGG 3’

5’ GTACCCACCTTCATGTCGTTGAACACCTTCATGACT 3'

Synthetic DNA oligonucleotides encoding the cofilin NLS, bipartite NLS and bipartite NLS mutations were made with 5’ SacII and 3’ XbaI overhangs (MOBIX, McMaster University) and cloned using the annealed products into EGFP-MCS-βGalactosidase (phM830 vector) to create EGFP-“synthetic NLS”- βGalactosidase.

Putative Cofilin NLS:

5’ GGCCAGAGGAGGTGAAGAAGCGCAAGAAGGCGGTGT 3’

5’CTAGACACCGCCTTCTTGCGCTTCTTCACCTCCTCTGGCCGC 3’

Putative Cofilin Bipartite NLS:

5’ GGAAGGTGCGTAAGTCTTCAACGCCAGAGGAGGTGAAGAAGCGCAAGAAGGCGT 3’

5’ CTAGACGCCTTCTTGCGCTTCTTCACCTCCTCTGGCGTTGAAGACTTACGCACCTTCCGC 3’

Putative cofilin bipartite NLS mutant:

5’ GGAAGGTGGCTGCGTCTTCAACGCCAGAGGAGGTGAAGGCAGCTAAGAAGGCGT 3’

5’ CTAGACGCCTTCTTAGCTGCCTTCACCTCCTCTGGCGTTGAAGACGCAGCCACCTTCCGC 3’

A1.3 Cofilin shRNA plasmids

Cofilin shRNA plasmids were purchased (HuSH Origene) in pRFP-C-RS vector. Cofilin shRNA F1575659 was used for all experiments and scrambled control TR30015 or vector control TR30014.

To make silent mutations in the EYFP-cofilin plasmid so that it would not be susceptible to the shRNA inverse PCR was used:

5’ GATTGTAGATACGCCCTCTATGATGCAACCTATG 3’

5’ TTTATCAGGTAACATCTTGACAAAGGTGGCGTAG 3’

These primers were used to mutate and introduce silent mutations into EYFP-Cofilin, EYFP-Cofilin RK21-22AA KR 31-32AA, EYFP-Cofilin V20A, YFP-cofilin R21A and YFP-Cofilin K22A.

To alter the shRNA plasmid so that the RFP was removed and the MCS had additional cut sites (ApaI and AscI were added) inverse PCR was used on the control shRNA vector TR30015 and the cofilin shRNA plasmid F1575659

5’GGGCCCGGTGGCAGATCTCCTC3’

5’GGCGCGCCCGATCGCAACGTTCGAA3’

Primers to express EYFP-cofilin or EYFP were made (McMaster Mobix facility) with 5' MluI and 3' PmeI overhangs and cloning was performed, using PCR product from all EYFP-cofilin plasmids (wildtype, NLS/NES mutations) or EYFP alone plasmid (previously described), between MluI/PmeI sites of the shRNA plasmids with the fluorophore removed - TR30015 and F1575659 to create EYFP-Cofilin-F1575659-R-CS, EYFP-F1575659-R-CS and EYFP-TR30015-R-CS. The same forward primer amplifying YFP was used on both EYFP alone and EYFP-cofilin

YFP forward:

5’GATCACGCGTATGGTGAGCAAGGGCGAG3’

YFP Reverse:

5’GATCGTTTAAACTTGTACAGCTCGTCCATGC3’

Cofilin Reverse:

5’GATCGTTTAAACCAAAGGCTTGCCCTCCAG3’

A1.4 GST-cofilin plasmids

Primers to express human cofilin1 were made (McMaster Mobix facility) with 5’ BamHI and 3’ EcoRI overhangs and cloning was performed, using PCR product from all EYFP-

cofilin plasmids previously made (wildtype and NLS/NES mutants), between BamHI/EcoRI cut sites of pGEX 5X-1 (GE) to create GST-Cofilin expression plasmid.

5’ GATCGGATCCAGATGGCCTCCGGTGTGGC 3’;

5’ GATCGAATTCCAAAGGCTTGCCCTCCAG 3’.

A1.5 Cofilin-3XFLAG plasmids

Primers to express human cofilin1 were made with 5’ Acc651 and 3’ XbaI overhangs and cloning was performed, using PCR product from our previously constructed EYFP-cofilin plasmids (wildtype and NLS/NES mutants), between Acc651/XbaI sites of 3xFLAG-CMV-14 (Sigma) to create the cofilin-3xFLAG plasmids.

5’ GATCGGTACCATGGCCTCCGGTGTGGC 3’

5’ GATCTCTAGACAAAGGCTTGCCCTCCAG 3’

A1.6 Cofilin phM830 plasmids

To make the GFP-cofilin RK21-22AA KR31-32AA- β-Galactosidase construct, primers to express human cofilin1 were made with 5’ SacII and 3’ XbaI overhangs and cloning was performed, using PCR product from our previously constructed EYFP-cofilin RK21-22AA, KR31-32AA plasmid between SacII/XbaI sites of phM830.

5’ GATCCCGCGGATGGCCTCCGGTGTGGC 3’

5’ GATCTCTAGACAAAGGCTTGCCCTCCAG 3’

BIBLIOGRAPHY

Abe, H., R. Nagaoka, and T. Obinata. 1993. Cytoplasmic localization and nuclear transport of cofilin in cultured myotubes. *Exp.Cell Res.* 206:1-10.

Agrawal, N., J. Pallos, N. Slepko, B.L. Apostol, L. Bodai, L.W. Chang, A.S. Chiang, L.M. Thompson, and J.L. Marsh. 2005. Identification of combinatorial drug regimens for treatment of Huntington's disease using Drosophila. *Proc.Natl.Acad.Sci.U.S.A*. 102:3777-3781.

Aiken, C.T., J.S. Steffan, C.M. Guerrero, H. Khashwji, T. Lukacsovich, D. Simmons, J.M. Purcell, K. Menhaji, Y.Z. Zhu, K. Green, F. Laferla, L. Huang, L.M. Thompson, and J.L. Marsh. 2009. Phosphorylation of threonine 3: implications for Huntingtin aggregation and neurotoxicity. *J.Biol.Chem.* 284:29427-29436.

Aiken, C.T., A.J. Tobin, and E.S. Schweitzer. 2004. A cell-based screen for drugs to treat Huntington's disease. *Neurobiology of disease*. 16:546-555.

Andrade, M.A., and P. Bork. 1995. HEAT repeats in the Huntington's disease protein. *Nature genetics*. 11:115-116.

Andrade, M.A., C. Petosa, S.I. O'Donoghue, C.W. Muller, and P. Bork. 2001. Comparison of ARM and HEAT protein repeats. *J.Mol.Biol.* 309:1-18.

Angeli, S., J. Shao, and M.I. Diamond. 2010. F-actin binding regions on the androgen receptor and huntingtin increase aggregation and alter aggregate characteristics. *PloS one*. 5:e9053.

Annis, M.G., N. Zamzami, W. Zhu, L.Z. Penn, G. Kroemer, B. Leber, and D.W. Andrews. 2001. Endoplasmic reticulum localized Bcl-2 prevents apoptosis when redistribution of cytochrome c is a late event. *Oncogene*. 20:1939-1952.

Arber, S., F.A. Barbayannis, H. Hanser, C. Schneider, C.A. Stanyon, O. Bernard, and P. Caroni. 1998. Regulation of actin dynamics through phosphorylation of cofilin by LIM-kinase. *Nature*. 393:805-809.

Arrasate, M., S. Mitra, E.S. Schweitzer, M.R. Segal, and S. Finkbeiner. 2004. Inclusion body formation reduces levels of mutant huntingtin and the risk of neuronal death. *Nature*. 431:805-810.

Attwell, D., and S.B. Laughlin. 2001. An energy budget for signaling in the grey matter of the brain. *Journal of cerebral blood flow and metabolism : official journal of the International Society of Cerebral Blood Flow and Metabolism*. 21:1133-1145.

Atwal, R.S., C.R. Desmond, N. Caron, T. Maiuri, J. Xia, S. Sipione, and R. Truant. 2011. Kinase inhibitors modulate huntingtin cell localization and toxicity. *Nature chemical biology*. 7:453-460.

Atwal, R.S., J. Xia, D. Pinchev, J. Taylor, R.M. Epand, and R. Truant. 2007. Huntingtin has a membrane association signal that can modulate huntingtin aggregation, nuclear entry and toxicity. *Human molecular genetics*. 16:2600-2615.

Bailey, C.D., and G.V. Johnson. 2005. Tissue transglutaminase contributes to disease progression in the R6/2 Huntington's disease mouse model via aggregate-independent mechanisms. *J.Neurochem.* 92:83-92.

Bamburg, J.R., B.W. Bernstein, R.C. Davis, K.C. Flynn, C. Goldsbury, J.R. Jensen, M.T. Maloney, I.T. Marsden, L.S. Minamide, C.W. Pak, A.E. Shaw, I. Whiteman, and O. Wiggan. 2010. ADF/Cofilin-actin rods in neurodegenerative diseases. *Curr.Alzheimer Res.* 7:241-250.

Bamburg, J.R., and O.P. Wiggan. 2002. ADF/cofilin and actin dynamics in disease. *Trends in Cell Biology*. 12:598-605.

Bao, J., A.H. Sharp, M.V. Wagster, M. Becher, G. Schilling, C.A. Ross, V.L. Dawson, and T.M. Dawson. 1996. Expansion of polyglutamine repeat in huntingtin leads to abnormal protein interactions involving calmodulin. *Proceedings of the National Academy of Sciences of the United States of America*. 93:5037-5042.

Bauer, P.O., H.K. Wong, F. Oyama, A. Goswami, M. Okuno, Y. Kino, H. Miyazaki, and N. Nukina. 2009. Inhibition of Rho kinases enhances the degradation of mutant huntingtin. *J.Biol.Chem.* 284:13153-13164.

Beal, M.F., N.W. Kowall, D.W. Ellison, M.F. Mazurek, K.J. Swartz, and J.B. Martin. 1986. Replication of the neurochemical characteristics of Huntington's disease by quinolinic acid. *Nature*. 321:168-171.

Belanger, M., I. Allaman, and P.J. Magistretti. 2011. Brain energy metabolism: focus on astrocyte-neuron metabolic cooperation. *Cell metabolism*. 14:724-738.

Benchaar, S.A., Y. Xie, M. Phillips, R.R. Loo, V.E. Galkin, A. Orlova, M. Thevis, A. Muhlrad, S.C. Almo, J.A. Loo, E.H. Egelman, and E. Reisler. 2007. Mapping the interaction of cofilin with subdomain 2 on actin. *Biochemistry*. 46:225-233.

Benn, C.L., T. Sun, G. Sadri-Vakili, K.N. McFarland, D.P. DiRocco, G.J. Yohrling, T.W. Clark, B. Bouzou, and J.H. Cha. 2008. Huntingtin modulates transcription, occupies gene promoters in vivo, and binds directly to DNA in a polyglutamine-dependent manner. *The Journal of neuroscience : the official journal of the Society for Neuroscience*. 28:10720-10733.

Bernstein, B.W., and J.R. Bamburg. 2003. Actin-ATP hydrolysis is a major energy drain for neurons. *J.Neurosci.* 23:1-6.

Bernstein, B.W., and J.R. Bamburg. 2010. ADF/cofilin: a functional node in cell biology. *Trends Cell Biol.* 20:187-195.

Bernstein, B.W., H. Chen, J.A. Boyle, and J.R. Bamburg. 2006. Formation of actin-ADF/cofilin rods transiently retards decline of mitochondrial potential and ATP in stressed neurons. *Am.J.Physiol Cell Physiol*. 291:C828-C839.

Bjorkqvist, M., E.J. Wild, J. Thiele, A. Silvestroni, R. Andre, N. Lahiri, E. Raibon, R.V. Lee, C.L. Benn, D. Soulet, A. Magnusson, B. Woodman, C. Landles, M.A. Pouladi, M.R. Hayden, A. Khalili-Shirazi, M.W. Lowdell, P. Brundin, G.P. Bates, B.R. Leavitt, T. Moller, and S.J. Tabrizi. 2008. A novel pathogenic pathway of immune activation detectable before clinical onset in Huntington's disease. *The Journal of experimental medicine*. 205:1869-1877.

Bogerd, H.P., R.A. Fridell, R.E. Benson, J. Hua, and B.R. Cullen. 1996. Protein sequence requirements for function of the human T-cell leukemia virus type 1 Rex nuclear export signal delineated by a novel in vivo randomization-selection assay. *Mol.Cell Biol.* 16:4207-4214.

Bonelli, R.M., F.A. Mahnert, and G. Niederwieser. 2002. Olanzapine for Huntington's disease: an open label study. *Clinical neuropharmacology*. 25:263-265.

Boudreau, R.L., J.L. McBride, I. Martins, S. Shen, Y. Xing, B.J. Carter, and B.L. Davidson. 2009. Nonallele-specific silencing of mutant and wild-type huntingtin demonstrates therapeutic efficacy in Huntington's disease mice. *Molecular therapy : the journal of the American Society of Gene Therapy*. 17:1053-1063.

Boudreau, R.L., A.M. Monteys, and B.L. Davidson. 2008. Minimizing variables among hairpin-based RNAi vectors reveals the potency of shRNAs. *RNA*. 14:1834-1844.

Bradley Zuchero, J., B. Belin, and R. Dyche Mullins. 2012. Actin Binding to WH2 Domains Regulates Nuclear Import of the Multifunctional Actin Regulator JMY. *Molecular Biology of the Cell*.

Brook, J.D., M.E. McCurrach, H.G. Harley, A.J. Buckler, D. Church, H. Aburatani, K. Hunter, V.P. Stanton, J.P. Thirion, T. Hudson, and et al. 1992. Molecular basis of myotonic dystrophy: expansion of a trinucleotide (CTG) repeat at the 3' end of a transcript encoding a protein kinase family member. *Cell*. 68:799-808.

Brouillet, E., C. Jacquard, N. Bizat, and D. Blum. 2005. 3-Nitropropionic acid: a mitochondrial toxin to uncover physiopathological mechanisms underlying striatal degeneration in Huntington's disease. *Journal of neurochemistry*. 95:1521-1540.

Browne, S.E., A.C. Bowling, U. MacGarvey, M.J. Baik, S.C. Berger, M.M. Muqit, E.D. Bird, and M.F. Beal. 1997. Oxidative damage and metabolic dysfunction in Huntington's disease: selective vulnerability of the basal ganglia. *Annals of neurology*. 41:646-653.

Browne, S.E., R.J. Ferrante, and M.F. Beal. 1999. Oxidative stress in Huntington's disease. *Brain Pathol.* 9:147-163.

Burnett, B.G., J. Andrews, S. Ranganathan, K.H. Fischbeck, and N.A. Di Prospero. 2008. Expression of expanded polyglutamine targets profilin for degradation and alters actin dynamics. *Neurobiology of disease*. 30:365-374.

Butters, N., J. Wolfe, M. Martone, E. Granholm, and L.S. Cermak. 1985. Memory disorders associated with Huntington's disease: verbal recall, verbal recognition and procedural memory. *Neuropsychologia*. 23:729-743.

Caine, E.D., M.H. Ebert, and H. Weingartner. 1977. An outline for the analysis of dementia. The memory disorder of Huntingtons disease. *Neurology*. 27:1087-1092.

Calabresi, P., M.M. De, A. Pisani, A. Stefani, G. Sancesario, N.B. Mercuri, and G. Bernardi. 1995. Vulnerability of medium spiny striatal neurons to glutamate: role of Na+/K+ ATPase. *Eur.J.Neurosci.* 7:1674-1683.

Caputo, I., M.V. Barone, S. Martucciello, M. Lepretti, and C. Esposito. 2009. Tissue transglutaminase in celiac disease: role of autoantibodies. *Amino acids*. 36:693-699.

Cardoso, F., K. Seppi, K.J. Mair, G.K. Wenning, and W. Poewe. 2006. Seminar on choreas. *Lancet Neurol.* 5:589-602.

Cariello, L., C.T. de, L. Zanetti, T. Cuomo, M.L. Di, G. Campanella, S. Rinaldi, P. Zanetti, L.R. Di, and S. Varrone. 1996. Transglutaminase activity is related to CAG repeat length in patients with Huntington's disease. *Hum.Genet.* 98:633-635.

Carlier, M.F., V. Laurent, J. Santolini, R. Melki, D. Didry, G.X. Xia, Y. Hong, N.H. Chua, and D. Pantaloni. 1997. Actin depolymerizing factor (ADF/cofilin) enhances the rate of filament turnover: implication in actin-based motility. *J.Cell Biol.* 136:1307-1322.

Carroll, J.B., S.C. Warby, A.L. Southwell, C.N. Doty, S. Greenlee, N. Skotte, G. Hung, C.F. Bennett, S.M. Freier, and M.R. Hayden. 2011. Potent and selective antisense oligonucleotides targeting single-nucleotide polymorphisms in the Huntington disease

gene / allele-specific silencing of mutant huntingtin. *Molecular therapy : the journal of the American Society of Gene Therapy*. 19:2178-2185.

Cattaneo, E., and L. Conti. 1998. Generation and characterization of embryonic striatal conditionally immortalized ST14A cells. *J.Neurosci.Res.* 53:223-234.

Cepeda, C., D.M. Cummings, V.M. Andre, S.M. Holley, and M.S. Levine. 2010. Genetic mouse models of Huntington's disease: focus on electrophysiological mechanisms. *ASN neuro*. 2:e00033.

Cha, J.H. 2007. Transcriptional signatures in Huntington's disease. *Progress in neurobiology*. 83:228-248.

Cheng, Y., Q. Peng, Z. Hou, M. Aggarwal, J. Zhang, S. Mori, C.A. Ross, and W. Duan. 2011. Structural MRI detects progressive regional brain atrophy and neuroprotective effects in N171-82Q Huntington's disease mouse model. *NeuroImage*. 56:1027-1034.

Choo, Y.S., G.V. Johnson, M. MacDonald, P.J. Detloff, and M. Lesort. 2004. Mutant huntingtin directly increases susceptibility of mitochondria to the calcium-induced permeability transition and cytochrome c release. *Human molecular genetics*. 13:1407-1420.

Chuang, D.M., Y. Leng, Z. Marinova, H.J. Kim, and C.T. Chiu. 2009. Multiple roles of HDAC inhibition in neurodegenerative conditions. *Trends in neurosciences*. 32:591-601.

Chun, W., M. Lesort, J. Tucholski, C.A. Ross, and G.V. Johnson. 2001. Tissue transglutaminase does not contribute to the formation of mutant huntingtin aggregates. *J.Cell Biol.* 153:25-34.

Cichon, J., C. Sun, B. Chen, M. Jiang, X.A. Chen, Y. Sun, Y. Wang, and G. Chen. 2012. Cofilin aggregation blocks intracellular trafficking and induces synaptic loss in hippocampal neurons. *The Journal of biological chemistry*. 287:3919-3929.

Colin, E., D. Zala, G. Liot, H. Rangone, M. Borrell-Pages, X.J. Li, F. Saudou, and S. Humbert. 2008. Huntingtin phosphorylation acts as a molecular switch for anterograde/retrograde transport in neurons. *The EMBO journal*. 27:2124-2134.

Cong, S.Y., B.A. Pepers, B.O. Evert, D.C. Rubinsztein, R.A. Roos, G.J. van Ommen, and J.C. Dorsman. 2005. Mutant huntingtin represses CBP, but not p300, by binding and protein degradation. *Molecular and cellular neurosciences*. 30:12-23.

Conneally, P.M. 1984. Huntington disease: genetics and epidemiology. *Am.J.Hum.Genet.* 36:506-526.

Cooper, A.J., K.F. Sheu, J.R. Burke, O. Onodera, W.J. Strittmatter, A.D. Roses, and J.P. Blass. 1997. Polyglutamine domains are substrates of tissue transglutaminase: does transglutaminase play a role in expanded CAG/poly-Q neurodegenerative diseases? *J.Neurochem.* 69:431-434.

Craufurd, D., J.C. Thompson, and J.S. Snowden. 2001. Behavioral changes in Huntington Disease. *Neuropsychiatry, neuropsychology, and behavioral neurology*. 14:219-226.

Cudkowicz, M., and N.W. Kowall. 1990. Degeneration of pyramidal projection neurons in Huntington's disease cortex. *Annals of neurology*. 27:200-204.

Dallocchio, C., C. Buffa, C. Tinelli, and P. Mazzarello. 1999. Effectiveness of risperidone in Huntington chorea patients. *Journal of clinical psychopharmacology*. 19:101-103.

Dalrymple, A., E.J. Wild, R. Joubert, K. Sathasivam, M. Bjorkqvist, A. Petersen, G.S. Jackson, J.D. Isaacs, M. Kristiansen, G.P. Bates, B.R. Leavitt, G. Keir, M. Ward, and S.J. Tabrizi. 2007. Proteomic profiling of plasma in Huntington's disease reveals

neuroinflammatory activation and biomarker candidates. *J.Proteome.Res.* 6:2833-2840.

Dana, C.L. 1895. The Pathology of Hereditary Chorea. Report of A Case With Autopsy. Record of Anomalies in A Degenerate Brain. *The Journal of Nervous and Mental Disease*. 20.

Davis, R.C., M.T. Maloney, L.S. Minamide, K.C. Flynn, M.A. Stonebraker, and J.R. Bamburg. 2009. Mapping Cofilin-Actin Rods in Stressed Hippocampal Slices and the Role of cdc42 in Amyloid-beta-Induced Rods. *J.Alzheimers.Dis.*

de Lanerolle, P., and L. Serebryannyy. 2011. Nuclear actin and myosins: life without filaments. *Nature cell biology*. 13:1282-1288.

de Yebenes, J.G., B. Landwehrmeyer, F. Squitieri, R. Reilmann, A. Rosser, R.A. Barker, C. Saft, M.K. Magnet, A. Sword, A. Rembratt, and J. Tedroff. 2011. Pridopidine for the treatment of motor function in patients with Huntington's disease (MermaiHD): a phase 3, randomised, double-blind, placebo-controlled trial. *Lancet neurology*. 10:1049-1057.

DeJesus-Hernandez, M., I.R. Mackenzie, B.F. Boeve, A.L. Boxer, M. Baker, N.J. Rutherford, A.M. Nicholson, N.A. Finch, H. Flynn, J. Adamson, N. Kouri, A. Wojtas, P. Sengdy, G.Y. Hsiung, A. Karydas, W.W. Seeley, K.A. Josephs, G. Coppola, D.H. Geschwind, Z.K. Wszolek, H. Feldman, D.S. Knopman, R.C. Petersen, B.L. Miller, D.W. Dickson, K.B. Boylan, N.R. Graff-Radford, and R. Rademakers. 2011. Expanded GGGGCC hexanucleotide repeat in noncoding region of C9ORF72 causes chromosome 9p-linked FTD and ALS. *Neuron*. 72:245-256.

Delanty, N., and M.A. Dichter. 2000. Antioxidant therapy in neurologic disease. *Archives of neurology*. 57:1265-1270.

Delmaire, C., E.M. Dumas, M.A. Sharman, S.J. van den Bogaard, R. Valabregue, C. Jauffret, D. Justo, R. Reilmann, J.C. Stout, D. Craufurd, S.J. Tabrizi, R.A. Roos, A. Durr, and S. Lehericy. 2012. The structural correlates of functional deficits in early huntington's disease. *Human brain mapping*.

Di Pardo, A., V. Maglione, M. Alpaugh, M. Horkey, R.S. Atwal, J. Sassone, A. Ciammola, J.S. Steffan, K. Fouad, R. Truant, and S. Sipione. 2012. Ganglioside GM1 induces phosphorylation of mutant huntingtin and restores normal motor behavior in Huntington disease mice. *Proceedings of the National Academy of Sciences of the United States of America*. 109:3528-3533.

DiFiglia, M., P. Pasik, and T. Pasik. 1976. A Golgi study of neuronal types in the neostriatum of monkeys. *Brain research*. 114:245-256.

DiFiglia, M., E. Sapp, K. Chase, C. Schwarz, A. Meloni, C. Young, E. Martin, J.P. Vonsattel, R. Carraway, S.A. Reeves, and et al. 1995. Huntingtin is a cytoplasmic protein associated with vesicles in human and rat brain neurons. *Neuron*. 14:1075-1081.

Dong, X.X., Y. Wang, and Z.H. Qin. 2009. Molecular mechanisms of excitotoxicity and their relevance to pathogenesis of neurodegenerative diseases. *Acta pharmacologica Sinica*. 30:379-387.

Dopie, J., K.P. Skarp, R.E. Kaisa, K. Tanhuanpaa, and M.K. Vartiainen. 2012. Active maintenance of nuclear actin by importin 9 supports transcription. *Proc.Natl.Acad.Sci.U.S.A*. 109:E544-E552.

Dragatsis, I., M.S. Levine, and S. Zeitlin. 2000. Inactivation of Hdh in the brain and testis results in progressive neurodegeneration and sterility in mice. *Nature genetics*. 26:300-306.

Drummond, I.A., S.A. McClure, M. Poenie, R.Y. Tsien, and R.A. Steinhardt. 1986. Large changes in intracellular pH and calcium observed during heat shock are not responsible for the induction of heat shock proteins in Drosophila melanogaster. *Mol.Cell Biol.* 6:1767-1775.

Dudek, N.L., Y. Dai, and N.A. Muma. 2010. Neuroprotective effects of calmodulin peptide 76-121aa: disruption of calmodulin binding to mutant huntingtin. *Brain Pathol*. 20:176-189.

Dumas, E.M., S.J. van den Bogaard, M.E. Ruber, R.R. Reilman, J.C. Stout, D. Craufurd, S.L. Hicks, C. Kennard, S.J. Tabrizi, M.A. van Buchem, J. van der Grond, and R.A. Roos. 2012. Early changes in white matter pathways of the sensorimotor cortex in premanifest Huntington's disease. *Human brain mapping*. 33:203-212.

Dunah, A.W., H. Jeong, A. Griffin, Y.M. Kim, D.G. Standaert, S.M. Hersch, M.M. Mouradian, A.B. Young, N. Tanese, and D. Krainc. 2002. Sp1 and TAFII130 transcriptional activity disrupted in early Huntington's disease. *Science*. 296:2238-2243.

Dundr, M., J.K. Ospina, M.H. Sung, S. John, M. Upender, T. Ried, G.L. Hager, and A.G. Matera. 2007. Actin-dependent intranuclear repositioning of an active gene locus in vivo. *The Journal of cell biology*. 179:1095-1103.

Eckert, A., K.L. Schulz, V. Rhein, and J. Gotz. 2010. Convergence of amyloid-beta and tau pathologies on mitochondria in vivo. *Molecular neurobiology*. 41:107-114.

Endo, M., K. Ohashi, and K. Mizuno. 2007. LIM kinase and slingshot are critical for neurite extension. *J.Biol.Chem.* 282:13692-13702.

Engelender, S., A.H. Sharp, V. Colomer, M.K. Tokito, A. Lanahan, P. Worley, E.L. Holzbaur, and C.A. Ross. 1997. Huntingtin-associated protein 1 (HAP1) interacts with the p150Glued subunit of dynactin. *Human molecular genetics*. 6:2205-2212.

Eskes, R., B. Antonsson, A. Osen-Sand, S. Montessuit, C. Richter, R. Sadoul, G. Mazzei, A. Nichols, and J.C. Martinou. 1998. Bax-induced cytochrome C release from mitochondria is independent of the permeability transition pore but highly dependent on Mg2+ ions. *J.Cell Biol.* 143:217-224.

Fahrenkrog, B., D. Stoffler, and U. Aebi. 2001. Nuclear pore complex architecture and functional dynamics. *Curr.Top.Microbiol.Immunol.* 259:95-117.

Feigin, A. 2011. Pridopidine in treatment of Huntington's disease: beyond chorea? *Lancet neurology*. 10:1036-1037.

Feldman, M.L., and A. Peters. 1972. Intranuclear rods and sheets in rat cochlear nucleus. *Journal of neurocytology*. 1:109-127.

Ferrante, R.J., N.W. Kowall, and E.P. Richardson, Jr. 1991. Proliferative and degenerative changes in striatal spiny neurons in Huntington's disease: a combined study using the section-Golgi method and calbindin D28k immunocytochemistry. *The Journal of neuroscience : the official journal of the Society for Neuroscience*. 11:3877-3887.

Folk, J.E. 1983. Mechanism and basis for specificity of transglutaminase-catalyzed epsilon-(gamma-glutamyl) lysine bond formation. *Advances in enzymology and related areas of molecular biology*. 54:1-56.

Fornerod, M., M. Ohno, M. Yoshida, and I.W. Mattaj. 1997. CRM1 is an export receptor for leucine-rich nuclear export signals. *Cell*. 90:1051-1060.

Friis, M.B., C.R. Friborg, L. Schneider, M.B. Nielsen, I.H. Lambert, S.T. Christensen, and E.K. Hoffmann. 2005. Cell shrinkage as a signal to apoptosis in NIH 3T3 fibroblasts. *J.Physiol*. 567:427-443.

Fu, Y.H., D.P. Kuhl, A. Pizzuti, M. Pieretti, J.S. Sutcliffe, S. Richards, A.J. Verkerk, J.J. Holden, R.G. Fenwick, Jr., S.T. Warren, and et al. 1991. Variation of the CGG repeat at the fragile X site results in genetic instability: resolution of the Sherman paradox. *Cell*. 67:1047-1058.

Fujikake, N., Y. Nagai, H.A. Popiel, Y. Okamoto, M. Yamaguchi, and T. Toda. 2008. Heat shock transcription factor 1-activating compounds suppress polyglutamine-induced neurodegeneration through induction of multiple molecular chaperones. *J.Biol.Chem.* 283:26188-26197.

Fukui, Y., and H. Katsumaru. 1979. Nuclear actin bundles in Amoeba, Dictyostelium and human HeLa cells induced by dimethyl sulfoxide. *Experimental cell research*. 120:451-455.

Gagnon, K.T., H.M. Pendergraff, G.F. Deleavey, E.E. Swayze, P. Potier, J. Randolph, E.B. Roesch, J. Chattopadhyaya, M.J. Damha, C.F. Bennett, C. Montaillier, M. Lemaitre, and D.R. Corey. 2010. Allele-selective inhibition of mutant huntingtin expression with antisense oligonucleotides targeting the expanded CAG repeat. *Biochemistry*. 49:10166-10178.

Gallo, G. 2007. Tau is actin up in Alzheimer's disease. *Nature cell biology*. 9:133-134.

Gatchel, J.R., and H.Y. Zoghbi. 2005. Diseases of unstable repeat expansion: mechanisms and common principles. *Nature reviews. Genetics*. 6:743-755.

Gauthier, L.R., B.C. Charrin, M. Borrell-Pages, J.P. Dompierre, H. Rangone, F.P. Cordelieres, M.J. De, M.E. MacDonald, V. Lessmann, S. Humbert, and F. Saudou. 2004. Huntingtin controls neurotrophic support and survival of neurons by enhancing BDNF vesicular transport along microtubules. *Cell*. 118:127-138.

Gibson, G.E., A. Starkov, J.P. Blass, R.R. Ratan, and M.F. Beal. 2010. Cause and consequence: mitochondrial dysfunction initiates and propagates neuronal dysfunction, neuronal death and behavioral abnormalities in age-associated neurodegenerative diseases. *Biochim.Biophys.Acta*. 1802:122-134.

Gimenez-Roldan, S., and D. Mateo. 1989. [Huntington disease: tetrabenazine compared to haloperidol in the reduction of involuntary movements]. *Neurologia*. 4:282-287.

Gines, S., I.S. Seong, E. Fossale, E. Ivanova, F. Trettel, J.F. Gusella, V.C. Wheeler, F. Persichetti, and M.E. MacDonald. 2003. Specific progressive cAMP reduction implicates energy deficit in presymptomatic Huntington's disease knock-in mice. *Human molecular genetics*. 12:497-508.

Giorgini, F., P. Guidetti, Q. Nguyen, S.C. Bennett, and P.J. Muchowski. 2005. A genomic screen in yeast implicates kynurenine 3-monooxygenase as a therapeutic target for Huntington disease. *Nature genetics*. 37:526-531.

Giralt, A., M. Puigdellivol, O. Carreton, P. Paoletti, J. Valero, A. Parra-Damas, C.A. Saura, J. Alberch, and S. Gines. 2012. Long-term memory deficits in Huntington's disease are associated with reduced CBP histone acetylase activity. *Human molecular genetics*. 21:1203-1216.

Gissi, C., G. Pesole, E. Cattaneo, and M. Tartari. 2006. Huntingtin gene evolution in Chordata and its peculiar features in the ascidian Ciona genus. *BMC genomics*. 7:288.

Godin, J.D., K. Colombo, M. Molina-Calavita, G. Keryer, D. Zala, B.C. Charrin, P. Dietrich, M.L. Volvert, F. Guillemot, I. Dragatsis, Y. Bellaiche, F. Saudou, L. Nguyen, and S. Humbert. 2010. Huntingtin is required for mitotic spindle orientation and mammalian neurogenesis. *Neuron*. 67:392-406.

Grinthal, A., I. Adamovic, B. Weiner, M. Karplus, and N. Kleckner. 2010. PR65, the HEAT-repeat scaffold of phosphatase PP2A, is an elastic connector that links force and catalysis. *Proceedings of the National Academy of Sciences of the United States of America*. 107:2467-2472.

Grunewald, T., and M.F. Beal. 1999. Bioenergetics in Huntington's disease. *Ann.N.Y.Acad.Sci.* 893:203-213.

Gu, X., E.R. Greiner, R. Mishra, R. Kodali, A. Osmand, S. Finkbeiner, J.S. Steffan, L.M. Thompson, R. Wetzel, and X.W. Yang. 2009. Serines 13 and 16 are critical determinants of full-length human mutant huntingtin induced disease pathogenesis in HD mice. *Neuron*. 64:828-840.

Guidetti, P., P.H. Reddy, D.A. Tagle, and R. Schwarcz. 2000. Early kynurenergic impairment in Huntington's disease and in a transgenic animal model. *Neuroscience letters*. 283:233-235.

Gunawardena, S., L.S. Her, R.G. Brusch, R.A. Laymon, I.R. Niesman, B. Gordesky-Gold, L. Sintasath, N.M. Bonini, and L.S. Goldstein. 2003. Disruption of axonal transport by loss of huntingtin or expression of pathogenic polyQ proteins in Drosophila. *Neuron*. 40:25-40.

Gusella, J.F., N.S. Wexler, P.M. Conneally, S.L. Naylor, M.A. Anderson, R.E. Tanzi, P.C. Watkins, K. Ottina, M.R. Wallace, and A.Y. Sakaguchi. 1983. A polymorphic DNA marker genetically linked to Huntington's disease. *Nature*. 306:234-238.

Gutekunst, C.A., S.H. Li, H. Yi, J.S. Mulroy, S. Kuemmerle, R. Jones, D. Rye, R.J. Ferrante, S.M. Hersch, and X.J. Li. 1999. Nuclear and neuropil aggregates in Huntington's disease: relationship to neuropathology. *The Journal of neuroscience : the official journal of the Society for Neuroscience*. 19:2522-2534.

Han, I., Y. You, J.H. Kordower, S.T. Brady, and G.A. Morfini. 2010. Differential vulnerability of neurons in Huntington's disease: the role of cell type-specific features. *Journal of neurochemistry*. 113:1073-1091.

Han, L., M.B. Stope, M.L. de Jesus, P.A. Oude Weernink, M. Urban, T. Wieland, D. Rosskopf, K. Mizuno, K.H. Jakobs, and M. Schmidt. 2007. Direct stimulation of receptor-controlled phospholipase D1 by phospho-cofilin. *EMBO J.* 26:4189-4202.

Harper, S.Q., P.D. Staber, X. He, S.L. Eliason, I.H. Martins, Q. Mao, L. Yang, R.M. Kotin, H.L. Paulson, and B.L. Davidson. 2005. RNA interference improves motor and neuropathological abnormalities in a Huntington's disease mouse model. *Proceedings of the National Academy of Sciences of the United States of America*. 102:5820-5825.

Harreman, M.T., T.M. Kline, H.G. Milford, M.B. Harben, A.E. Hodel, and A.H. Corbett. 2004. Regulation of nuclear import by phosphorylation adjacent to nuclear localization signals. *The Journal of biological chemistry*. 279:20613-20621.

Heiser, V., S. Engemann, W. Brocker, I. Dunkel, A. Boeddrich, S. Waelter, E. Nordhoff, R. Lurz, N. Schugardt, S. Rautenberg, C. Herhaus, G. Barnickel, H. Bottcher, H. Lehrach, and E.E. Wanker. 2002. Identification of benzothiazoles as potential polyglutamine aggregation inhibitors of Huntington's disease by using an automated filter retardation assay.

***Proceedings of the National Academy of Sciences of the United States of America*. 99 Suppl 4:16400-16406.**

Helton, T.D., T. Otsuka, M.C. Lee, Y. Mu, and M.D. Ehlers. 2008. Pruning and loss of excitatory synapses by the parkin ubiquitin ligase. *Proceedings of the National Academy of Sciences of the United States of America*. 105:19492-19497.

Heng, M.Y., P.J. Detloff, and R.L. Albin. 2008. Rodent genetic models of Huntington disease. *Neurobiology of disease*. 32:1-9.

Herman, J.F., L.S. Mangala, and K. Mehta. 2006. Implications of increased tissue transglutaminase (TG2) expression in drug-resistant breast cancer (MCF-7) cells. *Oncogene*. 25:3049-3058.

Hernandez-Espinosa, D., and A.J. Morton. 2006. Calcineurin inhibitors cause an acceleration of the neurological phenotype in a mouse transgenic for the human Huntington's disease mutation. *Brain research bulletin*. 69:669-679.

Heydari, A.R., S. You, R. Takahashi, A. Gutsmann-Conrad, K.D. Sarge, and A. Richardson. 2000. Age-related alterations in the activation of heat shock transcription factor 1 in rat hepatocytes. *Experimental cell research*. 256:83-93.

Hoffner, G., P. Kahlem, and P. Djian. 2002. Perinuclear localization of huntingtin as a consequence of its binding to microtubules through an interaction with beta-tubulin: relevance to Huntington's disease. *Journal of cell science*. 115:941-948.

Hofmann, W.A., L. Stojiljkovic, B. Fuchsova, G.M. Vargas, E. Mavrommatis, V. Philimonenko, K. Kysela, J.A. Goodrich, J.L. Lessard, T.J. Hope, P. Hozak, and P. de Lanerolle. 2004. Actin is part of pre-initiation complexes and is necessary for transcription by RNA polymerase II. *Nature cell biology*. 6:1094-1101.

Hosoi, T., and K. Ozawa. 2010. Endoplasmic reticulum stress in disease: mechanisms and therapeutic opportunities. *Clin.Sci.(Lond)*. 118:19-29.

Hotulainen, P., and C.C. Hoogenraad. 2010. Actin in dendritic spines: connecting dynamics to function. *J.Cell Biol.* 189:619-629.

Hotulainen, P., E. Paunola, M.K. Vartiainen, and P. Lappalainen. 2005. Actin-depolymerizing factor and cofilin-1 play overlapping roles in promoting rapid F-actin depolymerization in mammalian nonmuscle cells. *Mol.Biol.Cell*. 16:649-664.

Hu, P., S. Wu, and N. Hernandez. 2004. A role for beta-actin in RNA polymerase III transcription. *Genes & development*. 18:3010-3015.

Huang, T.Y., L.S. Minamide, J.R. Bamburg, and G.M. Bokoch. 2008. Chronophin mediates an ATP-sensing mechanism for cofilin dephosphorylation and neuronal cofilin-actin rod formation. *Dev.Cell*. 15:691-703.

Huntington-Study-Group. 2001. A randomized, placebo-controlled trial of coenzyme Q10 and remacemide in Huntington's disease. *Neurology*. 57:397-404.

Huntington-Study-Group. 2010. A futility study of minocycline in Huntington's disease. *Movement disorders : official journal of the Movement Disorder Society*. 25:2219-2224.

Huntington, G. 2003. On chorea. George Huntington, M.D. *J.Neuropsychiatry Clin.Neurosci.* 15:109-112.

Iida, K., S. Matsumoto, and I. Yahara. 1992. The KKRKK sequence is involved in heat shock-induced nuclear translocation of the 18-kDa actin-binding protein, cofilin. *Cell Struct.Funct.* 17:39-46.

Jeitner, T.M., W.R. Matson, J.E. Folk, J.P. Blass, and A.J. Cooper. 2008. Increased levels of gamma-glutamylamines in Huntington disease CSF. *J.Neurochem.* 106:37-44.

Jeitner, T.M., N.A. Muma, K.P. Battaile, and A.J. Cooper. 2009. Transglutaminase activation in neurodegenerative diseases. *Future neurology*. 4:449-467.

Johnson, G.V., T.M. Cox, J.P. Lockhart, M.D. Zinnerman, M.L. Miller, and R.E. Powers. 1997. Transglutaminase activity is increased in Alzheimer's disease brain. *Brain Res.* 751:323-329.

Junn, E., W.H. Jang, X. Zhao, B.S. Jeong, and M.M. Mouradian. 2009. Mitochondrial localization of DJ-1 leads to enhanced neuroprotection. *Journal of neuroscience research*. 87:123-129.

Kahlem, P., C. Terre, H. Green, and P. Djian. 1996. Peptides containing glutamine repeats as substrates for transglutaminase-catalyzed cross-linking: relevance to diseases of the nervous system. *Proc.Natl.Acad.Sci.U.S.A*. 93:14580-14585.

Kalderon, D., W.D. Richardson, A.F. Markham, and A.E. Smith. 1984. Sequence requirements for nuclear location of simian virus 40 large-T antigen. *Nature*. 311:33-38.

Karpuj, M.V., M.W. Becher, and L. Steinman. 2002. Evidence for a role for transglutaminase in Huntington's disease and the potential therapeutic implications. *Neurochem.Int.* 40:31-36.

Kaufman, A.M., A.J. Milnerwood, M.D. Sepers, A. Coquinco, K. She, L. Wang, H. Lee, A.M. Craig, M. Cynader, and L.A. Raymond. 2012. Opposing roles of synaptic and extrasynaptic NMDA receptor signaling in cocultured striatal and cortical neurons. *The Journal of neuroscience : the official journal of the Society for Neuroscience*. 32:3992-4003.

Kay, B.K., M.P. Williamson, and M. Sudol. 2000. The importance of being proline: the interaction of proline-rich motifs in signaling proteins with their cognate domains. *FASEB journal : official publication of the Federation of American Societies for Experimental Biology*. 14:231-241.

Kegel, K.B., A.R. Meloni, Y. Yi, Y.J. Kim, E. Doyle, B.G. Cuiffo, E. Sapp, Y. Wang, Z.H. Qin, J.D. Chen, J.R. Nevins, N. Aronin, and M. DiFiglia. 2002. Huntingtin is present in the nucleus, interacts with the transcriptional corepressor C-terminal binding protein, and represses transcription. *The Journal of biological chemistry*. 277:7466-7476.

Keller, J.N. 2006. Age-related neuropathology, cognitive decline, and Alzheimer's disease. *Ageing Research Reviews*. 5:1-13.

Kennedy, L., E. Evans, C.M. Chen, L. Craven, P.J. Detloff, M. Ennis, and P.F. Shelbourne. 2003. Dramatic tissue-specific mutation length increases are an early molecular event in Huntington disease pathogenesis. *Human molecular genetics*. 12:3359-3367.

Keryer, G., J.R. Pineda, G. Liot, J. Kim, P. Dietrich, C. Benstaali, K. Smith, F.P. Cordelieres, N. Spassky, R.J. Ferrante, I. Dragatsis, and F. Saudou. 2011. Ciliogenesis is regulated by a huntingtin-HAP1-PCM1 pathway and is altered in Huntington disease. *The Journal of clinical investigation*. 121:4372-4382.

Killoran, A., and K.M. Biglan. 2012. Therapeutics in Huntington's Disease. *Current treatment options in neurology*.

Kiraly, R., E. Csosz, T. Kurtan, S. Antus, K. Szigeti, Z. Simon-Vecsei, I.R. Korponay-Szabo, Z. Keresztessy, and L. Fesus. 2009. Functional significance of five noncanonical Ca2+-

binding sites of human transglutaminase 2 characterized by site-directed mutagenesis. *FEBS J.* 276:7083-7096.

Kirkwood, T.B., and S.N. Austad. 2000. Why do we age? *Nature*. 408:233-238.

Klamt, F., S. Zdanov, R.L. Levine, A. Pariser, Y. Zhang, B. Zhang, L.R. Yu, T.D. Veenstra, and E. Shacter. 2009. Oxidant-induced apoptosis is mediated by oxidation of the actin-regulatory protein cofilin. *Nat.Cell Biol.* 11:1241-1246.

Kobe, B., and A.V. Kajava. 2000. When protein folding is simplified to protein coiling: the continuum of solenoid protein structures. *Trends in biochemical sciences*. 25:509-515.

Koroshetz, W.J., B.G. Jenkins, B.R. Rosen, and M.F. Beal. 1997. Energy metabolism defects in Huntington's disease and effects of coenzyme Q10. *Ann.Neurol.* 41:160-165.

Kraus, R.L., R. Pasieczny, K. Lariosa-Willingham, M.S. Turner, A. Jiang, and J.W. Trauger. 2005. Antioxidant properties of minocycline: neuroprotection in an oxidative stress assay and direct radical-scavenging activity. *Journal of neurochemistry*. 94:819-827.

Kremer, B., E. Almqvist, J. Theilmann, N. Spence, H. Telenius, Y.P. Goldberg, and M.R. Hayden. 1995. Sex-dependent mechanisms for expansions and contractions of the CAG repeat on affected Huntington disease chromosomes. *American journal of human genetics*. 57:343-350.

Kubo, T., A. Yamaguchi, N. Iwata, and T. Yamashita. 2008. The therapeutic effects of Rho-ROCK inhibitors on CNS disorders. *Therapeutics and clinical risk management*. 4:605-615.

Kudo, N., B. Wolff, T. Sekimoto, E.P. Schreiner, Y. Yoneda, M. Yanagida, S. Horinouchi, and M. Yoshida. 1998. Leptomycin B inhibition of signal-mediated nuclear export by direct binding to CRM1. *Exp.Cell Res.* 242:540-547.

Kurita, S., E. Gunji, K. Ohashi, and K. Mizuno. 2007. Actin filaments-stabilizing and -bundling activities of cofilin-phosphatase Slingshot-1. *Genes Cells*. 12:663-676.

Kwan, W., A. Magnusson, A. Chou, A. Adame, M.J. Carson, S. Kohsaka, E. Masliah, T. Moller, R. Ransohoff, S.J. Tabrizi, M. Bjorkqvist, and P.J. Muchowski. 2012. Bone marrow transplantation confers modest benefits in mouse models of Huntington's disease. *The Journal of neuroscience : the official journal of the Society for Neuroscience*. 32:133-142.

Labbadia, J., H. Cunliffe, A. Weiss, E. Katsyuba, K. Sathasivam, T. Seredenina, B. Woodman, S. Moussaoui, S. Frentzel, R. Luthi-Carter, P. Paganetti, and G.P. Bates. 2011. Altered chromatin architecture underlies progressive impairment of the heat shock response in mouse models of Huntington disease. *The Journal of clinical investigation*. 121:3306-3319.

Lamprecht, M.R., D.M. Sabatini, and A.E. Carpenter. 2007. CellProfiler: free, versatile software for automated biological image analysis. *Biotechniques*. 42:71-75.

Lange, A., L.M. McLane, R.E. Mills, S.E. Devine, and A.H. Corbett. 2010. Expanding the definition of the classical bipartite nuclear localization signal. *Traffic.* 11:311-323.

Lange, A., R.E. Mills, C.J. Lange, M. Stewart, S.E. Devine, and A.H. Corbett. 2007. Classical nuclear localization signals: definition, function, and interaction with importin alpha. *J.Biol.Chem.* 282:5101-5105.

Leavitt, B.R., J.M. van Raamsdonk, J. Shehadeh, H. Fernandes, Z. Murphy, R.K. Graham, C.L. Wellington, L.A. Raymond, and M.R. Hayden. 2006. Wild-type huntingtin protects neurons from excitotoxicity. *Journal of neurochemistry*. 96:1121-1129.

Lee, J.M., E.M. Ramos, J.H. Lee, T. Gillis, J.S. Mysore, M.R. Hayden, S.C. Warby, P. Morrison, M. Nance, C.A. Ross, R.L. Margolis, F. Squitieri, S. Orobello, S. Di Donato, E. Gomez-Tortosa, C. Ayuso, O. Suchowersky, R.J. Trent, E. McCusker, A. Novelletto, M. Frontali, R. Jones, T. Ashizawa, S. Frank, M.H. Saint-Hilaire, S.M. Hersch, H.D. Rosas, D. Lucente, M.B. Harrison, A. Zanko, R.K. Abramson, K. Marder, J. Sequeiros, J.S. Paulsen, G.B. Landwehrmeyer, R.H. Myers, M.E. Macdonald, and J.F. Gusella. 2012. CAG repeat expansion in Huntington disease determines age at onset in a fully dominant fashion. *Neurology*. 78:690-695.

Lesort, M., W. Chun, G.V. Johnson, and R.J. Ferrante. 1999. Tissue transglutaminase is increased in Huntington's disease brain. *J.Neurochem.* 73:2018-2027.

Lesort, M., W. Chun, J. Tucholski, and G.V. Johnson. 2002. Does tissue transglutaminase play a role in Huntington's disease? *Neurochem.Int.* 40:37-52.

Levine, M.S., C. Cepeda, M.A. Hickey, S.M. Fleming, and M.F. Chesselet. 2004. Genetic mouse models of Huntington's and Parkinson's diseases: illuminating but imperfect. *Trends in neurosciences*. 27:691-697.

Levine, R.L. 2002. Carbonyl modified proteins in cellular regulation, aging, and disease. *Free radical biology & medicine*. 32:790-796.

Levine, R.L., J.A. Williams, E.R. Stadtman, and E. Shacter. 1994. Carbonyl assays for determination of oxidatively modified proteins. *Methods in enzymology*. 233:346-357.

Li, M., Y. Huang, A.A. Ma, E. Lin, and M.I. Diamond. 2009. Y-27632 improves rotarod performance and reduces huntingtin levels in R6/2 mice. *Neurobiol.Dis.* 36:413-420.

Li, S.H., G. Schilling, W.S. Young, 3rd, X.J. Li, R.L. Margolis, O.C. Stine, M.V. Wagster, M.H. Abbott, M.L. Franz, N.G. Ranen, and et al. 1993. Huntington's disease gene (IT15) is widely expressed in human and rat tissues. *Neuron*. 11:985-993.

Li, W., L.C. Serpell, W.J. Carter, D.C. Rubinsztein, and J.A. Huntington. 2006. Expression and characterization of full-length human huntingtin, an elongated HEAT repeat protein. *The Journal of biological chemistry*. 281:15916-15922.

Li, Z., C.A. Karlovich, M.P. Fish, M.P. Scott, and R.M. Myers. 1999. A putative Drosophila homolog of the Huntington's disease gene. *Human molecular genetics*. 8:1807-1815.

Lim, M.K., T. Kawamura, Y. Ohsawa, M. Ohtsubo, S. Asakawa, A. Takayanagi, and N. Shimizu. 2007. Parkin interacts with LIM Kinase 1 and reduces its cofilin-phosphorylation activity via ubiquitination. *Exp.Cell Res.* 313:2858-2874.

Liquori, C.L., K. Ricker, M.L. Moseley, J.F. Jacobsen, W. Kress, S.L. Naylor, J.W. Day, and L.P. Ranum. 2001. Myotonic dystrophy type 2 caused by a CCTG expansion in intron 1 of ZNF9. *Science*. 293:864-867.

Lleres, D., J. James, S. Swift, D.G. Norman, and A.I. Lamond. 2009. Quantitative analysis of chromatin compaction in living cells using FLIM-FRET. *J.Cell Biol.* 187:481-496.

Lleres, D., S. Swift, and A.I. Lamond. 2007. Detecting protein-protein interactions in vivo with FRET using multiphoton fluorescence lifetime imaging microscopy (FLIM). *Curr.Protoc.Cytom.* Chapter 12:Unit12.

Lovell, M.A., S.P. Gabbita, and W.R. Markesbery. 1999. Increased DNA oxidation and decreased levels of repair products in Alzheimer's disease ventricular CSF. *Journal of neurochemistry*. 72:771-776.

Luthi-Carter, R., and J.H. Cha. 2003. Mechanisms of transcriptional dysregulation in Huntington's disease. *Clinical Neuroscience Research*. 3:165-177.

Macario, A.J., and E. Conway de Macario. 2005. Sick chaperones, cellular stress, and disease. *The New England journal of medicine*. 353:1489-1501.

Macchi, G. 1999. Camillo Golgi: a clinical pathologist. *J.Hist Neurosci.* 8:141-150.

Macleod, M.D. 1881. Cases of Choreic Convulsions in Persons of Advanced Age. Vol. 27. The British Journal of Psychiatry. 194-200.

Maekawa, M., T. Ishizaki, S. Boku, N. Watanabe, A. Fujita, A. Iwamatsu, T. Obinata, K. Ohashi, K. Mizuno, and S. Narumiya. 1999. Signaling from Rho to the actin cytoskeleton through protein kinases ROCK and LIM-kinase. *Science*. 285:895-898.

Maglione, V., P. Marchi, A. Di Pardo, S. Lingrell, M. Horkey, E. Tidmarsh, and S. Sipione. 2010. Impaired ganglioside metabolism in Huntington's disease and neuroprotective role of GM1. *The Journal of neuroscience : the official journal of the Society for Neuroscience*. 30:4072-4080.

Maloney, M.T., and J.R. Bamburg. 2007. Cofilin-mediated neurodegeneration in Alzheimer's disease and other amyloidopathies. *Mol.Neurobiol.* 35:21-44.

Maloney, M.T., L.S. Minamide, A.W. Kinley, J.A. Boyle, and J.R. Bamburg. 2005. Beta-secretase-cleaved amyloid precursor protein accumulates at actin inclusions induced in neurons by stress or amyloid beta: a feedforward mechanism for Alzheimer's disease. *The Journal of neuroscience : the official journal of the Society for Neuroscience*. 25:11313-11321.

Mannherz, H.G., E. Ballweber, M. Galla, S. Villard, C. Granier, C. Steegborn, A. Schmidtmann, K. Jaquet, B. Pope, and A.G. Weeds. 2007. Mapping the ADF/cofilin binding site on monomeric actin by competitive cross-linking and peptide array: evidence for a second binding site on monomeric actin. *J.Mol.Biol*. 366:745-755.

Margolis, R.L., D.D. Rudnicki, and S.E. Holmes. 2005. Huntington's disease like-2: review and update. *Acta neurologica Taiwanica*. 14:1-8.

Mastroberardino, P.G., M.G. Farrace, I. Viti, F. Pavone, G.M. Fimia, G. Melino, C. Rodolfo, and M. Piacentini. 2006. "Tissue" transglutaminase contributes to the formation of disulphide bridges in proteins of mitochondrial respiratory complexes. *Biochimica et biophysica acta*. 1757:1357-1365.

Mastroberardino, P.G., C. Iannicola, R. Nardacci, F. Bernassola, L.V. De, G. Melino, S. Moreno, F. Pavone, S. Oliverio, L. Fesus, and M. Piacentini. 2002. 'Tissue' transglutaminase ablation reduces neuronal death and prolongs survival in a mouse model of Huntington's disease. *Cell Death.Differ.* 9:873-880.

Matthews, R.T., L. Yang, B.G. Jenkins, R.J. Ferrante, B.R. Rosen, R. Kaddurah-Daouk, and M.F. Beal. 1998. Neuroprotective effects of creatine and cyclocreatine in animal models of Huntington's disease. *The Journal of neuroscience : the official journal of the Society for Neuroscience*. 18:156-163.

McBride, J.L., M.R. Pitzer, R.L. Boudreau, B. Dufour, T. Hobbs, S.R. Ojeda, and B.L. Davidson. 2011. Preclinical safety of RNAi-mediated HTT suppression in the rhesus macaque as a potential therapy for Huntington's disease. *Molecular therapy : the journal of the American Society of Gene Therapy*. 19:2152-2162.

McConoughey, S.J., M. Basso, Z.V. Niatsetskaya, S.F. Sleiman, N.A. Smirnova, B.C. Langley, L. Mahishi, A.J. Cooper, M.A. Antonyak, R.A. Cerione, B. Li, A. Starkov, R.K. Chaturvedi, M.F. Beal, G. Coppola, D.H. Geschwind, H. Ryu, L. Xia, S.E. Iismaa, J. Pallos, R. Pasternack, M. Hils, J. Fan, L.A. Raymond, J.L. Marsh, L.M. Thompson, and R.R. Ratan.

2010. Inhibition of transglutaminase 2 mitigates transcriptional dysregulation in models of Huntington disease. *EMBO Mol.Med.*

McGeer, E.G., and P.L. McGeer. 1976. Duplication of biochemical changes of Huntington's chorea by intrastriatal injections of glutamic and kainic acids. *Nature*. 263:517-519.

McGough, A., B. Pope, W. Chiu, and A. Weeds. 1997. Cofilin changes the twist of F-actin: implications for actin filament dynamics and cellular function. *The Journal of cell biology*. 138:771-781.

McNeil, S.M., A. Novelletto, J. Srinidhi, G. Barnes, I. Kornbluth, M.R. Altherr, J.J. Wasmuth, J.F. Gusella, M.E. MacDonald, and R.H. Myers. 1997. Reduced penetrance of the Huntington's disease mutation. *Human molecular genetics*. 6:775-779.

Menalled, L.B. 2005. Knock-in mouse models of Huntington's disease. *NeuroRx : the journal of the American Society for Experimental NeuroTherapeutics*. 2:465-470.

Menalled, L.B., M. Patry, N. Ragland, P.A. Lowden, J. Goodman, J. Minnich, B. Zahasky, L. Park, J. Leeds, D. Howland, E. Signer, A.J. Tobin, and D. Brunner. 2010. Comprehensive behavioral testing in the R6/2 mouse model of Huntington's disease shows no benefit from CoQ10 or minocycline. *PloS one*. 5:e9793.

Mendel, G. 1865. Experiments in Plant Hybridization. Electronic Scholarly Publishing Project(1996): http://www.esp.org/foundations/genetics/classical/gm-65.pdf

Miguel-Hidalgo, J.J., X.A. Alvarez, R. Cacabelos, and G. Quack. 2002. Neuroprotection by memantine against neurodegeneration induced by beta-amyloid(1-40). *Brain research*. 958:210-221.

Mila, S., A.G. Albo, D. Corpillo, S. Giraudo, M. Zibetti, E.M. Bucci, L. Lopiano, and M. Fasano. 2009. Lymphocyte proteomics of Parkinson's disease patients reveals cytoskeletal protein dysregulation and oxidative stress. *Biomark.Med.* 3:117-128.

Milnerwood, A.J., C.M. Gladding, M.A. Pouladi, A.M. Kaufman, R.M. Hines, J.D. Boyd, R.W. Ko, O.C. Vasuta, R.K. Graham, M.R. Hayden, T.H. Murphy, and L.A. Raymond. 2010. Early increase in extrasynaptic NMDA receptor signaling and expression contributes to phenotype onset in Huntington's disease mice. *Neuron*. 65:178-190.

Milnerwood, A.J., and L.A. Raymond. 2010. Early synaptic pathophysiology in neurodegeneration: insights from Huntington's disease. *Trends Neurosci.* 33:513-523.

Minamide, L.S., S. Maiti, J.A. Boyle, R.C. Davis, J.A. Coppinger, Y. Bao, T.Y. Huang, J. Yates, G.M. Bokoch, and J.R. Bamburg. 2010. Isolation and characterization of cytoplasmic cofilin-actin rods. *J.Biol.Chem.* 285:5450-5460.

Minamide, L.S., A.M. Striegl, J.A. Boyle, P.J. Meberg, and J.R. Bamburg. 2000. Neurodegenerative stimuli induce persistent ADF/cofilin-actin rods that disrupt distal neurite function. *Nat.Cell Biol.* 2:628-636.

Mitchell, I.J., A.J. Cooper, and M.R. Griffiths. 1999. The selective vulnerability of striatopallidal neurons. *Progress in neurobiology*. 59:691-719.

Modregger, J., N.A. DiProspero, V. Charles, D.A. Tagle, and M. Plomann. 2002. PACSIN 1 interacts with huntingtin and is absent from synaptic varicosities in presymptomatic Huntington's disease brains. *Human molecular genetics*. 11:2547-2558.

Mohr, D., S. Frey, T. Fischer, T. Guttler, and D. Gorlich. 2009. Characterisation of the passive permeability barrier of nuclear pore complexes. *EMBO J.* 28:2541-2553.

Monsonego, A., I. Friedmann, Y. Shani, M. Eisenstein, and M. Schwartz. 1998. GTP-dependent conformational changes associated with the functional switch between Galpha and

cross-linking activities in brain-derived tissue transglutaminase. *J.Mol.Biol.* 282:713-720.

Moon, A., and D.G. Drubin. 1995. The ADF/cofilin proteins: stimulus-responsive modulators of actin dynamics. *Mol Biol Cell*. 6:1423-1431.

Morimoto, R.I. 2008. Proteotoxic stress and inducible chaperone networks in neurodegenerative disease and aging. *Genes & development*. 22:1427-1438.

Morimoto, R.I. 2012. The Heat Shock Response: Systems Biology of Proteotoxic Stress in Aging and Disease. *Cold Spring Harbor symposia on quantitative biology*.

Moriyama, K., K. Iida, and I. Yahara. 1996. Phosphorylation of Ser-3 of cofilin regulates its essential function on actin. *Genes Cells*. 1:73-86.

Mortiboys, H., K.K. Johansen, J.O. Aasly, and O. Bandmann. 2010. Mitochondrial impairment in patients with Parkinson disease with the G2019S mutation in LRRK2. *Neurology*. 75:2017-2020.

Moscovich, M., R.P. Munhoz, N. Becker, E.R. Barbosa, A.J. Espay, R. Weiser, and H.A. Teive. 2011. Americo Negrette and Huntington's disease. *Arq Neuropsiquiatr.* 69:711-713.

Muma, N.A. 2007. Transglutaminase is linked to neurodegenerative diseases. *Journal of neuropathology and experimental neurology*. 66:258-263.

Munsie, L., N. Caron, R.S. Atwal, I. Marsden, E.J. Wild, J.R. Bamburg, S.J. Tabrizi, and R. Truant. 2011. Mutant huntingtin causes defective actin remodeling during stress: defining a new role for transglutaminase 2 in neurodegenerative disease. *Hum.Mol.Genet.* 20:1937-1951.

Nasir, J., S.B. Floresco, J.R. O'Kusky, V.M. Diewert, J.M. Richman, J. Zeisler, A. Borowski, J.D. Marth, A.G. Phillips, and M.R. Hayden. 1995. Targeted disruption of the Huntington's disease gene results in embryonic lethality and behavioral and morphological changes in heterozygotes. *Cell*. 81:811-823.

Nishida, E., K. Iida, N. Yonezawa, S. Koyasu, I. Yahara, and H. Sakai. 1987. Cofilin is a component of intranuclear and cytoplasmic actin rods induced in cultured cells. *Proc.Natl.Acad.Sci.U.S.A*. 84:5262-5266.

Norlund, M.A., J.M. Lee, G.M. Zainelli, and N.A. Muma. 1999. Elevated transglutaminase-induced bonds in PHF tau in Alzheimer's disease. *Brain Res.* 851:154-163.

Nuss, J.E., K.B. Choksi, J.H. DeFord, and J. Papaconstantinou. 2008. Decreased enzyme activities of chaperones PDI and BiP in aged mouse livers. *Biochemical and biophysical research communications*. 365:355-361.

Obrdlik, A., A. Kukalev, E. Louvet, A.K. Farrants, L. Caputo, and P. Percipalle. 2008. The histone acetyltransferase PCAF associates with actin and hnRNP U for RNA polymerase II transcription. *Molecular and cellular biology*. 28:6342-6357.

Obrdlik, A., and P. Percipalle. 2011. The F-actin severing protein cofilin-1 is required for RNA polymerase II transcription elongation. *Nucleus.* 2:72-79.

Ohta, Y., E. Nishida, H. Sakai, and E. Miyamoto. 1989. Dephosphorylation of cofilin accompanies heat shock-induced nuclear accumulation of cofilin. *J.Biol Chem.* 264:16143-16148.

Okano, I., J. Hiraoka, H. Otera, K. Nunoue, K. Ohashi, S. Iwashita, M. Hirai, and K. Mizuno. 1995. Identification and characterization of a novel family of serine/threonine kinases containing two N-terminal LIM motifs. *The Journal of biological chemistry*. 270:31321-31330.

Ono, S., H. Abe, R. Nagaoka, and T. Obinata. 1993. Colocalization of ADF and cofilin in intranuclear actin rods of cultured muscle cells. *J.Muscle Res.Cell Motil.* 14:195-204.

Orr, H.T. 2011. Are polyglutamine diseases expanding? *Neuron*. 70:377-378.

Orr, H.T., and H.Y. Zoghbi. 2007. Trinucleotide repeat disorders. *Annual review of neuroscience*. 30:575-621.

Osborn, M., and K. Weber. 1980. Damage of cellular functions by trifluoperazine, a calmodulin-specific drug. *Experimental cell research*. 130:484-488.

Osborn, M., and K. Weber. 1984. Actin paracrystal induction by forskolin and by db-cAMP in CHO cells. *Experimental cell research*. 150:408-418.

Pal, A., F. Severin, B. Lommer, A. Shevchenko, and M. Zerial. 2006. Huntingtin-HAP40 complex is a novel Rab5 effector that regulates early endosome motility and is up-regulated in Huntington's disease. *J.Cell Biol.* 172:605-618.

Paleacu, D. 2007. Tetrabenazine in the treatment of Huntington's disease. *Neuropsychiatric disease and treatment*. 3:545-551.

Park, S.H., T.J. Park, and I.K. Lim. 2010. Reduction of exportin 6 activity leads to actin accumulation via failure of RanGTP restoration and NTF2 sequestration in the nuclei of senescent cells. *Exp.Cell Res.*

Pawlowski, R., E.K. Rajakyla, M.K. Vartiainen, and R. Treisman. 2010. An actin-regulated importin alpha/beta-dependent extended bipartite NLS directs nuclear import of MRTF-A. *EMBO J.* 29:3448-3458.

Percipalle, P., J. Zhao, B. Pope, A. Weeds, U. Lindberg, and B. Daneholt. 2001. Actin bound to the heterogeneous nuclear ribonucleoprotein hrp36 is associated with Balbiani ring mRNA from the gene to polysomes. *The Journal of cell biology*. 153:229-236.

Pfister, E.L., L. Kennington, J. Straubhaar, S. Wagh, W. Liu, M. DiFiglia, B. Landwehrmeyer, J.P. Vonsattel, P.D. Zamore, and N. Aronin. 2009. Five siRNAs targeting three SNPs may provide therapy for three-quarters of Huntington's disease patients. *Current biology : CB*. 19:774-778.

Pillon, B., B. Dubois, and Y. Agid. 1991. Severity and specificity of cognitive impairment in Alzheimer's, Huntington's, and Parkinson's diseases and progressive supranuclear palsy. *Annals of the New York Academy of Sciences*. 640:224-227.

Plotkin, J.L., M. Day, and D.J. Surmeier. 2011. Synaptically driven state transitions in distal dendrites of striatal spiny neurons. *Nature neuroscience*. 14:881-888.

Pollitt, S.K., J. Pallos, J. Shao, U.A. Desai, A.A. Ma, L.M. Thompson, J.L. Marsh, and M.I. Diamond. 2003. A rapid cellular FRET assay of polyglutamine aggregation identifies a novel inhibitor. *Neuron*. 40:685-694.

Pontrello, C.G., M.Y. Sun, A. Lin, T.A. Fiacco, K.A. DeFea, and I.M. Ethell. 2012. Cofilin under control of beta-arrestin-2 in NMDA-dependent dendritic spine plasticity, long-term depression (LTD), and learning. *Proceedings of the National Academy of Sciences of the United States of America*. 109:E442-451.

Porras, G., Q. Li, and E. Bezard. 2012. Modeling Parkinson's Disease in Primates: The MPTP Model. *Cold Spring Harbor perspectives in medicine*. 2:a009308.

Posse de Chaves, E., and S. Sipione. 2010. Sphingolipids and gangliosides of the nervous system in membrane function and dysfunction. *FEBS letters*. 584:1748-1759.

Prime, M.E., O.A. Andersen, J.J. Barker, M.A. Brooks, R.K. Cheng, I. Toogood-Johnson, S.M. Courtney, F.A. Brookfield, C.J. Yarnold, R.W. Marston, P.D. Johnson, S.F. Johnsen, J.J.

Palfrey, D. Vaidya, S. Erfan, O. Ichihara, B. Felicetti, S. Palan, A. Pedret-Dunn, S. Schaertl, I. Sternberger, A. Ebneth, A. Scheel, D. Winkler, L. Toledo-Sherman, M. Beconi, D. Macdonald, I. Munoz-Sanjuan, C. Dominguez, and J. Wityak. 2012. Discovery and structure-activity relationship of potent and selective covalent inhibitors of transglutaminase 2 for Huntington's disease. *Journal of medicinal chemistry*. 55:1021-1046.

Przedborski, S., K. Tieu, C. Perier, and M. Vila. 2004. MPTP as a mitochondrial neurotoxic model of Parkinson's disease. *Journal of bioenergetics and biomembranes*. 36:375-379.

Puszkin, E.G., and V. Raghuraman. 1985. Catalytic properties of a calmodulin-regulated transglutaminase from human platelet and chicken gizzard. *The Journal of biological chemistry*. 260:16012-16020.

Quarrell, O.W., A.S. Rigby, L. Barron, Y. Crow, A. Dalton, N. Dennis, A.E. Fryer, F. Heydon, E. Kinning, A. Lashwood, M. Losekoot, L. Margerison, S. McDonnell, P.J. Morrison, A. Norman, M. Peterson, F.L. Raymond, S. Simpson, E. Thompson, and J. Warner. 2007. Reduced penetrance alleles for Huntington's disease: a multi-centre direct observational study. *Journal of medical genetics*. 44:e68.

Rauskolb, S., M. Zagrebelsky, A. Dreznjak, R. Deogracias, T. Matsumoto, S. Wiese, B. Erne, M. Sendtner, N. Schaeren-Wiemers, M. Korte, and Y.A. Barde. 2010. Global deprivation of brain-derived neurotrophic factor in the CNS reveals an area-specific requirement for dendritic growth. *The Journal of neuroscience : the official journal of the Society for Neuroscience*. 30:1739-1749.

Rawlins, M. 2010. Huntington's disease out of the closet? *Lancet*. 376:1372-1373.

Reiner, A., R.L. Albin, K.D. Anderson, C.J. D'Amato, J.B. Penney, and A.B. Young. 1988. Differential loss of striatal projection neurons in Huntington disease. *Proceedings of the National Academy of Sciences of the United States of America*. 85:5733-5737.

Reinhart, P.H., L.S. Kaltenbach, C. Essrich, D.E. Dunn, J.A. Eudailey, C.T. DeMarco, G.J. Turmel, J.C. Whaley, A. Wood, S. Cho, and D.C. Lo. 2011. Identification of anti-inflammatory targets for Huntington's disease using a brain slice-based screening assay. *Neurobiology of disease*. 43:248-256.

Renton, A.E., E. Majounie, A. Waite, J. Simon-Sanchez, S. Rollinson, J.R. Gibbs, J.C. Schymick, H. Laaksovirta, J.C. van Swieten, L. Myllykangas, H. Kalimo, A. Paetau, Y. Abramzon, A.M. Remes, A. Kaganovich, S.W. Scholz, J. Duckworth, J. Ding, D.W. Harmer, D.G. Hernandez, J.O. Johnson, K. Mok, M. Ryten, D. Trabzuni, R.J. Guerreiro, R.W. Orrell, J. Neal, A. Murray, J. Pearson, I.E. Jansen, D. Sondervan, H. Seelaar, D. Blake, K. Young, N. Halliwell, J.B. Callister, G. Toulson, A. Richardson, A. Gerhard, J. Snowden, D. Mann, D. Neary, M.A. Nalls, T. Peuralinna, L. Jansson, V.M. Isoviita, A.L. Kaivorinne, M. Holtta-Vuori, E. Ikonen, R. Sulkava, M. Benatar, J. Wuu, A. Chio, G. Restagno, G. Borghero, M. Sabatelli, D. Heckerman, E. Rogaeva, L. Zinman, J.D. Rothstein, M. Sendtner, C. Drepper, E.E. Eichler, C. Alkan, Z. Abdullaev, S.D. Pack, A. Dutra, E. Pak, J. Hardy, A. Singleton, N.M. Williams, P. Heutink, S. Pickering-Brown, H.R. Morris, P.J. Tienari, and B.J. Traynor. 2011. A hexanucleotide repeat expansion in C9ORF72 is the cause of chromosome 9p21-linked ALS-FTD. *Neuron*. 72:257-268.

Richfield, E.K., K.A. Maguire-Zeiss, H.E. Vonkeman, and P. Voorn. 1995. Preferential loss of preproenkephalin versus preprotachykinin neurons from the striatum of Huntington's disease patients. *Ann.Neurol.* 38:852-861.

Rigamonti, D., J.H. Bauer, C. De-Fraja, L. Conti, S. Sipione, C. Sciorati, E. Clementi, A. Hackam, M.R. Hayden, Y. Li, J.K. Cooper, C.A. Ross, S. Govoni, C. Vincenz, and E. Cattaneo. 2000. Wild-type huntingtin protects from apoptosis upstream of caspase-3. *The Journal of neuroscience : the official journal of the Society for Neuroscience*. 20:3705-3713.

Rizzo, M.A., G.H. Springer, B. Granada, and D.W. Piston. 2004. An improved cyan fluorescent protein variant useful for FRET. *Nat.Biotechnol.* 22:445-449.

Robbins, J., S.M. Dilworth, R.A. Laskey, and C. Dingwall. 1991. Two interdependent basic domains in nucleoplasmin nuclear targeting sequence: identification of a class of bipartite nuclear targeting sequence. *Cell*. 64:615-623.

Rockabrand, E., N. Slepko, A. Pantalone, V.N. Nukala, A. Kazantsev, J.L. Marsh, P.G. Sullivan, J.S. Steffan, S.L. Sensi, and L.M. Thompson. 2007. The first 17 amino acids of Huntingtin modulate its sub-cellular localization, aggregation and effects on calcium homeostasis. *Hum.Mol.Genet.* 16:61-77.

Roos, W.P., and B. Kaina. 2006. DNA damage-induced cell death by apoptosis. *Trends in molecular medicine*. 12:440-450.

Rosenstock, T.R., O.M. de Brito, V. Lombardi, S. Louros, M. Ribeiro, S. Almeida, I.L. Ferreira, C.R. Oliveira, and A.C. Rego. 2011. FK506 ameliorates cell death features in Huntington's disease striatal cell models. *Neurochemistry international*. 59:600-609.

Ross, C.A., and M.A. Poirier. 2005. Opinion: What is the role of protein aggregation in neurodegeneration? *Nature reviews. Molecular cell biology*. 6:891-898.

Ruan, Q., and G.V. Johnson. 2007. Transglutaminase 2 in neurodegenerative disorders. *Front Biosci.* 12:891-904.

Rust, M.B., C.B. Gurniak, M. Renner, H. Vara, L. Morando, A. Gorlich, M. Sassoe-Pognetto, M.A. Banchaabouchi, M. Giustetto, A. Triller, D. Choquet, and W. Witke. 2010. Learning, AMPA receptor mobility and synaptic plasticity depend on n-cofilin-mediated actin dynamics. *The EMBO journal*. 29:1889-1902.

Sassone, J., C. Colciago, G. Cislaghi, V. Silani, and A. Ciammola. 2009. Huntington's disease: the current state of research with peripheral tissues. *Experimental neurology*. 219:385-397.

Saudou, F., S. Finkbeiner, D. Devys, and M.E. Greenberg. 1998. Huntingtin acts in the nucleus to induce apoptosis but death does not correlate with the formation of intranuclear inclusions. *Cell*. 95:55-66.

Savas, J.N., B. Ma, K. Deinhardt, B.P. Culver, S. Restituito, L. Wu, J.G. Belasco, M.V. Chao, and N. Tanese. 2010. A role for huntington disease protein in dendritic RNA granules. *The Journal of biological chemistry*. 285:13142-13153.

Schaertl, S., M. Prime, J. Wityak, C. Dominguez, I. Munoz-Sanjuan, R.E. Pacifici, S. Courtney, A. Scheel, and D. Macdonald. 2010. A Profiling Platform for the Characterization of Transglutaminase 2 (TG2) Inhibitors. *J.Biomol.Screen.* 15:478-487.

Scherzinger, E., R. Lurz, M. Turmaine, L. Mangiarini, B. Hollenbach, R. Hasenbank, G.P. Bates, S.W. Davies, H. Lehrach, and E.E. Wanker. 1997. Huntingtin-encoded polyglutamine expansions form amyloid-like protein aggregates in vitro and in vivo. *Cell*. 90:549-558.

Schnell, U., F. Dijk, K.A. Sjollema, and B.N. Giepmans. 2012. Immunolabeling artifacts and the need for live-cell imaging. *Nat.Methods*. 9:152-158.

Schoenfeld, M., R.H. Myers, L.A. Cupples, B. Berkman, D.S. Sax, and E. Clark. 1984. Increased rate of suicide among patients with Huntington's disease. *Journal of neurology, neurosurgery, and psychiatry*. 47:1283-1287.

Schroder, M., and R.J. Kaufman. 2005. ER stress and the unfolded protein response. *Mutat.Res.* 569:29-63.

Schulte, J., K.J. Sepp, C. Wu, P. Hong, and J.T. Littleton. 2011. High-content chemical and RNAi screens for suppressors of neurotoxicity in a Huntington's disease model. *PloS one*. 6:e23841.

Schwarcz, R. 2004. The kynurenine pathway of tryptophan degradation as a drug target. *Current opinion in pharmacology*. 4:12-17.

Seibel, N.M., J. Eljouni, M.M. Nalaskowski, and W. Hampe. 2007. Nuclear localization of enhanced green fluorescent protein homomultimers. *Anal.Biochem.* 368:95-99.

Seong, I.S., E. Ivanova, J.M. Lee, Y.S. Choo, E. Fossale, M. Anderson, J.F. Gusella, J.M. Laramie, R.H. Myers, M. Lesort, and M.E. MacDonald. 2005. HD CAG repeat implicates a dominant property of huntingtin in mitochondrial energy metabolism. *Hum.Mol.Genet.* 14:2871-2880.

Seong, I.S., J.M. Woda, J.J. Song, A. Lloret, P.D. Abeyrathne, C.J. Woo, G. Gregory, J.M. Lee, V.C. Wheeler, T. Walz, R.E. Kingston, J.F. Gusella, R.A. Conlon, and M.E. MacDonald. 2010. Huntingtin facilitates polycomb repressive complex 2. *Human molecular genetics*. 19:573-583.

Shao, J., W.J. Welch, N.A. Diprospero, and M.I. Diamond. 2008. Phosphorylation of profilin by ROCK1 regulates polyglutamine aggregation. *Mol.Cell Biol.* 28:5196-5208.

Sharp, A.H., S.J. Loev, G. Schilling, S.H. Li, X.J. Li, J. Bao, M.V. Wagster, J.A. Kotzuk, J.P. Steiner, A. Lo, and et al. 1995. Widespread expression of Huntington's disease gene (IT15) protein product. *Neuron*. 14:1065-1074.

Shiwach, R. 1994. Psychopathology in Huntington's disease patients. *Acta psychiatrica Scandinavica*. 90:241-246.

Silvestroni, A., R.L. Faull, A.D. Strand, and T. Moller. 2009. Distinct neuroinflammatory profile in post-mortem human Huntington's disease. *Neuroreport*. 20:1098-1103.

Singaraja, R.R., K. Huang, S.S. Sanders, A.J. Milnerwood, R. Hines, J.P. Lerch, S. Franciosi, R.C. Drisdel, K. Vaid, F.B. Young, C. Doty, J. Wan, N. Bissada, R.M. Henkelman, W.N. Green, N.G. Davis, L.A. Raymond, and M.R. Hayden. 2011. Altered palmitoylation and neuropathological deficits in mice lacking HIP14. *Human molecular genetics*. 20:3899-3909.

Sittler, A., R. Lurz, G. Lueder, J. Priller, H. Lehrach, M.K. Hayer-Hartl, F.U. Hartl, and E.E. Wanker. 2001. Geldanamycin activates a heat shock response and inhibits huntingtin aggregation in a cell culture model of Huntington's disease. *Hum.Mol.Genet.* 10:1307-1315.

Smith, K.M., S. Matson, W.R. Matson, K. Cormier, S.J. Del Signore, S.W. Hagerty, E.C. Stack, H. Ryu, and R.J. Ferrante. 2006. Dose ranging and efficacy study of high-dose coenzyme Q10 formulations in Huntington's disease mice. *Biochimica et biophysica acta*. 1762:616-626.

Sorg, G., and T. Stamminger. 1999. Mapping of nuclear localization signals by simultaneous fusion to green fluorescent protein and to beta-galactosidase. *Biotechniques*. 26:858-862.

Sorolla, M.A., G. Reverter-Branchat, J. Tamarit, I. Ferrer, J. Ros, and E. Cabiscol. 2008. Proteomic and oxidative stress analysis in human brain samples of Huntington disease. *Free radical biology & medicine*. 45:667-678.

Spencer, V.A., S. Costes, J.L. Inman, R. Xu, J. Chen, M.J. Hendzel, and M.J. Bissell. 2011. Depletion of nuclear actin is a key mediator of quiescence in epithelial cells. *Journal of cell science*. 124:123-132.

Steffan, J.S., N. Agrawal, J. Pallos, E. Rockabrand, L.C. Trotman, N. Slepko, K. Illes, T. Lukacsovich, Y.Z. Zhu, E. Cattaneo, P.P. Pandolfi, L.M. Thompson, and J.L. Marsh. 2004. SUMO modification of Huntingtin and Huntington's disease pathology. *Science*. 304:100-104.

Strehlow, A.N., J.Z. Li, and R.M. Myers. 2007. Wild-type huntingtin participates in protein trafficking between the Golgi and the extracellular space. *Human molecular genetics*. 16:391-409.

Sturrock, A., and B.R. Leavitt. 2010. The clinical and genetic features of Huntington disease. *J.Geriatr.Psychiatry Neurol.* 23:243-259.

Stuven, T., E. Hartmann, and D. Gorlich. 2003. Exportin 6: a novel nuclear export receptor that is specific for profilin.actin complexes. *EMBO J.* 22:5928-5940.

Swami, M., A.E. Hendricks, T. Gillis, T. Massood, J. Mysore, R.H. Myers, and V.C. Wheeler. 2009. Somatic expansion of the Huntington's disease CAG repeat in the brain is associated with an earlier age of disease onset. *Human molecular genetics*. 18:3039-3047.

Szegezdi, E., S.E. Logue, A.M. Gorman, and A. Samali. 2006. Mediators of endoplasmic reticulum stress-induced apoptosis. *EMBO reports*. 7:880-885.

Tabrizi, S.J., A.M. Blamire, D.N. Manners, B. Rajagopalan, P. Styles, A.H. Schapira, and T.T. Warner. 2005. High-dose creatine therapy for Huntington disease: a 2-year clinical and MRS study. *Neurology*. 64:1655-1656.

Tabrizi, S.J., R. Reilmann, R.A. Roos, A. Durr, B. Leavitt, G. Owen, R. Jones, H. Johnson, D. Craufurd, S.L. Hicks, C. Kennard, B. Landwehrmeyer, J.C. Stout, B. Borowsky, R.I. Scahill, C. Frost, and D.R. Langbehn. 2012. Potential endpoints for clinical trials in premanifest and early Huntington's disease in the TRACK-HD study: analysis of 24 month observational data. *Lancet neurology*. 11:42-53.

Tang, T.S., E. Slow, V. Lupu, I.G. Stavrovskaya, M. Sugimori, R. Llinas, B.S. Kristal, M.R. Hayden, and I. Bezprozvanny. 2005. Disturbed Ca2+ signaling and apoptosis of medium spiny neurons in Huntington's disease. *Proc.Natl.Acad.Sci.U.S.A*. 102:2602-2607.

Taniguchi, E., F. Toyoshima-Morimoto, and E. Nishida. 2002. Nuclear translocation of plk1 mediated by its bipartite nuclear localization signal. *J.Biol.Chem.* 277:48884-48888.

The-Huntington's-Disease-Research-Collaborative-Group. 1993. A novel gene containing a trinucleotide repeat that is expanded and unstable on Huntington's disease chromosomes. The Huntington's Disease Collaborative Research Group. *Cell*. 72:971-983.

Thies, E., and E.M. Mandelkow. 2007. Missorting of tau in neurons causes degeneration of synapses that can be rescued by the kinase MARK2/Par-1. *The Journal of neuroscience : the official journal of the Society for Neuroscience*. 27:2896-2907.

Thompson, L.M., C.T. Aiken, L.S. Kaltenbach, N. Agrawal, K. Illes, A. Khoshnan, M. Martinez-Vincente, M. Arrasate, J.G. O'Rourke, H. Khashwji, T. Lukacsovich, Y.Z. Zhu, A.L. Lau, A. Massey, M.R. Hayden, S.O. Zeitlin, S. Finkbeiner, K.N. Green, F.M. LaFerla, G. Bates, L. Huang, P.H. Patterson, D.C. Lo, A.M. Cuervo, J.L. Marsh, and J.S. Steffan. 2009. IKK phosphorylates Huntingtin and targets it for degradation by the proteasome and lysosome. *The Journal of cell biology*. 187:1083-1099.

Toshima, J., J.Y. Toshima, T. Amano, N. Yang, S. Narumiya, and K. Mizuno. 2001. Cofilin phosphorylation by protein kinase testicular protein kinase 1 and its role in integrin-mediated actin reorganization and focal adhesion formation. *Mol Biol Cell*. 12:1131-1145.

Trettel, F., D. Rigamonti, P. Hilditch-Maguire, V.C. Wheeler, A.H. Sharp, F. Persichetti, E. Cattaneo, and M.E. MacDonald. 2000. Dominant phenotypes produced by the HD mutation in STHdh(Q111) striatal cells. *Hum.Mol.Genet.* 9:2799-2809.

Trushina, E., R.B. Dyer, J.D. Badger, 2nd, D. Ure, L. Eide, D.D. Tran, B.T. Vrieze, V. Legendre-Guillemin, P.S. McPherson, B.S. Mandavilli, B. Van Houten, S. Zeitlin, M. McNiven, R. Aebersold, M. Hayden, J.E. Parisi, E. Seeberg, I. Dragatsis, K. Doyle, A. Bender, C. Chacko, and C.T. McMurray. 2004. Mutant huntingtin impairs axonal trafficking in mammalian neurons in vivo and in vitro. *Molecular and cellular biology*. 24:8195-8209.

Tukamoto, T., N. Nukina, K. Ide, and I. Kanazawa. 1997. Huntington's disease gene product, huntingtin, associates with microtubules in vitro. *Brain research. Molecular brain research*. 51:8-14.

Turunen, M., J. Olsson, and G. Dallner. 2004. Metabolism and function of coenzyme Q. *Biochimica et biophysica acta*. 1660:171-199.

Valente, E.M., P.M. Abou-Sleiman, V. Caputo, M.M. Muqit, K. Harvey, S. Gispert, Z. Ali, D. Del Turco, A.R. Bentivoglio, D.G. Healy, A. Albanese, R. Nussbaum, R. Gonzalez-Maldonado, T. Deller, S. Salvi, P. Cortelli, W.P. Gilks, D.S. Latchman, R.J. Harvey, B. Dallapiccola, G. Auburger, and N.W. Wood. 2004. Hereditary early-onset Parkinson's disease caused by mutations in PINK1. *Science*. 304:1158-1160.

Varma, H., C. Voisine, C.T. DeMarco, E. Cattaneo, D.C. Lo, A.C. Hart, and B.R. Stockwell. 2007. Selective inhibitors of death in mutant huntingtin cells. *Nature chemical biology*. 3:99-100.

Vartiainen, M.K., S. Guettler, B. Larijani, and R. Treisman. 2007. Nuclear actin regulates dynamic subcellular localization and activity of the SRF cofactor MAL. *Science*. 316:1749-1752.

Venezula-Project-Collaborators. 2008. The Venezuela Huntington's Disease Project. http://www.hdfoundation.org/html/venezuela_huntington.php.

Vonsattel, J.P., R.H. Myers, T.J. Stevens, R.J. Ferrante, E.D. Bird, and E.P. Richardson, Jr. 1985. Neuropathological classification of Huntington's disease. *Journal of neuropathology and experimental neurology*. 44:559-577.

Wallrabe, H., and A. Periasamy. 2005. Imaging protein molecules using FRET and FLIM microscopy. *Curr.Opin.Biotechnol.* 16:19-27.

Wang, J., S. Gines, M.E. MacDonald, and J.F. Gusella. 2005a. Reversal of a full-length mutant huntingtin neuronal cell phenotype by chemical inhibitors of polyglutamine-mediated aggregation. *BMC neuroscience*. 6:1.

Wang, W., W. Duan, S. Igarashi, H. Morita, M. Nakamura, and C.A. Ross. 2005b. Compounds blocking mutant huntingtin toxicity identified using a Huntington's disease neuronal cell model. *Neurobiology of disease*. 20:500-508.

Wang, Y., F. Shibasaki, and K. Mizuno. 2005c. Calcium signal-induced cofilin dephosphorylation is mediated by Slingshot via calcineurin. *The Journal of biological chemistry*. 280:12683-12689.

Wexler, A. 2008. The Woman Who Walked into the Sea. Yale University Press. 1-100.

Wexler, N.S., A.B. Young, R.E. Tanzi, H. Travers, S. Starosta-Rubinstein, J.B. Penney, S.R. Snodgrass, I. Shoulson, F. Gomez, M.A. Ramos Arroyo, and et al. 1987. Homozygotes for Huntington's disease. *Nature*. 326:194-197.

White, J.K., W. Auerbach, M.P. Duyao, J.P. Vonsattel, J.F. Gusella, A.L. Joyner, and M.E. MacDonald. 1997. Huntingtin is required for neurogenesis and is not impaired by the Huntington's disease CAG expansion. *Nature genetics*. 17:404-410.

Whitesell, L., E.G. Mimnaugh, B. De Costa, C.E. Myers, and L.M. Neckers. 1994. Inhibition of heat shock protein HSP90-pp60v-src heteroprotein complex formation by benzoquinone ansamycins: essential role for stress proteins in oncogenic transformation. *Proceedings of the National Academy of Sciences of the United States of America*. 91:8324-8328.

Wilburn, B., D.D. Rudnicki, J. Zhao, T.M. Weitz, Y. Cheng, X. Gu, E. Greiner, C.S. Park, N. Wang, B.L. Sopher, A.R. La Spada, A. Osmand, R.L. Margolis, Y.E. Sun, and X.W. Yang. 2011. An antisense CAG repeat transcript at JPH3 locus mediates expanded polyglutamine protein toxicity in Huntington's disease-like 2 mice. *Neuron*. 70:427-440.

Wild, E., M. Bjorkqvist, and S.J. Tabrizi. 2008. Immune markers for Huntington's disease? *Expert review of neurotherapeutics*. 8:1779-1781.

Wilhelmus, M.M., S.C. Grunberg, J.G. Bol, A.M. van Dam, J.J. Hoozemans, A.J. Rozemuller, and B. Drukarch. 2009. Transglutaminases and transglutaminase-catalyzed cross-links colocalize with the pathological lesions in Alzheimer's disease brain. *Brain Pathol.* 19:612-622.

Wolff, B., J.J. Sanglier, and Y. Wang. 1997. Leptomycin B is an inhibitor of nuclear export: inhibition of nucleo-cytoplasmic translocation of the human immunodeficiency virus type 1 (HIV-1) Rev protein and Rev-dependent mRNA. *Chemistry & biology*. 4:139-147.

Wyttenbach, A., J. Swartz, H. Kita, T. Thykjaer, J. Carmichael, J. Bradley, R. Brown, M. Maxwell, A. Schapira, T.F. Orntoft, K. Kato, and D.C. Rubinsztein. 2001. Polyglutamine expansions cause decreased CRE-mediated transcription and early gene expression changes prior to cell death in an inducible cell model of Huntington's disease. *Human molecular genetics*. 10:1829-1845.

Xia, J., D.H. Lee, J. Taylor, M. Vandelft, and R. Truant. 2003. Huntingtin contains a highly conserved nuclear export signal. *Human molecular genetics*. 12:1393-1403.

Xifro, X., J.M. Garcia-Martinez, D. Del Toro, J. Alberch, and E. Perez-Navarro. 2008. Calcineurin is involved in the early activation of NMDA-mediated cell death in mutant huntingtin knock-in striatal cells. *Journal of neurochemistry*. 105:1596-1612.

Xu, Y.Z., T. Thuraisingam, D.A. Morais, M. Rola-Pleszczynski, and D. Radzioch. 2010. Nuclear translocation of beta-actin is involved in transcriptional regulation during macrophage differentiation of HL-60 cells. *Mol Biol Cell*. 21:811-820.

Yahara, I., F. Harada, S. Sekita, K. Yoshihira, and S. Natori. 1982. Correlation between effects of 24 different cytochalasins on cellular structures and cellular events and those on actin in vitro. *The Journal of cell biology*. 92:69-78.

Yang, N., O. Higuchi, K. Ohashi, K. Nagata, A. Wada, K. Kangawa, E. Nishida, and K. Mizuno. 1998. Cofilin phosphorylation by LIM-kinase 1 and its role in Rac-mediated actin reorganization. *Nature*. 393:809-812.

Zainelli, G.M., C.A. Ross, J.C. Troncoso, J.K. Fitzgerald, and N.A. Muma. 2004. Calmodulin regulates transglutaminase 2 cross-linking of huntingtin. *The Journal of neuroscience : the official journal of the Society for Neuroscience*. 24:1954-1961.

Zhang, H., Q. Li, R.K. Graham, E. Slow, M.R. Hayden, and I. Bezprozvanny. 2008. Full length mutant huntingtin is required for altered Ca2+ signaling and apoptosis of striatal neurons in the YAC mouse model of Huntington's disease. *Neurobiol.Dis.* 31:80-88.

Zhang, J., G. Perry, M.A. Smith, D. Robertson, S.J. Olson, D.G. Graham, and T.J. Montine. 1999. Parkinson's disease is associated with oxidative damage to cytoplasmic DNA and RNA in substantia nigra neurons. *The American journal of pathology*. 154:1423-1429.

Zhang, J., P.L. Yang, and N.S. Gray. 2009. Targeting cancer with small molecule kinase inhibitors. *Nature reviews. Cancer*. 9:28-39.

Zhang, X., D.L. Smith, A.B. Meriin, S. Engemann, D.E. Russel, M. Roark, S.L. Washington, M.M. Maxwell, J.L. Marsh, L.M. Thompson, E.E. Wanker, A.B. Young, D.E. Housman, G.P. Bates, M.Y. Sherman, and A.G. Kazantsev. 2005. A potent small molecule inhibits polyglutamine aggregation in Huntington's disease neurons and suppresses neurodegeneration in vivo. *Proceedings of the National Academy of Sciences of the United States of America*. 102:892-897.

Zhang, Y., M. Li, M. Drozda, M. Chen, S. Ren, R.O. Mejia Sanchez, B.R. Leavitt, E. Cattaneo, R.J. Ferrante, M.R. Hayden, and R.M. Friedlander. 2003. Depletion of wild-type huntingtin in mouse models of neurologic diseases. *Journal of neurochemistry*. 87:101-106.

Zhao, L., and S.L. Ackerman. 2006. Endoplasmic reticulum stress in health and disease. *Current Opinion in Cell Biology*. 18:444-452.

Zheng, B., M. Han, M. Bernier, and J.K. Wen. 2009. Nuclear actin and actin-binding proteins in the regulation of transcription and gene expression. *FEBS J.* 276:2669-2685.

Zoghbi, H.Y., and H.T. Orr. 2000. Glutamine repeats and neurodegeneration. *Annual review of neuroscience*. 23:217-247.

Zuccato, C., A. Ciammola, D. Rigamonti, B.R. Leavitt, D. Goffredo, L. Conti, M.E. MacDonald, R.M. Friedlander, V. Silani, M.R. Hayden, T. Timmusk, S. Sipione, and E. Cattaneo. 2001. Loss of huntingtin-mediated BDNF gene transcription in Huntington's disease. *Science*. 293:493-498.

Zuccato, C., D. Liber, C. Ramos, A. Tarditi, D. Rigamonti, M. Tartari, M. Valenza, and E. Cattaneo. 2005. Progressive loss of BDNF in a mouse model of Huntington's disease and rescue by BDNF delivery. *Pharmacological research : the official journal of the Italian Pharmacological Society*. 52:133-139.

Zuccato, C., M. Tartari, A. Crotti, D. Goffredo, M. Valenza, L. Conti, T. Cataudella, B.R. Leavitt, M.R. Hayden, T. Timmusk, D. Rigamonti, and E. Cattaneo. 2003. Huntingtin interacts

with REST/NRSF to modulate the transcription of NRSE-controlled neuronal genes. *Nature genetics*. 35:76-83.

Zuddas, A., G. Oberto, F. Vaglini, F. Fascetti, F. Fornai, and G.U. Corsini. 1992. MK-801 prevents 1-methyl-4-phenyl-1,2,3,6-tetrahydropyridine-induced parkinsonism in primates. *Journal of neurochemistry*. 59:733-739.

Zwilling, D., S.Y. Huang, K.V. Sathyasaikumar, F.M. Notarangelo, P. Guidetti, H.Q. Wu, J. Lee, J. Truong, Y. Andrews-Zwilling, E.W. Hsieh, J.Y. Louie, T. Wu, K. Scearce-Levie, C. Patrick, A. Adame, F. Giorgini, S. Moussaoui, G. Laue, A. Rassoulpour, G. Flik, Y. Huang, J.M. Muchowski, E. Masliah, R. Schwarcz, and P.J. Muchowski. 2011. Kynurenine 3-monooxygenase inhibition in blood ameliorates neurodegeneration. *Cell*. 145:863-874.